AD-A127 226 AN ANALYSIS OF FULL SCALE MEASUREMENTS ON M/V STEWART J CORT DURING THE 1..(U) STEVENS INST OF TECH HOBOKEN NJ DAVIDSON LAB J F DALZELL FEB 82 SIT-DL-81-9-2221 1/3

UNCLASSIFIED USCG-D-25-82 DTCG23-81-C-2031 F/G 13/10 NL

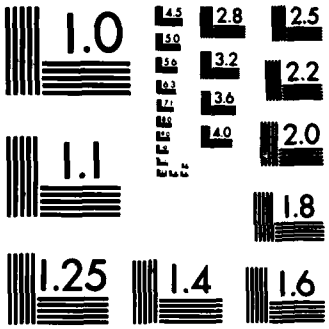

MICROCOPY RESOLUTION TEST CHART
NATIONAL BUREAU OF STANDARDS-1963-A

Report No. CG-D-25-82

(10)

AD A127226

AN ANALYSIS OF FULL SCALE MEASUREMENTS ON M/V STEWART J. CORT DURING THE 1979 AND 1980 TRIAL PROGRAMS

Davidson Laboratory
Stevens Institute of Technology
Castle Point Station
Hoboken, NJ 07030

FINAL REPORT
February 1982

Document is available to the U. S. public through the National Technical Information Service, Springfield, Virginia 22161

APR 26 1983

A

PREPARED FOR

U.S. DEPARTMENT OF TRANSPORTATION
UNITED STATES COAST GUARD
OFFICE OF RESEARCH AND DEVELOPMENT
WASHINGTON, D.C. 20590

DTIC FILE COPY

83 04 26 013

NOTICE

This document is disseminated under the sponsorship of the Department of Transportation in the interest of information exchange. The United States Government assumes no liability for its contents or use thereof.

The contents of this report do not necessarilv reflect the official view or policy of the Coast Guard; and they do not constitute a standard, specification, or regulation.

This report, or portions thereof may not be used for advertising or sales promotion purposes. Citation of trade names and manufacturers does not constitute endorsement or approval of such products.

Technical Report Documentation Page

1. Report No. CG-D-25-82	2. Government Accession No. AD-A127226	3. Recipient's Catalog No.
4. Title and Subtitle AN ANALYSIS OF FULL SCALE MEASUREMENTS ON M/V STEWART J. CORT DURING THE 1979 AND 1980 TRIAL PROGRAMS		5. Report Date February 1982
		6. Performing Organization Code
7. Author(s) J. F. DALZELL		8. Performing Organization Report No. SIT-DL-81-9-2221 (Part I) SIT-DL-82-9-2257 (Part II)
9. Performing Organization Name and Address Stevens Institute of Technology Davidson Laboratory Castle Point Station Hoboken, NJ 07030		10. Work Unit No. (TRAIS)
		11. Contract or Grant No. DTCG23-81-C-20031
12. Sponsoring Agency Name and Address U.S. Coast Guard (G-DMT-1/54) 2100 Second Street, SW Washington, DC 20593		13. Type of Report and Period Covered Final Report May 1981 - February 1982
		14. Sponsoring Agency Code

15. Supplementary Notes

Report SIT-DL-81-9-2221 (Part I) was issued in August 1981.

Report SIT-DL-81-9-2257 (Part II) was issued in February 1982

16. Abstract

The work documented herein represents a small part of a program of research on the longitudinal strength standards for Great Lakes vessels, and was carried out in two distinct but related parts.

The purpose of Part I of the work was to provide an independent review of wave induced springing data obtained aboard the M/V STEWART J. CORT in the Fall of 1979, and the subsequent analysis of this data. The emphasis in this work was to be upon the question of sampling variability, upon some exploratory alternative analysis of data, and upon the resulting implications for projected trials with the same ship in the Fall of 1981. The important finding from this work was that a significant part of the scatter of results derived from the 1979 data may be ascribed to sampling variability. The fact that the statistical coherency between observed stress and wave elevation was found to be of the order of 0.4 raises some important conceptual problems, among which is the possibility of nonlinear response. Evidence was found that quadratic nonlinearities of some significance may exist in the springing response to waves. Recommendations for the projected 1981 trials were formulated.

The purpose of Part II of the present work was to continue the qualification of a previously developed numerical simulation of combined, springing and wave induced stresses. Previous qualification efforts had been inconclusive with respect to main deck bending stresses observed in the 1979 trials of the M/V STEWART J. CORT. Subsequently discovered problems with the main deck bending measurement suggested that the bottom bending stress information should be more suitable, and accordingly, the present analysis has been made with bottom bending stress data from the 1979 and 1980 trials.

17. Key Words Longitudinal Strength, Wave Induced Stress, Bulk Carriers, Vibration Stress, Stress Combination, Springing Stress, Great Lakes Waves	18. Distribution Statement Document is available to the public through the National Technical Information Service, Springfield, VA 22161.

19. Security Classif. (of this report)	20. Security Classif. (of this page)	21. No. of Pages	22. Price
UNCLASSIFIED	UNCLASSIFIED	200	

Form DOT F 1700.7 (8-72) Reproduction of completed page authorized

It was found that the numerical simulation was credible with respect to this data. Essentially, the statistics derivable from typical samples of observed and simulated data are statistically indistinguishable. Because the basic assumptions of the simulation are identical to the state of the art statistical model which is employed for combined wave induced and springing response, this finding reinforces the state of the art approach. This report also contains a preface that summarizes the entire Great Lakes Research Project.

Distribution/
Availability Codes
Avail and/or
Dist Special
A

DTIC
COPY
INSPECTED
2

TABLE OF CONTENTS

PREFACE.....ii

RETROSPECTIVE COMMENTS ON THE FULL SCALE TRIALS PROGRAM OBJECTIVES.....v

GENERAL RECOMMENDATIONS FOR PHASE IV.....vii

PART I

INTRODUCTION.....1

OVERVIEW.....2

FINDINGS.....3

RECOMMENDATIONS FOR THE PROJECTED 1981 TRIALS.....5

APPENDIX A: SELECTION AND PREPROCESSING OF DATA FOR EXPLORATORY ANALYSES.....A-1 through A-23

APPENDIX B: MAXIMUM LIKELIHOOD METHOD SPECTRAL ANALYSES.....B-1 through B-14

APPENDIX C: CROSS SPECTRAL ANALYSES.....C-1 through C-30

APPENDIX D: CROSS-BI-SPECTRAL ANALYSES.....D-1 through D-12

PART II

INTRODUCTION.....II-1

OVERVIEW.....II-3

FINDINGS.....II-5

APPENDIX A: SELECTION AND PREPROCESSING OF 1979 TRIAL DATA.....II-7

APPENDIX B: SELECTION AND PREPROCESSING OF 1980 TRIAL DATA.....II-12

APPENDIX C: AUTOCORRELATION ANALYSIS OF RUN 8 OF THE 1980 TRIALS.....II-19

APPENDIX D: BASIC PROCESSING.....II-21

APPENDIX E: SIMULATION OF DATA.....II-48

APPENDIX F: STATISTICAL INDEPENDENCE OF MAXIMA.....II-50

APPENDIX G: COMPARISONS OF STATISTICS FROM REAL DATA AND SIMULATIONS.....II-54

REFERENCES.....II-101

PREFACE

This document is the last of a series of reports on a segment of the overall program of research on the longitudinal strength standards for Great Lakes vessels. It is a compilation of two separate reports summarizing the last work performed during this segment, known as Phase III. Phase III was carried to its present state in part by efforts of the Coast Guard technical staff and in part by the combined efforts of the following (in order of approximate chronological entry):

Bethlehem Steel Corporation
Naval Research Laboratory (NRL)
David W. Taylor Naval Ship Research and Development Center (DTNSRDC)
American Bureau of Shipping (ABS)
University of Michigan (UM)
Det norske Veritas (DnV)
Stevens Institute of Technology (SIT)

The broad objectives of the overall research program were to assess the magnitude of the springing component of Great Lakes bulk carriers, to develop a new formulation of the rules, to verify the assumptions with full and model scale experiments and to revise, if necessary, the rules for longitudinal strength. The three phases of the research, which started in the early 1960's can be outlined as follows:

Phase I - began in 1963 with full scale stress measurements of the RYERSON. Alarmingly large stresses were recorded on the RYERSON in Lake Michigan during the same storm in which the DANIEL J. MORRELL was lost in Lake Huron. This phase was fully reported in 1971 at the SNAME Symposium (Bulletin S-3) in Ottawa, Canada.

Phase II - included extensive full scale trials on the new 1000-foot carrier M/V STEWART J. CORT and the CHARLES M. BEEGHLY. This phase was concluded September 9, 1975 at SNAME HS-1, HS-1-1, and HS-1-2 meeting in Cleveland, Ohio.

It was concluded at this joint panel meeting that a third phase, where there was a simultaneous measurement of the encountered waves and the hull stress, was absolutely necessary.

Phase III - was comprised of the adaption of two wave measurement systems, three seasons of data collection on the M/V CORT, and the subsequent analysis of this data. This phase closed nominally in early 1982 and its major conclusions are included in this report.

The specific objective of Phase III was to verify, through data analysis, and if possible to improve upon, the present longitudinal strength standards for Great Lakes vessels. These standards, developed in 1977, are complicated by the observed "springing" vibratory stresses, which are of significantly greater magnitude relative to wave induced stresses than is the case in most ocean going ships. The technical questions posed in the program were essentially: How well can the magnitude of springing stresses be predicted analytically? How do springing and wave induced stresses combine to form extreme stresses? And, how might the results of the program be used to improve present day strength standards?

In order to approach the first question in the context of full scale observations it was necessary to obtain some objective measure of the waves encountered by the ship. A wave height measurement system had to be utilized. The first part of the program involved the development, installation and verification of wave measuring devices aboard the Bethlehem Steel Corporation vessel, M/V STEWART J. CORT, which was to be the trials vessel. This portion of the work was carried out by NRL and Coast Guard personnel in 1978 and is documented in Reference 3*.

---

*References on Page II-101.

Sufficiently encouraged, a full scale instrumented trials program was carried out aboard the M/V CORT in the Fall of 1979 by DTNSRDC with the wave measuring equipment previously developed, and an on-board data processing system. These full scale ship trials were the first in history with the objective of directly obtaining springing response amplitude operators (RAO's). With the co-operation of Coast Guard Search and Rescue Units, techniques were developed for encountered wave measurement verification. In this method, wave buoys were dropped and picked up by helicopter in the vicinity of the moving ship. Unfortunately during these trials no heavy wave conditions were encountered, with the result that the wave meter verification data was not extensive enough. However, the notable result from the trials was the acquisition of the first full scale springing response amplitude operators in which some confidence could be felt. These trials are documented in Reference 1 along with direct comparison of observed and theoretical response amplitude operators as predicted by ABS, UM, Webb, and DnV.

In the fall of 1980 a third trials program was carried out aboard the M/V CORT by Coast Guard personnel. These trials involved fewer measurements than the 1979 trials since their objective was to obtain better data with which to verify the wave measurement systems. However, since the main deck bending stress gauges were found to have malfunctioned bottom bending stresses were also recorded. Reasonable success was enjoyed with respect to validation of the wave measurement systems, and some additional springing stress operator data was obtained. These trials are documented in Reference 11.

Concurrently with the 1980 trials, work was underway at SIT on a numerical approach to the question of how springing and wave induced stresses combine to form extremes, Reference 2. In this work it was necessary to further analyze some of the 1979 main deck bending stress data. A peculiar systematic asymmetry in the main deck bending stress data was noted. Systematic assymetry of stresses, is not present in the previously obtained data, References 17 and 18, and is not allowed for in the present state of analytical technology (Reference 19 for example).

It is also not a possible result in the simulations of Reference 2. The credibility of the simulation technique of Reference 2 was thus questioned. In view of the finding of the 1980 trials with respect to main deck bending gages, questions arose about some of the 1979 data.

Consequently, a third measurement program was scheduled for the Fall of 1981. At the conclusion of the 1980 trials and Reference 2 there had been several questions posed about the 1979 results. It was at this point in the overall program that the present analytical work was started in two phases. The objective of the first phase of the present work was to link the 1979 and the projected 1981 full scale measurements with an independent review and analysis of the 1979 data, and to make recommendations, if necessary, for the 1981 trials. Since recommendations, to be used in the 1981 trials, had to be in hand by August 1981, the results of that phase were documented in a technical report prior to the initiation of the second work phase. It is this first technical report which is included (slightly edited) in the present document as "Part I".

The objective of the second phase of the work was to continue the validation studies of Reference 2 using bottom bending stress data from the 1979 and 1980 trials, in order to extend if possible the present ideas about the method of combination of wave induced and springing stresses. The present program thus resulted in a second technical report which is included herein (slightly edited) as "Part II".

RETROSPECTIVE COMMENTS ON THE FULL SCALE TRIALS PROGRAM OBJECTIVES

The existing longitudinal strength standard of the American Bureau of Shipping is contained in Reference 20. The assumptions on which this standard is based are not stated. It appears from the statement that "consideration will be given to the combined dynamic as well as the wave-induced and springing moments and vibration calculations..." that the assumptions used are a blend of proven practice and one or more of the approaches of Reference 19.

Because the permissible bending stresses given for ordinary strength steel do not appear to involve major factors of ignorance, it must be assumed that the rule dynamic longitudinal moments are intended to represent values which have a very low probability of being exceeded within a normal ship life. Thus, there should be an exceedingly low probability that dynamic bending stresses observed in a brief trial program, after augmentation by calculated still water stresses, will approach the permissible. It is clear that direct comparison of observed maximum dynamic stresses with the standard cannot be a serious objective of the present type of trials unless the standard itself is an order of magnitude wrong. Nevertheless, once the trials had been made, simple comparisons can be made of the extremes of the observations with previous data from the same ship, with data from other ships, and with the standard. Clearly, nothing approaching the extremes stresses experienced in 1973 (References17,18) was experienced in either the 1979 or the 1980 trials.

Unless all or most existing large lake carriers were instrumented with maximum reading (scratch) gauges for a very long period of time, no direct "verification" of the extreme magnitudes of combined dynamic stresses is possible. Extrapolation of standards (as contrasted to interpolation) to longer, wider or deeper ships can only be attempted indirectly by computations according to the best available methods.

Assuming, that the strength standard for very long ships has evolved through the application of contemporary analytical methods as outlined in Reference 19, the most important objective in analyses of the present type of trial data is to verify, so far as possible, these analytical methods. The first is the computation of the basic springing response functions (RAO's) and the second is the method whereby the statistics of the maxima of the combined responses are extrapolated. These two aspects of the problem are explicitly noted in the overall objectives cited in the preface, and both have been addressed in the work completed thus far.

GENERAL RECOMMENDATIONS FOR PHASE IV

At the time of assembly of the present document, the 1981 trials program had been carried out, but the data had not yet been reduced. It is thought that somewhat more severe weather was experienced in these trials than in 1979 and 1980. If so, it would be of benefit to attempt analysis similar to that of Part I herein with data in which wave induced stresses are significant.

Part I raises some serious conceptual problems. These include low coherence between encountered wave and springing s sses, and the possibility of nonlinear response in more severe wave tions. The low coherence problem implies a significant sampli. variability in the derived RAO results. Because of this the standard of comparison between analytical predictions and observed response cannot be a close one. Secondly, the indications of nonlinear response raises the spector that the underlying assumptions of the present analytical state of are may be partially in error. Both problems need further examination.

The indication from the analysis of Part II was that the statistics of observed maxima of stresses conform with those expected by virtue of the latest statistical assumptions. This indication suffers from lack of analyzed cases in which wave induced stress was significant. A concurrent statistical work by DnV (Reference 21) suggests the potential for using alternative statistical models; their results should then be compared to those obtained in this report. Application of these in analysis of Great Lakes vessel stresses is recommended.

General recommendations for future Phase IV of the Great Lakes Ship Strength Research are:

- Complete analytical review of the 1980 and 1981 trials data.
- Compare the implied nonlinear response from data analysis with the theoretical results from the University of Michigan model tests.
- Incorporate the new statistical models and the simulation methods for the combination of high and low frequency stresses.
- Final verification of the strength standard.

INTRODUCTION

The problem of providing adequate provision in longitudinal strength standards for the stresses produced by wave induced vibration is particularly important for Great Lakes ships since the vibratory stress (springing) levels experienced have been found to be of significantly greater magnitude relative to wave induced stresses than the vibratory response of most ocean going vessels. The present work is a contribution to an ongoing USCG research program for Great Lakes ore carriers.

Under contract to the U.S. Coast Guard, David W. Taylor Naval Ship Research and Development Center (DTNSRDC) performed full scale measurements on board the M/V STEWART J. CORT during the fall of 1979. During the data analysis phase, RAO's (response amplitude operators) were developed from the stress and wave measurements which were then compared with theoretical RAO's computed by American Bureau of Shipping (ABS), Webb Institute of Naval Architecture, the University of Michinga (UM) and Det norske Veritas (DnV). The results of this work are contained in Reference 1.* A continuation of these full scale measurements is projected for the fall of 1981.

The primary purpose of the present work is to link the 1979 and the projected 1981 full scale wave and stress measurements with an independent review of the 1979 data. The intent was to build upon the research performed to date and to insure the interpretation of the 1979 data is as complete as possible. In particular, the emphasis in the present work was to be upon the question of the sampling variability of the estimates produced in Reference 1, and upon exploratory alternate analyses of the data.

In documenting the present work it has been found convenient to follow the Summary/Appendix report organization. In this style the main body of the report consists of an overview and summary of findings. Following the brief main body of the report are a series of Appendices which contain the detail of the work.

---

*References on Page II-101.

OVERVIEW

The details of the present work are contained in Appendices A through D.

In order to accomplish the objectives of the present work a small subset of the data produced in Reference 1 was selected for analysis. Fundamentally the concern was with the relationship of deck bending stress and the measured wave elevations since these were the data primarily analyzed in Reference 1. One by-product of the work described in Reference 2 was a set of problems involving the basic data. The first problem was that the maxima and minima of the deck bending stresses were statistically asymmetric, a situation which does not agree with the concepts of the present state of springing theory, or with the basic assumptions made in the interpretation of data. The second problem was that the ratio between deck and the more symmetric bottom bending stresses appeared to change with time during the experiments of Reference 1--by an amount which was difficult to accept on physical grounds. Thus in the present work it was thought prudent to analyze deck and bottom bending stresses in parallel in hopes of throwing some light upon these problems. Appendix A contains the detail of which particular runs were selected for analysis, which channels of data were of importance, and an account of some pre-processing operations which it was of advantage to carry out. Also included in Appendix A are plots of the basic time domain data, the results of a qualitative analysis of these data, and a review of the basic processing which is required to derive encountered wave elevations from the radar altimeter and ship motions data actually measured.

Appendix B is an account of the application of a new (to springing data) method of spectrum analysis to the present problem. The method is called "Maximum Likelihood Method Spectrum Analysis", and is data adaptive in the sense that the spectral window is chosen in an optimum way according to the spectral content of the data itself. The original applications of this approach were toward the detection of very narrow frequency band components buried in noise. It was thought worthwhile to make an exploratory application of these methods to the present data in hopes of refining current ideas about the frequency bandwidth of the springing component of stress, and (possibly) of finding a better method of deriving springing response operators.

In order to obtain some sort of estimate of the sampling variability of the RAO estimates of Reference 1 it was necessary to perform cross spectral analyses of the data subset. Appendix C documents these analyses. Some estimates

of the magnitude of possible bias errors were made, and, once the analyses were in hand a measure of the possible sampling variability of the results of Reference 1 was estimated.

Documentation of the final part of the present analysis is contained in Appendix D. The objective of the analysis of Appendix D was to attempt to discover if the observed springing response data contains any indication of non-linear response of quadratic degree. The approach involved cross-bi-spectral analyses of the wave and stress data according to methods originally developed in the study of ship resistance induced by waves.

FINDINGS

Nothing particularly surprising appeared in the initial examination of the time domain records. Deck bending stresses were consistently asymmetric, bottom bending stresses were not, and the relative magnitudes were different than the nominal location of the ship's neutral axis would imply. Unfortunately, no evidence surfaced in the present analysis which would explain the deck bending asymmetry.

As a method to improve estimates of springing stress spectra the Maximum Likelihood Method of analysis does not appear promising--either technically or economically. The analyses carried out suggest two things of importance. First, half power bandwidths of springing stress spectral peaks may be as low as 0.04 times the springing frequency (0.08 rad/sec or 0.012 Hz for the CORT). Secondly, some evidence exists of low level periodic components of springing stress of the order of 1 kpsi amplitude, such as might be produced by engine or propeller. A similar analysis of zero speed runs, and runs where the ship was in sheltered water might throw some light on the source of this response.

The present work suggests that the effective statistical bandwidth of the analysis of Reference 1 was slightly wide relative to the narrowest band springing response in the data set. However the analysis also suggested that the good level of statistical stability in the estimates of Reference 1 probably out-weighs the potential for bias errors inherent in the bandwidth chosen. The net conclusion was that the choice of analysis parameters in Reference 1, given the fixed sample length, is not likely to have seriously affected the variability of the results.

The present results suggest that a significant part of the variability in the RAO estimates of Reference 1 is due to sampling error. The differences

between the theoretical predictions and the experimental estimates for the peak of the springing RAO for the particular cases shown in Reference 1 appear generally to be less than the scatter which might be expected from run to run under the same nominal ship conditions. It is thus difficult to judge which of the two (theory or experiment) is least wrong on the basis of the evidence to date. In this light many of the theoretical/experimental comparisons of Reference 1 may be considered in "reasonable" agreement.

The results of the present parallel analyses of deck and bottom bending stresses differed significantly only with respect to the absolute magnitude of the RAO estimates. This is apparently a direct result only of the problem with the scale factor previously mentioned. Otherwise, run to run scatter appears much the same. The asymmetry in deck stresses apparently has had little effect upon the results derived in Reference 1.

The main problem which the present analysis suggests is a coherency between wave elevation and stress of about 0.4. For purposes of deriving relationships between stress and encountered wave this is a very low magnitude. Such low coherencies significantly widen the estimated sampling variability, and raise some serious conceptual problems.

There are four more or less standard explanations for low computed coherency between input and output of a system.

1. Extraneous noise is present in the measurements.
2. Analysis bandwidths are chosen so that the fluctuations in the real and imaginary part of the cross spectrum are poorly resolved.
3. The response is due to the measured input <u>as well as</u> other inputs which are not measured.
4. The system relating input and response is not linear.

Pertaining to the first two explanations just cited, only the presence of some higher frequency than expected content in the wave elevations can be cited. Only by comparison of radar and buoy derived wave elevations can the adequacy of the radar system and the meaning of the high frequency content be judged.

The presence of significant propeller excited vibration would be a contributing factor to low coherence. Such vibration is in effect due to an unmeasured input.

Implicit in the statement that coherencies are low is that perfect coherency is unity. In short crested seas* it has been shown that the theoretical coherency for purely linear, noiseless, systems is less than unity. How much less depends in all probability upon how much short cresting is present. This is a possibility which may require an analytical investigation of the range of coherency to be expected in a theoretical noiseless system having perfect instrumentation. Such a result might yield a better standard of comparison for the observed coherencies and indicate what, if anything, is wrong.

The present investigation into the possibility of quadratic nonlinearities in springing response has indicated that they exist. The magnitude of the nonlinearity, however, did not appear sufficient to explain all of the low coherency problem. Because of the spectral distribution of wave elevation in the runs examined, large quadratic response might not have been expected at all. The fact that the contribution is apparently of visible magnitude suggests that relatively much more significant nonlinear response may be expected in the event that waves become more severe than the worst experienced in the 1979 trials.

RECOMMENDATIONS FOR THE PROJECTED 1981 TRIALS

The data used in the present analysis included some of the most severe waves observed in the 1979 season. Nevertheless, the corrections to the radar altimeter data necessary to derive wave elevation were quite minor. Some evidence surfaced that the accelerometer records contained some quite high frequencies. If serious aliasing is present in this channel, a significant error might be injected into derived wave elevations when and if data is ever obtained during a really severe storm. Some re-examination is indicated of the possibility of filtering this, and possibly the radar, with low pass analog filters.

With reference to selection of digitizing rates and analysis parameters for the projected trials, the present work suggests that a somewhat smaller analysis bandwidth might be of advantage. The digitizing rate certainly can be reduced to 5 samples/second, and probably to 3.33, without harm and with the

*"Short cresting" refers to irregularities in wave profile at right angles to the dominant direction of propagation, and is caused conceptually by the superposition of many wave components coming from a broad sector of direction about the dominant one.

advantage of a drastically reduced volume of data. Serious consideration should be given to doubling the sample length from the order of 25 minutes to 45 or 50 when it is reasonable to suspect that ship will continue on course for this length of time. If double length records show evidence of serious non-stationarity they can be considered in two parts. If not, double sample length would allow spectrum analyses with about the same statistical stability and half the bandwidth used in Reference 1. If there is the possibility that analyses of the sort carried out in the present work might eventually be required, it would be helpful to set sample times so that multiples of 4100 or 4200 points are acquired. (For example, at a sampling interval of 0.2 seconds, 14, 28, 42, ... minutes.)

It might be useful to characterize, with the present data acquisition system, the level of springing which occurs under calm wave conditions in both load and ballast ship loadings.

APPENDIX A

SELECTION AND PREPROCESSING OF DATA FOR EXPLORATORY ANALYSES

Introduction

In order to accomplish the exploratory analysis objectives of the present work, it was necessary to select a small number of data runs obtained in the 1979 CORT trials, Reference 1*. Because there was a certain amount of time pressure, it was advantageous to select the data from those runs which were available as a by-product of the work in Reference 2*. The purpose of this Appendix is to document the selection, certain pre-processing operations which were carried out, provide a look at the time domain data for stresses and the radar wave measuring system, and to indicate the basic method of deriving the encountered wave elevations.

Selection of Data Runs

In the work of Reference 2 data tape 4 and a portion of tape 7 produced in Reference 1 were made available. Everything which could be read by the Stevens Institute computer had to be extracted from these tapes in order to get the two runs required for the previous work. The result was that Runs 68 through 77, and Runs 116 through 118 of Reference 1 were immediately available. Since one of the present problems was to assess sampling variability, it was of interest to have available 3 or 4 runs which were obtained one after the other during a period when the nominal ship and wave conditions were constant. It was also thought wise for the sake of continuity to select at least one of the runs which were analyzed in Reference 2.

The log data for the five runs eventually selected for the present work is summarized in Table A-1. It will be noted that Runs 74 through 77 form a sequence where the nominal ship and wave conditions were relatively constant and which contains one of the special runs which was specially treated in both

---

*1. Swanek, R.A., and Kihl, D.P., "Investigation of Springing Responses on the Great Lakes Ore Carrier M/V STEWART J. CORT", Structures Department, David W. Taylor Naval Ship Research and Development Center, CG-D-17-81, December 1980, NTIS No. ADA100293

*2. Dalzell, J.F., "Numerical Simulation of Combined, Springing and Wave Induced Stress Response", Davidson Laboratory Report SIT-DL-81-9-2141, Coast Guard Report CG-M-6-81

TABLE A-1

LOG-DATA FOR THE RUNS SELECTED FOR ANALYSIS

RUN	74	75	77	116	117
Data Tape	4	4	4	7	7
Date	16-Nov-79	16-Nov-79	16-Nov-79	9-Dec-79	9-Dec-79
Time	10:02	10:10	10:26	13:42	15:04
Ship Position:					
Lake	Superior	Superior	Superior	Michigan	Michigan
North Latitude	47° 22'	47° 21'	47° 15'	44° 8'	43° 20'
West Longitude	89° 0'	89° 5'	89° 20'	87° 7'	87° 13'
Ship Draft (Mean, ft.)	20.6	20.6	20.6	27.0	27.0
Load Condition	Ballast	Ballast	Ballast	Full Load	Full Load
Ship Speed (MPH)	14.7	14.4	14.4	13.5	13.5
Heading	256°	256°	256°	189°	188°
Wind Direction	235°	240°	240°	247°	263°
Wind Speed (kt)	29	29	29	18	14
Wave Direction	250°	250°	250°	212°	198°
Estimated Wave Height, ft.	6	6	6	4	3

Reference 1 and 2. Run 76 was omitted from the sequence because the computer clock used in timing the digitization was apparently running at twice the nominal rate--sorting this out was not thought worth the extra effort for the present work. Runs 116 and 117, in addition to being two of the runs specially treated in Reference 1, involve apparently constant full load ship conditions and were thought a reasonable choice to round out the set of five runs for exploratory analysis. A close inspection of Table A-1 discloses that on the 16th of November it was apparently possible to record 25 minutes of data in about 8 minutes. Because the value of the springing frequency computed from the records is as expected, and because the changes in ship position noted are about what might be expected for 25 or 30 minute time intervals, it is suspected that the time of day clock was somehow in error.

The Data Channels of Interest

In order to produce results comparable to those of Reference 1, the main deck midship bending stress data channel is of primary interest. In view of the problems and uncertainties raised about this channel in Reference 2, it was thought prudent to also consider the midship bottom bending stress channel. In effect it was determined to process the deck and bottom bending stresses in parallel. Ideally, a data channel of encountered wave elevation as measured by the Collins radar is also required. However, wave elevation is not measured directly and there are six channels of data which may potentially influence the wave elevation estimates.

The data channels of potential interest which were produced in the work described in Reference 1 are as follows:

Channel No.	Item
1	Main Deck Combined Bending Stress
4	Bottom Bending Stress
7	Pitch
8	Roll
25	Collins Radar Range
26	Collins Vertical Acceleration
27	Collins Horizontal Acceleration
30	Collins Error Signal

The general ideas in processing the data to produce estimates of the encountered wave elevation include use of the roll and pitch data to determine the instantaneous angular orientation of the radar beam so that its vertical component may be derived. In the present data set maximum roll and pitch angles were of the order of ±0.5 degrees. Thus the effort in carrying out the compensation for roll and pitch was unjustified. Similarly, in the absence of significant lateral plane motions the horizontal accelerometer (Channel 27) is of no use. What remains in the derivation of wave elevation is to correct radar range by the vertical motion of the antenna derived from the vertical acceleration data. The purpose of the "Collins Error Signal", Channel 30, is evidently to flag low levels of radar return or malfunction of the Collins Radar. Unfortunately, there appears no documentation of what to expect of this signal in either Reference 1 or 3*.

Pre-processing: Filtering and Decimation

The net effect of the preceding is that it was necessary to consider and process five of the data channels previously mentioned (Numbers 1, 4, 25, 26 and 30). Many of the projected operations involved Fast Fourier Transform operations. In each of the runs of interest the data had been sampled at 0.1 second time intervals for 25 minutes so that the resulting time series were 15000 points in length--too short for a 16K FFT analysis, and too long for a single 8K analysis. It had been found in both References 1 and 2 that the 0.1 second interval is unnecessarily short. For present purposes it was attractive to employ the filtering/decimation scheme developed in Reference 2 as a first processing step.

Accordingly, the following operations were carried out on each of the five data channels of interest for each of the five runs noted in Table A-1:

1. Filter each time series with a recursive 6-pole sine-butterworth low pass digital filter. The characteristics of this filter include:

*3. Hammond, D.L., "Great Lakes Wave Height Radar System", prepared by the Naval Research Laboratory, issued as Coast Guard Report CG-D-6-80, January 1980, NTIS ADA083647

- 0.1% or less attenuation of signal and and sensibly linear phase shift from D.C. to 0.6 Hertz.
- Nominal cutoff frequency 1.4 Hertz.
- 98.5% or more attenuation of signal between 3.33 and 5.0 Hertz.

2. Perform the 1½th point decimation procedure described in Reference 2 on each time series.

The effect of these operations is first to eliminate signal content between 3.33 and 5.0 Hz so as to minimize the possibility of aliasing, and then to create a shorter time series which has a time step of 0.15 seconds rather than 0.1 seconds, and a folding frequency of 3.33 Hz rather than 5.0 Hz. The first 2^{13} points of the resulting series represent 20½ minutes of the original 25 minutes of data; that is, a loss of 18% of the original data was accepted in order to facilitate the projected analyses.

The practical result of this pre-processing step was five new data files. These pre-processed time series data were the starting point in all the subsequent analyses.

The Basic Time Domain Data

When the issue is the discovery of the odd spike or other nonsense in a time history, the human eye is far superior to and more efficient than the computer. Accordingly, the first step in the present analysis was to plot the time series data of interest and look at it. The resulting plots are included here as Figures A-1 through A-5. Each figure is in two parts so that most of the individual oscillations of the 20½ minutes of data are visible. The five data channels mentioned are plotted to the same time scale. Compressive stresses are positive in these figures.

Time histories of the stress channels for Runs 77 and 116 had previously been looked at in Reference 2. Given this preparation, there were no surprises in the stress channels for Runs 74, 75 and 117. There is a positively biased asymmetry in Runs 74 and 75 similar to that previously discovered in Run 77, and a negatively biased asymmetry in Run 117 similar to that previously observed in Run 116. The previously noted apparent scale factor disparity between deck and bottom bending stresses carries over in the new runs.

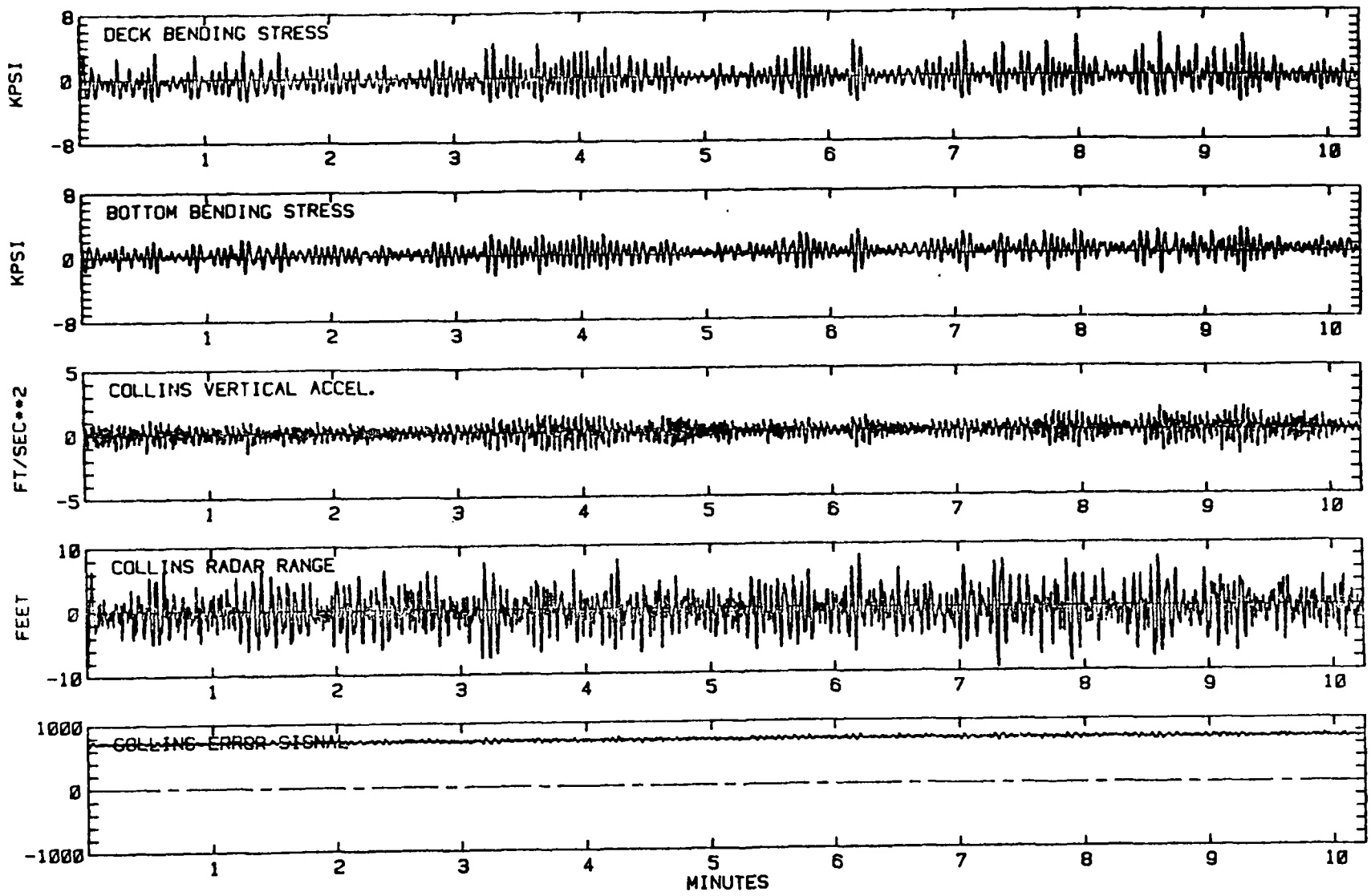

FIGURE A-1a THE TIME DOMAIN DATA OF INTEREST--RUN 74

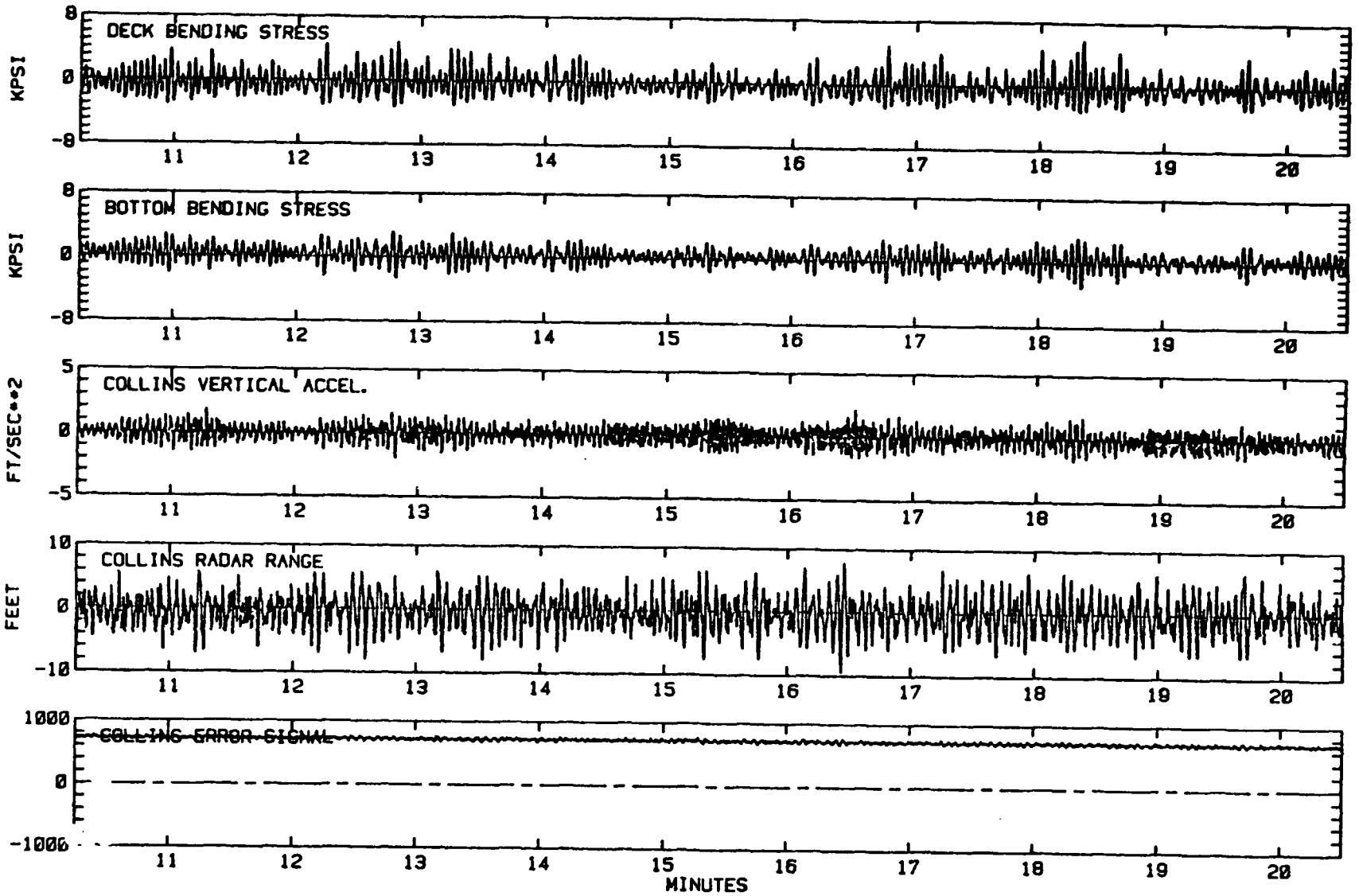

FIGURE A-1b THE TIME DOMAIN DATA OF INTEREST--RUN 74

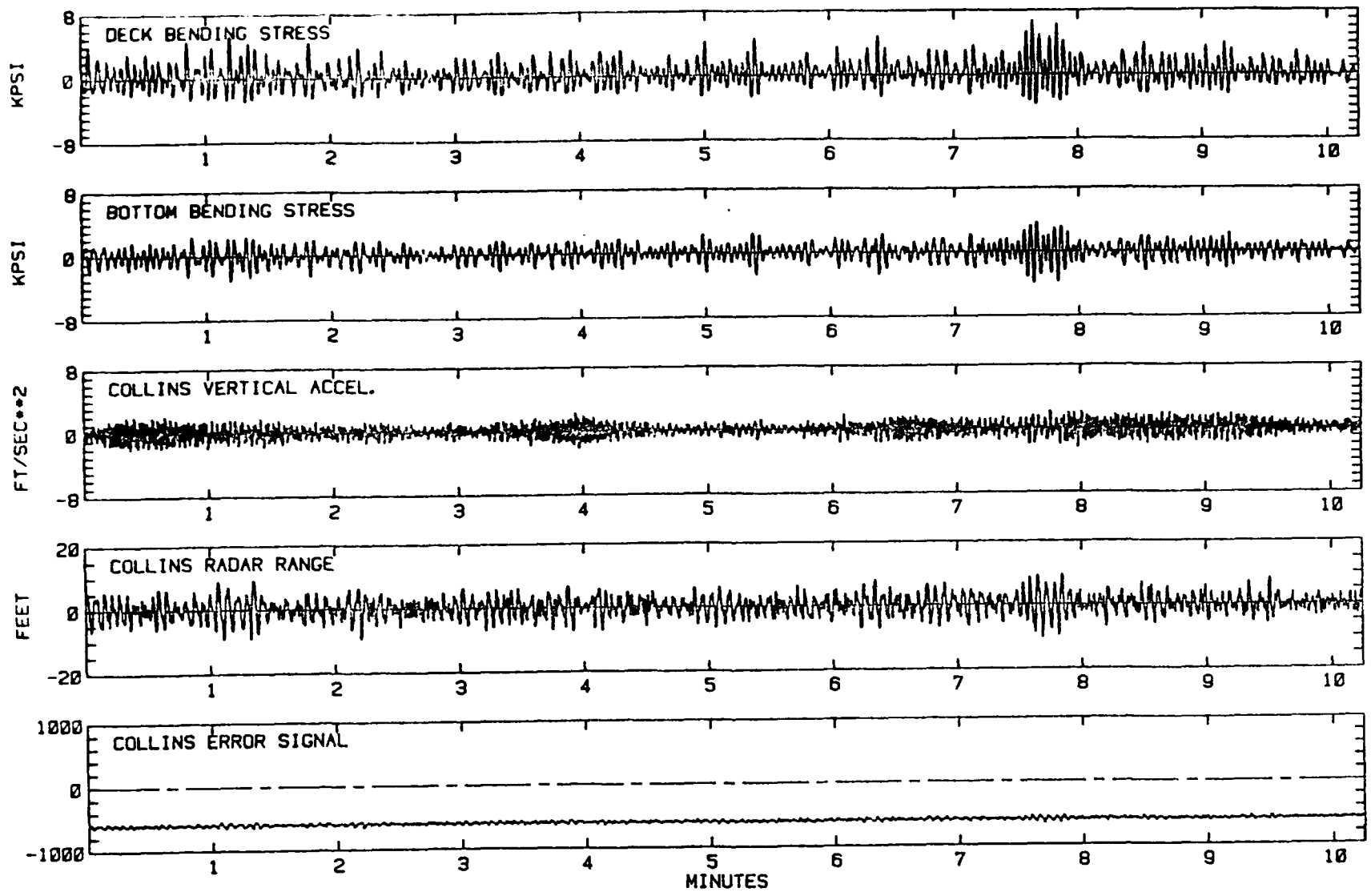

FIGURE A-2a THE TIME DOMAIN DATA OF INTEREST--RUN 75

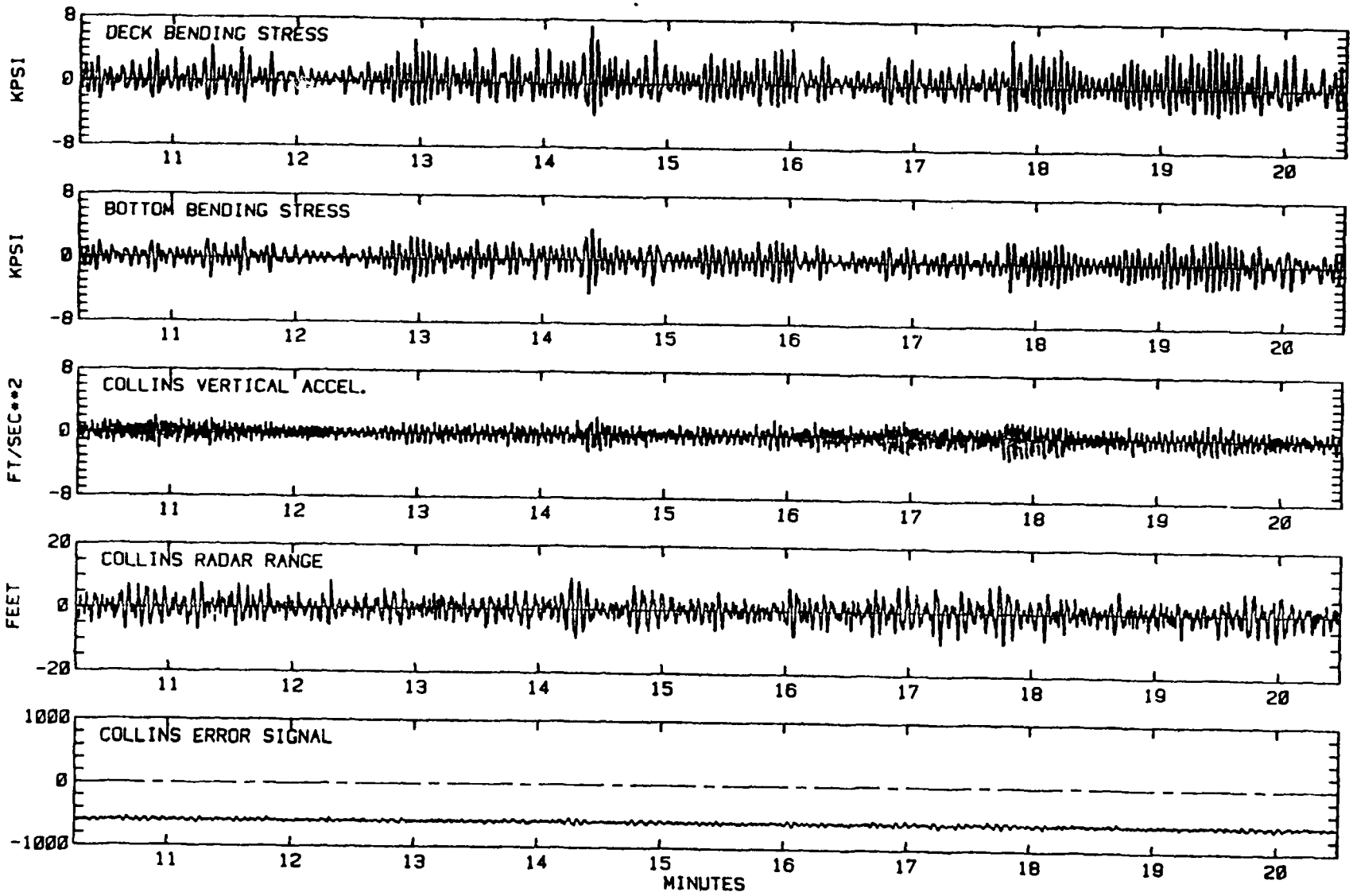

FIGURE A-2b THE TIME DOMAIN DATA OF INTEREST--RUN 75

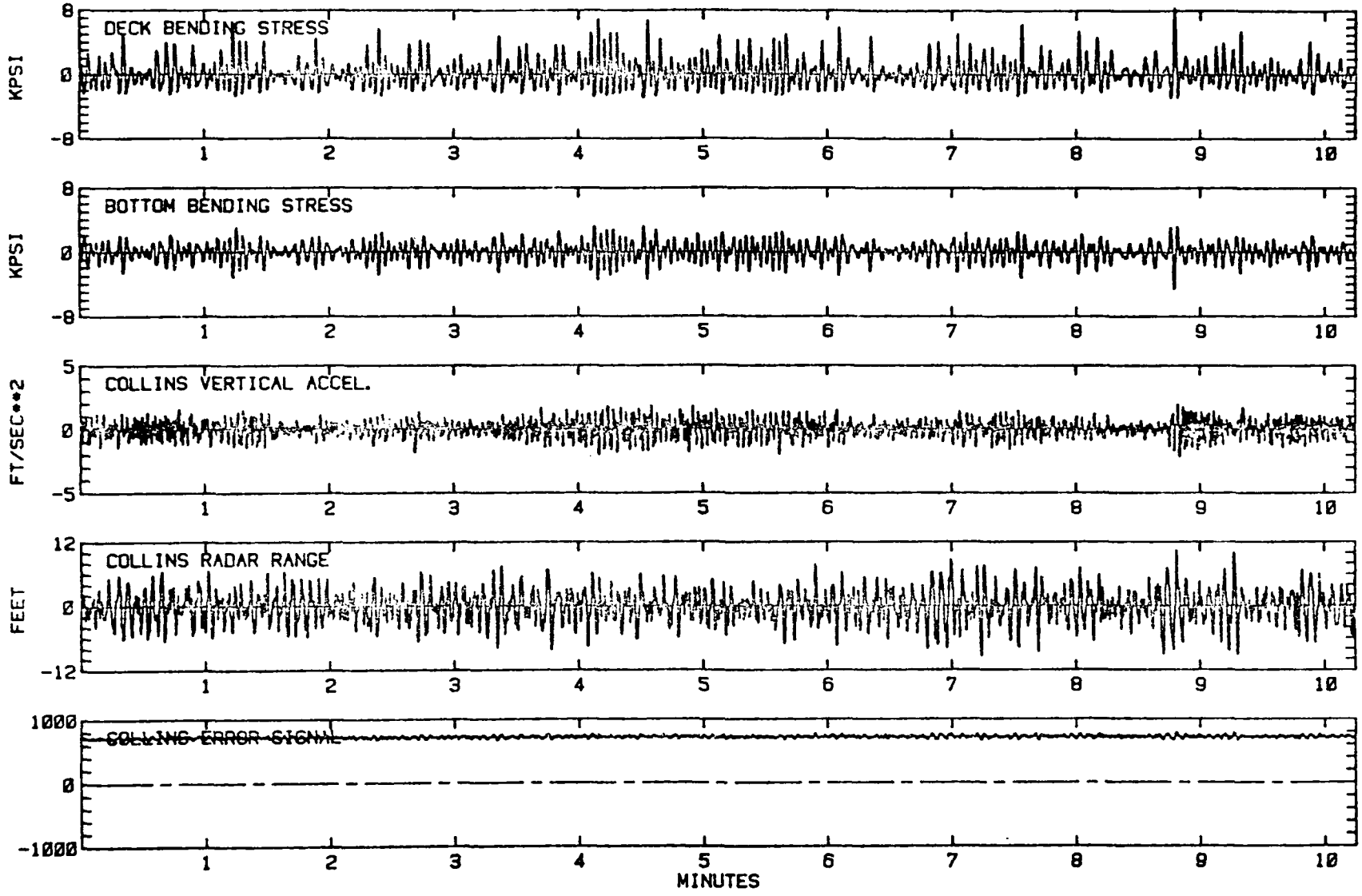

FIGURE A-3a THE TIME DOMAIN DATA OF INTEREST--RUN 77

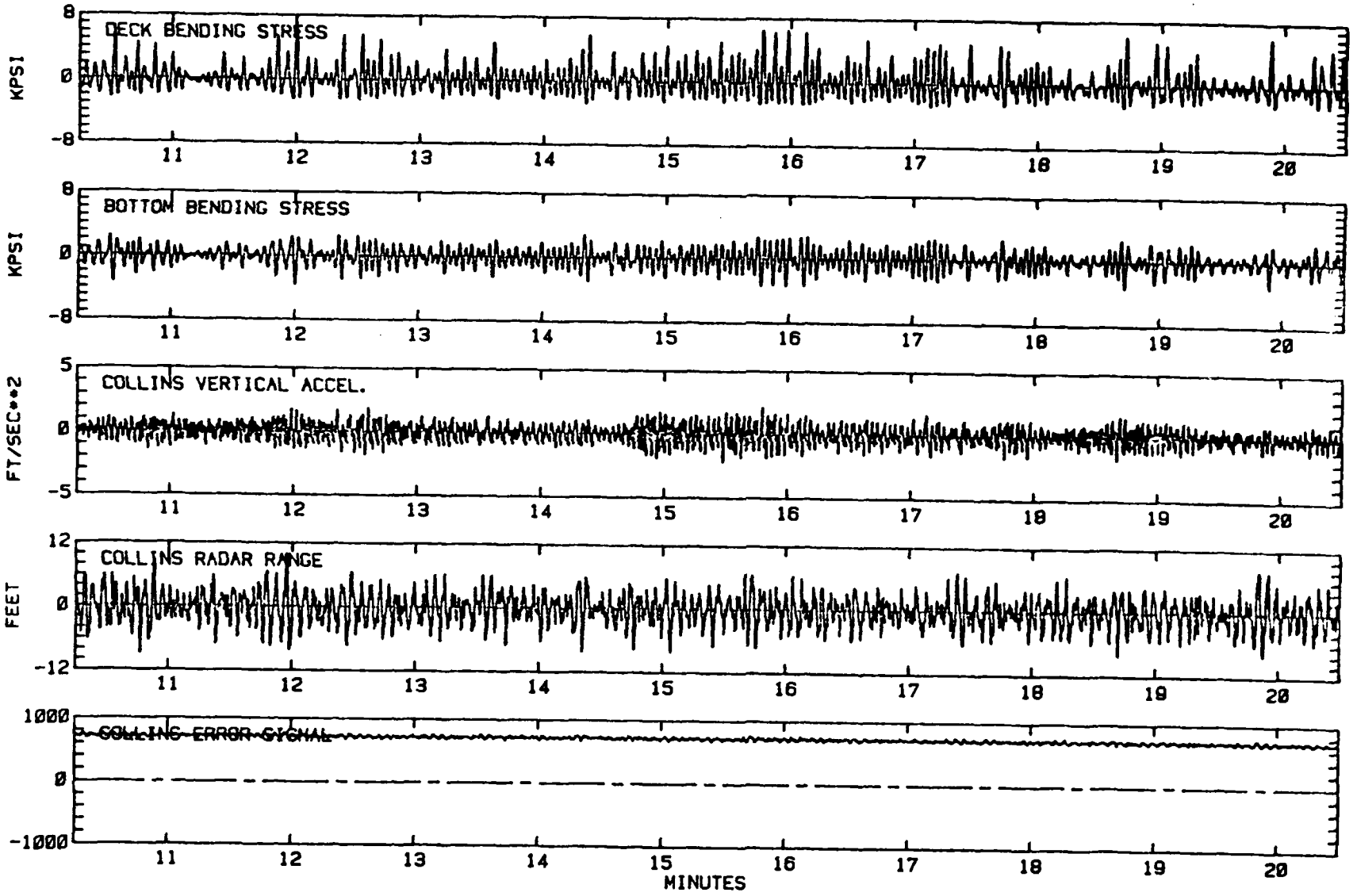

FIGURE A-3b THE TIME DOMAIN DATA OF INTEREST--RUN 77

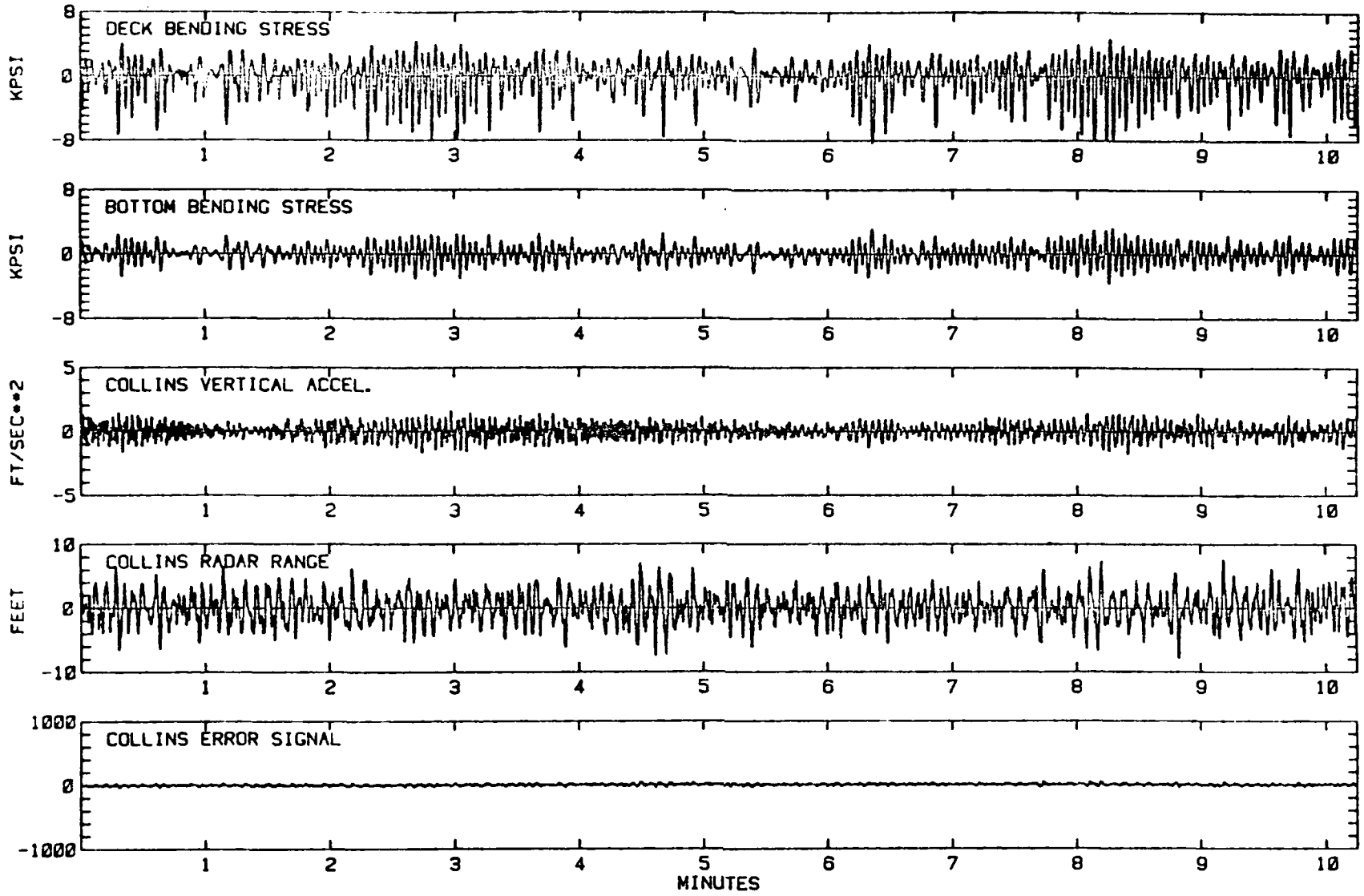

FIGURE A-4a THE TIME DOMAIN DATA OF INTEREST--RUN 116

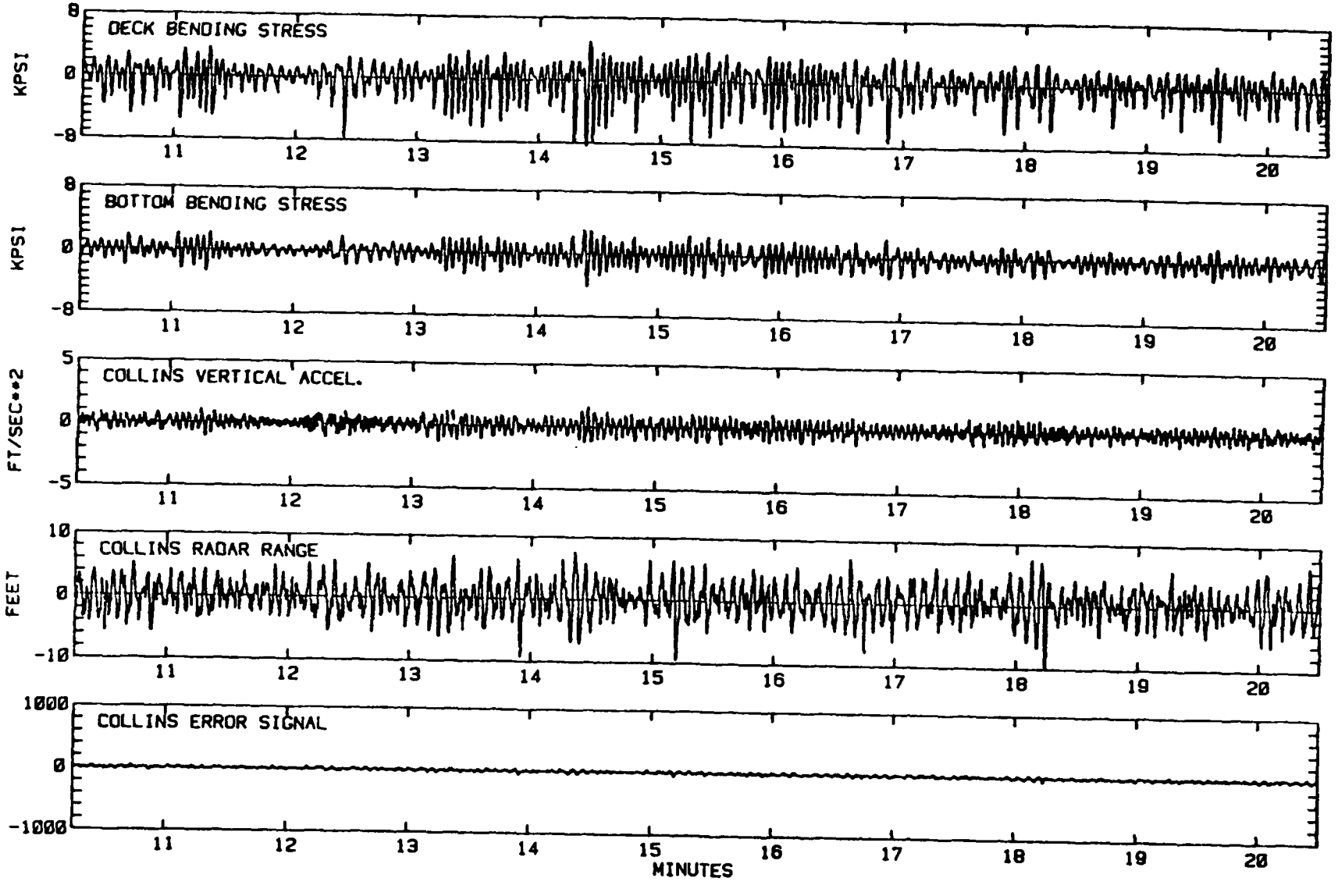

FIGURE A-4b THE TIME DOMAIN DATA OF INTEREST--RUN 116

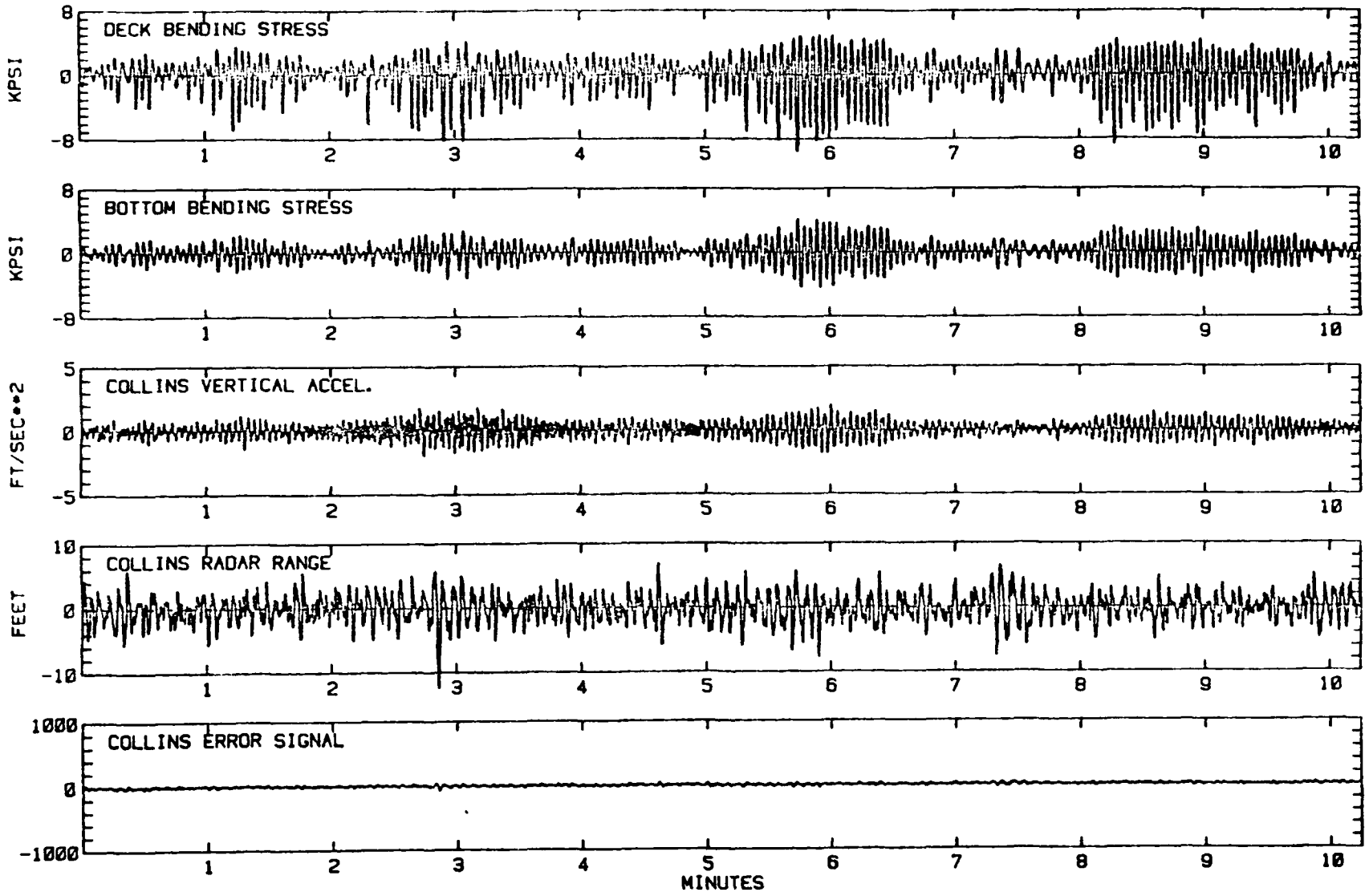

FIGURE A-5a THE TIME DOMAIN DATA OF INTEREST--RUN 117

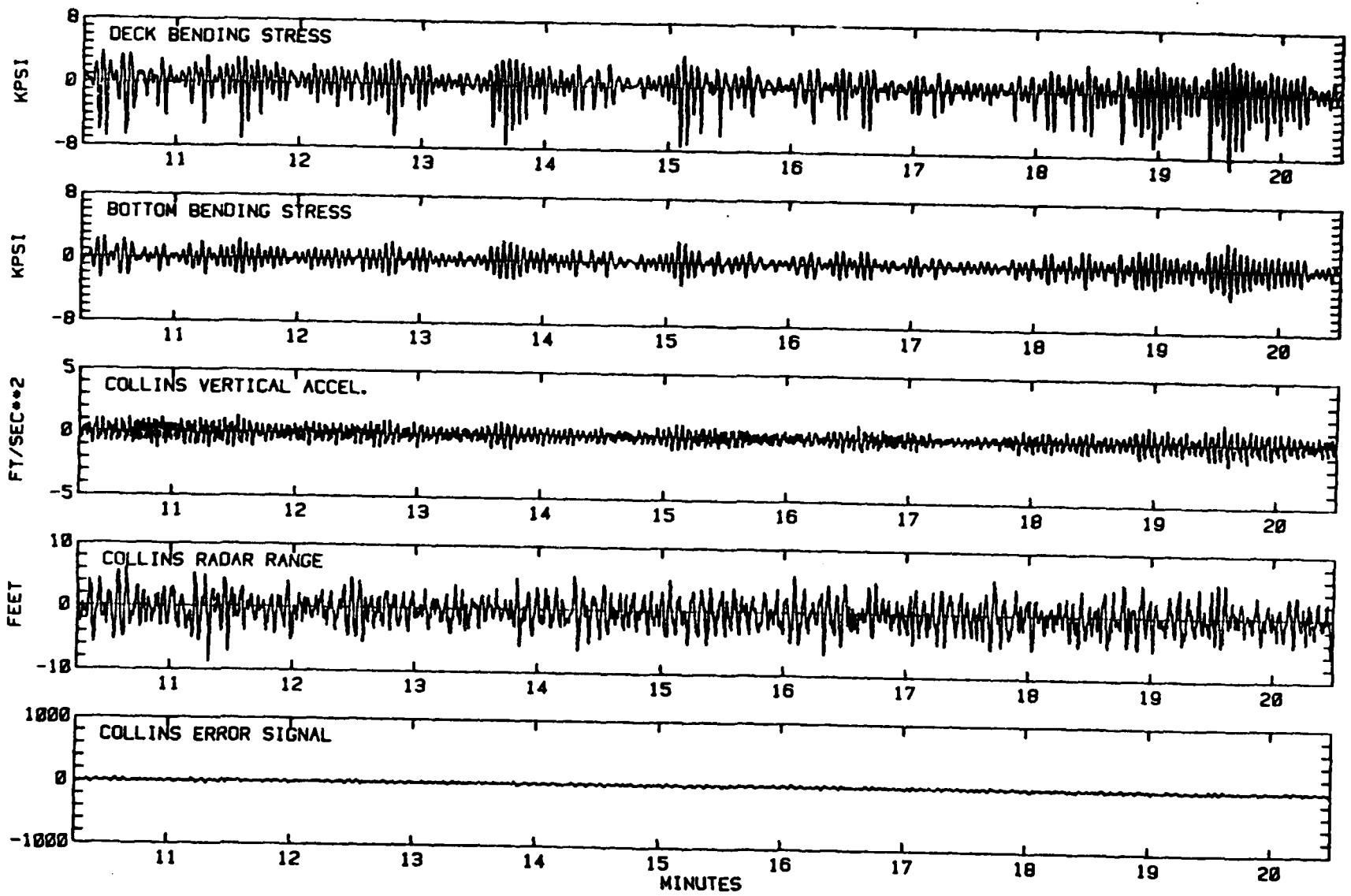

FIGURE A-5b THE TIME DOMAIN DATA OF INTEREST--RUN 117

The Collins Vertical Acceleration time histories clearly have some fairly strong content at a much higher frequency than that of the springing. To see what it might be, portions of the record were plotted to expanded time scales. Figure A-6 is a typical result. The filtered accelerometer clearly contains vibration at 2 or 3 times the springing frequency. It seems reasonable to suppose that this frequency may correspond to vibration of the boom upon which the radar antenna and accelerometer are supported. When plotting the results in Figures A-1 through A-5 it was noticed that the maximum excursions of these filtered accelerations were about half what the computer said the maxima of the original data were. Obviously the present filtering operation eliminated some high frequency noise. Reference 3 implies that the accelerometer natural frequency is about 350 Hz, and mentions no analog filtering. If the actual resonant frequency deviates from 350 Hz by as little as ±1½%, transient vibration of the accelerometer itself may alias to anywhere in the DC to 5 Hz range in which it is assumed that all of the present signal content exists. In the present context it just had to be assumed that no such aliasing effects exist.

Inspection of the Collins Range and Error discloses no obvious nonsense. The error signal is flat and it is reasonable to assume that the radar was working nominally during the runs examined. There is rather more high frequency content in the range signal than the present analyst would have expected, but nothing which appears physically impossible.

Derived Wave Elevations

The geometry for the present radar wave measuring system is simpler than that described in Reference 4* because the vertical acceleration is measured at the radar antenna.

Taking a fixed horizontal reference plane in the water, the vertical position of the radar may be denoted by $Z_a(t)$, positive upward, positive for the antenna above the water. The radar beam is directed downward at a 25° angle to the vertical and the sense conventions of Reference 1 are that positive excursions of signal correspond to increasing range. Denoting the total range

*4. Dalzell, J.F., "Wavemeter Data Reduction Method and Initial Data for the SL-7 Containership", Ship Structure Committee, SSC-278, September 1978, AD-A062391.

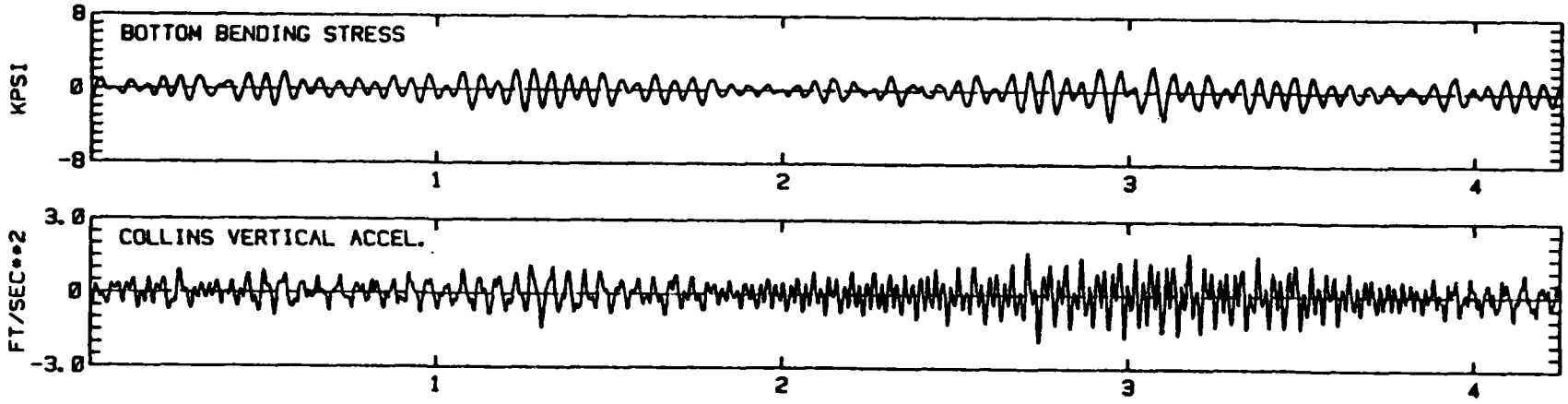

FIGURE A-6 EXPANDED PORTION OF ACCELERATION AND BOTTOM BENDING STRESS TIME HISTORIES--RUN 117

from antenna to water surface as $R_a(t)$, the vertical component becomes $R_a(t) \cos 25^o$. This is because it is permissible in the present case to neglect the time varying angular motion of the radar. Now define the instantaneous position of the water surface above the reference plane as $\zeta(t)$ (positive upward). Then:

$$\zeta(t) = Z_a(t) - R_a(t) \cos 25^o \tag{A-1}$$

In actuality the interest is not in wave elevations above some absolute datum but in the variations about mean water level. Taking the time mean of Equation (A-1):

$$\eta(t) = Z(t) - R(t) \cos 25^o \tag{A-2}$$

where:

$\eta(t) = \zeta(t) - \overline{\zeta}(t)$ = Corrected wave elevation

$Z(t) = Z_a(t) - \overline{Z}_a(t)$ = Dynamic vertical motion of radar antenna

$R(t) = R_a(t) - \overline{R}_a(t)$

The various mean values drop out because

$$\overline{Z}_a(t) = \overline{\zeta}(t) + \overline{R}_a(t) \cos 25^o$$

by the definition of the problem.

Essentially, R(t) in Equation A-2 corresponds closely to the quantity recorded and displayed as "radar range" in Figures A-1 through A-5. It might be noted that the total range will have to be derived somehow should it ever be required to make the corrections for roll and pitch. In practice, R(t) is derived from the recorded data by correcting the signal to zero sample mean.

The quantity Z(t) is the dynamic fluctuation of the vertical position of the antenna. What is available to derive this quantity is the vertical acceleration. Since upward acceleration is considered positive in Reference 1 the quantity Z(t) is the doubly integrated acceleration signal corrected to zero mean:

$$Z(t) = \iint_{-\infty}^{t} A_v(t)dt - (\text{time mean of the integral})$$

The procedure developed in Reference 4 for deriving Z(t) in the time domain are applicable in this case also. In two of the exploratory analyses to be described the wave elevation needs to be defined in the time domain. Accordingly, the procedures of Reference 4 were applied to the present data when this was required. It is instructive to see in the time domain the magnitude of the influence of the correction for antenna motion. Figures A-7 and A-8 show the various derived quantities for selected portions of Runs 77 and 117. The portions selected were chosen so as to include relatively high magnitudes of the Collins Vertical Acceleration signal. The first ("a") part of each figure contains the acceleration signal and the derived double integration. The second ("b") part shows the bottom bending stress, the derived wave elevation and the radar range signal. For comparative purposes the sign of the range was changed. Had the vertical component of range been plotted ($R(t) \cos 25^{\circ}$) it would have been hard to tell the difference between wave elevation and radar range. In general, the largest excursions of Z(t) are out of phase with the range signal, and the net effect of the antenna motion correction is quite small.

Closing Comments

Nothing particularly surprising appeared in the initial examination of the time domain records. It is seen that for the runs of interest the influence of the vertical acceleration of the radar antenna upon the derived wave elevations is small. The ship was evidently not moving much, and under these circumstances the corrections for antenna motion are almost not worth making. This will not be the case when and if data is ever taken in a really severe storm. Against this eventually two things seem worth considering. The first is that when radar range must be corrected for roll and pitch, the entire range is required. Data for computing this range does not appear in the data files. The second is the possibility of aliasing very high frequency vibration of accelerometers back into the principal alias of the digital record. To a lesser extent this worry applies to other channels as well. There is only one way to insure against allasing when the basic recording is all digital and that is to interpose suitable low pass analog filters between the analog signal and the A/D converter.

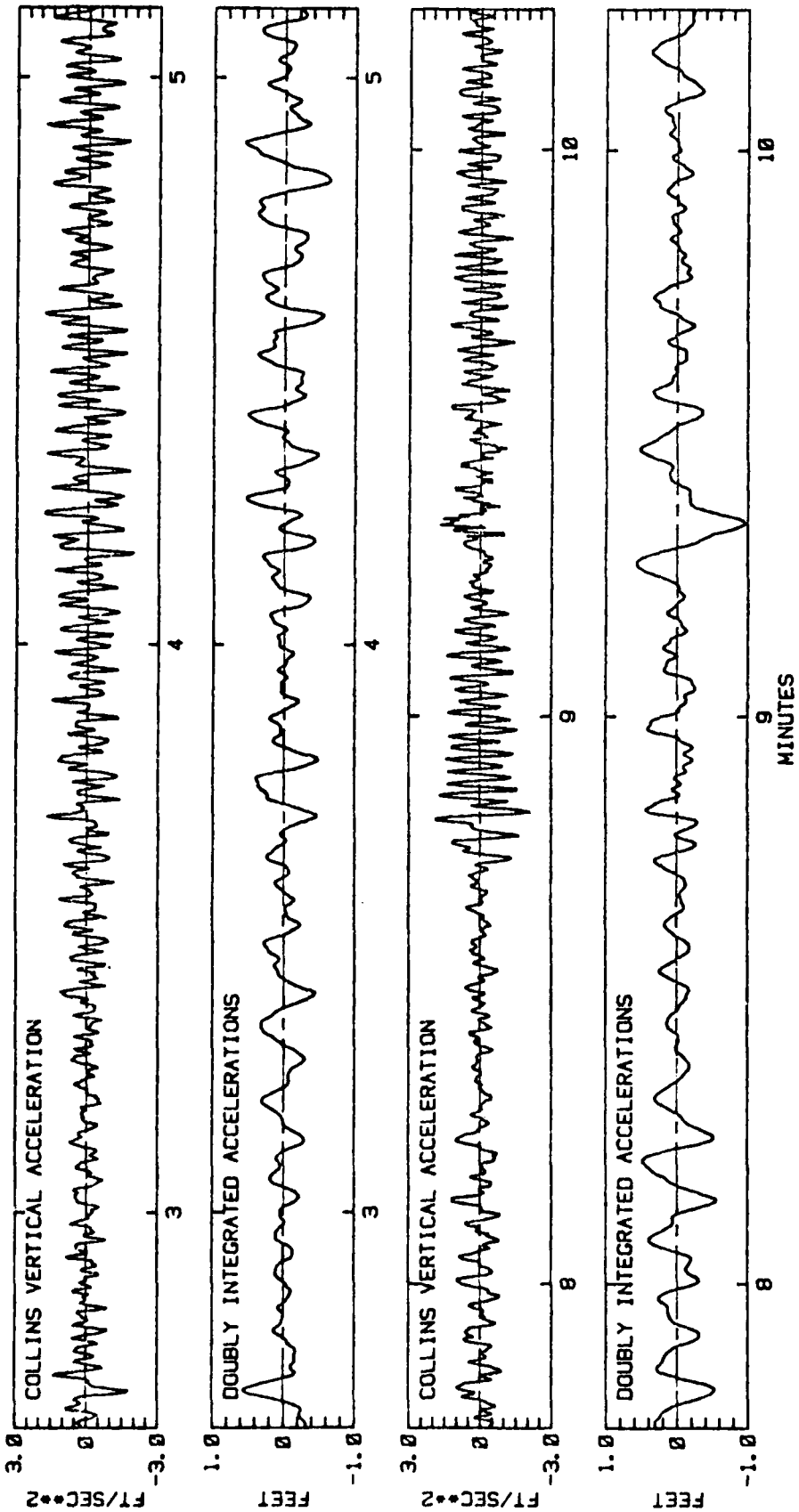

FIGURE A-7a SAMPLES OF COLLINS VERTICAL ACCELERATION AND ITS DOUBLE INTEGRAL--RUN 77

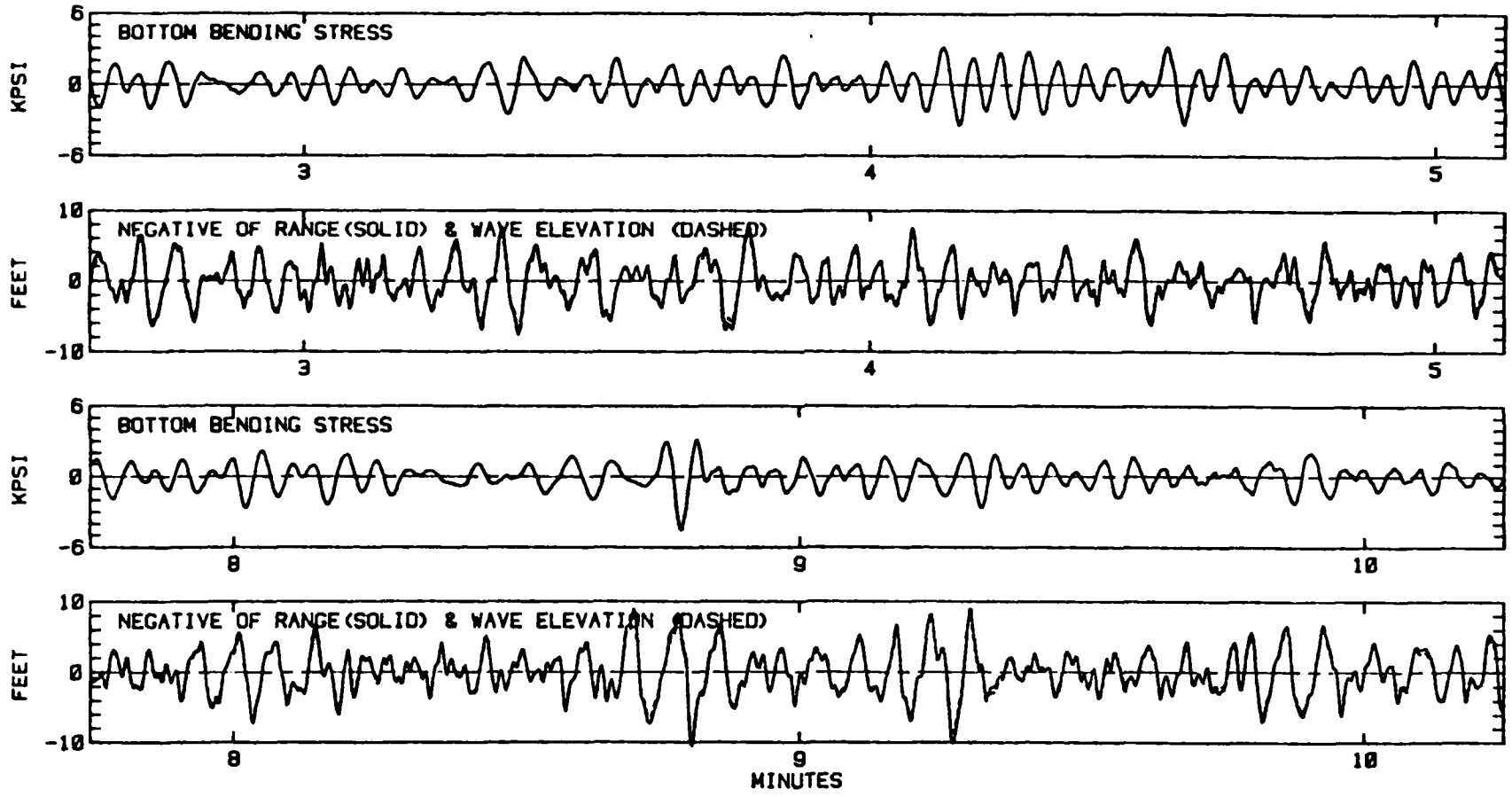

FIGURE A-7b SAMPLES OF RADAR RANGE AND DERIVED WAVE ELEVATION--RUN 77

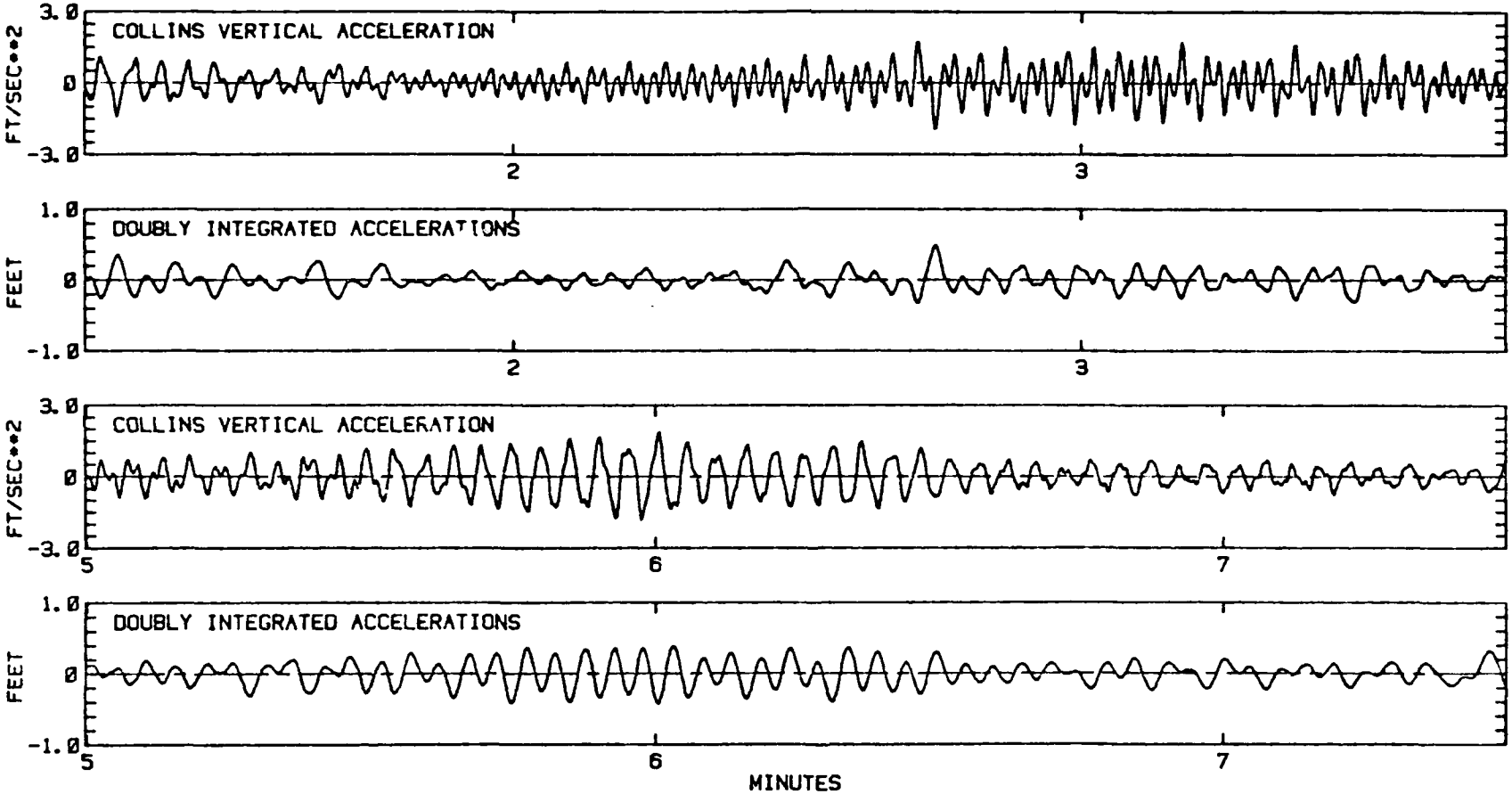

FIGURE A-8a SAMPLES OF COLLINS VERTICAL ACCELERATION AND ITS DOUBLE INTEGRAL--RUN 117

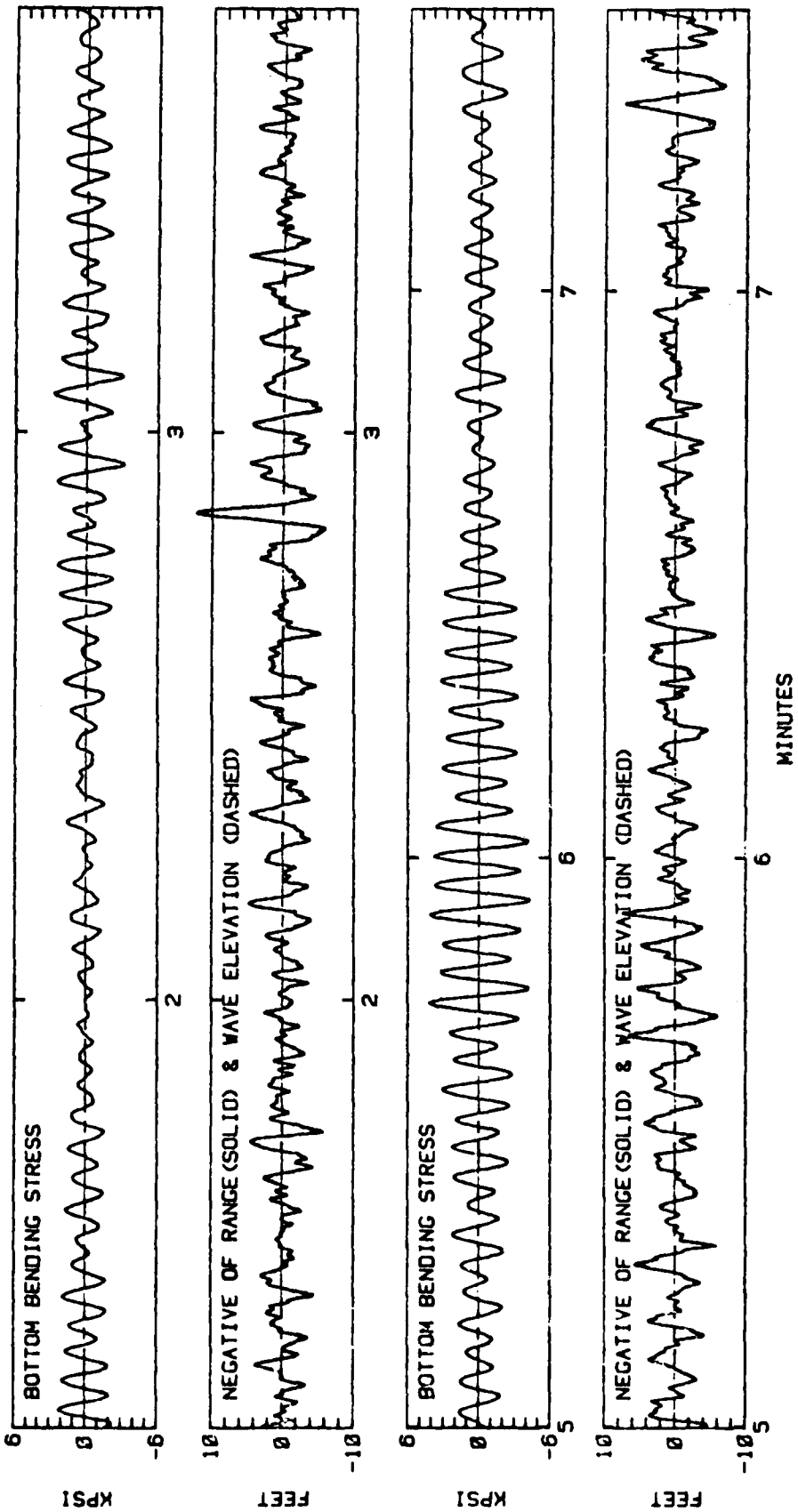

FIGURE A-8b SAMPLES OF RADAR RANGE AND DERIVED WAVE ELEVATION--Run 117

APPENDIX B

MAXIMUM LIKELIHOOD METHOD SPECTRUM ANALYSES

Introduction

One objective of the work of Reference 1 was to derive springing response amplitude operators (RAO's) from the stress and wave elevation data. In the derivation utilized the RAO was estimated as the square root of the ratio of stress and wave elevation spectral densities. Thus one of the basic problems of spectral analysis may be potentially important. The problem is that of possible bias errors in the estimates for very narrow band processes. In general the analysis bandwidth should be small relative to the bandwidth of the spectrum. At the same time the analysis bandwidth should be as wide as possible to increase statistical confidence in the results. Selection of analysis bandwidth is essentially a trade-off problem in conventional analysis methods. "Maximum Likelihood Method" analyses are one of a class of methods largely developed in the geophysical field starting in the mid 1960's, Reference 5*. The method is data adaptive in the sense that the spectral window is chosen in an optimum way to suit the data. Some of the original applications of this approach were to detect very narrow band frequency components buried in random noise. Accordingly, it was thought worthwhile to apply these methods to the present data in hopes of refining current ideas about the bandwidth of the springing component of stress, and (possibly) of finding a better method of deriving RAO's via the spectral ratio technique.

The methods used in the present analyses are based entirely upon the exposition in Reference 5. Initial programming and checkout was performed by Mr. P. F. Wang as an academic project within the Ocean Engineering Department of Stevens Institute.

Autocorrelation Functions

The first step in the maximum likelihood method is to estimate sampled autocorrelation functions from the data. This was done for each of the time

*5. Lacoss, T., "Data Adaptive Spectral Analysis Methods", Geophysics, Vol. 36, No. 4, August 1971, pp. 661.

series using the customary estimator, Reference 6*, pp. 311. An immediate problem was seen when the basic data defined at time steps of 0.15 seconds was used. The 30 seconds of stress autocorrelation functions obtainable by considering lagged products separated by up to 200 time steps obviously defined only a part of the function since the general tendency was for the function to decay very slowly with time. Because the stress records were free enough of high frequency content that a reduction in folding frequency to 0.66 Hz (4.2 rad/sec) appeared safe, new time series were made by considering every 5th point. The result was time series "sampled" at 0.75 second intervals and 1637 "points" long. Normalized autocorrelation functions were computed using these time series, and the results for each channel are shown in Figures B-1 through B-5. It should be noted that the "wave elevation" time series was derived as described in the last part of Appendix A. The computation was carried out to 200 "lags" or 150 seconds. Carrying out computations of this sort over lags much in excess of 10% of the record length is not generally recommended. Thus the results shown in Figures B-1 through B-5 are about as much of the stress autocorrelation functions as it was thought prudent to estimate.

The fact that the functions for Runs 116 and 117 appear to settle into a fairly steady oscillation at about the springing period flags a potentially serious problem. When an autocorrelation function does this sort of thing it implies that there is a periodic component in the data.* The autocorrelation of a cosine wave of frequency ω and amplitude a is $(\frac{1}{2}a^2 \cos \omega\tau)$. Applying this formula to the five cases shown in Figures B-1 through B-5, using rough estimates of the amplitude of the autocorrelation function for large time lag and the computed sample variances, results in the following estimates for the amplitude of the possible periodic springing component.

Runs	Amplitude
74 through 77	≈0.5 kpsi
116 and 117	≈1.3 kpsi

It should be remarked that "periodic" is defined relative to the available length of record and that no truly periodic response can exist. The evidence simply indicates that there may exist somehow an extremely narrow band vibration excitation which cannot be characterized within the available record length.

*6. Bendat, J.S. and Piersol, A.G., "Random Data: Analysis and Measurement Procedures", John Wiley & Sons, Inc., 1971.

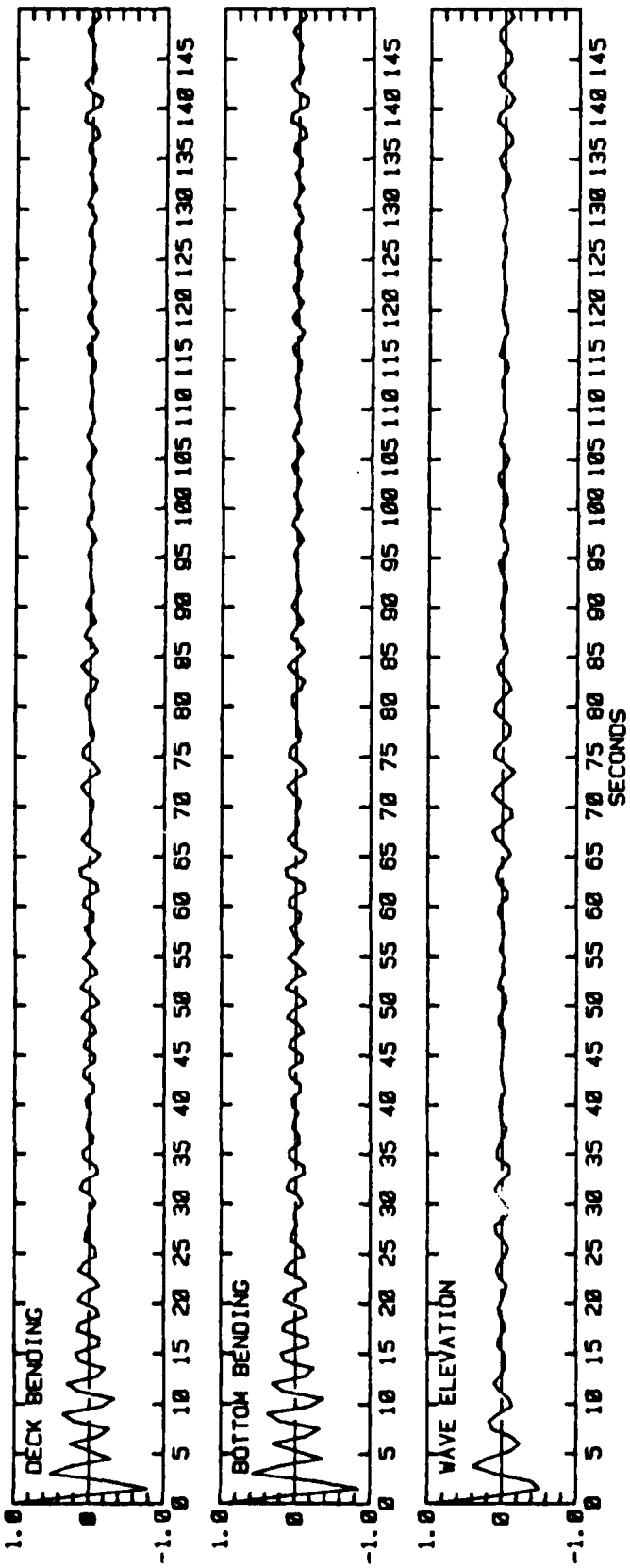

FIGURE B-1 NORMALIZED AUTOCORRELATION FUNCTIONS--RUN 74

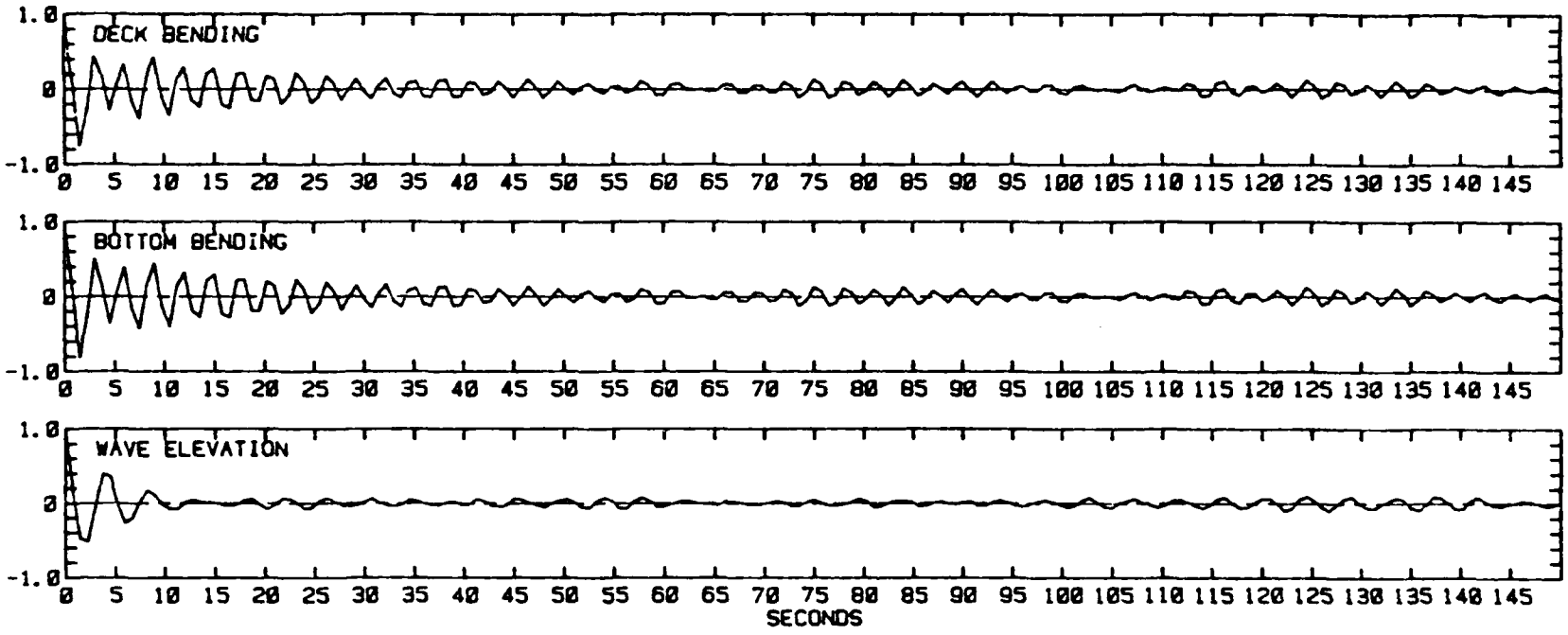

FIGURE B-2 NORMALIZED AUTOCORRELATION FUNCTION--RUN 75

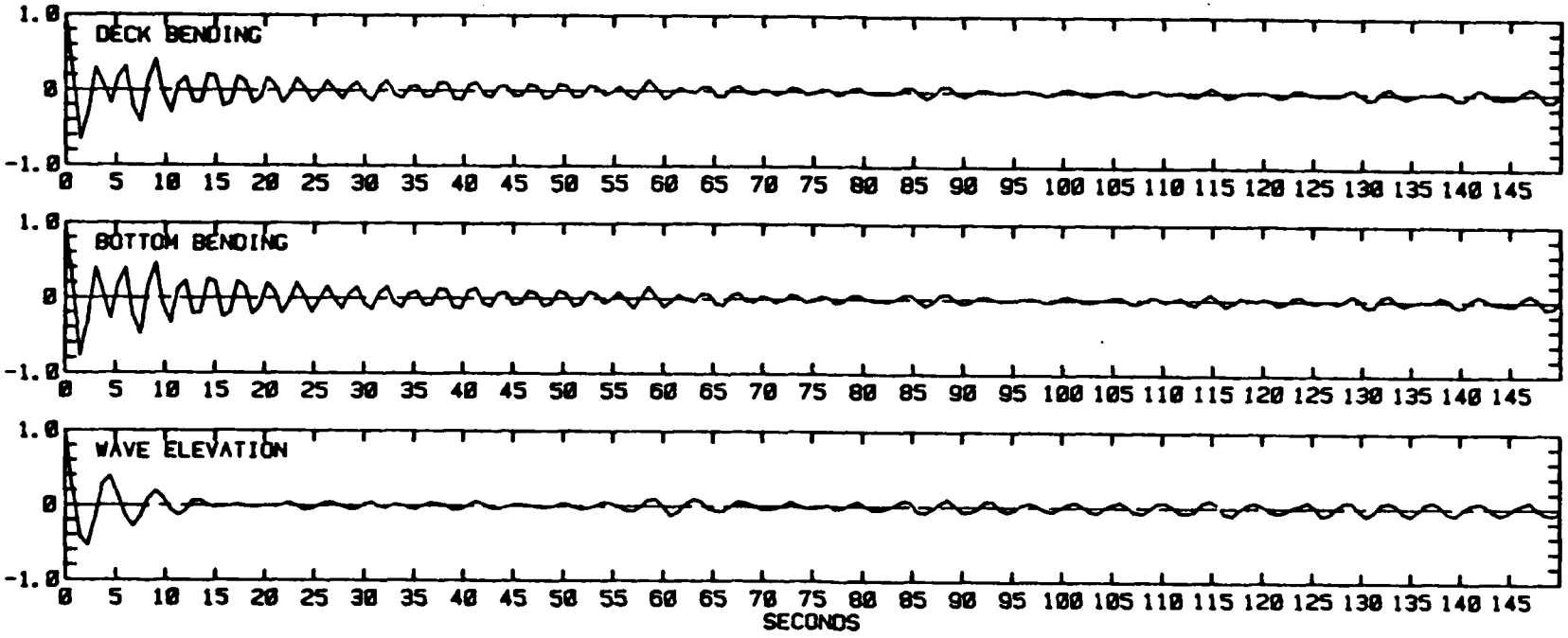

FIGURE B-3 NORMALIZED AUTOCORRELATION FUNCTIONS--RUN 77

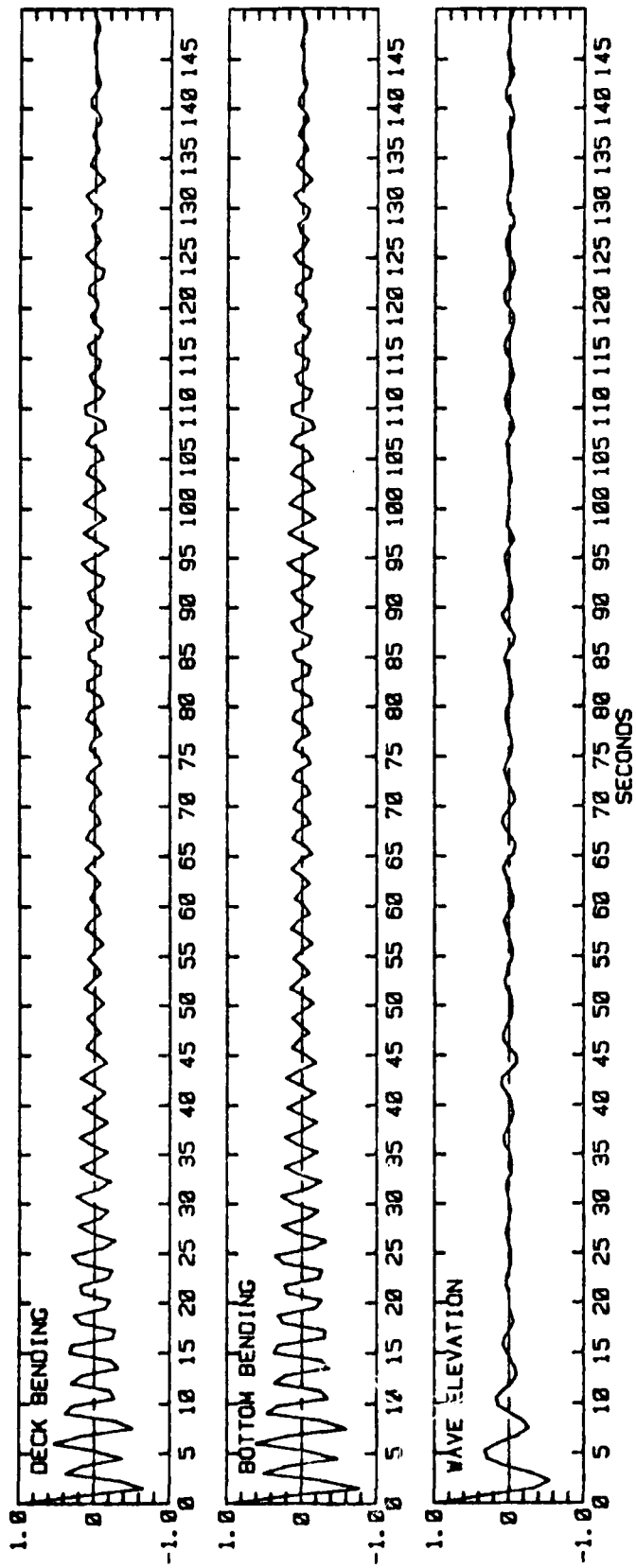

FIGURE B-4 NORMALIZED AUTOCORRELATION FUNCTIONS--RUN 116

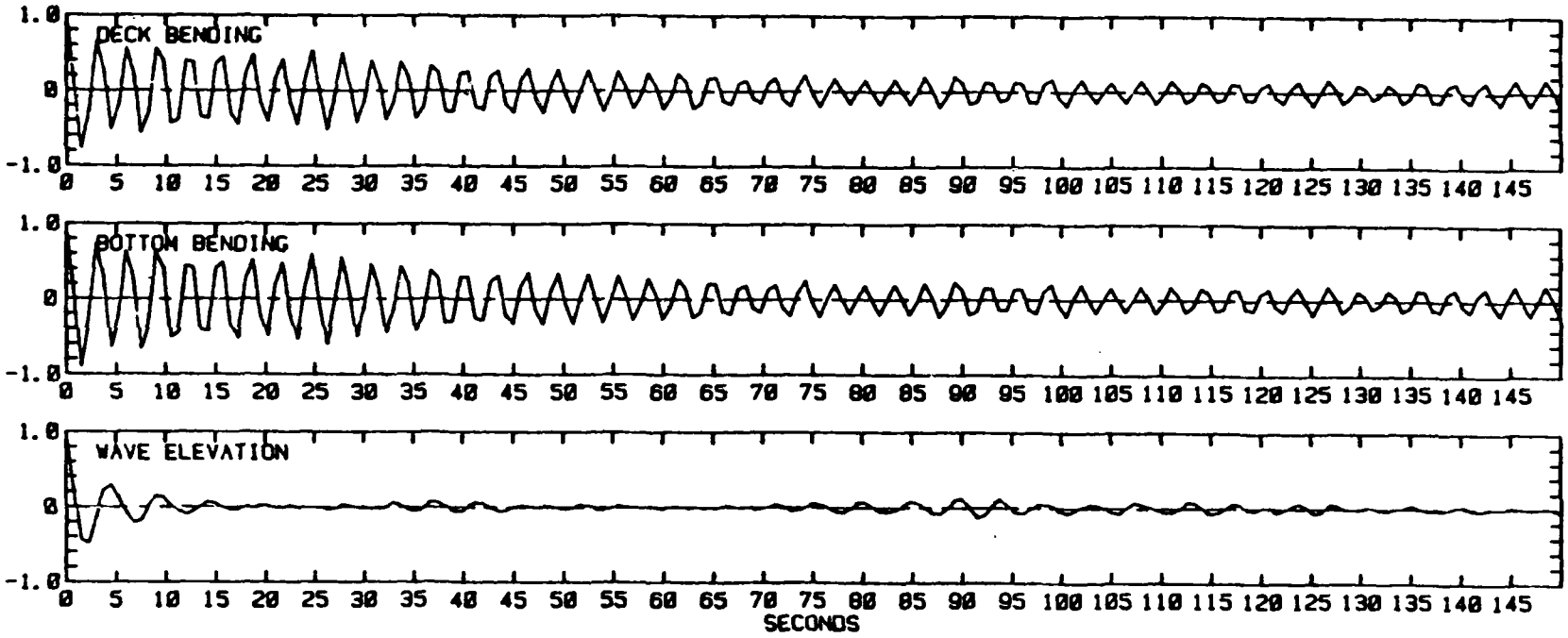

FIGURE B-5 NORMALIZED AUTOCORRELATION FUNCTIONS--RUN 117

MLM Spectral Esimtates

In the maximum likelihood method (MLM) the spectral estimate is of the form:

$$S(\omega) = \frac{1}{g_o + \sum_{n=1}^{m} 2g_n \cos(n\omega\Delta t)} \qquad \text{(B-1)}$$

where: m = the number of lags of autocorrelation function used

g_n = a series of coefficients derived from the autocorrelation function.

Once the "g" coefficients are estimated Equation (B-1) may be evaluated at whatever values of ω are required. Figures B-6 through B-10 indicate the MLM spectral density estimates obtained for the 5 runs using 100, 150 and 200 lags (half, 3/4 and all the autocorrelation functions shown in Figures B-1 through B-5).

In general, the more lags used, the more apparent detail of the spectrum is resolved. One of the attractions of MLM estimates according to Reference 5 is that highly resolved spectra may be estimated from very short samples of autocorrelation function. Indeed, this was found to be so when the present programs were checked out with simulated springing stress records as produced by the methods of Reference 2. Real data, apparently, is another matter. (Most of the assertions of Reference 5 are based on simulated data.)

In the figures, the apparent peak of the springing spectral density marches upward as the number of lags is increased. This is what might be expected from conventional methods if there is a periodic component in the data. It appears that most of the detail is resolved very little differently by 150 and 200 lag analyses. On this, largely intuitive, basis very little difference in the answer might be expected were the number of lags increased moderately. It was decided not to press the MLM analysis any further lest errors in estimating the autocorrelation function for too many lags increase the confusion.

Relative to the second objective of this exercise (finding a better method) the results just shown were quite disappointing. The main attraction of MLM estimates is that the analyst is not supposed to worry too much about resolution. The results show that judgement is still necessary.

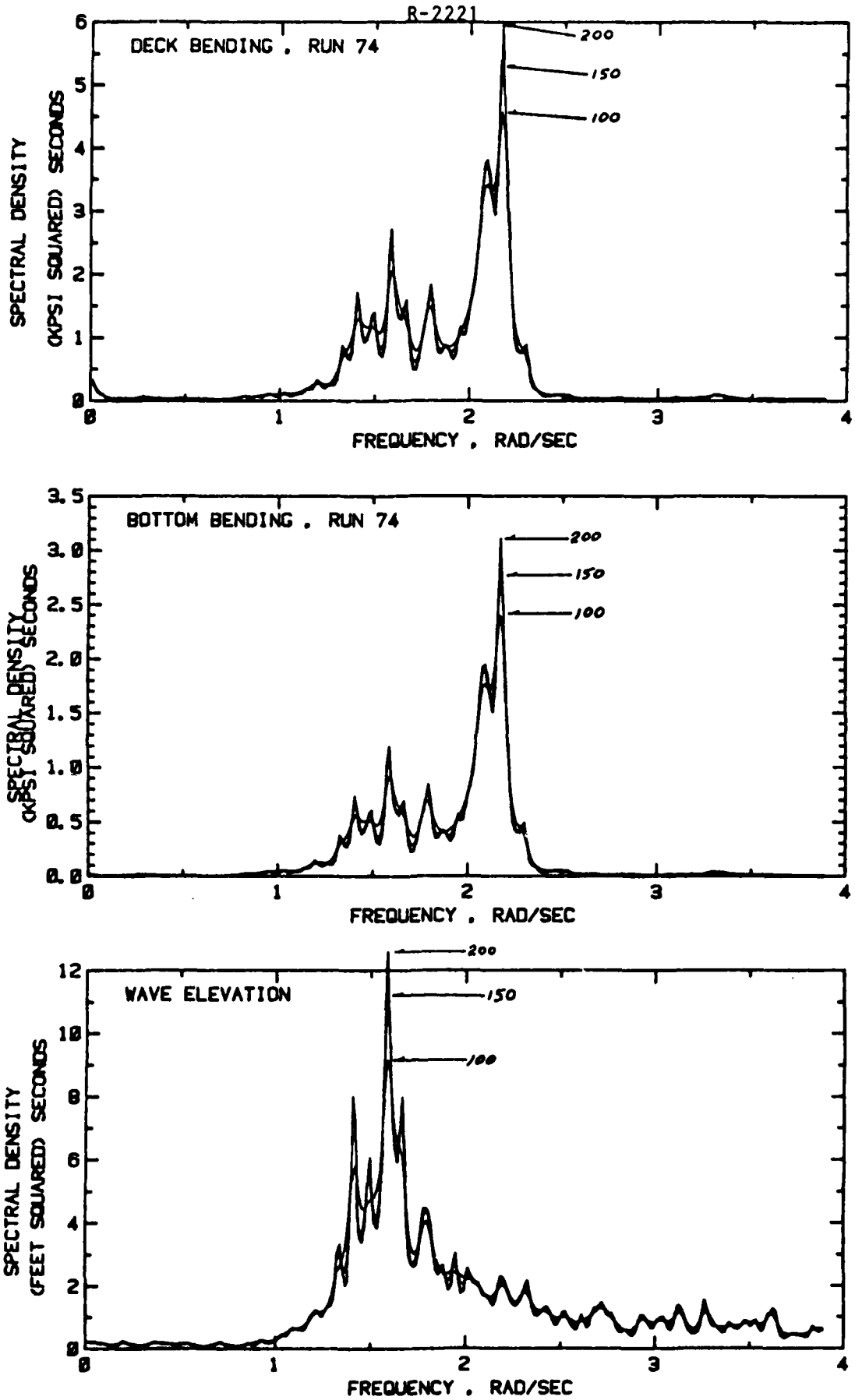

FIGURE B-6 MLM SPECTRAL ESTIMATES FOR 100, 150 AND 200 LAGS--RUN 74

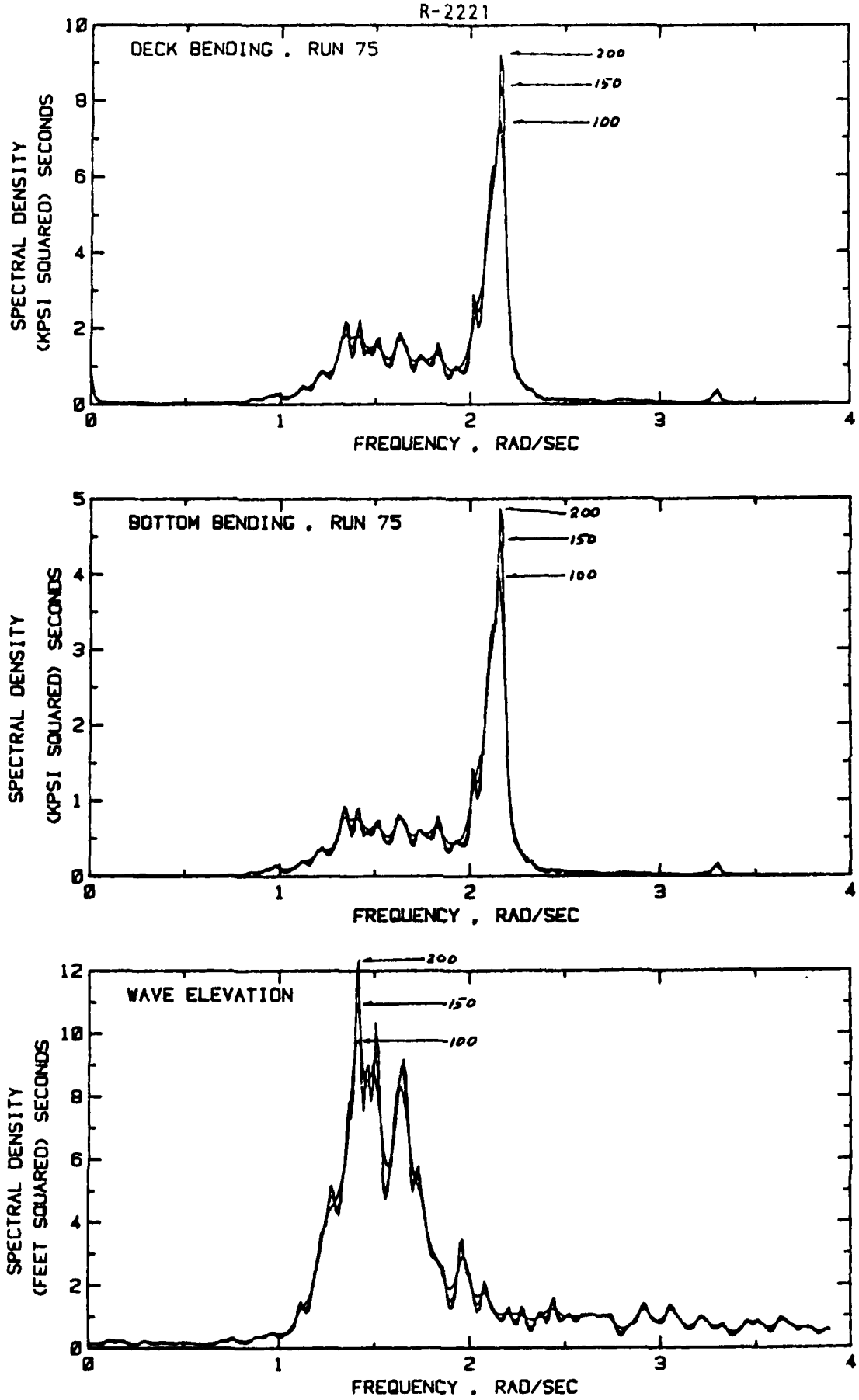

FIGURE B-7 MLM SPECTRAL ESTIMATES FOR 100, 150 AND 200 LAGS--RUN 75

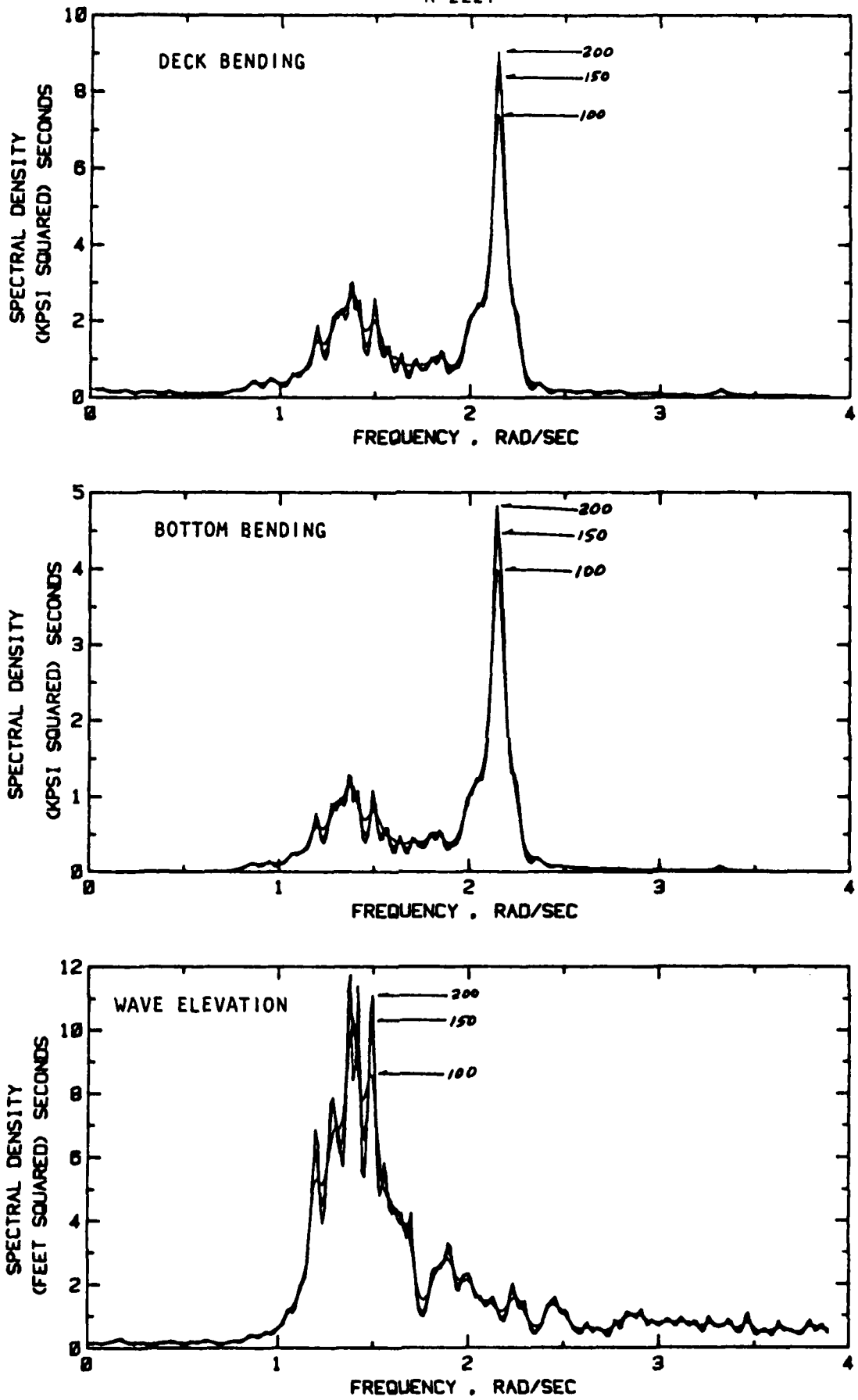

FIGURE B-8 MLM SPECTRAL ESTIMATES FOR 100, 150 AND 200 LAGS--RUN 77

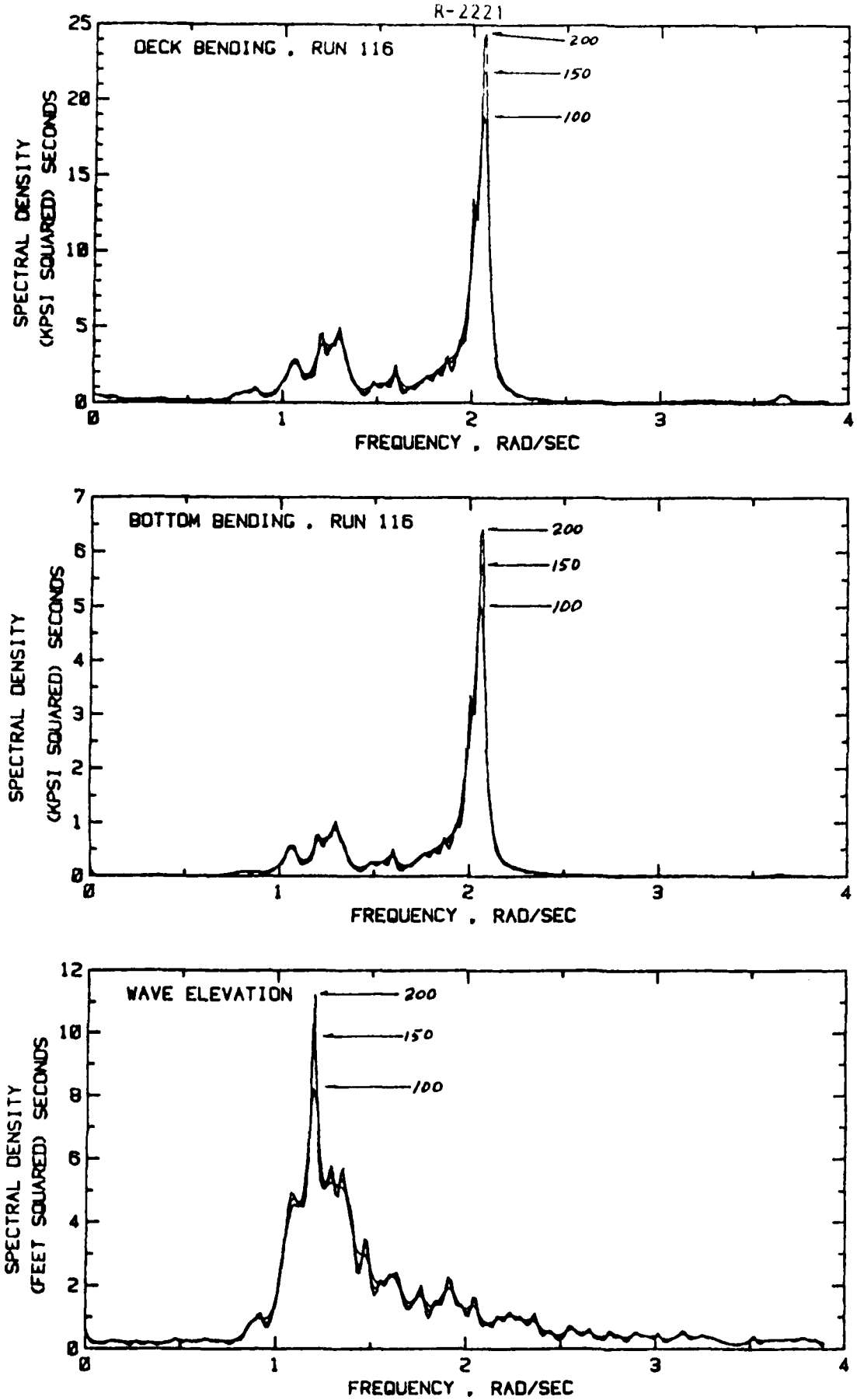

FIGURE B-9 MLM SPECTRAL ESTIMATES FOR 100, 150 AND 200 LAGS-- RUN 116

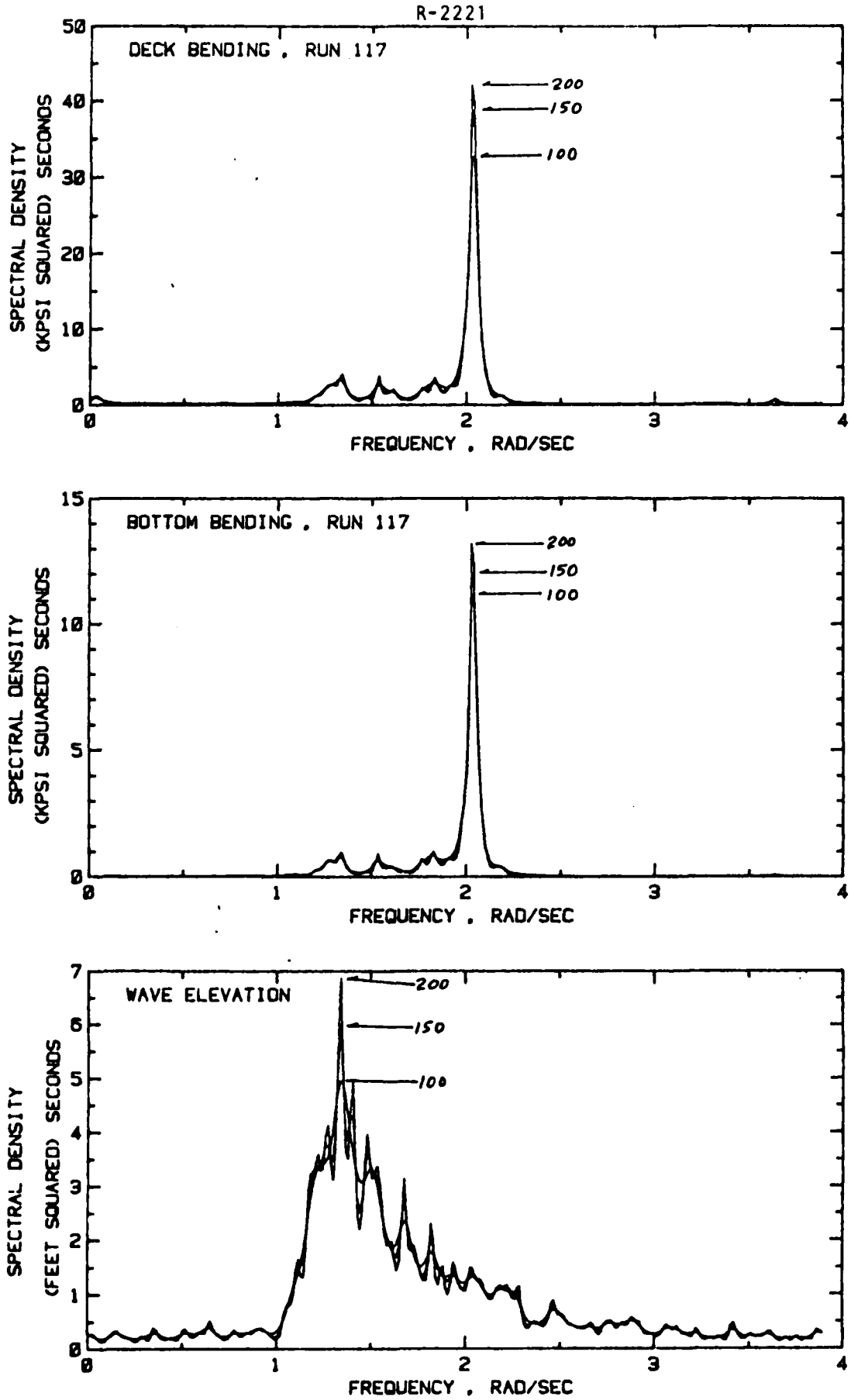

FIGURE B-10 MLM SPECTRAL ESTIMATES FOR 100, 150 AND 200 LAGS--RUN 117

It appears that autocorrelation functions for as many as 200 lags would be required to handle springing data. The main computation problem in a 200 lag MLM analysis is the inversion of a special 201 x 201 matrix. Through this is done indirectly with only 6 x 201 memory locations, the net results of a 200 lag specification is more computing time and cost than the familiar FFT based methods.

It may be noted from Figures B-6 through B-10 that the half power bandwidth of the springing peak is not seriously altered by differences in the number of lags used in the analysis. Measuring from the charts, the half power bands of deck and bottom bending stresses are about the same, and the values range from 0.08 to 0.15 rad/sec (0.012 to 0.023 Hz), or between 0.04 and 0.07 times the springing frequency. These values are consistent with results of previous conventional spectral analyses of springing (reference 2), but the lower figure is less than the minimum quoted in Reference 2.

Closing Comments

As a method to improve estimates of springing stress spectra the Maximum Likelihood Method of analysis does not appear promising--either technically or economically. The analyses carried out suggest two things of possible importance. First, half power bandwidths of springing stress spectral peaks may be as low as 0.04 times the springing frequency (0.08 rad/sec or 0.012 Hz for the CORT). Secondly, some evidence exists of low level "periodic" components of springing stress of the order of 1 kpsi amplitude, such as might conceivably be produced by engine or propeller.

APPENDIX C

CROSS SPECTRAL ANALYSES

Introduction

Because one of the objectives of the present work was to analyze the statistical variability of the response estimates of Reference 1, it was necessary to do some trial cross-spectral analyses of the five run data set so as to provide estimates of the coherency between the measured wave and the stresses.

Analytical Form of the Analysis

What is required of the analysis is to estimate gain (which is another estimate of RAO), phase and coherency between wave elevation and stresses, in addition to the spectral ratio estimate of RAO. To fix notation:

$$\text{RAO} = \{S_{ss}(\omega)/S_{\eta\eta}(\omega)\}^{\frac{1}{2}} \tag{C-1}$$

$$\text{GAIN} = |S_{\eta s}(\omega)|/S_{\eta\eta}(\omega) \tag{C-2}$$

$$\text{PHASE} = \tan^{-1}\{Q_{\eta s}(\omega)/C_{\eta s}(\omega)\} \tag{C-3}$$

$$\text{COHERENCY} = |S_{\eta s}(\omega)|^2/\{S_{\eta\eta}(\omega)\ S_{ss}(\omega)\} \tag{C-4}$$

where:

$S_{ss}(\omega)$ = stress spectrum

$S_{\eta\eta}(\omega)$ = wave elevation spectrum

$S_{\eta s}(\omega)$ = wave-stress cross spectrum
= $C_{\eta s}(\omega) + i\ Q_{\eta s}(\omega)$
= (co-spectrum) + i (quad-spectrum)

As noted in Appendix A, the wave elevation is not available directly. For present purposes it was convenient to do the corrections to radar range in the frequency domain. From Equation A-2, Appendix A, the wave elevations, n(t), is:

$$n(t) = Z(t) - R(t) \cos 25^{\circ} \tag{C-5}$$

with $Z(t)$ = motion of radar antenna
$R(t)$ = fluctuation of radar range about the mean

Let:

$$r(t) = R(t) \cos 25^{o}$$

The autocorrelation function of wave is then:

$$\rho_{\eta\eta}(\tau) = \langle [Z(t) - r(t)][Z(t + \tau) - r(t + \tau)] \rangle$$
$$= \rho_{zz}(\tau) + \rho_{rr}(\tau) - \rho_{rz}(\tau) - \rho_{zr}(\tau)$$

Accordingly the spectrum of wave elevation becomes:

$$S_{\eta\eta}(\omega) = S_{rr}(\omega) + S_{zz}(\omega) - 2C_{zr}(\omega) \qquad \text{(C-6)}$$

where:

$S_{rr}(\omega)$ = spectrum of $r(t)$

$S_{zz}(\omega)$ = spectrum of $Z(t)$

$C_{zr}(\omega)$ = co-spectrum of $Z(t)$ and $r(t)$

Doing the double integration of acceleration in the frequency domain the wave spectrum becomes:

$$S_{\eta\eta}(\omega) = S_{rr}(\omega) + \frac{1}{\omega^4} \cdot S_{aa}(\omega) + \frac{2}{\omega^2} \cdot C_{ar}(\omega) \qquad \text{(C-7)}$$

where:

$S_{aa}(\omega)$ = spectrum of acceleration

$C_{ar}(\omega)$ = co-spectrum of acceleration and $r(t)$

Equation C-7 provides a form in which the available data can be used directly.

Turning to the cross spectrum between wave and stress, the cross correlation function becomes:

$$\rho_{\eta s}(\tau) = \langle [Z(t) - r(t)] S(t + \tau) \rangle$$
$$= \rho_{zs} - \rho_{rs}$$

Then the wave-stress cross spectrum is:

$$S_{\eta s}(\omega) = S_{zs}(\omega) - S_{rs}(\omega) \qquad \text{(C-8)}$$

and doing the double integration in the frequency domain:

$$S_{\eta s}(\omega) = -\frac{1}{\omega^2} S_{as}(\omega) - S_{rs}(\omega) \tag{C-9}$$

where:

$S_{as}(\omega)$ = cross spectrum of acceleration and stress

$S_{rs}(\omega)$ = cross spectrum of r(t) and stress.

Equation C-9 is also in a form where the available data can be used directly.

The estimating forms of Equation C-7 and C-9 were used in assembling programming to estimate stress and wave spectra, and cross spectra for both the deck and bending stress channels. The method used was the relatively standard Fast Fourier Transform approach noted in Reference 6. This includes for two given time histories:

1. Correct each time history to zero mean and remove linear trends.
2. Apply the Tukey 10% taper to each.
3. Perform the direct FFT, considering one tapered series the real part and one the imaginary part of the required complex array.
4. Unscramble the resulting complex transform array, compute raw FFT spectra and cross spectra, and compensate for the scale factor due to tapering. In the present case this resulted in estimates for frequencies defined by:

   $$k(\Delta\omega) = 2\pi k/8192/.15 = 0.00511k \text{ rad/sec}$$

   or:

   $$k(\Delta f) = k/8192/.15 = 0.000814k \text{ Hz}$$

   where $k = 0, 1.....4096$.

5. Perform frequency smoothing by averaging the raw estimates in non-overlapping frequency bands of width ℓ to obtain the final smoothing estimates at frequencies defined by:

   $$k\ell(\Delta\omega) \text{ rad/sec}$$

The final effective statistical frequency bandwidth for this procedure is roughly $k\ell(\Delta\omega)$ for reasonably large ℓ, and the degrees of freedom per spectral estimate is 2ℓ.

Bandwidth, Bias and Stability Considerations

Reference 6 gives estimates of bias errors for a second order system response to noise which seems applicable to the springing response. The results are given in terms of the normalized bias error:

$$\varepsilon = |1 - E[\phi]/\phi|$$

(where $E[\phi]$ stands for the expected value of the estimate of the spectral density ϕ) as a function of B_e/B_r where B_e is the effective statistical bandwidth of the analysis, and B_r is the half power bandwidth of the spectral peak. Table C-1 gives some approximate numerical values read from the graphical presentation of Reference 6. Included in the table is a column of the statistical bandwidth, B_e under the assumption that the half power bandwidth of the spectrum is the minimum found in Appendix B.

The values given in Table C-1 suggested that the present analysis should be carried out so that a statistical bandwidth of about 0.02 rad/sec would be achieved. However with the sample length fixed, the relations given in the last section result in a 9 degree of freedom analysis for this bandwidth, a figure which is so low that the statistical variability of final estimates would likely be orders of magnitude larger than the bias error. In the event it was decided to do analyses at two frequency resolutions, aiming at the bandwidths which Table C-1 suggests might yield bias errors of 10 and 20%.

Table C-2 summarizes the parameters selected for the two analyses carried out in the present work (labeled "A" and "B"), and the analysis parameters implied in Reference 1 for the prior analysis of the data. It may be noted that the degrees of freedom for analyses A and B are on the low side--it would be preferable to design for 30 at least. Much better statistical stability is implied for the analysis of Reference 1 (55 degrees of freedom). It should be noted that the statistical bandwidth of the analysis method of Reference 1 is roughly twice the resolution (Reference 7*) on the frequency scale. Thus the improvement in statistical stability relative to the present analyses A and B is partly because of an 18% longer sample and partly because larger potential bias errors were accepted.

---

*7. Nuttal, A.H., "Spectral Estimation by Means of Overlapped Fast Fourier Transform Processing of Windowed Data", Report 4169, Naval Underwater Systems Center, October 1971.

TABLE C-1

APPROXIMATE BIAS ERROR ESTIMATES

B_e/B_r	B_e(for B_r = 0.08 rps)	ε
1.5	0.12 rps ≈ 0.018 Hz	52%
1.0	0.08 rps ≈ 0.012 Hz	28%
0.75	0.06 rps ≈ 0.009 Hz	18%
0.50	0.04 rps ≈ 0.006 Hz	10%
0.25	0.02 rps ≈ 0.003 Hz	3%

TABLE C-2

ANALYSIS PARAMETERS

Analysis	A	B	DTNSRDC, Reference 1
Method	FFT, Frequency smoothing	FFT, Frequency smoothing	Overlapped FFT, cosine window, 50% overlap
Frequency Resolution:			
RPS	0.0460	0.0614	0.0614
Hz	0.00732	0.00976	0.00976
Statistical Bandwidth, RPS	0.046+	0.061+	≈0.12
Sample Duration, sec	1229	1229	1500
Degrees Freedom/ Spectral Estimate	18	24	55
Estimated bias, ε for Spectrum Half Power Band of 0.08 RPS	≈10%	≈20%	30→50%

Sample Spectra and Cross Spectra

Figures C-1 through C-5 indicate the results of cross-spectral analysis A of wave elevation and deck bending for the 5 runs. Qualitatively, the results for bottom bending were nearly identical except for the stress scale. The results for analysis B differed from those of analysis A in that fluctuations in the spectra and the cross-spectrum were slightly less well defined because of the wider analysis bandwidth. In both cases however the resolution of the cross spectrum was judged adequate, if not outstanding, for the derivation of gains, phases and coherency. As may be noted in Figures C-4 and C-5 for Runs 116 and 117, more resolution would have been particularly desirable in these cases, but, as noted, that selected was accepted as a trade-off with statistical stability.

Estimated Coherencies, Gains, Phases and RAO's

Analyses were carried out with both type A and B frequency resolutions for all five runs. Spectra and cross-spectra were estimated for both deck and bottom stresses in each case. Once these were available the estimates of coherency, gain, phase and RAO could be carried out as defined by Equations C-1 through C-4. In order to present the results graphically the runs obtained on the same day were grouped. Figures C-6 through C-9 are the results from analysis A (delta frequency of 0.046 rad/sec). Figure C-6 involves deck bending for Runs 74 through 77, Figure C-7 involves bottom bending for the same runs, and Figures C-8 and C-9 involve deck and bottom bending for Runs 116 and 117.

It will be noted that the frequency scale has been expanded in these figures. Previous experience has strongly suggested that no estimates of the sort presented should be made at frequencies where either input (wave) or output (stress) spectra are less than 5 or 10% of their peak values. Such a truncation results in estimates only in the frequency range between 1 and 2.3 rad/sec.

The only results for deck and bottom bending stresses which appear qualitatively different are those for phase. Deck and bending stresses should be 180° out of phase and the results obtained reflect this quite clearly. The changes in magnitude of deck and bending stresses gain and RAO reflect the scaling uncertainty noted in Reference 2. The relative scatter from run to run of bottom bending stresses is the same as that of the deck stresses. The asymmetry of deck bending evidently does not materially influence the scatter in RAO or gain.

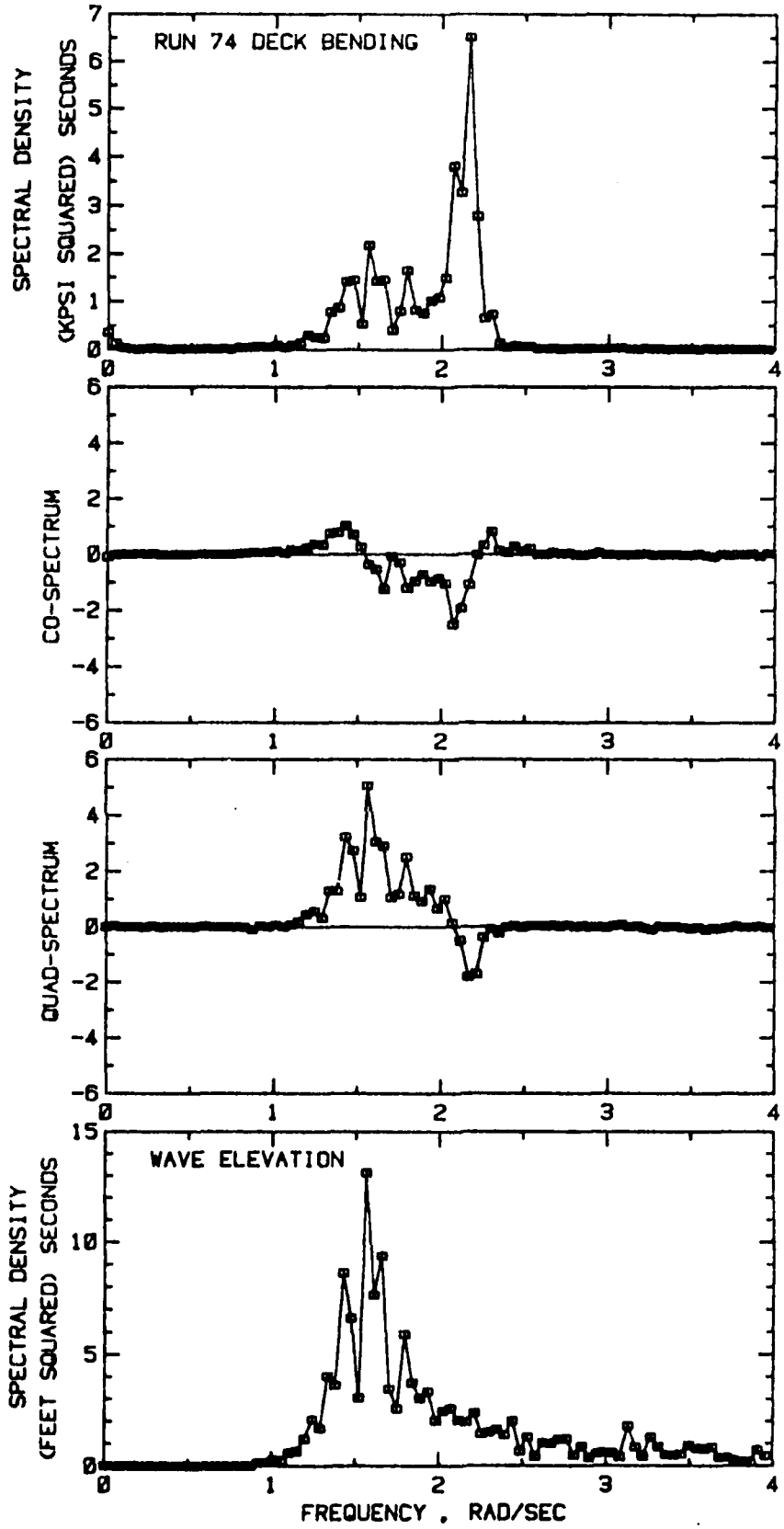

FIGURE C-1 RUN 74 - RESULTS OF CROSS-SPECTRAL ANALYSIS A, DECK BENDING

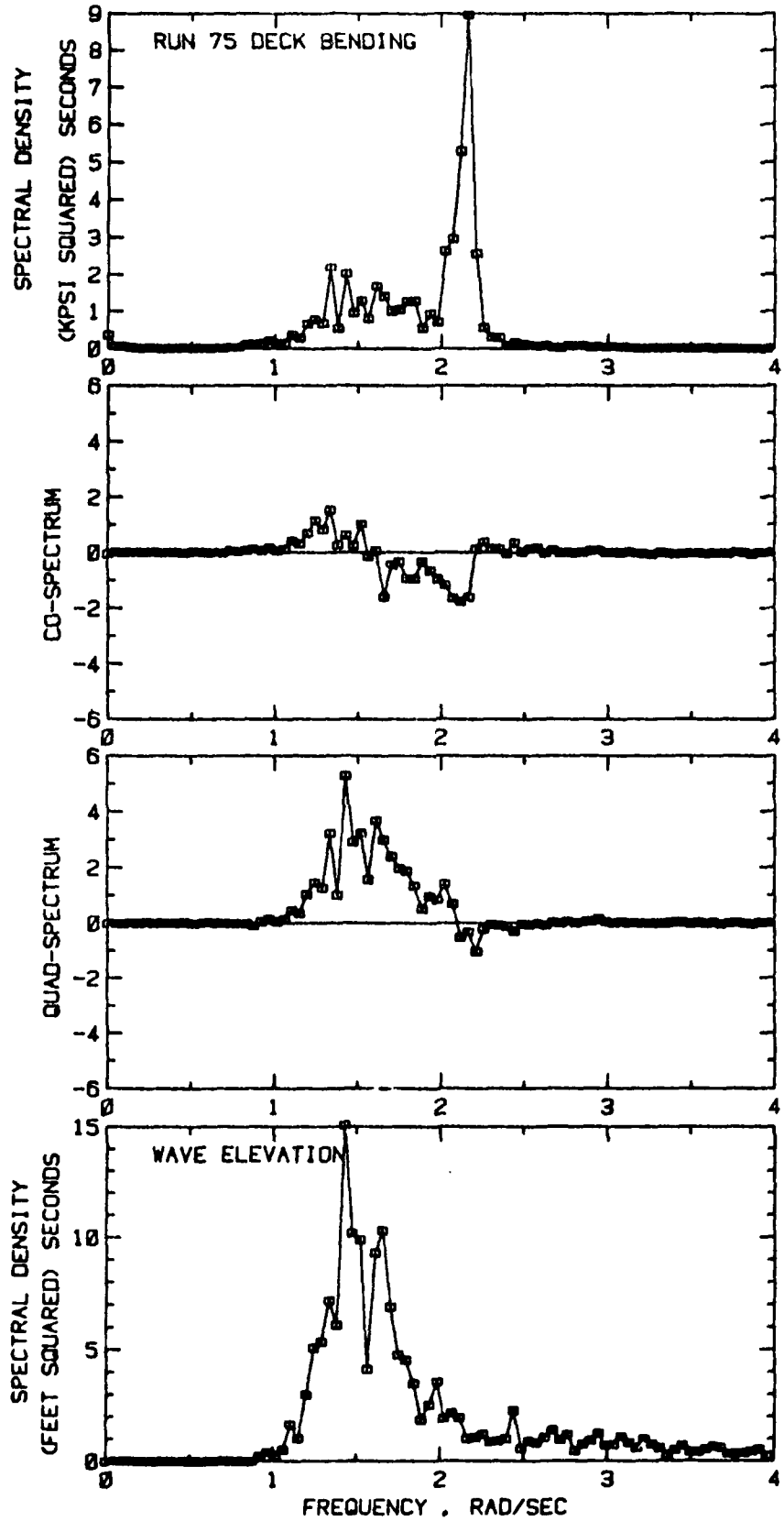

FIGURE C-2 RUN 75 - RESULTS OF CROSS-SPECTRAL ANALYSIS A, DECK BENDING

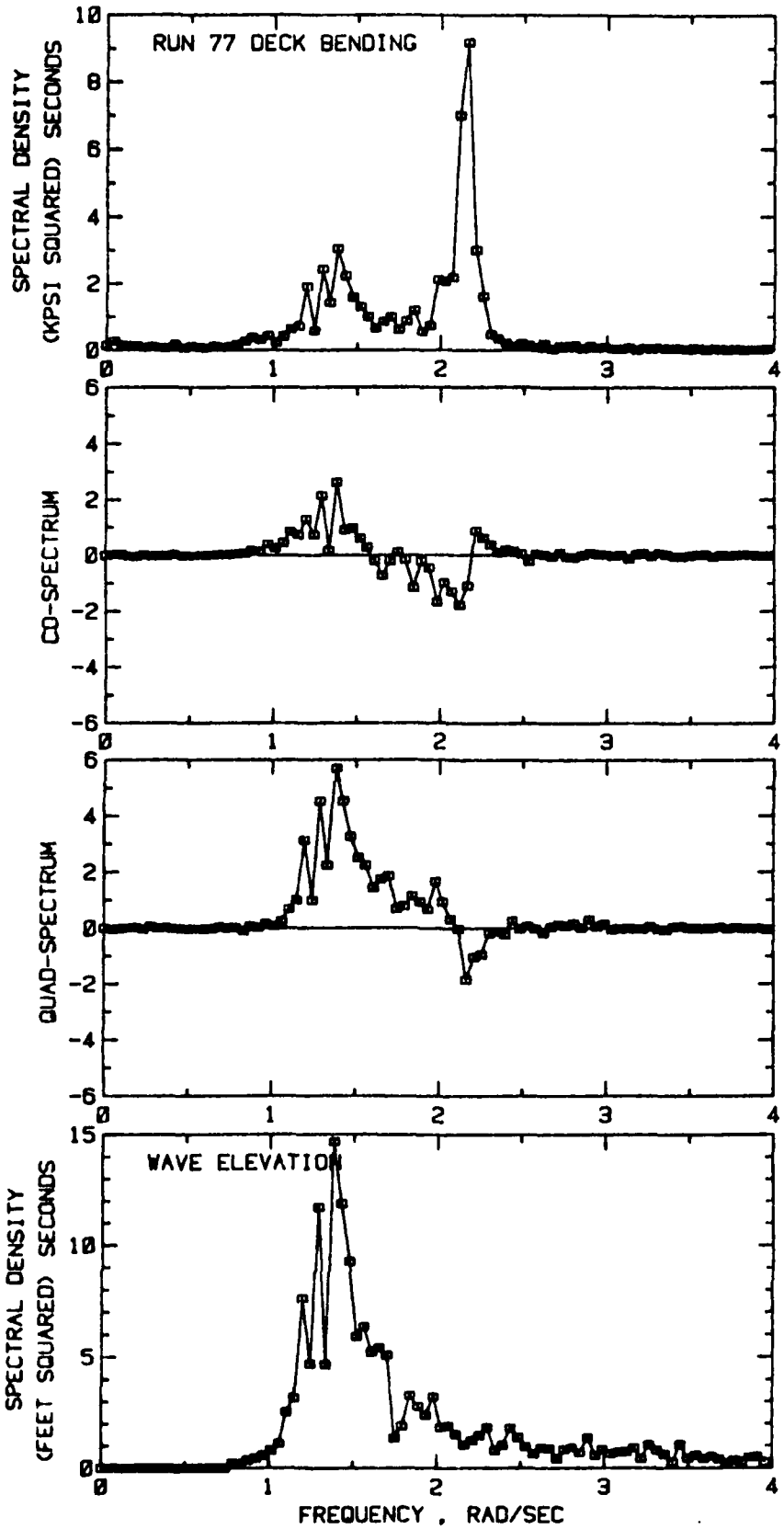

FIGURE C-3 RUN 77 - RESULTS OF CROSS-SPECTRAL ANALYSIS A, DECK BENDING

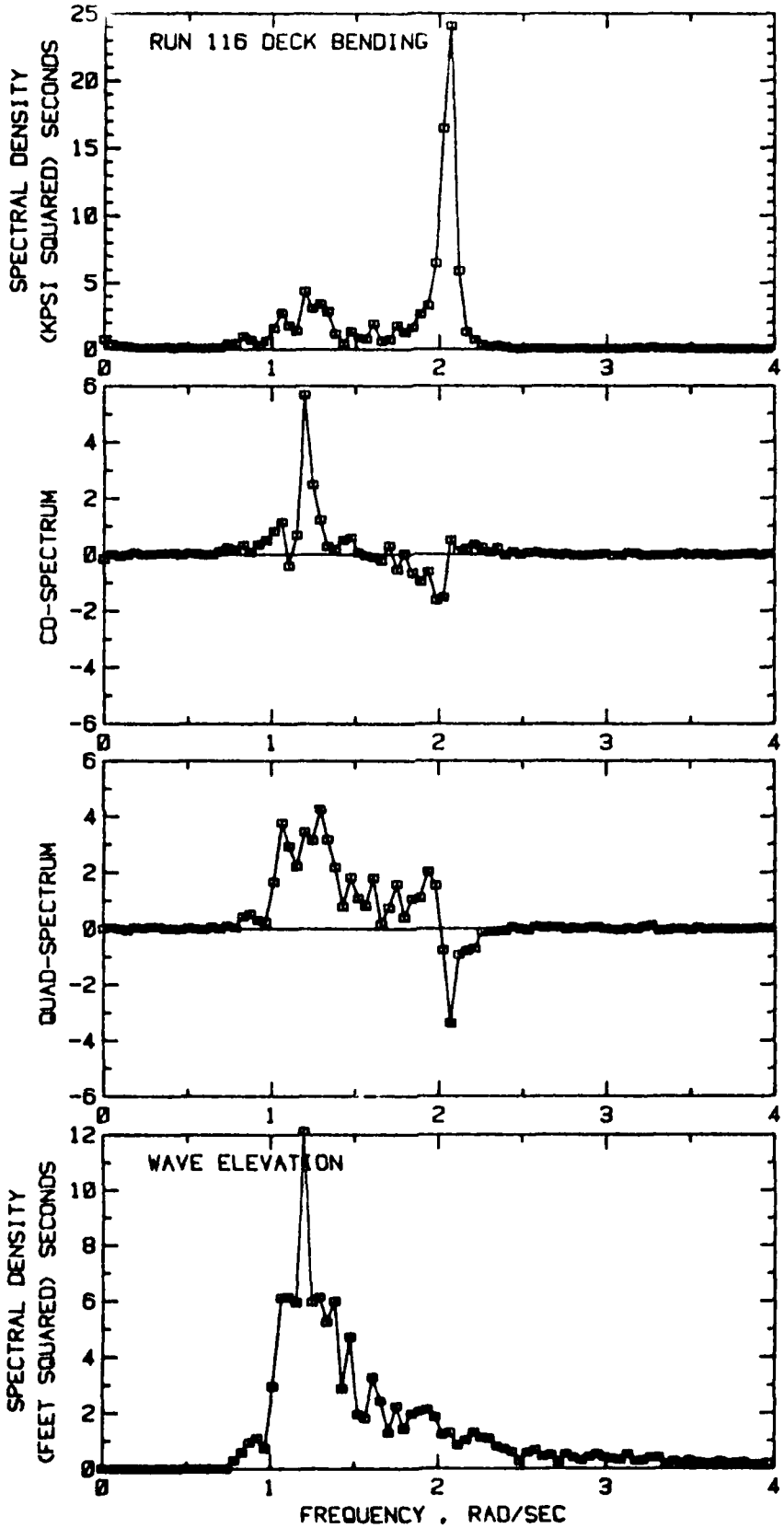

FIGURE C-4 RUN 116 - RESULTS OF CROSS-SPECTRAL ANALYSIS A, DECK BENDING

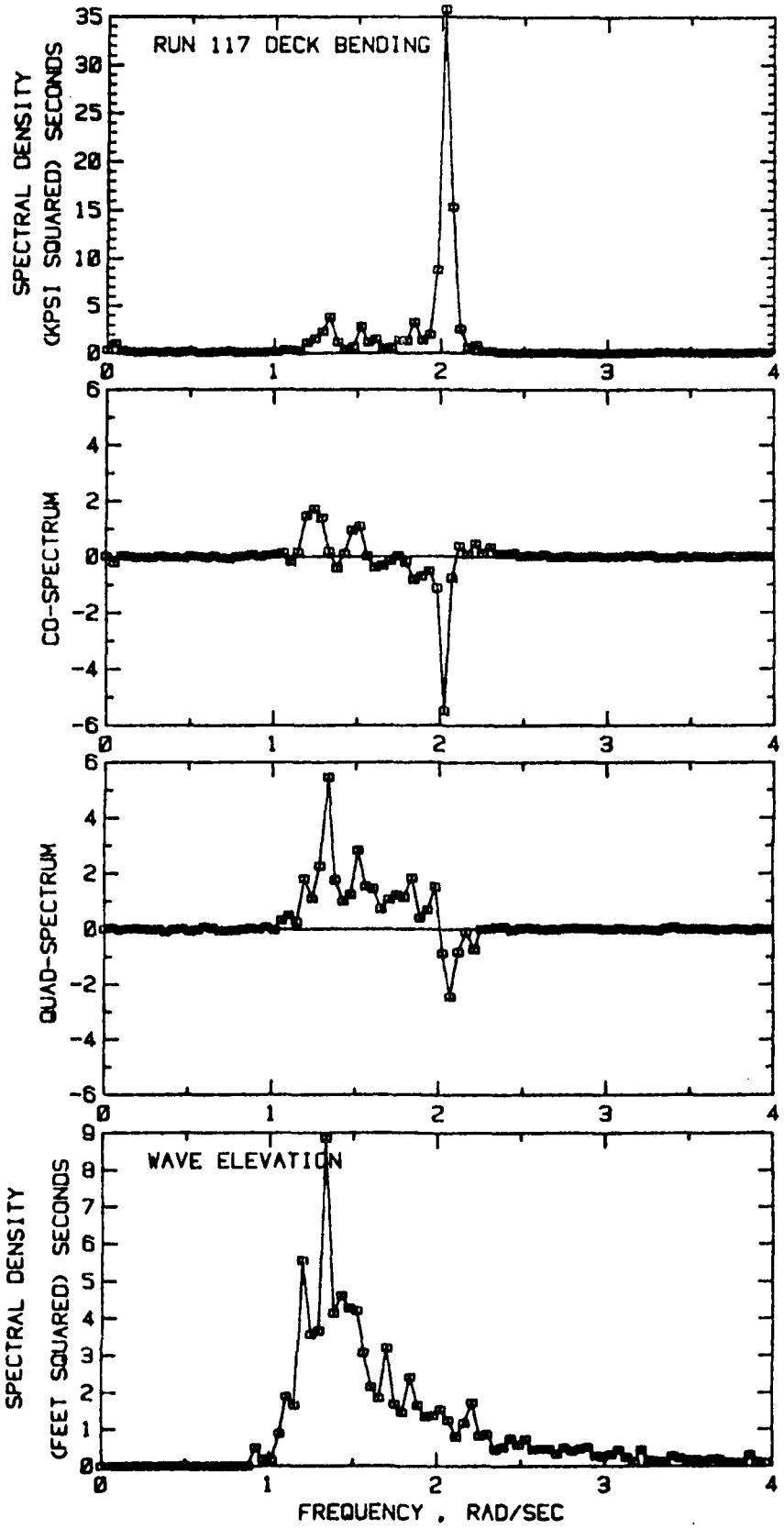

FIGURE C-5 RUN 117 - RESULTS OF CROSS-SPECTRAL ANALYSIS A, DECK BENDING

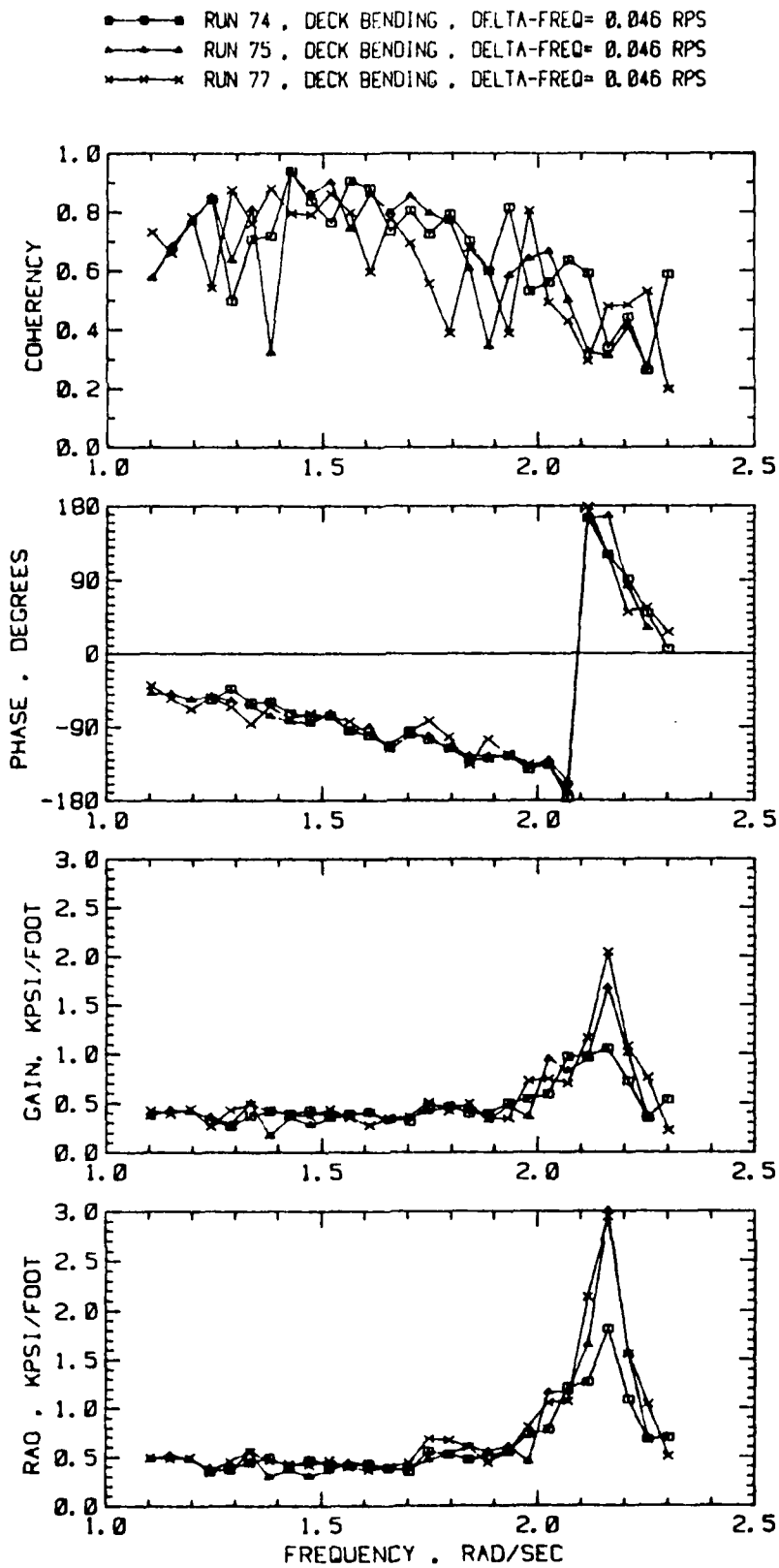

FIGURE C-6 GAIN, PHASE, COHERENCY AND RAO ESTIMATES FROM DECK BENDING ANALYSIS A, RUNS 74-77

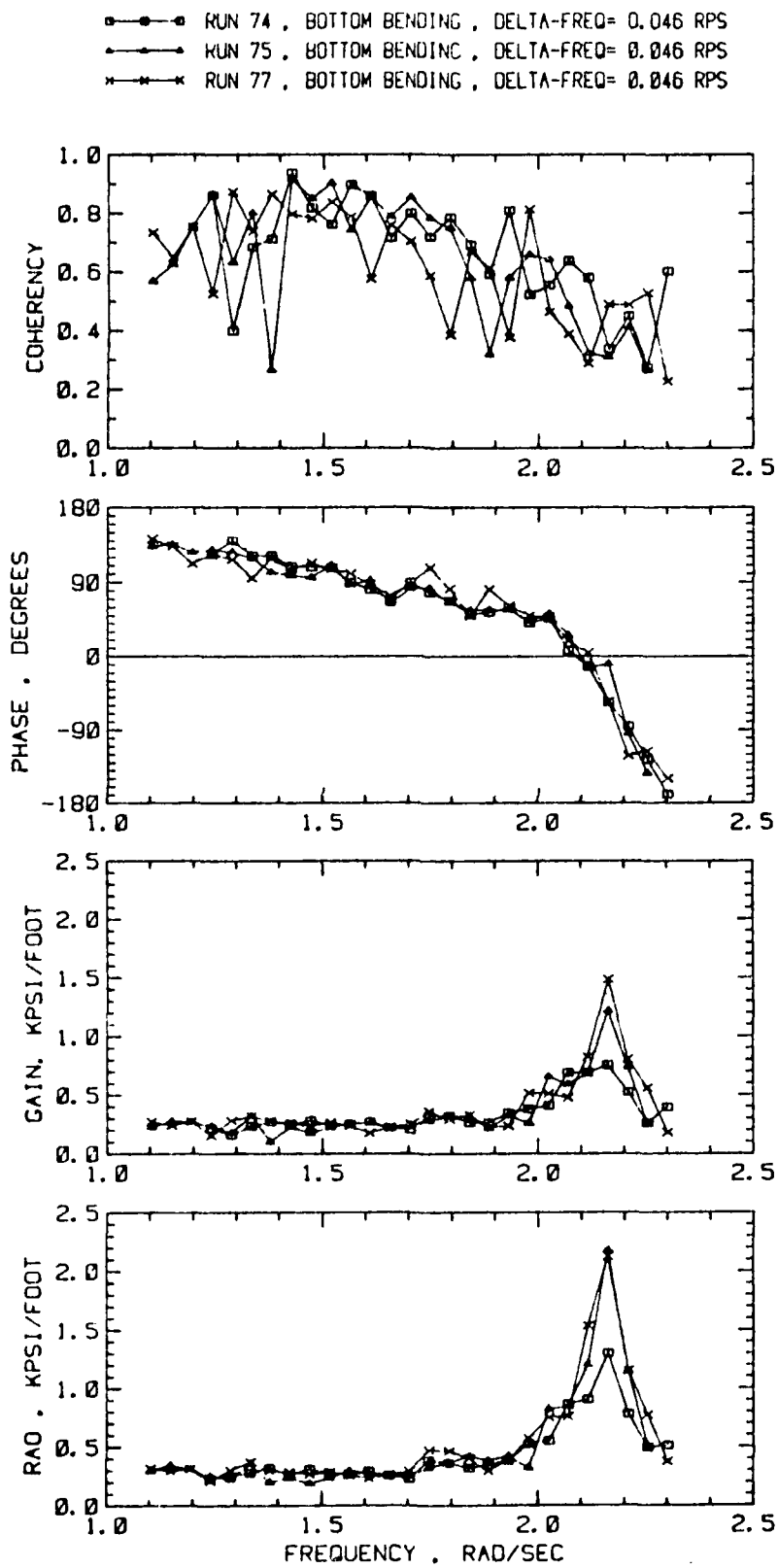

FIGURE C-7 GAIN, PHASE, COHERENCY AND RAO ESTIMATES FROM BOTTOM BENDING ANALYSIS A, RUNS 74-77

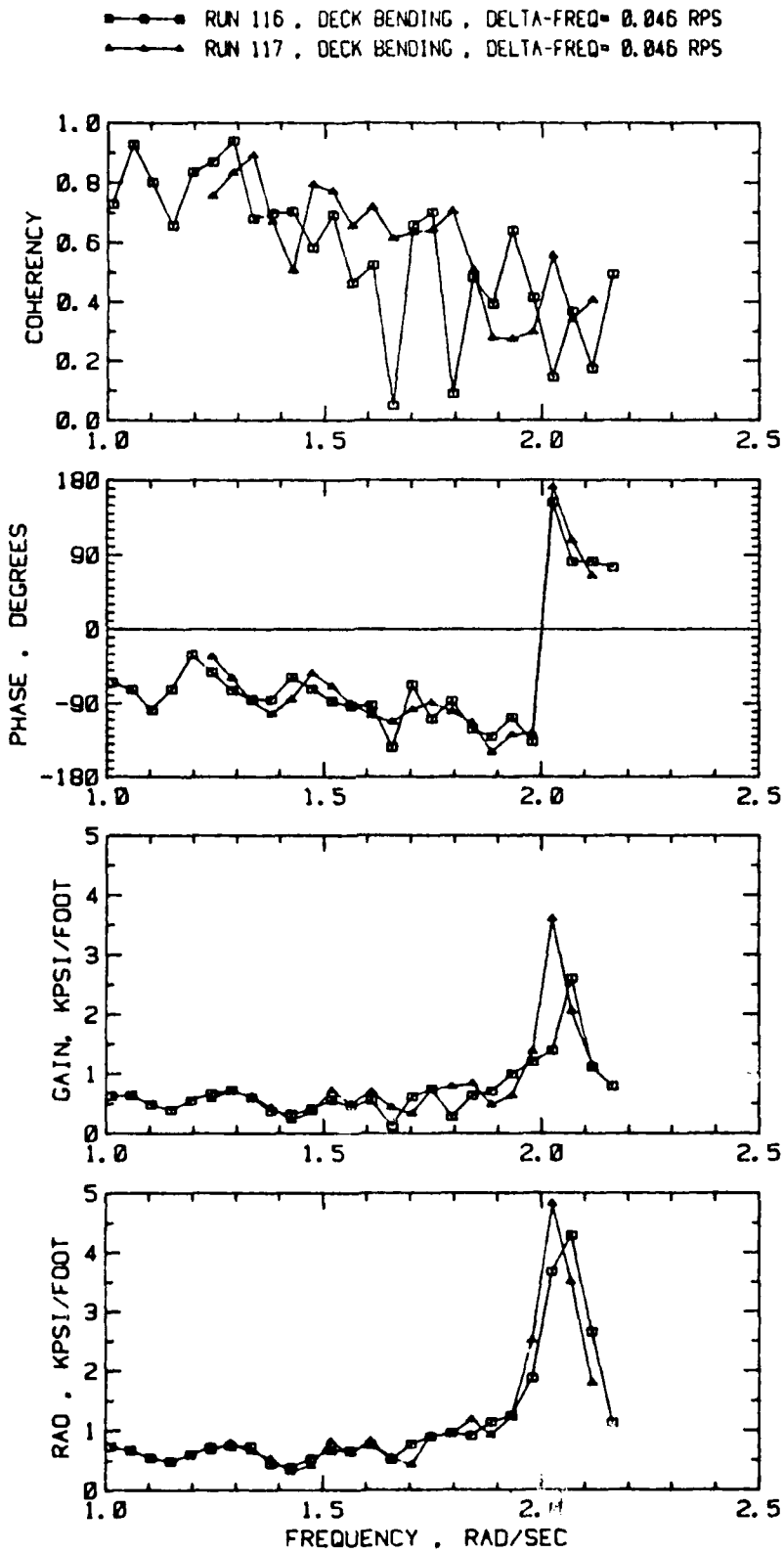

FIGURE C-8 GAIN, PHASE, COHERENCY AND RAO ESTIMATES FROM DECK BENDING ANALYSIS A, RUNS 116 & 117

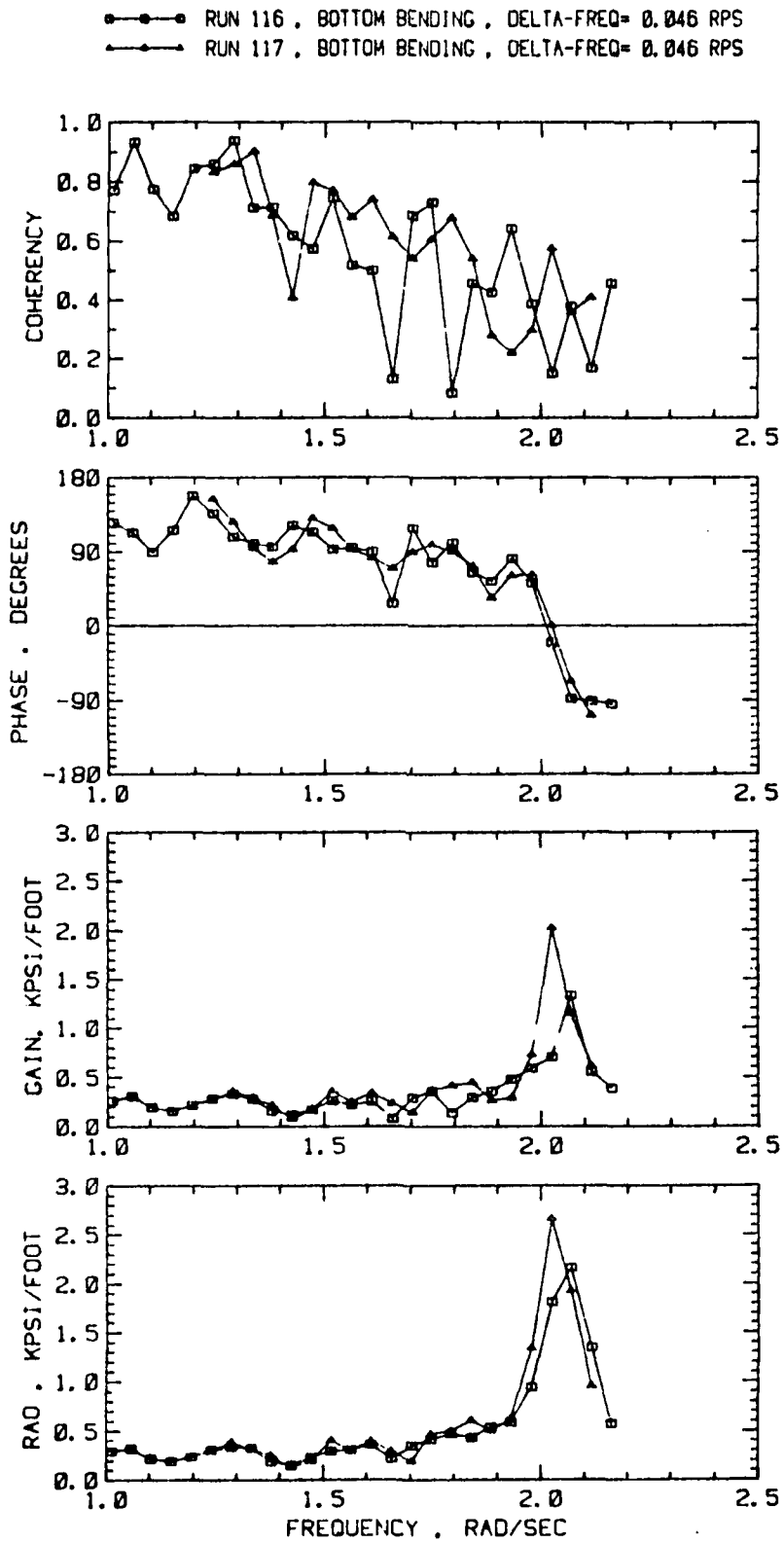

FIGURE C-9 GAIN, PHASE, COHERENCY AND RAO ESTIMATES FROM BOTTOM BENDING ANALYSIS A, RUNS 116 & 117

Figures C-10 through C-13 correspond exactly to Figures C-6 through C-9 except that the analysis frequency resolution was 0.061 rad/sec (analysis B). The remarks made with respect to the lack of qualitative difference between deck and bottom bending results for analysis A apply equally well to Analysis B.

The results just indicated suggested that there was little to be gained by continuing to consider deck and bending stresses in parallel, so that the next comparison involves only the deck stresses. Figures C-14 through C-18 involve a superposition of results from all the available analyses of each individual run. The first two analyses shown are the cross-spectral analyses A and B, the present FFT analyses. From the MLM results of Appendix B an estimate of RAO can be made. The estimate formed from the 200 lag MLM spectral analysis is shown. Finally, the peak value of RAO estimated in Reference 1 by the overlapped FFT method is indicated for 4 of the 5 runs.

It is clear from these results that the estimates of gain and RAO from all the different analyses are very much in line. The bias estimates shown in Table C-2 imply that at the springing peaks the RAO and gain estimates from analysis B (0.061 = delta frequency) should be about 4% lower than the results of analysis A; and similarly that the results of Reference 1 should be between 8 and 16% lower. Though there is a tendency for this to be true for analysis B, it is not so for the results of Reference 1. Quite possibly the bias errors of the methods of Reference 1 have been overestimated in the present work. Alternately, the result may be due to the better statistical stability of the analyses of Reference 1.

Estimated Sampling Variability

For present purposes the most improtant of the estimates just discussed is the coherency. The present interest is primarily in estimates of gain and RAO in the vicinity of the springing frequency. Looking over the results in Figures C-10 through C-18, the sample coherencies drop from about 0.8 in the frequency range where wave excitation is present to between 0.2 and 0.5 at the springing frequency. The coherency estimates have their own sampling variability so that scatter is expected. However it is thought that a reasonable round number average for the results shown is about 0.4. This, according to past experience, is terribly low.

Since it has been indicated that bias errors in the estimates of gain

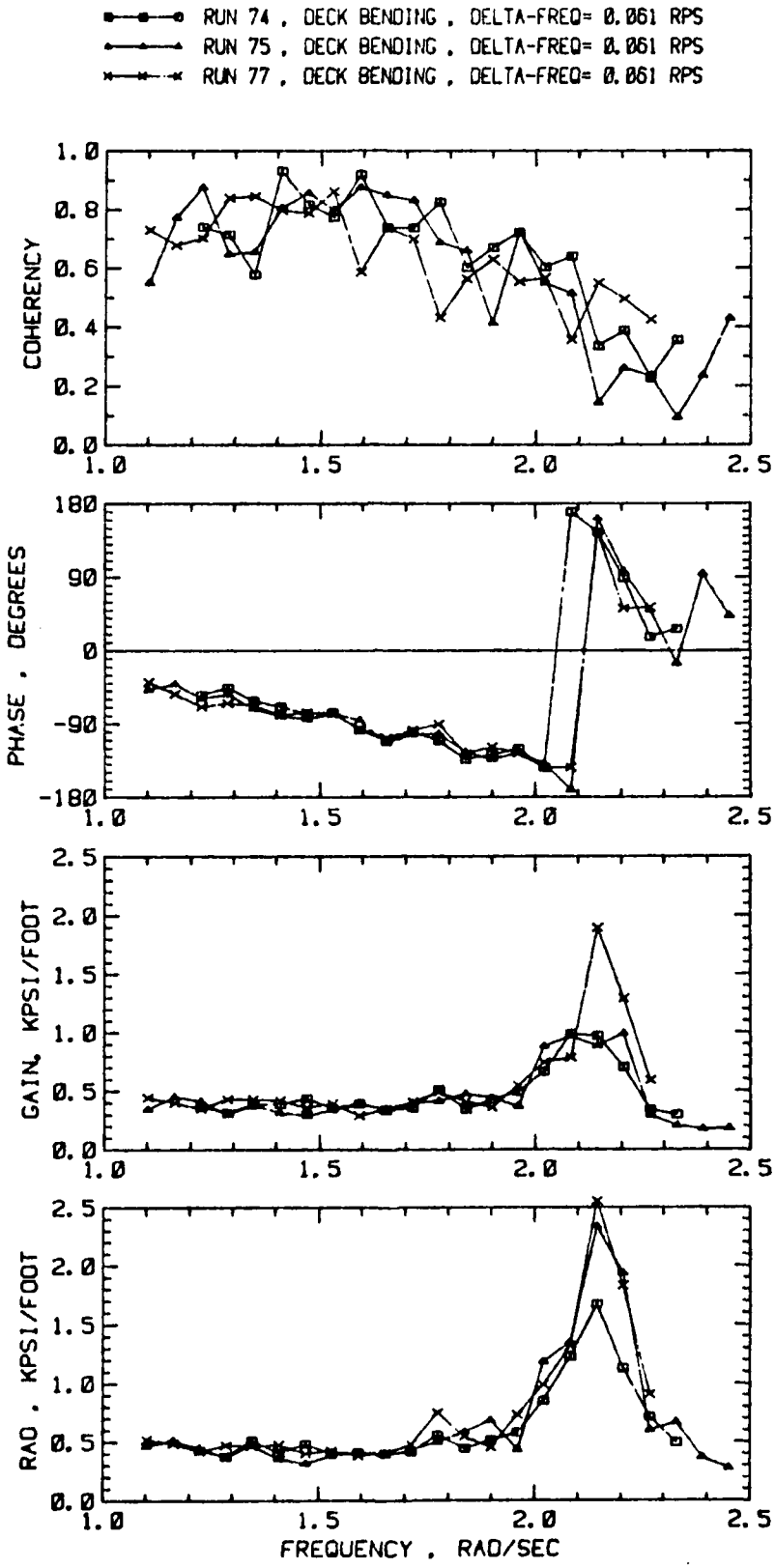

FIGURE C-11 GAIN, PHASE, COHERENCY AND RAO ESTIMATES FROM DECK BENDING ANALYSIS B, RUNS 74-77

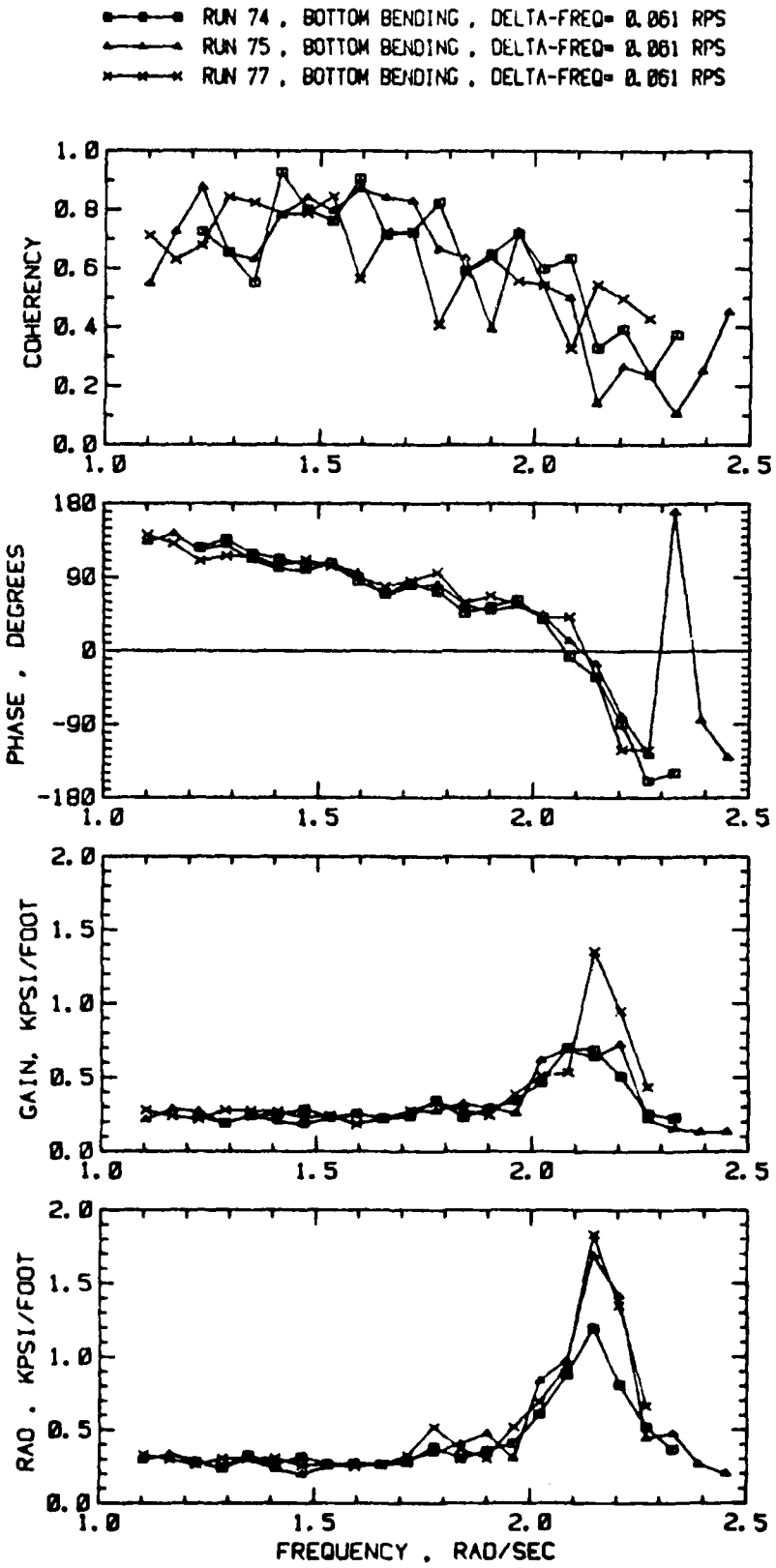

FIGURE C-11 GAIN, PHASE, COHERENCY AND RAO ESTIMATES FROM BOTTOM BENDING ANALYSIS B, RUNS 74-77

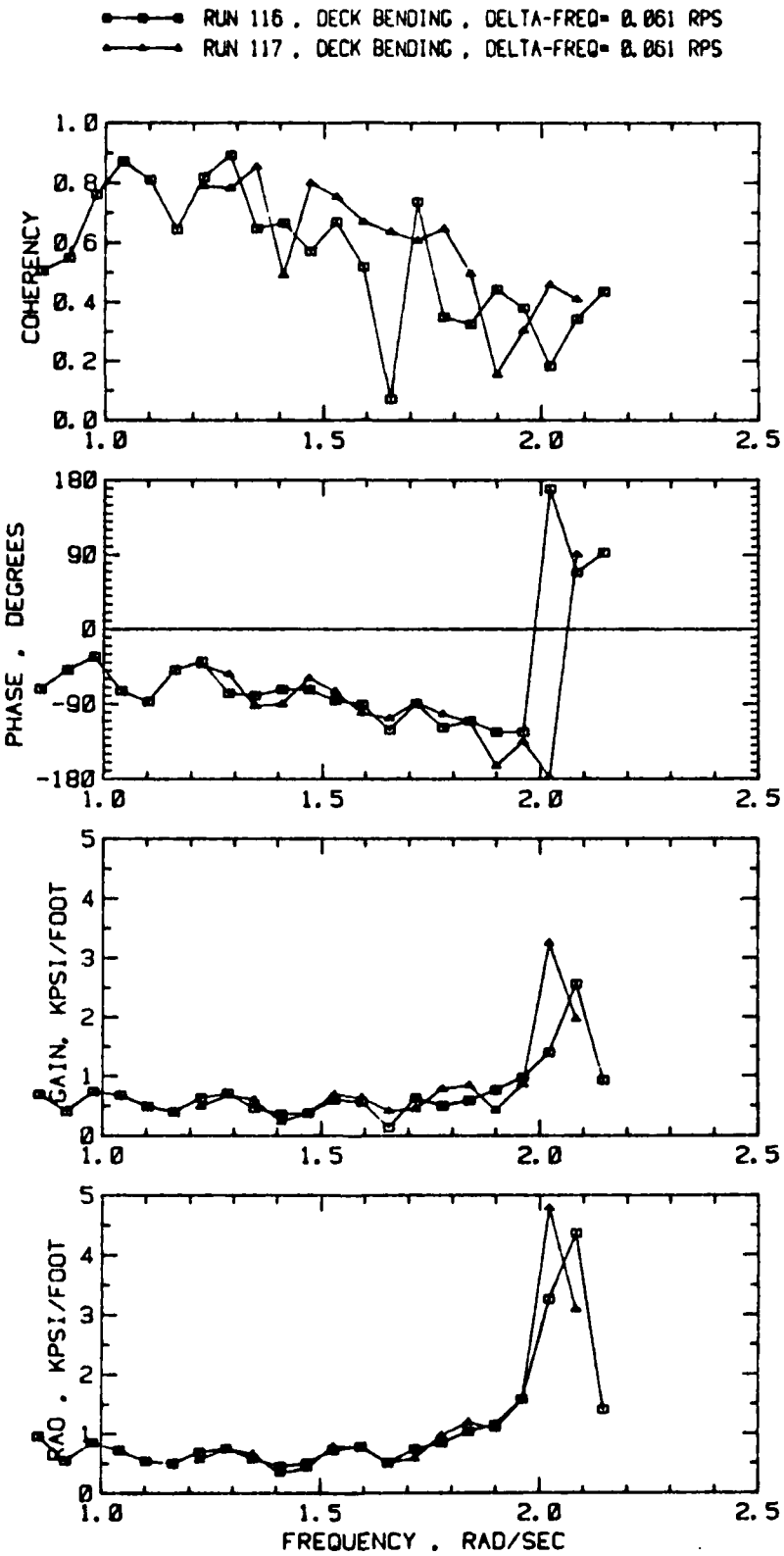

FIGURE C-12 GAIN, PHASE, COHERENCY AND RAO ESTIMATES FROM DECK BENDING ANALYSIS B, RUNS 116 & 117

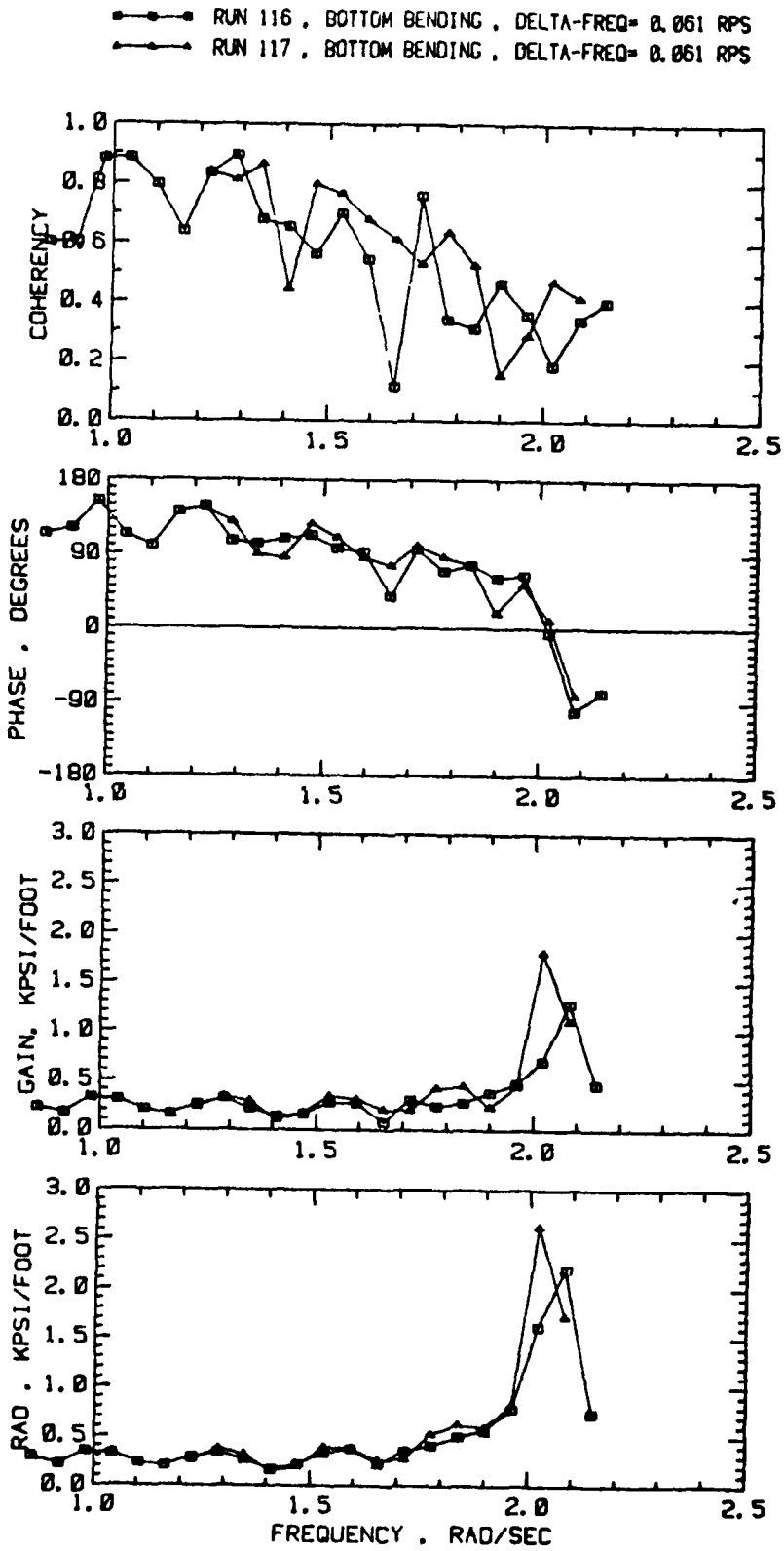

FIGURE C-13 GAIN, PHASE, COHERENCY AND RAO ESTIMATES FROM BOTTOM BENDING ANALYSIS B, RUNS 116 & 117

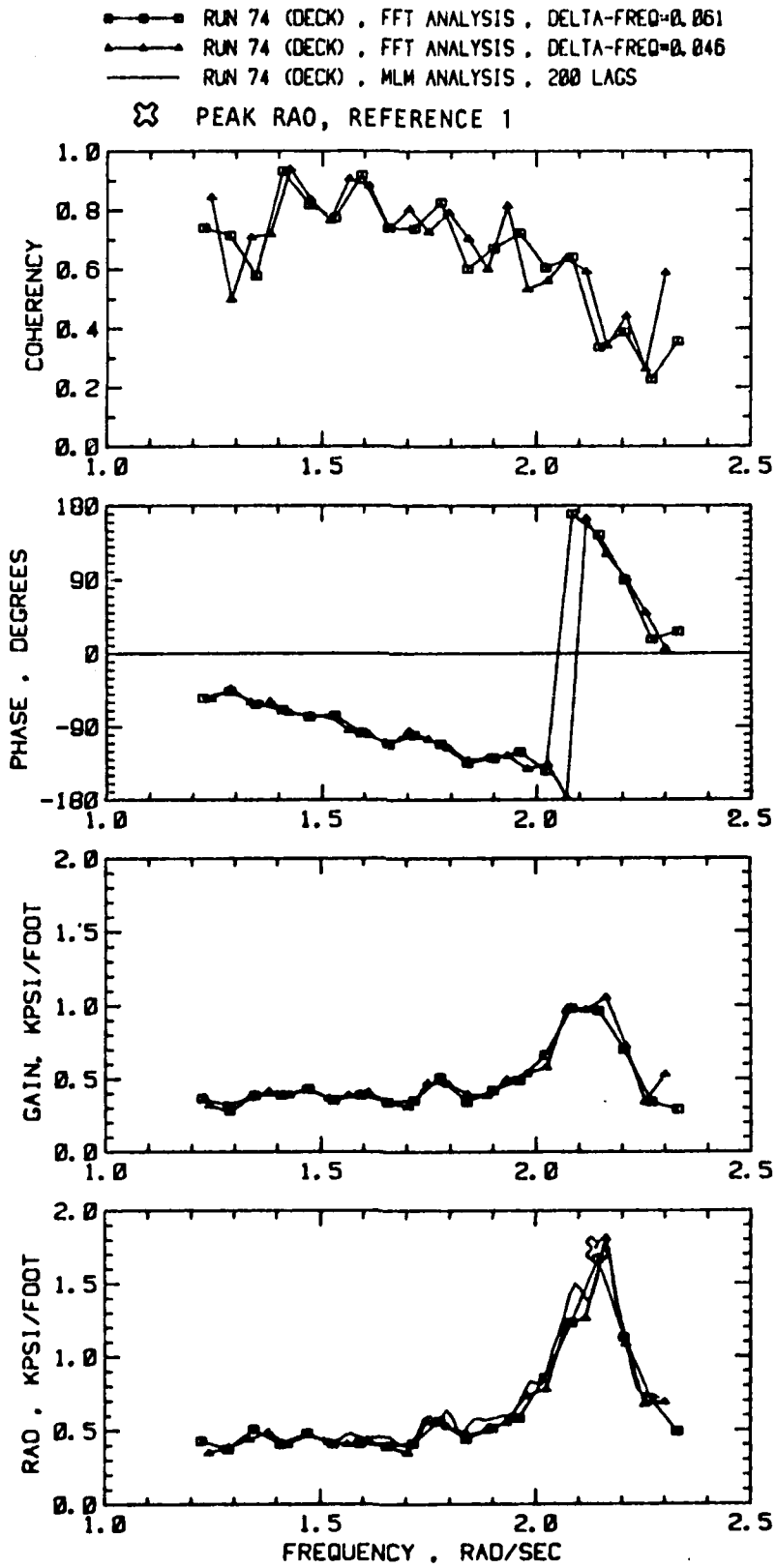

FIGURE C-14 RUN 74, COMPARISON OF RESULTS FROM VARIOUS ANALYSES

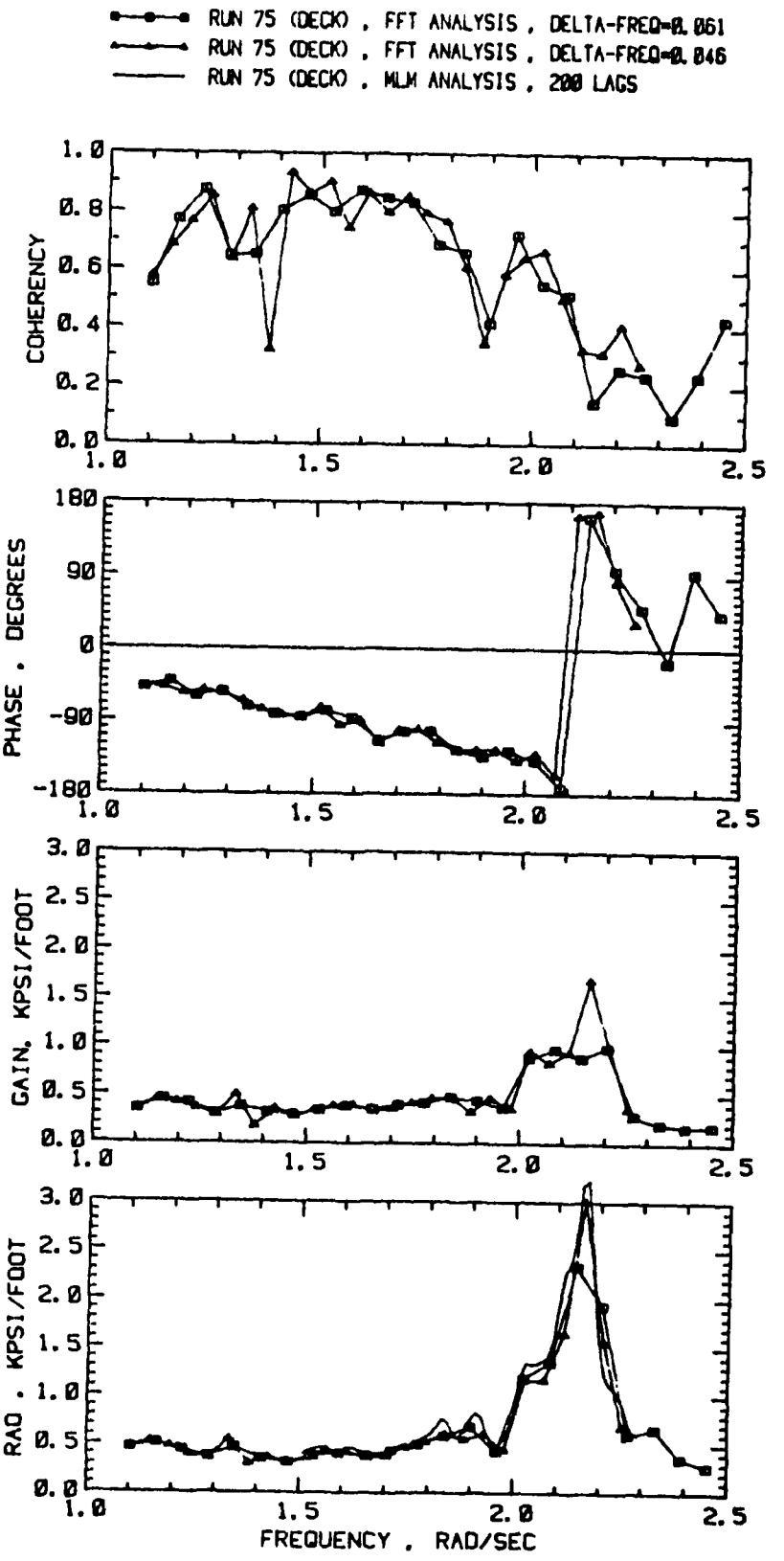

FIGURE C-15 RUN 75, COMPARISON OF RESULTS FROM VARIOUS ANALYSES

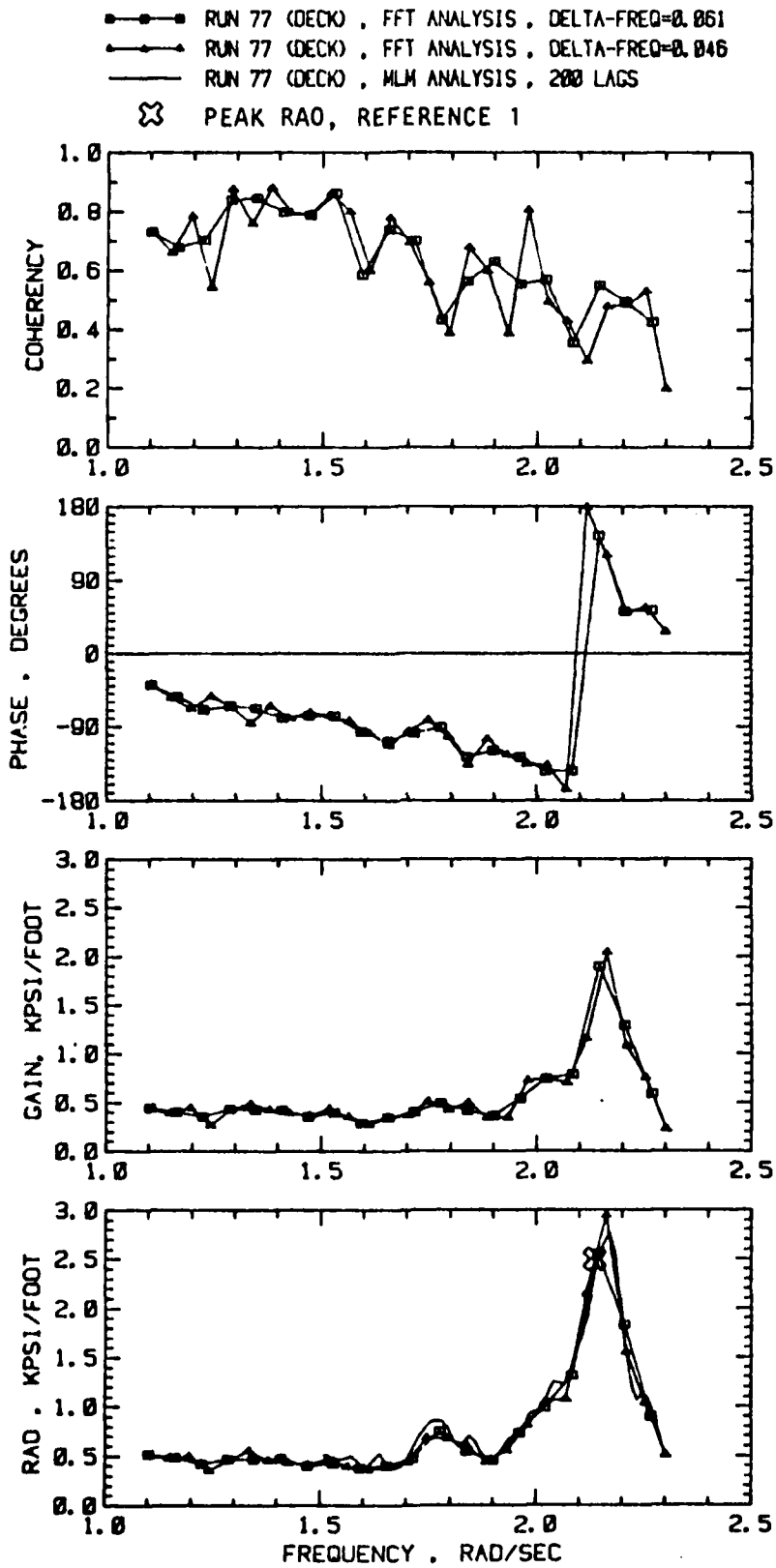

FIGURE C-16 RUN 77, COMPARISON OF RESULTS FROM VARIOUS ANALYSES

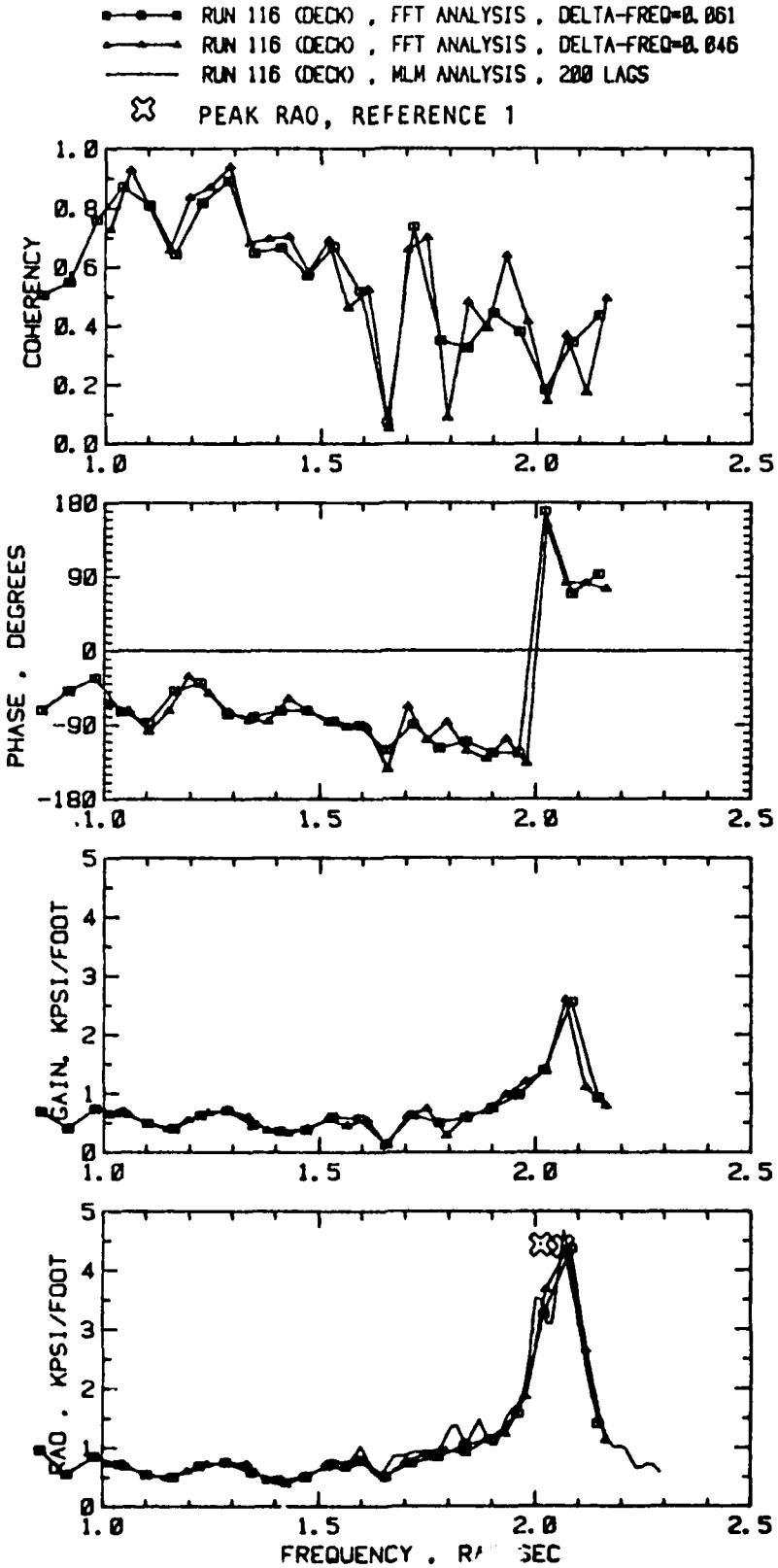

FIGURE C-17 RUN 116, COMPARISON OF RESULTS FROM VARIOUS ANALYSES

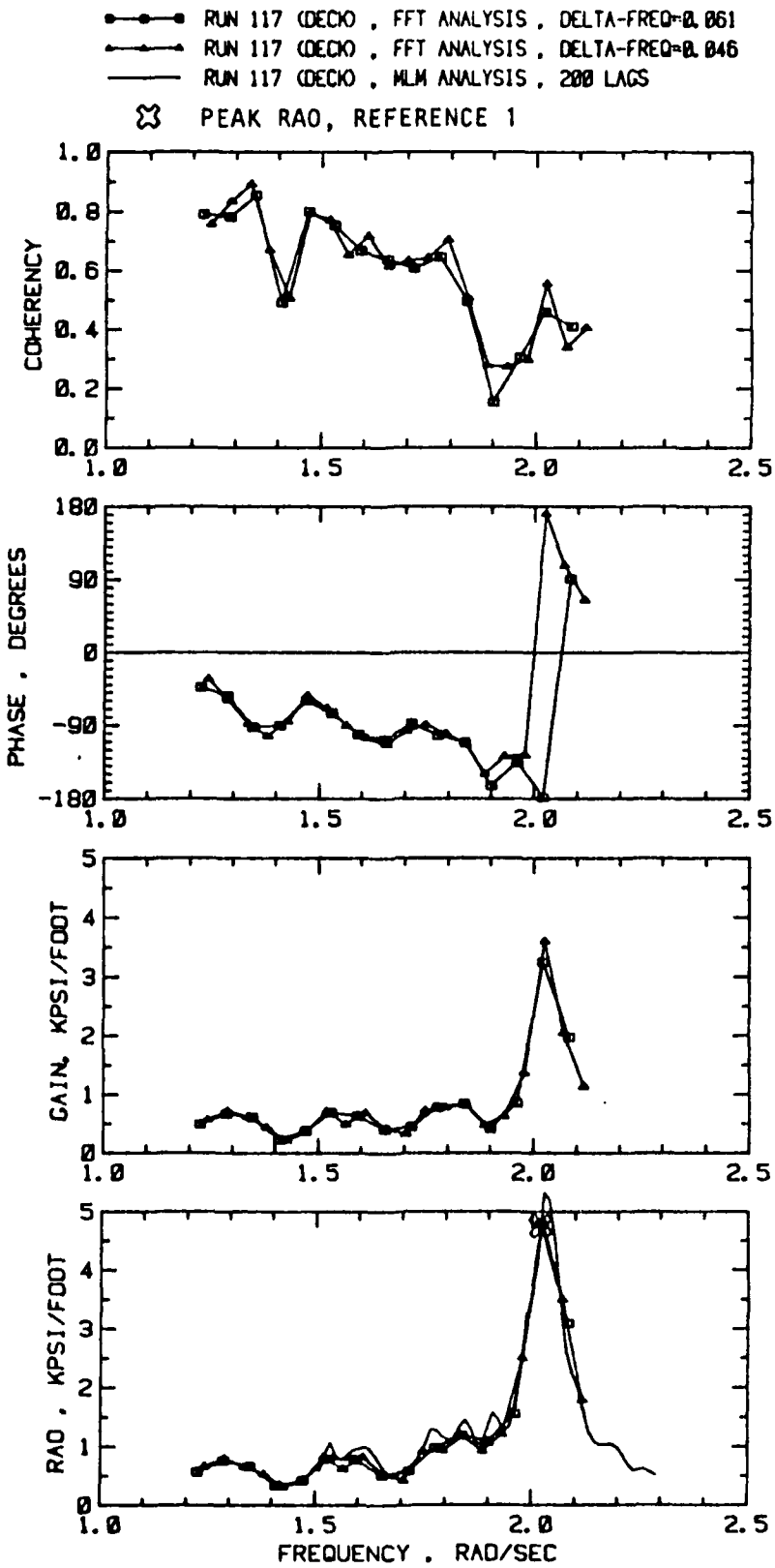

FIGURE C-18 RUN 117, COMPARISON OF RESULTS FROM VARIOUS ANALYSES

are probably not too serious, the methods given in Reference 6 for the analysis of random sampling errors appears applicable. A straight forward manipulation of Equations 6.146 and 6.147 of Reference 6 results in the following expressions for the 90% confidence bounds on the estimates of gain:

$$(\text{Sample Gain})[1 - \Lambda] \leq (\text{True Gain}) \leq (\text{Sample Gain})[1 + \Lambda] \quad \text{(C-10)}$$

where the parameter Λ and the gains are considered functions of frequency and:

$$\Lambda = \left[\frac{2}{n - 2} \; F_{2,n-2,.05} \; \frac{1 - \hat{\gamma}^2}{\hat{\gamma}^2}\right]^{\frac{1}{2}} \quad \text{(C-11)}$$

where:

$\hat{\gamma}^2$ = sample coherency, a function of frequency

n = degrees of freedom for each spectral estimate.

$F_{2,n-2,.05}$ = the 5 percentage point of the "F" distribution with 2 and $n-2$ degrees of freedom.

Roughly, Equation C-10 implies that in about 90% of similar estimates from statistically independent samples the computed sample gain should be within $\pm 100\Lambda$ percent of the truth. Table C-3 contains results of an evaluation of Equation C-11 for various choices of degrees of freedom and sample coherency.

An analogous treatment for the RAO estimate, Equation C-1, is not available. However, previous experience and the close resemblense of the gain and RAO scatter from run to run in Figures C-6 through C-13 suggests that the order of magnitude of sampling variability of RAO estimates is not wildly different than those for gain. Assuming this, and that sample coherencies near the springing frequency in the entire data set of Reference 1 are about 0.4, Table C-3 indicates that for the 55 degree of freedom analyses of Reference 1 the estimated RAO's should scatter ±40 or 50% about the truth. Perusal of Reference 1 discloses scatter of this order of the springing RAO estimates about the mean estimate for nominally similar ship and wave heading conditions. It appears that a significant part of the large variability of springing RAO estimates in Reference 1 may be ascribed to sampling variability.

TABLE C-3

VALUES OF Λ (IN PERCENT) COMPUTED FOR 90% CONFIDENCE BOUNDS ON ESTIMATES OF GAIN

Degrees of Freedom (n)	Sample Coherency 0.4	0.6	0.8
18	81%	54%	33%
24	68%	45%	28%
30	60%	40%	24%
40	50%	34%	21%
55	42%	28%	17%
80	34%	23%	14%
100	31%	20%	12.5%

Discussion

The numerical results in Table C-3 fairly clearly indicate the source of the conclusion just arrived at. Once the degrees of freedom chosen for an analysis are above about 30 the magnitude of sampling variability is strongly controlled by coherency. In the present case coherencies of about 0.4 are the problem.

There are four more or less standard explanations for low computed coherency between input and output of a system.

1. Extraneous noise is present in the measurements.
2. Analysis bandwidths are chosen so that the fluctuations in the real and imaginary part of the cross spectrum are poorly resolved.
3. The response is due to the measured input as well as other inputs which are not measured.
4. The system relating input and response is not linear.

It is suspected that cause 1 does not apply to the stress measurements on the basis that the bottom bending appears free of unexpected frequency components, and the final estimates of coherency for deck bending differ very little. The situation for the wave elevation is not so clear. The records contain content at higher frequencies than might be expected. Cause 2 is not suspected in the present case. Fluctuations in cross spectra at frequencies where coherencies were relatively high are not significantly better defined than those near the springing frequency.

There are two possibilities which can be mentioned in conjunction with cause 3. The first is the suggestion of a contribution of propeller induced vibration (which should be largely uncorrelated with waves). The second is that the trials involve a real ship in real waves. The response to short crested seas may be likened to a system which responds to multiple inputs. In this case waves coming from different directions correspond to the various inputs. Indeed, Reference 8* shows that the theoretical coherency between wave and response in short crested seas should be less than unity. (The theoretical

*8. Pierson, W.J., Jr., "On the Phases of the Motions of Ships in Confused Seas", New York University, Report 9, NONR 285(17), November 1957.

coherency for a linear single input system is unity.)

A brief investigation of cause 4 (nonlinearity) will be described in Appendix D.

Closing Comments

The purpose of the present analysis was to help shed light upon the large variability in estimates of springing RAO shown in Reference 1. The present rough estimates suggest that a significant part of the variability in the estimates of Reference 1 is due to random sampling error.

The present analysis, coupled with that of Appendix B suggests that the effective statistical bandwidth of the analysis of Reference 1 was slightly wide relative to the narrowest band springing response in the data set. However the analysis also suggested that the good level of statistical stability in the estimates of Reference 1 probably out-weighs the potential for bias errors inherent in the bandwidth chosen. The net conclusion is that the choice of analysis parameters in Reference 1, given the fixed sample length, is not likely to have seriously affected the variability of the result.

The results of the parallel analyses of deck and bottom bending stresses differed significantly only with respect to the absolute magnitude of the gain and RAO estimates. This is apparently a direct result only of the problem with the scale factor which was discussed in Reference 2. Otherwise, run to run scatter in gain, RAO, and coherency estimates are much the same. The asymmetry in deck stresses apparently has had little effect upon the results.

The main problem which the present analysis suggests is a coherency between wave elevation and springing stress of about 0.4. For purposes of deriving relationships between stress and encountered wave this is a very low magnitude. Such low coherencies significantly widen the estimated sampling variability, and raise some serious conceptual problems. Coherencies in the range of frequency where the stress may be considered to be a quasi-static direct result of the waves are close to 80%. This suggests that the estimates of wave induced stress RAO's are of much better quality. The consistent trend downward of the sample coherencies may reflect an increasing tendency toward short-crestedness as the wave components get shorter and shorter.

APPENDIX D

CROSS-BI-SPECTRAL ANALYSES

Introduction

Among the many reasons for the low coherencies noted in Appendix C, is the spector of nonlinear response. Unless nonlinearities are very dramatic there are limited means of deducing system response from random data. Given an input and a response it is possible in theory at least to estimate values of a "quadratic frequency response function" in which quadratic or "second order" relationships between input and response are imbedded. The technique is called cross-bi-spectral analysis, and the background as well as computational techniques are discussed in References 9* and 10*. It seemed reasonable, even before the low coherencies arose, to apply the technique to some of the present data to see if any indication of quadratic nonlinearities could be found.

Theory

In simplest terms, the theory assumes that weak nonlinearities of second degree may be modeled as a perturbation about an underlying linear system so that the relationship between output, Y(t) and input X(t) may be expressed as:

$$Y(t) = \int g_1(\tau)\, X(t - \tau)\, d\tau + \iint g_2(\tau_1, \tau_2)\, X(t - \tau_1)\, X(t - \tau_2)\, d\tau_1 d\tau_2 \quad \text{(D-1)}$$

Under fairly non-restrictuve conditions the kernels in Equation D-1 may be Fourier transformed. The transform of $g_1(\tau)$ in the first term is $G_1(\omega)$ and this is just the linear frequency response function. The transform of the kernel of the second term is denoted:

$$G_2(\omega_1, \omega_2)$$

and this is the "Quadratic Frequency Response Function". This function is

---

*9. Dalzell, J.F., "Application of Cross-Bi-Spectral Analysis to Ship Resistance in Waves", SIT-DL-72-1606, Davidson Laboratory, May 1972, AD 749102.

*10. Dalzell, J.F., "Application of the Functional Polynominal to the Ship Added Resistance Problem", Eleventh Symposium on Naval Hydrodynamics, London, 1976.

defined in a "bi-frequency plane". The complete function essentially contains the amplitudes of the response at the sum and difference frequencies which may be generated by any combination of two excitation frequencies, ω_1, and ω_2. Figure D-1 indicates a portion of the bi-frequency plane and some useful transformations. First, the quadratic frequency response function is symmetric about the line $\omega_1 = \omega_2$. The real part of the function is also symmetric about the line $\omega_2 = -\omega_1$, and the imaginary part is anti-symmetric about this line. Thus only a quadrant of the plane needs to be considered, and this is reflected in the sketch, Figure D-1. the frequency transformation shown in the figure is;

$$\Omega_2 = \omega_1 + \omega_2 \qquad \text{(Sum frequency)}$$

$$\Omega_1 = \omega_1 - \omega_2 \qquad \text{(Difference frequency)}$$

It turns out that Ω_2 is numerically equal to the output frequency produced by interactions between two frequencies ω_1 and ω_2. In the present case the interest is in the possibility of quadratic nonlinearities in springing response which is at a frequency of about 2 rad/sec. By the above, such response might be generated by any combination of frequencies adding to about 2. For example:

$$\omega_1 = 1,\ \omega_2 = 1 \qquad \text{(Response is second harmonic)}$$

$$\omega_1 = 1.1,\ \omega_2 = .9$$

$$\omega_1 = .5,\ \omega_2 = 1.5$$

Since springing is sharply tuned, what would be expected is that $|G_2(\omega_1,\omega_2)|$ would be appreciable near the line $\Omega_2 \approx 2 = \omega_1 + \omega_2$ in the upper octant of the bi-frequency plane--<u>if</u> appreciable quadratic response exists. Further, <u>if</u> this is so there is the possibility that springing could be induced by combinations of wave components of much lower frequency than that of springing itself.

Another result from theory which pertinent is the expression for the scalar spectrum of output of a linear plus quadratic system:

$$S_{ss}(\omega) = |G_1(\omega)|^2\, S_{\eta\eta}(\omega) + \int_{-\infty}^{\infty} |G_2(\omega-\xi,\xi)|^2\, S_{\eta\eta}(|\omega-\xi|)\, S_{\eta\eta}(|\xi|)\, d\xi \qquad \text{(D-2)}$$

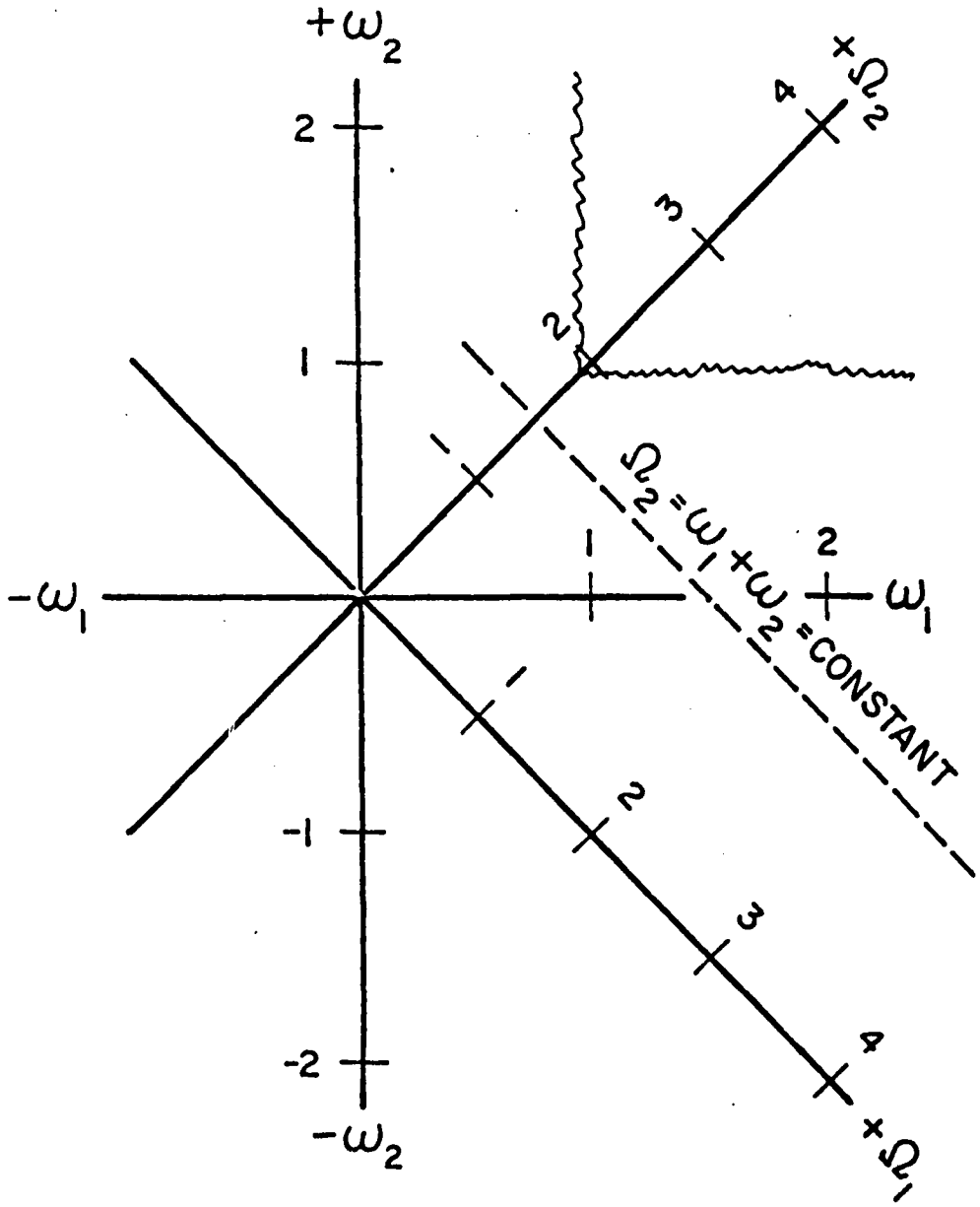

FIGURE D-1 BI-FREQUENCY PLANE

where:

$S_{ss}(\omega)$ = the response (stress) spectrum

$S_{\eta\eta}(\omega)$ = the input (wave) spectrum

The first term in Equation D-2 is the familiar linear one, and the second is the quadratic contribution. Note in the second term that in order to make a significant contribution to the integral the value of input spectral density has to be appreciable at two frequencies. If, as in the present case, $S_{\eta\eta}(\omega)$ is small or nil below a frequency of ≈1 rad/sec, significant contributions to the output spectrum can only arise if the quadratic frequency response function is appreciable in the region where ω_1 and ω_2 are both greater than 1, and this is indicated in Figure D-1 by the wiggly lines.

Cross-Bi-Spectral Analysis Techniques

Both the numerical processes and the computer subroutines used in the present analysis are fully documented in Reference 9. These are by no means the most computationally efficient programs possible for the analysis. In the present case they were used because they were immediately available and documented. The routines require "input" and "output" arrays corrected to zero mean. The wave elevation arrays were generated as described in Appendix A. With reference to Figure D-1 each execution of the routine yields cross-bi-spectral densities and estimates of the quadratic response function along a line of constant Ω_2 or Ω_1. Multiple executions are necessary to build up a map of the whole plane. Analysis parameters were chosen so as to resolve the plane at 0.046 rad/sec intervals in either the Ω_1 or Ω_2 direction.

Cross-Bi-Spectral Analyses

The analysis started by exploring the lines $\Omega_1 = 0$ and $\Omega_2 = 0$, Figure D-1. These are the lines of symmetry. Values of the quadratic frequency response function along these lines reflect second harmonic and shifts in the mean of the response. There is no theory of sampling variability available for this type of estimate, only the empirical work described in References 9 and 10. The first part of the rule of thumb developed there was that cross-bi-spectral estimates of the quadratic frequency response function should not be accepted at bi-frequencies ω_1, ω_2 where the product $S_{\eta\eta}(\omega_1)S_{\eta\eta}(\omega_2)$ is less than about 10% of the maximum values of the same product. In the case of the present data the spectral product is always less than the stated criterian for bi-

frequencies near the line $\Omega_2 = 2$, the region of primary importance in the present case. In fact, in order to obtain results, the estimates had to be accepted in the region where $S_{\eta\eta}(\omega_1)\ S_{\eta\eta}(\omega_2)$ is of the order of 2% of peak. Accordingly, the estimates of $G_2(\omega_s/2,\ \omega_s/2)$, which reflect possible springing response at frequency ω_s, as the second harmonic of a wave component of frequency $\omega_s/2$ were quite variable. Absolute values of the function $G_2(\omega_s/2,\ \omega_s/2)$ for Runs 74 through 77 ranged from 2 to 6 kpsi/ft^2, between 0.7 and 5 kpsi/ft^2 for Runs 116 and 117. Elsewhere, where the estimates of $G_2(\omega,\omega)$ should have been reasonable, the magnitudes were much lower. The exploration of the bi-frequency plane along $\Omega_2 = 0$ (Figure D-1) was to see if any significant shifts in the mean stress might be expected. The values of $G_2(\omega,-\omega)$ along this line were quite small in relation to the peaks just cited. The exploration of the plane continued along lines of Ω_1 = a constant = k(0.046) rad/sec. in order to see if the quadratic response function was appreciable near the line $\Omega_2 \approx 2$. The net result of these investigations was an indication that the quadratic frequency response function relating stress and encountered wave is probably appreciable only in the vicinity of the line $\Omega_2 \approx$ springing frequency (Figure D-1). Unfortunately, all of the estimates which appeared significant were in a portion of the bi-frequency plane where previous work and the given input spectra indicated that large distortions due to sampling variability would be present. Essentially, the magnitude of a response to sub-harmonic frequencies cannot be estimated well unless there is some spectral content at the sub-harmonic frequencies. In the case of the present data the analysis indicated that if quadratic springing stress response was present, it would arise largely as the second harmonic response to wave components of frequency equal to half the springing frequency because the input wave spectrum becomes very small for frequencies a little less than half the springing frequency.

Estimates of the Magnitude of Quadratic Springing Response

In the analysis just described the result was a qualitative indication that there might, indeed, be some quadratic springing response, but the numerical values of the estimates of quadratic frequency response function were considered of marginal accuracy where they could be accepted at all. The objective herein was more to explore the magnitude of the influence than pin it down exactly, and in order to proceed it was assumed that the magnitude of the estimates was correct.

In so far as the low coherency results of the last appendix are concerned the most important thing is to assess the relative magnitude of the springing spectral density which might be contributed by the second term of Equation D-2. It may be noted in this equation that when the integrand involves a spectral density which is nil, it does not matter much what the value of the quadratic frequency response function is. In the present case spectral densities were considered negligible for frequencies less than 0.9, and this (with the previous analysis) means that the integral of the second term of Equation D-2 would for practical purposes be non-negligible only in the region bounded by wiggly lines in Figure D-1. This meant that only a relatively small portion of the quadratic frequency response function needs to be known. Thus, in order to produce some kind of estimate of the quadratic part of the stress spectrum, the estimated values of $|G_2(\omega_1,\omega_2)|$ were used in place of the true values implied by Equation D-2, and an integration over the domain $\omega_1 > 0.9$, $\omega_2 > 0.9$ was carried out numerically.

The results of this procedure are shown graphically in Figures D-2 through D-6 for each of the five runs of interest. Both deck and bottom bending were processed in each case. The estimated quadratic contribution (second term of Equation D-2) is shown as a solid line. The corresponding FFT spectra computed from the stress records (analysis A, $\Delta\omega = 0.046$ rps) is shown for comparison. A third estimate is shown by dashed lines. What this represents is the stress spectrum which would be predicted if the gain estimates from the cross spectral analysis of Appendix C are correct.

It happens (Reference 9) that a cross spectral analysis of a linear plus quadratic system (Equation D-1) ignores the quadratic term and thus cross spectral estimates of "gain" should reflect the linear frequency response without distortion. Thus if the hypothesis is made that the low coherencies noted in Appendix C arise solely because of quadratic nonlinearities, the observed spectrum should be the sum of the quadratic contribution and "(gain squared) times the wave spectrum". Figures D-2 through D-6 indicate clearly that this is not so. Quadratic nonlinearities appear at most to be only a part of the low coherency problem.

The quadratic spectral contributions shown in Figures D-2 through D-6 amount to between 5 and 15% of peak springing spectral density. Relatively, the contributions are larger for the deck than the bottom stresses. This should

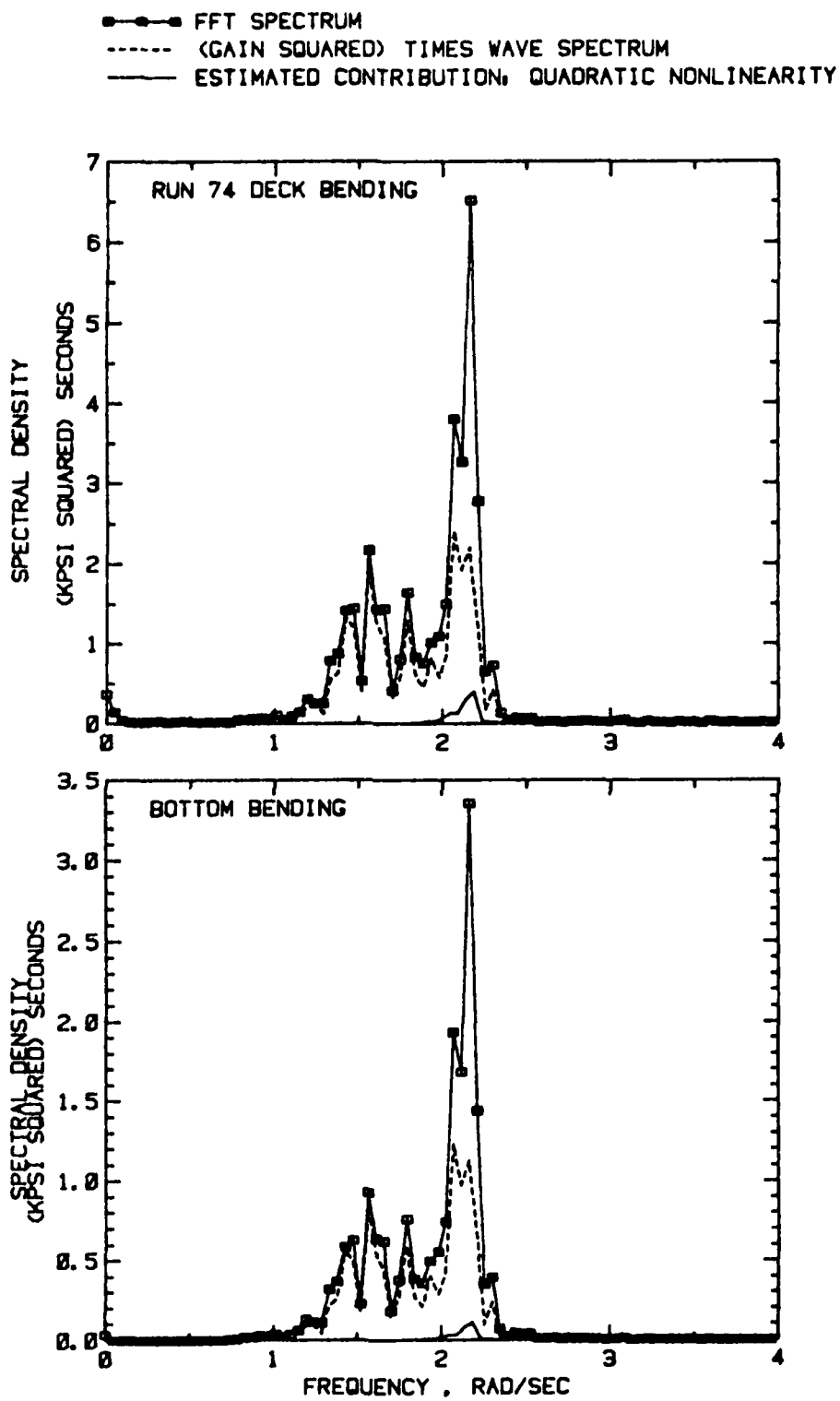

FIGURE D-2 RUN 74, QUADRATIC CONTRIBUTION TO SPRINGING STRESS SPECTRA

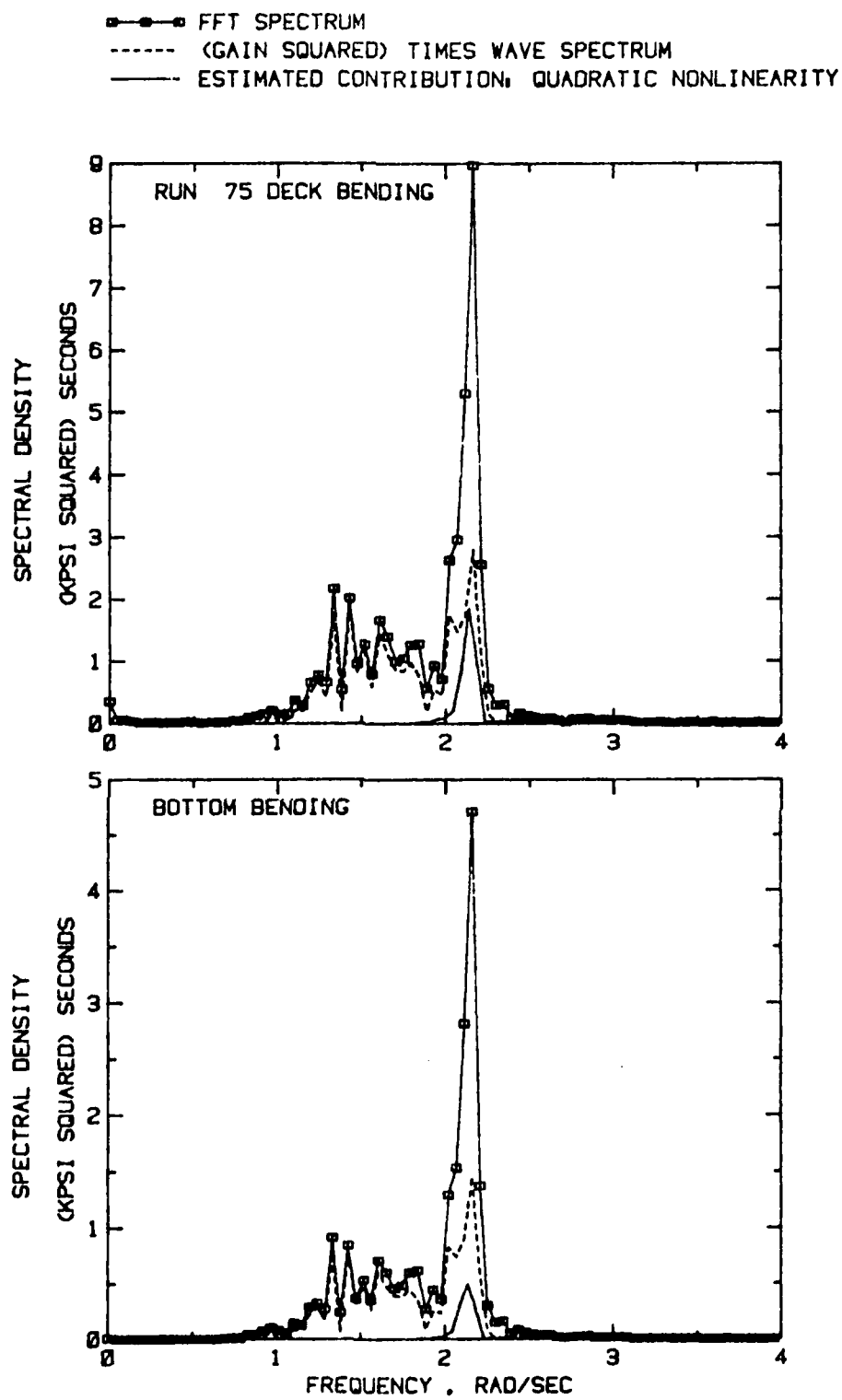

FIGURE D-3 RUN 75, QUADRATIC CONTRIBUTION TO SPRINGING STRESS SPECTRA

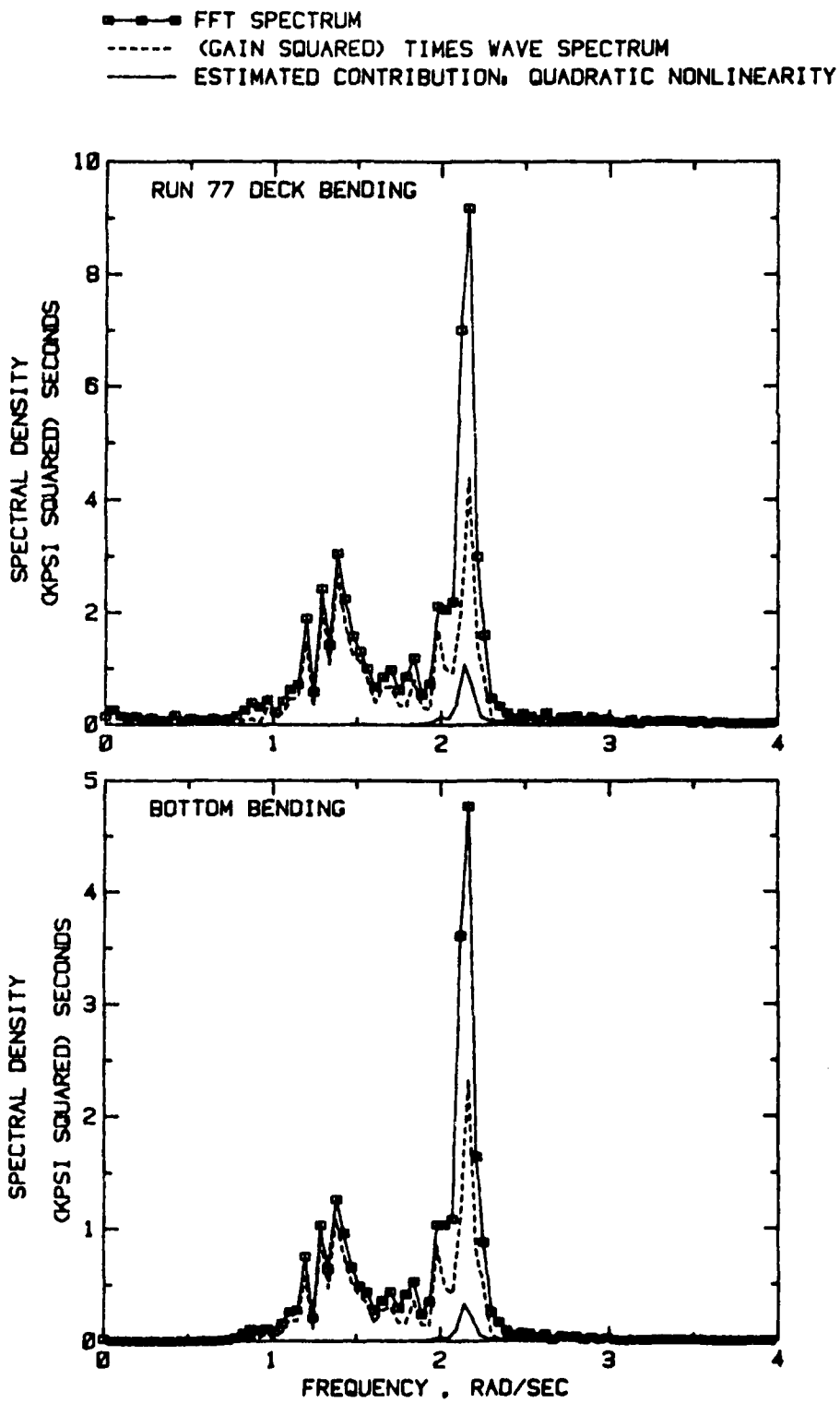

FIGURE D-4 RUN 77, QUADRATIC CONTRIBUTION TO SPRINGING STRESS SPECTRA

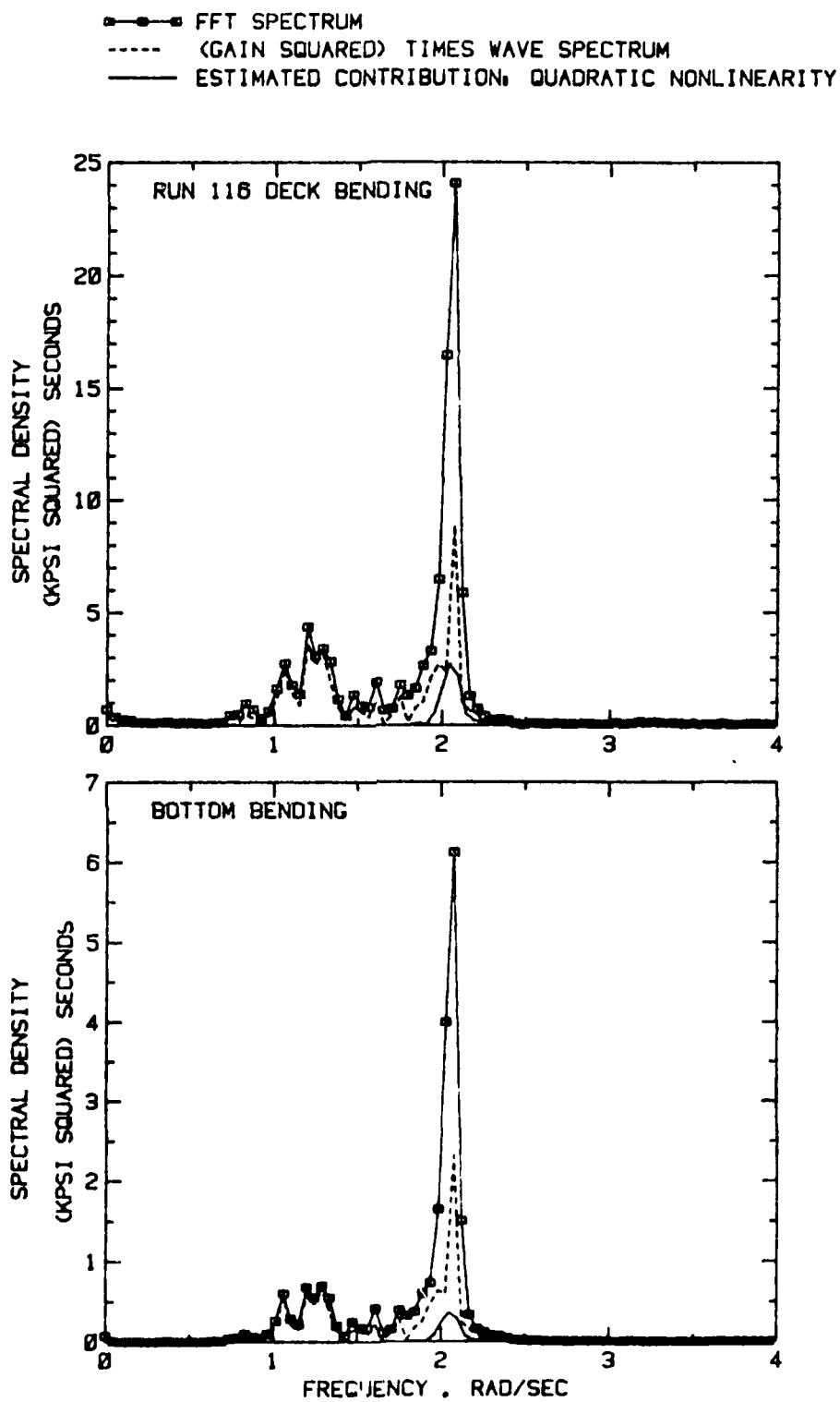

FIGURE D-5 RUN 116, QUADRATIC CONTRIBUTION TO SPRINGING STRESS SPECTRA

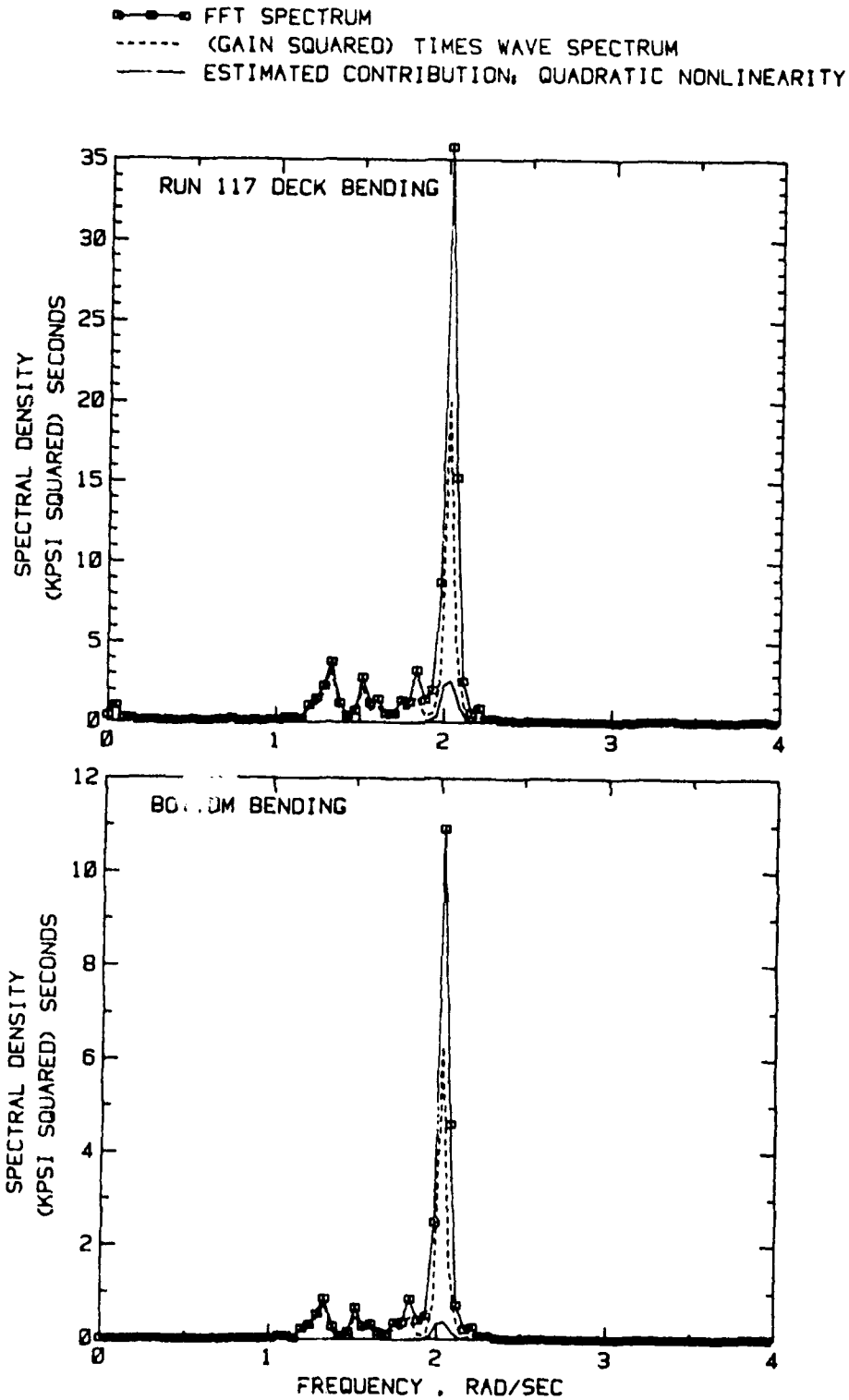

FIGURE D-6 RUN 117, QUADRATIC CONTRIBUTION TO SPRINGING STRESS SPECTRA

not be too surprising since the asymmetry in deck stress has some of the features of a linear plus quadratic system. If the deck stresses are asymmetric because of some extraneous quadratic instrumentation distortion, it might be expected that the quadratic contribution to deck bending stress spectra would be from this source, and the contributions to bottom bending spectra would be nil. However quadratic contributions are evident in the bottom bending as well.

As far as an exploration of possible quadratic stress response is concerned, the present data is not optimum because relatively little encountered wave spectral density is found at half the springing frequency. Given the low level of excitation it might not have been surprising to find no appreciable quadratic contribution for these data. If the present crude estimates are of the correct magnitude, the fact that the quadratic contribution to the stress spectra is visible in the present data is thought of potential significance. Quadratic response goes as the square of the input. Relatively much stronger quadratic response might be expected in the event that the waves become more severe than those experienced in the 1979 trials.

AD-A127 226 AN ANALYSIS OF FULL SCALE MEASUREMENTS ON M/V STEWART J CORT DURING THE 1..(U) STEVENS INST OF TECH HOBOKEN NJ DAVIDSON LAB J F DALZELL FEB 82 SIT-DL-81-9-2221 2/3

UNCLASSIFIED USCG-D-25-82 DTCG23-81-C-2031 F/G 13/10 NL

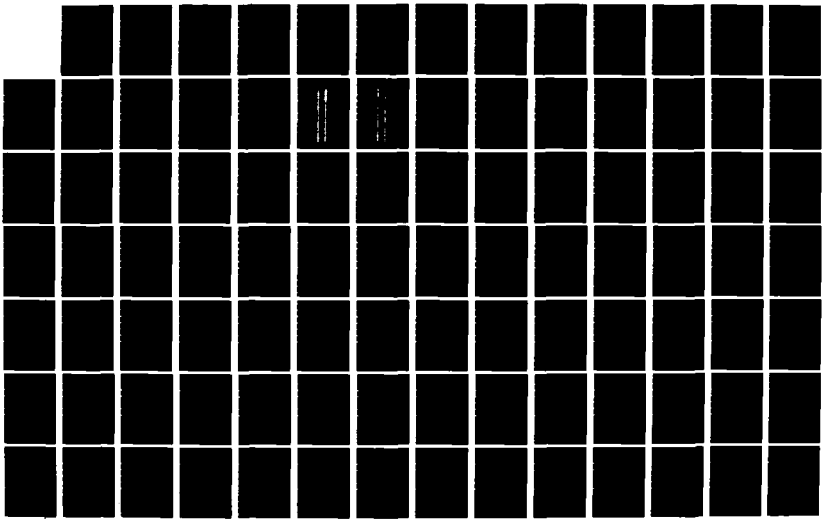

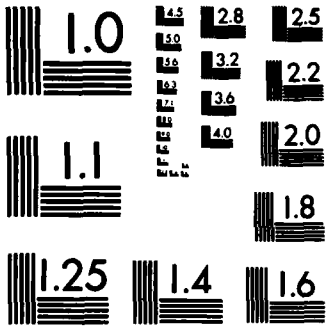

MICROCOPY RESOLUTION TEST CHART
NATIONAL BUREAU OF STANDARDS-1963-A

Technical Report Documentation Page

1. Report No.	2. Government Accession No.	3. Recipient's Catalog No.
CG-D-25-82		

4. Title and Subtitle	5. Report Date
AN ANALYSIS OF BOTTOM BENDING STRESS DATA OBSERVED ON M/V STEWART J. CORT DURING THE 1979 AND 1980 TRIAL PROGRAMS	February 1982
	6. Performing Organization Code
	8. Performing Organization Report No.
7. Author(s) J.F. Dalzell	SIT-DL-82-9-2257
9. Performing Organization Name and Address Stevens Institute of Technology Davidson Laboratory Castle Point Station Hoboken, NJ 07030	10. Work Unit No. (TRAIS)
	11. Contract or Grant No. DTCG23-81-C-20031
12. Sponsoring Agency Name and Address U.S. COAST GUARD (G-DMT-1/54) 2100 Second Street, SW Washington, DC 20593	13. Type of Report and Period Covered FINAL REPORT September 1981-February 1982
	14. Sponsoring Agency Code

15. Supplementary Notes This report documents Part II of a two part project. In support of the intention of the Coast Guard to print both reports in one volume, references to the first part of the project are made by citing "Part I". Part I of this contract was issued August 1981 as report SIT-DL-81-9-2221.

16. Abstract

The purpose of the work documented herein was to continue the qualification of a previously developed numerical simulation of combined, springing and wave induced stresses. Previous qualification efforts had been inconclusive with respect to main deck bending stresses observed in the 1979 trials of the M/V STEWART J. CORT. Subsequently uncovered problems with the main deck bending measurement suggested that the bottom bending stress information should be more suitable, and accordingly, the present analysis has been made with bottom bending stress data from the 1979 and 1980 trials. It was found that the numerical simulation was credible with respect to this data. Essentially, the statistics derivable from typical samples of observed and simulated data are statistically indistinguishable. Because the basic assumptions of the simulation are identical to the state-of-art statistical model which is employed for combined wave induced and springing response, this finding re-inforces the state-of-art approach.

17. Key Words	18. Distribution Statement
Longitudinal Strength Great Lakes Waves Bulk Carriers Vibration Stress Stress Combinations Springing Stress Wave Induced Stress	Document is available to the public through the National Technical Information Service, Springfield, VA 22161.

19. Security Classif. (of this report)	20. Security Classif. (of this page)	21. No. of Pages	22. Price
UNCLASSIFIED	UNCLASSIFIED	106	

Form DOT F 1700.7 (8-72) Reproduction of completed page authorized

INTRODUCTION

The provision of adequate longitudinal strength standards for the stresses produced by wave induced vibration is particularly important for Great Lakes ships since the vibratory stress (springing) levels experienced have been found to be of significantly greater magnitude relative to wave induced stresses than the vibratory response of most ocean going vessels. The present work is a contribution to an ongoing USCG research program for Great Lakes ore carriers.

Under contract to the U.S. Coast Guard, David W. Taylor Naval Ship Research and Development Center (DTNSRDC) performed full scale measurements on board the M/V STEWART J. CORT during the fall of 1979. During the data analysis phase, RAO's (response amplitude operators) were developed from the stress and wave measurements which were then compared with theoretical RAO's computed by American Bureau of Shipping, Webb Institute of Naval Architecture, the University of Michigan and Det Norske Veritas. The results of the work are contained in Reference 1*.

An abbreviated continuation of this trial program was carried out by the Coast Guard in the fall of 1980, Reference 11. The emphasis in this program was upon validation of the wave measurement devices rather than the gathering of stress data. Nevertheless, main deck and bottom bending stress data was recorded. It appeared at the outset of these trials that the deck bending bridge was malfunctioning, and this finding suggested that the peculiar asymmetry later found in the 1979 main deck bending stress in Reference 2 was due to some sort of instrumentation failure. The bottom bending stresses recorded in the 1980 trials were, however, considered free of similar problems.

The purpose of the work performed under the present contract was two-fold. An extension of the 1979 trials program was planned for 1981. The primary purpose of the first part of the present work was to link the 1979 and the projected 1981 full scale wave and stress measurements with an independent review of the 1979 data. The intent

*References on Page II-101

was to build upon the research performed to that time. The emphasis in this part of the work was upon the question of sampling variability of the estimates produced in Reference 1, and upon exploratory alternate analyses of the data. Part I summarizes these efforts. Among the recommendations of Part I for the 1981 trials was one that it might be useful to characterize the level of springing which occurs in the absence of waves since some tenuous evidence of nearly periodic springing response was found.

The present report describes the work performed in support of the secondary objective of the present contract. Because of the asymmetry found in the 1979 deck bending stresses in the simulation study of Reference 2, it had to be concluded that the credibility of that simulation was not completely resolved. The problems with the main deck bending bridge found in Reference 11 suggested that the qualification of the simulation would have been more realistically carried out with the bottom bending stress channel from the 1979 data. Thus the objective of the second part of the present work was to continue the validation of the simulation methods of Reference 2, using bottom stress data from both the 1979 and 1980 trials, in order to extend if possible the present ideas about the method of combination of wave induced and springing stresses.

In documenting the present work it has been found convenient to follow the Summary/Appendix report organization. In this style the main body of the report consists of an overview and summary of findings. Following the brief main body of the report are a series of Appendices which contain the detail of the work.

OVERVIEW

The details of the present work are contained in Appendices A through G.

The first step in the present work was to choose a total of 20 data runs, 10 each from the 1979 and the 1980 trials program, and extract, calibrate, and qualify the bottom bending stress records observed in each run. Appendices A and B document the choice of records, the associated log book data, and the necessary pre-processing of the records as required for the present analysis.

One of the records selected for analysis from the 1980 trial data was a run at zero ship speed. This run was of interest in the context of the inference of Part I that a small part of the springing response was perhaps the result of propeller excited vibration. Accordingly, the opportunity was taken to perform a brief autocorrelation analysis on this run as a possible complement to the analysis of Part I, and the results of this brief diversion are summarized in Appendix C.

In order to carry out the comparisons with simulations which were the objective of the present work it was necessary to carry out three basic processing operations on the observed time histories. These operations include: Spectral Analysis; Filtering operations to derive time histories of springing and wave induced stresses from the observed combined stresses; and a peak finding operation to define all the maxima and minima in each resulting record. Documentation of methods and the results of this phase are contained in Appendix D.

Methods for the simulation of time history data and the development of raw statistics of maxima are documented in Reference 2, and were the methods employed herein. Appendix E describes the organization of the present simulation. Conceptually, the 20 pieces of observed data which form the starting point of the present work are each a short term sample from an infinite population. The present simulation was

designed to mimic this situation by producing one randomly drawn simulation for each of the twenty conceptual populations which are defined by the observed stress spectra.

Virtually all of the objective inferential procedures which may be brought to bear on the problem of comparing the statistics of maxima observed and simulated require that each sample of maxima be randomly drawn. When all the maxima in a stress record are considered this requirement is almost always violated. Thus it was necessary to examine each of the sets of maxima and minima in the present data for evidence of statistical independence. Little was found, and it was necessary to work out an approach to analysis which would remove the problem or at least blunt its more serious consequences. Appendix F documents the approach (which is not new, Reference 12) as well as some indirect comparisons between observation and simulation which were a by-product.

The last part of the work is documented in Appendix G. In essence what was done was to hypothesize that the observed stress maxima and minima followed the theoretical probability density which is derived from the basic assumption that the stresses are ergodic Gaussian processes--and then apply several standard statistical test procedures which are designed to provide relatively objective means of accepting or rejecting the hypothesis. The simulated maxima and minima must follow the theoretical probability density by the basic assumptions of the simulation method. Throughout the analysis observed and simulated data were treated in exactly the same manner, with the result that numerous relatively direct statistical comparisons could be made.

FINDINGS

In the single unplanned diversion of the present work, the autocorrelation analysis of a single zero ship speed record, the decay time of the autocorrelation was found to be about as long as in the at-speed conditions treated in Part I. Less indication of a peridocity was evident, but overall no radical qualitative difference. The result does not rule out propeller excited vibration as a cause of the long decay of the autocorrelation functions of Part I, but suggests that it is less likely than implied in that reference.

The discovery of asymmetry in the 1979 main deck bending stress records in Reference 2 was the main reason for questioning the simulation in that reference, though no such problem seemed to exist in the pre-1979 data. The present analysis included only bottom bending stress data from 1979 and 1980 trials because it appeared subsequently that the main deck bending transducer was malfunctioning. However, a statistically valid systematic asymmetry between maxima and minima in any observation has a most serious effect on the credibility of the methods of Reference 2. Throughout the present analysis the data has been examined for evidence of asymmetry. At no stage in the analysis were significant differences between the statistics of observed maxima and minima found. This is not to say that there were no differences, but that what differences there were appeared to be generally less than the uncertainty which is introduced by sampling variability. The same conclusion is arrived at by comparing the magnitude of the differences between simulated maxima and minima with those observed. In effect the apparent level of statistical symmetry is the same for the observations of bottom bending stress as it is for the simulated process which is known to be symmetric.

In the analysis three approaches were made to checking that the "goodness of fit" of the sampled maxima and minima (both observed and simulated) to the theoretical distribution of maxima of an ergodic Gaussion process. The simulated maxima and minima should of course

follow this distribution because the simulation methods follow the ergodic Gaussian model to a high degree of accuracy. The first basic finding was that the fit of the observed data to the theoretical distribution is statistically indistinguishable from the fit of simulated data. The second basic finding is that the hypothesis should generally be accepted that the observed maxima and minima fit the theoretical probability density. This last finding is identical to the findings in Reference 12 where data from several smaller lakes vessels was considered.

A final statistical study was made upon the extremes in each sample (the largest maximum and the smallest minimum). Differences between the simulated and observed extremes appear statistically insignificant when compared to the probable magnitude of sample to sample variability. It appeared also that the magnitude of the observed sample extremes was what might reasonably be expected in samples of the given size if the maxima follow the hypothesized theoretical density.

The net effect of the above findings is that the simulation methods of Reference 2 appear to be credible with respect to the bottom bending stress records analyzed herein. However, none of these records represent particularly severe wave conditions, or high stresses relative to the most severe conditions which have been measured on the CORT. Credibility of the simulation with respect to these latter conditions has been addressed in Reference 2.

The state-of-art statistical model which has been adopted for the combined stress response is that it may be represented by an ergodic Gaussian process. Consequently the theoretical probability structure of the maxima and minima of the stresses is known. The work herein confirms that this statistical model for stress maxima is reasonable, and thus tends to reinforce the state-of-art approach.

APPENDIX A

SELECTION AND PREPROCESSING OF 1979 TRIAL DATA

Introduction

The general objective was to select 10 of the more than 100 data runs recorded in Reference 1 for the present analysis. In Reference 1* eight particular runs were selected for special treatment (Runs 77, 81, 90, 99, 101, 116, 117, and 119) on the basis of either high springing stresses or relatively high seas, and it was of interest to include these in the 10 finally selected. In order to acquire the data for the present work, four digital data tapes from the 1979 season were furnished by the Coast Guard.

Selection of the Data Runs

Unfortunately the digital data tapes involved are written in a highly machine dependent format and are at best a trial to translate for use in the Stevens DEC-10 computer system. The four tapes of interest were numbers 4 through 7. As matters turned out Tapes 4 and 7 were physically the same duplicates previously furnished in support of Reference 2* so that data Runs 68 through 77 and 116 through 118 were available as well as all that could be recovered from these tapes since Run 119 (one of the special runs) had never been duplicated. Tape 5 contains Runs 80 through 91 of the 1979 program. This tape as furnished was evidently the original and was completely unreadable on the available machinery. Tape 6, which was a duplicate, contains Runs 93 through 109 of

---

*1. Swanek, R. A. and Kihl, D. P., "Investigation of Springing Responses on the Great Lakes Ore Carrier M/V STEWART J. CORT," Structures Department, David W. Taylor Naval Ship Research and Development Center, CG-D-17-81, December 1980, NTIS AD A100 293.

*2. Dalzell, J. F., "Numerical Simulation of Combined, Sprining and Wave Induced Stress Response," Davidson Laboratory Report SIT-DL-81-9-2141, Coast Guard Report CG-M-6-81, August 1981.

the program and could be completely read. The net result of these very practical matters was that of the eight special runs of Reference 1, Runs 77, 99, 101, 116, and 117 were available, and these were the obvious choices for 5 of the 10 runs. In Part I a parallel analysis of deck and bending stress had been carried out for five runs (including three of the above) and it was thought worthwhile for the sake of continuity to continue with these. This left the problem of selecting three runs from Tape 6 in addition to Runs 99 and 101. The log data of Reference 1 suggested that the runs immediately adjacent to numbers 99 and 101 were of the most interest on the basis of essentially head and relatively high seas so that the final selection for this tape became Runs 99 through 103. The log data for the ten runs thus selected is summarized in Tables A-1a and A-1b. Also included is the rms bottom bending stress derived from the spectral analyses to be described.

Preprocessing of Data

As noted in Reference 2 and Part I many of the analyses to be carried out involved Fast Fourier Transform processing. In the 1979 trials the sampling interval was 0.1 seconds and the record was 15000 points in length--too short for a 16K FFT analysis, and too long for a single 8K analysis. It had been found in both References 1 and 2 that the 0.1 second interval is unnecessarily short. For present purposes the filtering/decimation scheme developed in Reference 2 was employed as a first processing step.

Accordingly, the following operations were carried out on the bottom bending stress channel of the ten runs noted in Table A-1:

1. Filter each time series with a recursive 6-pole sine-butterworth low pass digital filter. The characteristics

TABLE A-1a

LOG-DATA FOR THE 1979 RUNS SELECTED FOR ANALYSIS

RUN	74	75	77	116	117
Data Tape	4	4	4	7	7
Date	16-Nov-79	16-Nov-79	16-Nov-79	9-Dec-79	9-Dec-79
Time	10:02	10:10	10:26	13:42	15:04
Ship Position:					
Lake	Superior	Superior	Superior	Michigan	Michigan
North Latitude	47° 22'	47° 21'	47° 15'	44° 8'	43° 20'
West Longitude	89° 0'	89° 5'	89° 20'	87° 7'	87° 13'
Ship Draft (mean, ft.)	20.6	20.6	20.6	27.0	27.0
Load Condition	Ballast	Ballast	Ballast	Full Load	Full Load
Ship Speed (mph)	14.7	14.4	14.4	13.5	13.5
Heading	256°	256°	256°	189°	188°
Wind Direction	235°	240°	240°	247°	263°
Wind Speed (kt)	29	29	29	18	14
Wave Direction	250°	250°	250°	212°	198°
Estimated Wave Height, ft.	6	6	6	4	3
RMS Bottom Bending Stress (kpsi)	.92	1.01	1.09	1.02	1.10

TABLE A-1b

LOG-DATA FOR THE 1979 RUNS SELECTED FOR ANALYSIS

RUN	99	100	101	102	103
Data Tape	6	6	6	6	6
Date	5-Dec-79	5-Dec-79	5-Dec-79	5-Dec-79	5-Dec-79
Time	14:11	14:16	14:53	15:27	16:17
Ship Position:					
Lake	Superior	Superior	Superior	Superior	Superior
West Longitude	88° 0'	88° 5'	88° 20'	88° 55'	88° 50'
North Latitude	47° 35'	47° 35'	47° 30'	47° 25'	47° 25'
Ship Draft (mean, ft.)	19.0	19.0	20.6	20.6	20.6
Load Condition	Ballast	Ballast	Ballast	Ballast	Ballast
Ship Speed (mph)	11.6	11.6	11.6	11.6	15.5
Heading	270°	270°	260°	260°	260°
Wind Direction	270°	270°	350°	350°	340°
Wind Speed (kt)	15	15	27	27	28
Wave Direction	270°	270°	240°	[illegible]	240°
Estimated Wave Height, ft.	5	5	5	[illegible]	6
RMS Bottom Bending Stress (kpsi)	.88	1.00	1.12	.98	.97

of this filter include:

- 0.1% or less attenuation of signal and sensibly linear phase shift from D.C. to 0.6 Hertz.
- Nominal cutoff frequency 1.4 Hertz.
- 98.5% or more attenuation of signal between 3.33 and 5.0 Hertz.

2. Perform the 1 1/2th point decimation procedure described in Reference 2 on each time series.

The effect of these operations is first to eliminate signal content between 3.33 and 5.0 Hertz so as to minimize the possibility of aliasing, and then to create a shorter time series which has a time step of 0.15 seconds rather than 0.1 seconds, and a folding frequency of 3.33 Hertz rather than 5.0 Hertz. The first 2^{13} points of the resulting series represent 20 1/2 minutes of the original 25 minutes of data; that is, a loss of 18% of the original data was accepted in order to facilitate the projected analyses.

The practical result of this preprocessing was ten new bottom bending stress data files. These preprocessed time series were the starting point in all the subsequent analyses of the 1979 data.

Examination of Basic Time Domain Data

An examination of the basic data for nonsense had been carried out for the 5 runs of Table A-1a in Part I. Compressed plots for Runs 99 and 101 are shown in Reference 1. All these data are reasonable in appearance, and it was thought adequate to examine the time domain data for Runs 100, 102, and 103 only in the vicinity of the maximum stress since it is the maximum apparent stress which is most likely to be nonsense. The results will be presented later, but the conclusion was that these runs were also of reasonable quality.

APPENDIX B

SELECTION AND PREPROCESSING OF 1980 TRIAL DATA

Introduction

The results of the 1980 trials program, Reference 11*, involve 36 data runs recorded on five digital tapes. The original tapes were furnished by the Coast Guard for present purposes. Some analyses were made in Part I of 16 of these runs. The objective was to select 10 of the 1980 runs for the present project, emphasizing runs already analyzed in Reference 11.

Selection of Data Runs

A simple tabulation for each run of headings and wave heights from the log-data suggested that the contents of Tape 4 would be of little interest (and was evidently of little interest in Reference 11). Accordingly it was decided to try to read everything on 1980 Tapes 1, 2, 3, and 5. Some incompatability between the run format on the data tapes and what is expected by the Stevens systems software was evident. None of the five runs on Tape 5 could be recovered, nor could one run on each of Tapes 1, 2, and 3. Three runs read were short or had been aborted during the trials. Excluding these, the net practical result was that just 15 runs were available from which to make a choice of 10 (Runs 2, 3, 4, 5, 7, 8, 11, 13, 14, 15, 16, 17, 18, 20, and 21).

The 1980 trials included two pieces of data of interest in the context of the Recommendations of Part I that data under calm conditions would be of interest. The first was Run 10, which was apparently taken in seas of 1 foot height, and the other was Run 8 which was taken (mostly) at zero ship speed. Run 10 was unreadable,

---

*11. Walden, D. A. and Noll, M. D., "Springing Research of a Great Lakes Ore Carrier," Coast Guard Report No. CG-D-13-82, April 1981.

but Run 8 was available so that this run was accepted as one of the ten.

Preliminary spectral analyses were made of all 15 of the available runs to aid in the selection. Runs 2, 7, 11, 17, and 18 showed little, and in some cases negligible, wave induced stress response, and the final selection on this basis boiled down to Runs 3, 4, 5, 8, 13, 14, 15, 16, 20, and 21. The log-data for these runs is summarized in Tables B-1a and B-1b. Also included are RMS bottom bending stresses from the spectral analyses to be described.

Preprocessing of Data

Two minor differences in data recording between the 1979 and 1980 trials exist. In the 1979 trials the calibrations were imbedded in the data tapes, while they were not in the 1980 trials. The Coast Guard furnished the only calibration required for the present analysis, that for bottom bending stress, as 19.21 psi/computer count. The other difference is that the records were 1800 seconds in length instead of 1500, thus with the same sampling interval of 0.1 seconds, the 1980 time series were 18000 points in length. As in the case of the 1979 data a filtering and decimation scheme was employed to include as much data as possible in an 8192 point array. The following operations were carried out on the bending stress channel of the ten runs noted in Table B-1:

1. Filter each time series with a recursive 6-pole sine-butterworth low pass digital filter. The characteristics of this filter include:

   - 0.1% or less attenuation of signal and sensibly linear phase shift from D.C. to 0.5 Hertz.
   - Nominal cutoff frequency 1.2 Hertz.
   - 98.5% or more attenuation of signal between 2.85 and 5.0 Hertz.

TABLE B-1a

LOG-DATA FOR THE 1980 RUNS SELECTED FOR ANALYSIS

RUN	3	4	5	8	13
Data Tape	1	1	1	2	3
Date	23-Oct-80	23-Oct-80	23-Oct-80	25-Oct-80	18-Nov-80
Time	11:02	11:27	14:45	11:26	19:52
Ship Position:					
Lake	Superior	Superior	Superior	Superior	Superior
North Latitude	47° 35'	47° 35'	47° 20'	43° 26'	47° 29'
West Longitude	80° 55'	80° 55'	86° 45'	87° 10'	88° 21'
Ship Draft (mean, ft.)	27.0	27.0	27.0	27.0	17.0
Load Condition	Full Load	Full Load	Full Load	Full Load	Ballast
Ship Speed (mph)	11.7	11.7	11.1	0.0	10.9
Heading	106°	106°	113°	275°	258°
Wind Direction	135°	135°	126°	285°	260°
Wind Speed (kt)	32	32	32	30	34
Wave Direction	120°	120°	126°	195°	258°
Estimated Wave Height, ft.	7	7	8	4	4
RMS Bottom Bending Stress (kpsi)	1.10	1.12	1.28	.36	.97

TABLE B-1b

LOG-DATA FOR THE 1980 RUNS SELECTED FOR ANALYSIS

RUN	14	15	16	20	21
Data Tape	3	3	3	3	3
Date	18-Nov-80	18-Nov-80	18-Nov-80	20-Nov-80	20-Nov-80
Time	20:01	20:08	22:59	14:46	18:47
Ship Position:					
Lake	Superior	Superior	Superior	Superior	Superior
North Latitude	47° 28'	47° 26'	47° 24'	47° 28'	47° 17'
West Longitude	88° 31'	88° 38'	88° 38'	87° 14'	86° 32'
Ship Draft (mean, ft.)	17.0	19.0	19.0	27.0	27.0
Load Condition	Ballast	Ballast	Ballast	Full Load	Full Load
Ship Speed (mph)	10.9	8.5	10.9	11.4	11.4
Heading	258°	258°	258°	112°	114°
Wind Direction	260°	260°	270°	140°	183°
Wind Speed (kt)	34	28	26	16	12
Wave Direction	258°	258°	258°	147°	150°
Estimated Wave Height, ft.	4	4	4	3	3
RMS Bottom Bending Stress (kpsi)	.91	1.02	1.06	.55	.52

2. Decimate the time series by using every other point.

The effect of these operations is first to eliminate signal content between 2.85 and 5.0 Hertz so as to minimize the possibility of aliasing, and then to create a shorter time series which has a time step of 0.20 seconds reather than 0.1 seconds, and a folding frequency of 2.5 Hertz rather than 5.0 Hertz. The first 2^{13} points of the resulting series represent 27.3 minutes of the original 30 minutes of data; that is, a loss of 9% of the original data was accepted in order to facilitate the projected analyses.

The practical result of this pre-processing step was ten new data files. These pre-processed time series data were the starting point in the subsequent analyses of the 1980 data.

Examination of Basic Time Domain Data

The first operation was to plot and examine the data for Run 8, the zero speed run, because the comments in the experimental log implied that the ship had got up speed and changed course about 20 minutes into the run. Figure B-1 is the result. There is clearly a radical increase in stress level at around 24 minutes, and it seemed within reason to assume that the last 5 minutes of the run were not at zero speed as billed. Accordinly, the original record was re-filtered and decimated according to the scheme used on the 1979 data, Appendix A. The effect of this was to retain only the first 20 minutes of the record. Figure B-2 is a plot of the bottom bending stress time history after this revised pre-processing step.

Some of the other time histories of interest had been plotted in the preparation of Reference 11, so that for present purposes only an examination of each of the ten records near the time of maximum stress was carried out, and all records appeared qualitatively reasonable.

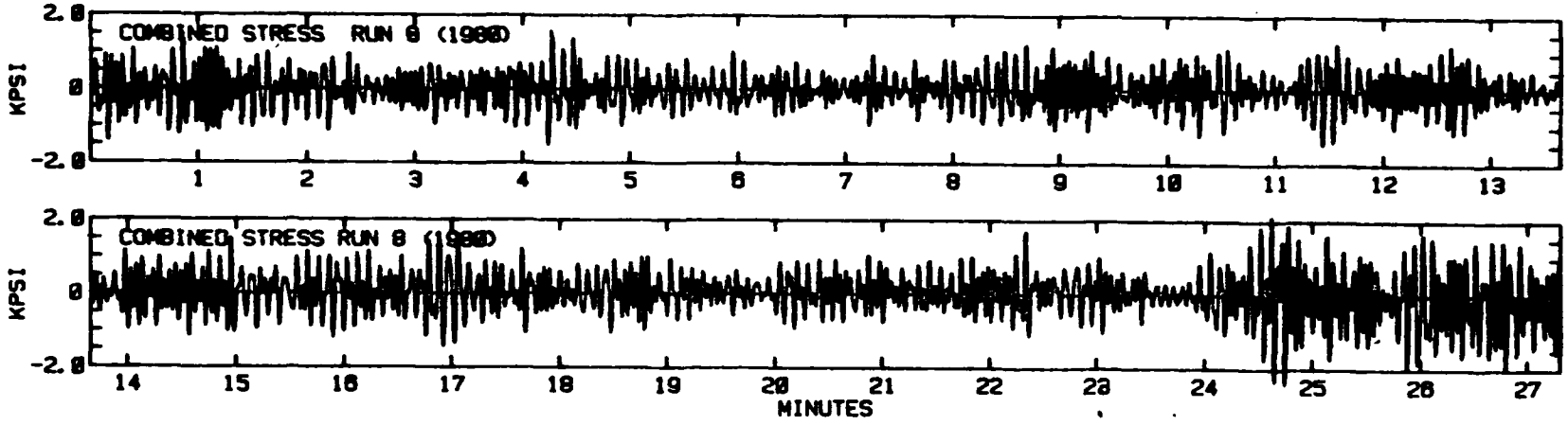

FIGURE B-1 TIME HISTORY OF COMBINED BOTTOM BENDING STRESS, RUN 8, ORIGINAL FILTERING AND DECIMATION

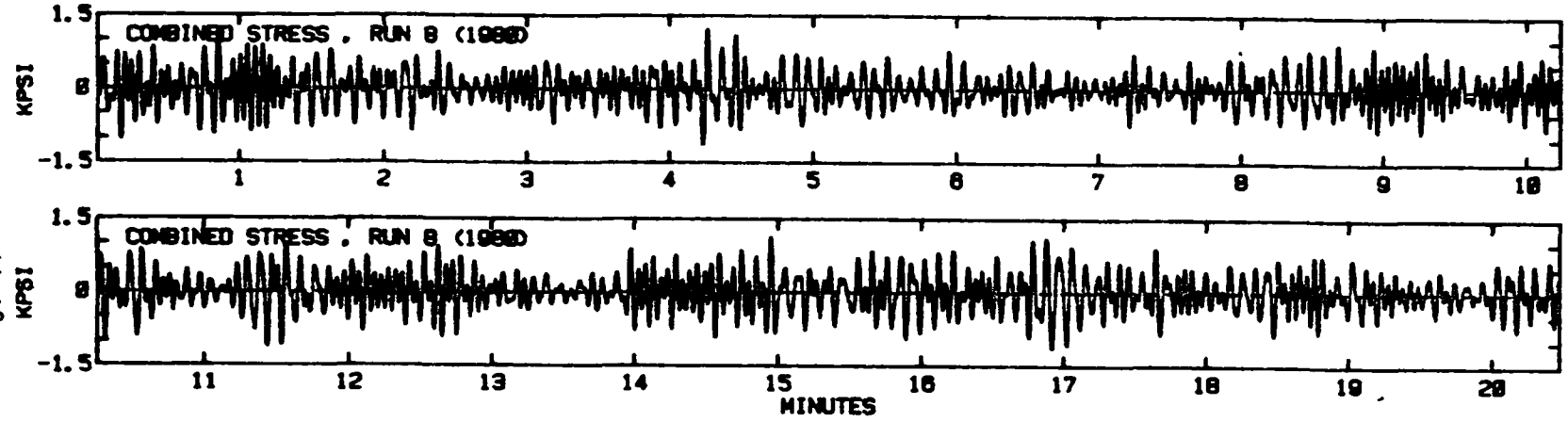

FIGURE B-2 TIME HISTORY OF COMBINED BOTTOM BENDING STRESS, RUN 8, REVISED FILTERING AND DECIMATION

APPENDIX C

AUTOCORRELATION ANALYSIS OF RUN 8 OF THE 1980 TRIALS

Introduction

In Part I an inference was drawn from an autocorrelation analysis that a small part of the springing stress response was nearly periodic, perhaps the result of propeller excited vibration rather than of wave action. This inference resulted in the recommendation to look for some calm water data in the 1981 trials. As has been noted, two runs of the 1980 trials were of interest in this context. One of these runs was conveniently available and the opportunity was taken to make a brief autocorrelation investigation of this run.

Autocorrelation Analysis of Run 8

Given the final form of the time history data for Run 8, Figure B-2, the programming used in the autocorrelation analyses of Part I was applicable without modification. These programs were applied to the Run 8 bottom bending stress data to compute the normalized autocorrelation function out to 200 lags of 0.75 second time intervals. The result is shown in Figure C-1.

Commentary

Comparison of Figures B-1 through B-5 of Part I with the present Figure C-1 indicates that the decay time of the autocorrelation function is about as long at zero ship speed (very low or no propeller revolutions) as it is when the ship is proceeding in waves. There is less indication of an almost periodicity shown in Figure C-1 than in some of the records of Part I, but overall no radical qualitative difference. Because the stress level in Run 8 is about a third of that of the runs of Part I the present results does not rule out propeller excited vibration as a cause of the long decay of the autocorrelation function but suggests that it is less likely than implied in Part I.

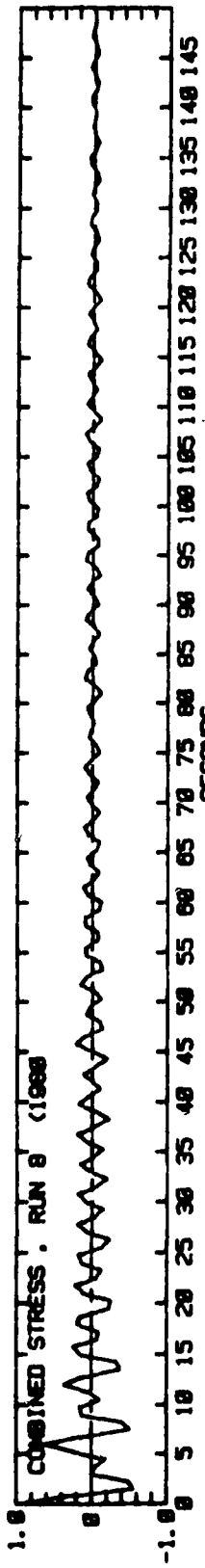

FIGURE C-1 NORMALIZED BOTTOM BENDING STRESS AUTOCORRELATION FUNCTION--RUN 8

APPENDIX D

BASIC PROCESSING

Introduction

In order to carry out comparisons with simulations as described in Reference 2 it was necessary to carry out three basic data processing steps on each of the 20 bottom bending stress time histories. These are:

1. Spectral Analysis
2. A filtering operation to derive from the given combined stress time history, the time histories of "wave induced" and "springing" stresses.
3. A peak finding operation to define and store all the maxima and minima of each of the three time histories developed in Step 2.

Spectral Analysis

The analysis of each bottom bending stress time history was carried out by the Fast Fourier Transform with frequency smoothing method outlined in Reference 6*, and utilized in the cross-spectral analyses of Part I. The sharp springing stress peaks in the present data require better resolution than the present lengths of sample can supply with the desirable 30 or more degrees of freedom per spectral estimate so that more than the usual compromise on analysis parameters was necessary. It was decided to use 24 degrees of freedom per spectral estimate throughout the analyses. This decision results in 90% confidence bound multipliers on spectral esimates of 0.66 and 1.73. In order to get this amount of stability, 12 adjacent values of the raw FFT spectrum must be averaged. Evaluation of the average was carried out at intervals of 6 raw FFT's which produces

---

*6. Bendat, J. S. and Piersol, A. G., "RANDOM DATA: Analysis and Measurement Procedures," John Wiley and Sons, Inc., 1971.

a slightly smeared spectrum similar to that produced by the Tukey autocorrelation method. The resulting frequency resolutions and statistical bandwidths worked out as follows:

	1979 Data, Plus Run 8 (1980)	1980 Data (Excluding Run 8)
Delta Frequency	0.0307 RPS (.005 Hz)	0.023 RPS (0.0036 Hz)
Statistical Bandwidth	0.0614 RPS (.01 Hz)	0.046 RPS (0.0073 Hz)

The resulting 20 bottom bending stress spectra are shown in the top part of Figures D-1 through D-20 which are grouped at the end of this appendix. The spectral estimates are shown as crosses and these are connected by straight lines. Spectral densities for frequencies greater than 3 radians/second were generally much smaller than the smallest shown on the plots and have been omitted. Spectral areas are equal to the sample variance.

The numerical values of spectral density shown in Figures D-1 through D-20 are essentially the input data to the time domain simulator of Reference 2. An additional piece of information is required and that is a "cut-off" frequency which separates the frequencies associated with "springing" from those associated with "wave induced" stresses. The cutoff frequencies were selected by inspection and are indicated in the Figures by vertical dashed lines typically located at 1.9 radians/second.

Development of Springing and Wave Induced Stress Time Histories

The details of the method of separating the combined stress into its springing and wave induced components are contained in Reference 2. Briefly, the method utilized is "Fast Convolution" type filtering. The cutoff frequency defines ideal low and high pass filters which are applied in the frequency domain to the direct Fast Fourier Transform of the data. The inverse transform then yields the filtered time histories. (This is the primary reason for the decimation of the original data into 8192 (2^{13}) point time histories.) In the present case

virtually the same programs were used to produce the filtered time histories as were used in Reference 2.

In addition to confirming that the original time history contains no obvious nonsense, it is comforting to check the filtering operation graphically. To this end a "representative" two minute sample of each time history was plotted. These results are contained in the lower part of Figures D-1 through D-20. In each figure the maximum combined stress excursion found in the sample is centered in the two minute frame. Positive stress excursions mean increasing tension, zero stress is the sample mean.

Generation of Maxima and Minima

Given the filtered time histories, the last step in the basic processing is to find and store all the maxima and minima in each record for later use. This was done in accordance with the programs and conventions of the "Data Base Generator" described in Appendix C to Reference 2, so that at the conclusion the raw statistics for each of the 20 runs were stored in exactly the same form as the simulation results.

The peak finding operation is somewhat sensitive to noise. The analyses of Reference 2 indicated that this was not a problem with typical 1979 data. To confirm that the operation was successful with the 1980 data, half cycle count analyses were performed on Runs 3, 8, and 15 in accordance with the description of Reference 2. The results are included herein as Figures D-21 through D-23, and indicate that the 1980 data is no different than the 1979 data in-so-far as noise is concerned. The results also confirm that the bottom bending stress is reasonable statistically symmetric.

Commentary

Nothing really unexpected qualitatively appears in the spectra or the time histories. The typical spectrum involves a sharp peak at

the springing frequency, and typically a relatively low level of wave induced stress. This is probably to be expected since no exceptionally severe waves were encountered in either trial program. In so far as the relative magnitudes of springing and wave induced stress are concerned, Run 8 most closely resembles the most severe conditions measured on the CORT (Interval 43, May 1973), Reference 3, but the rms stress for Run 8 is about a tenth as great. In all cases results for groups of runs which were taken the same day are qualitatively the same.

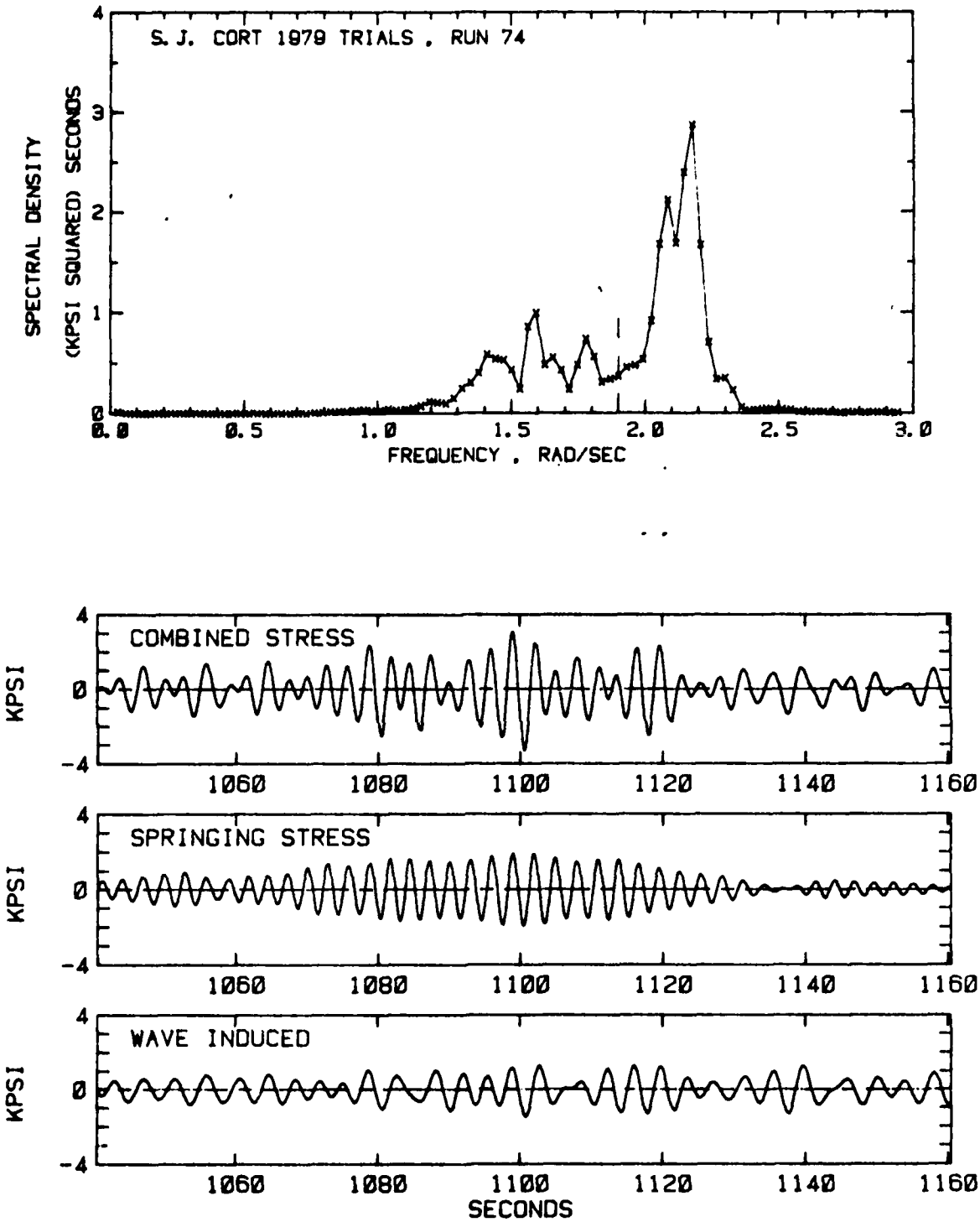

FIGURE D-1 BOTTOM BENDING STRESS SPECTRUM AND REPRESENTATIVE TIME HISTORIES--RUN 74 (1979)

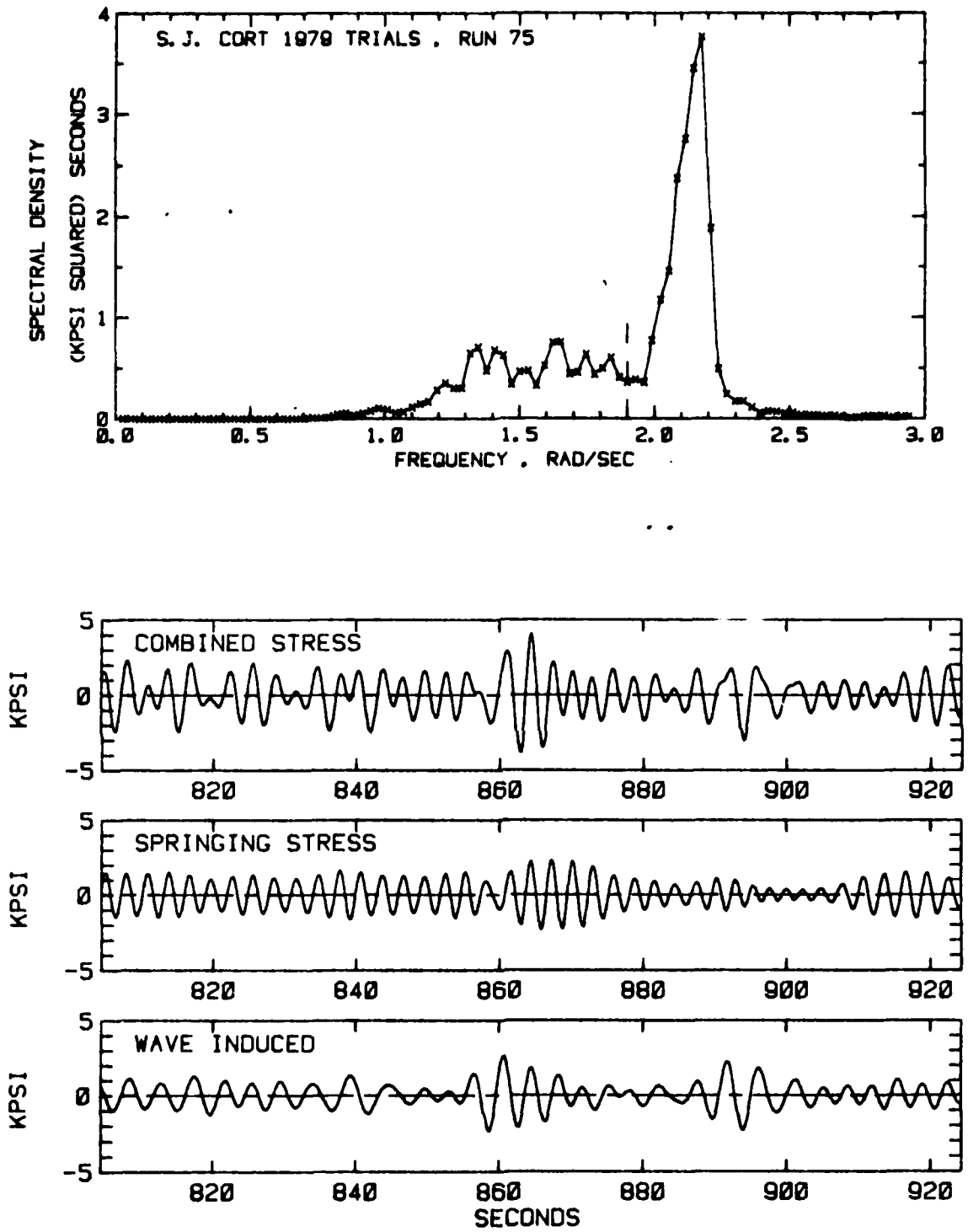

FIGURE D-2 BOTTOM BENDING STRESS SPECTRUM AND REPRESENTATIVE TIME HISTORIES--RUN 75 (1979)

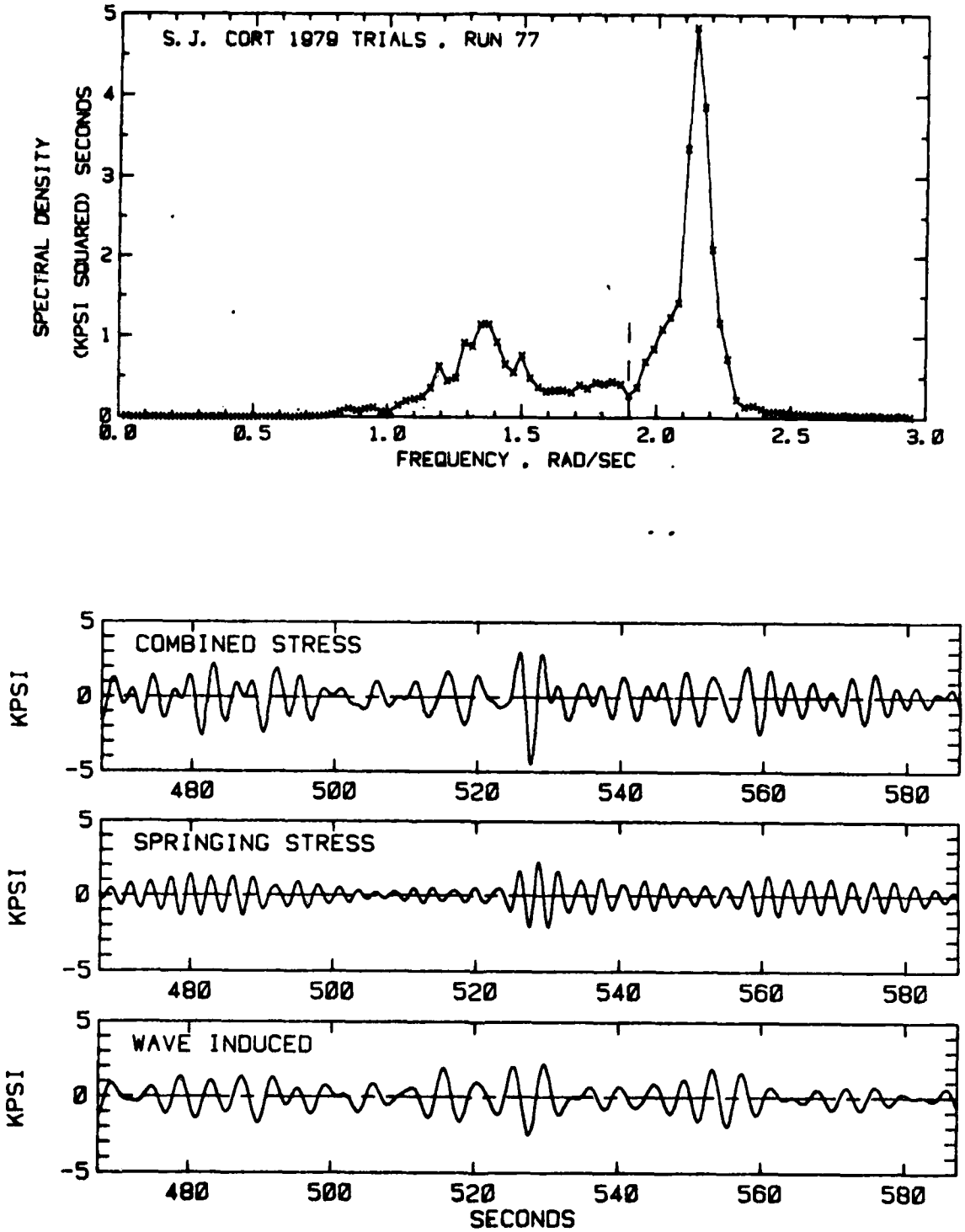

FIGURE D-3 BOTTOM BENDING STRESS SPECTRUM AND REPRESENTATIVE TIME HISTORIES--RUN 77 (1979)

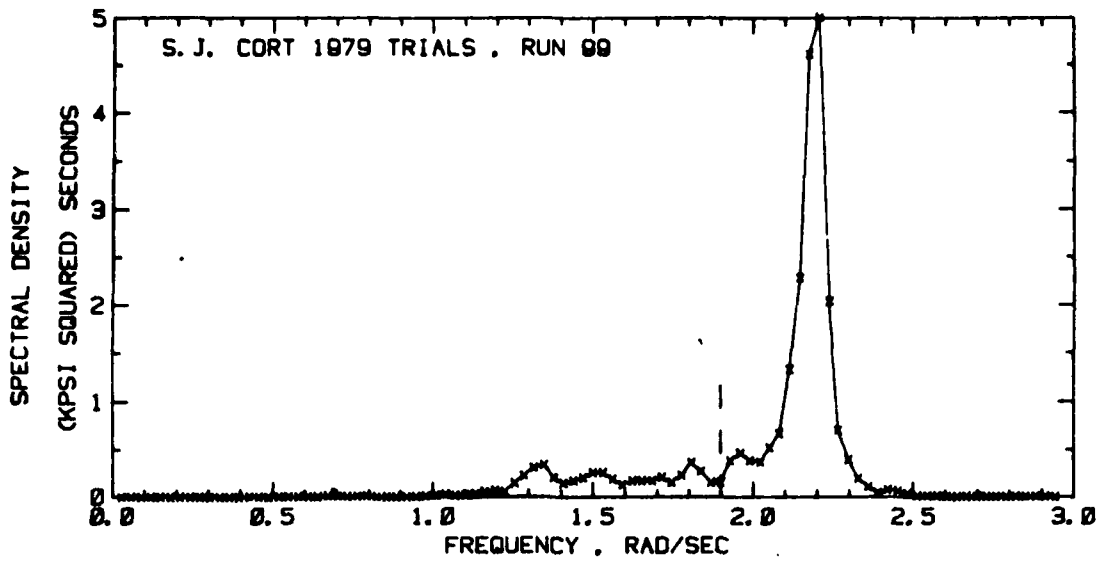

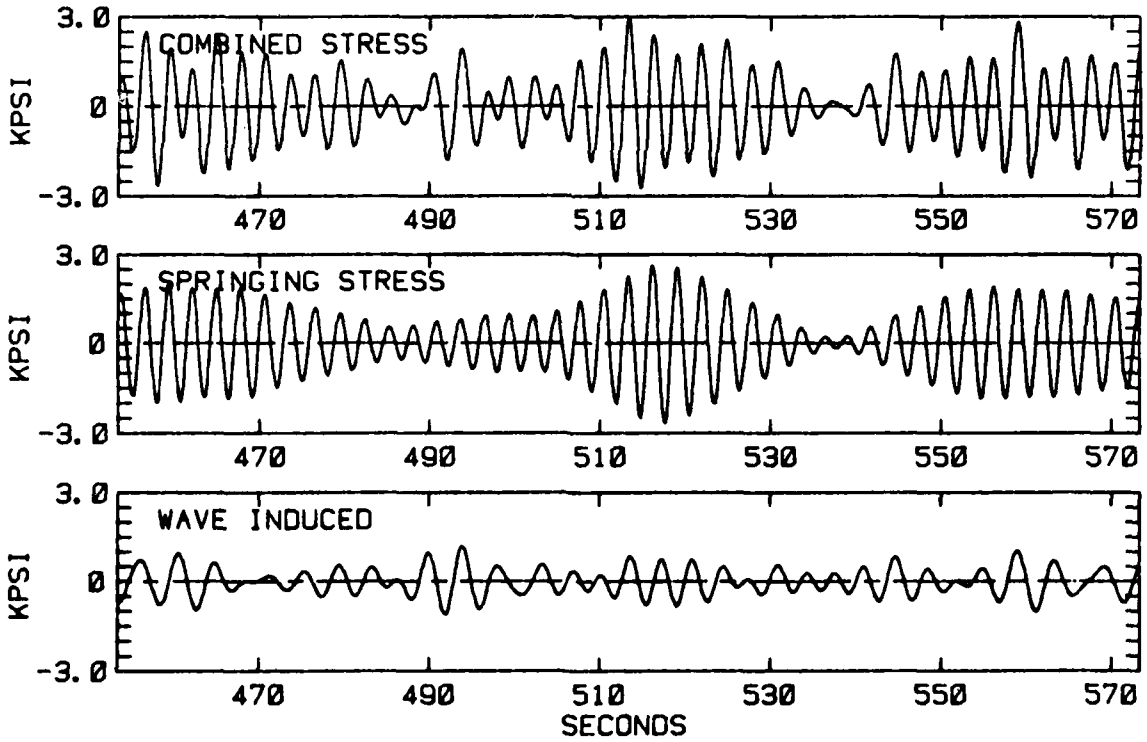

FIGURE D-4 BOTTOM BENDING STRESS SPECTRUM AND REPRESENTATIVE TIME HISTORIES--RUN 99 (1979)

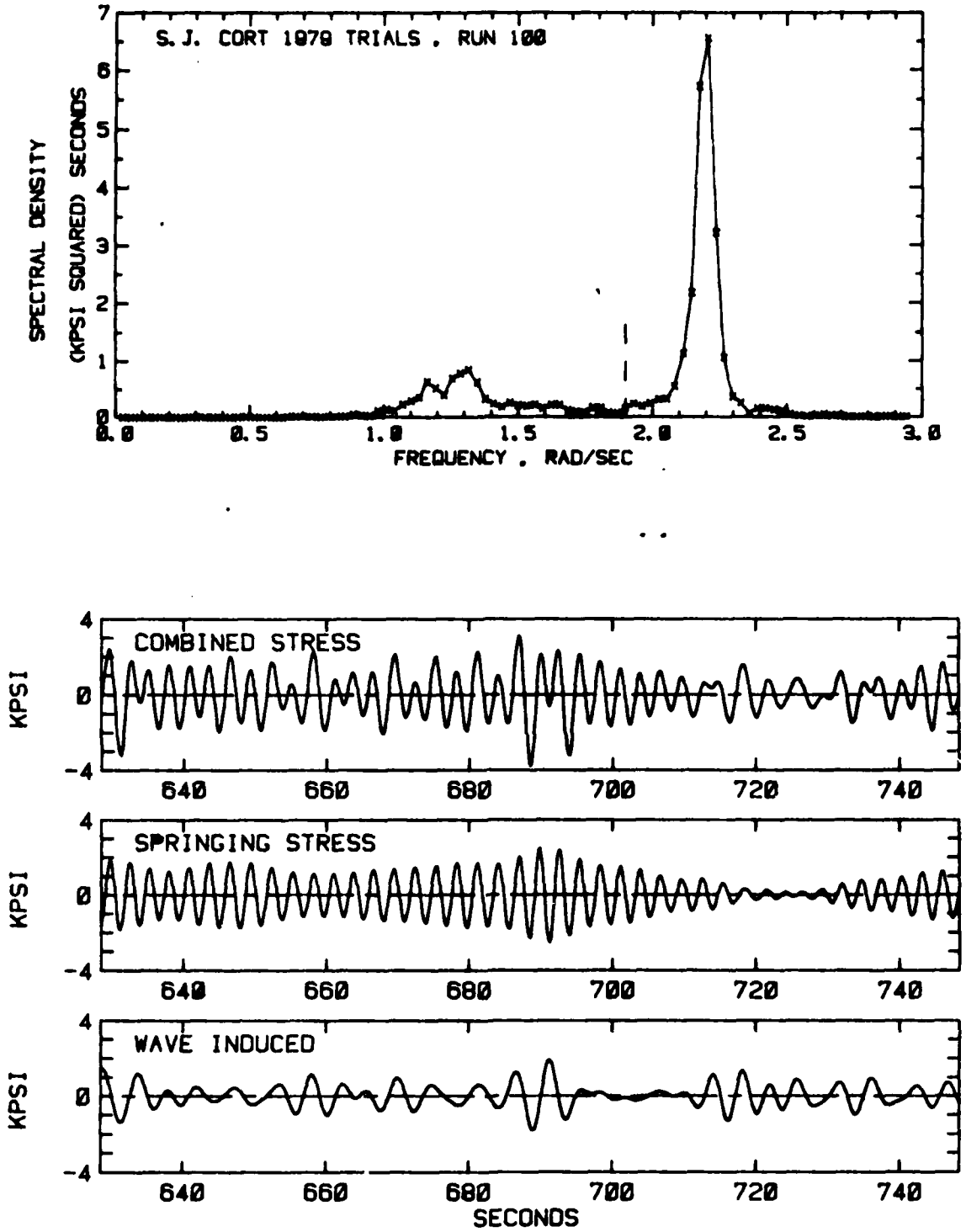

FIGURE D-5 BOTTOM BENDING STRESS SPECTRUM AND REPRESENTATIVE TIME HISTORIES--RUN 100 (1979)

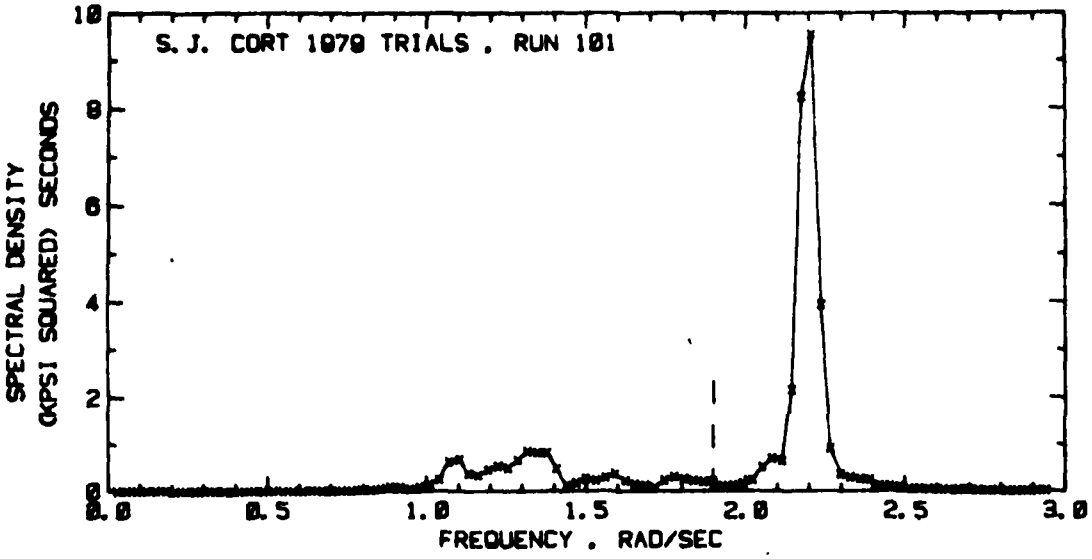

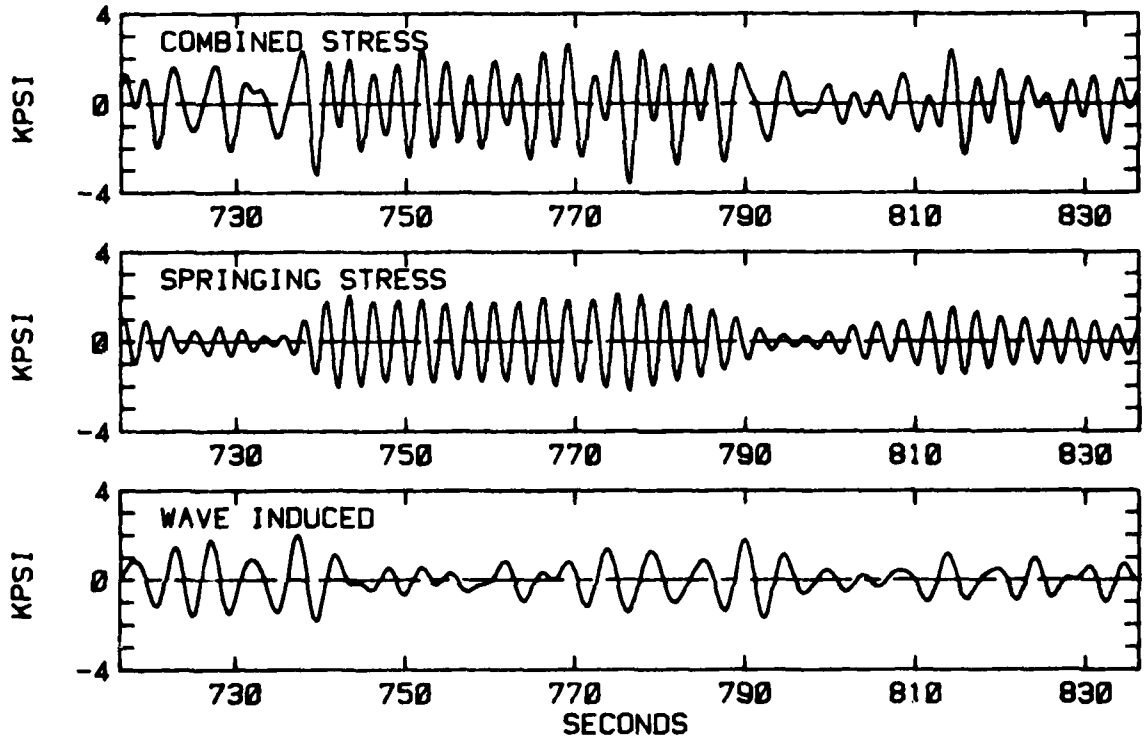

FIGURE D-6 BOTTOM BENDING STRESS SPECTRUM AND REPRESENTATIVE TIME HISTORIES--RUN 101 (1979)

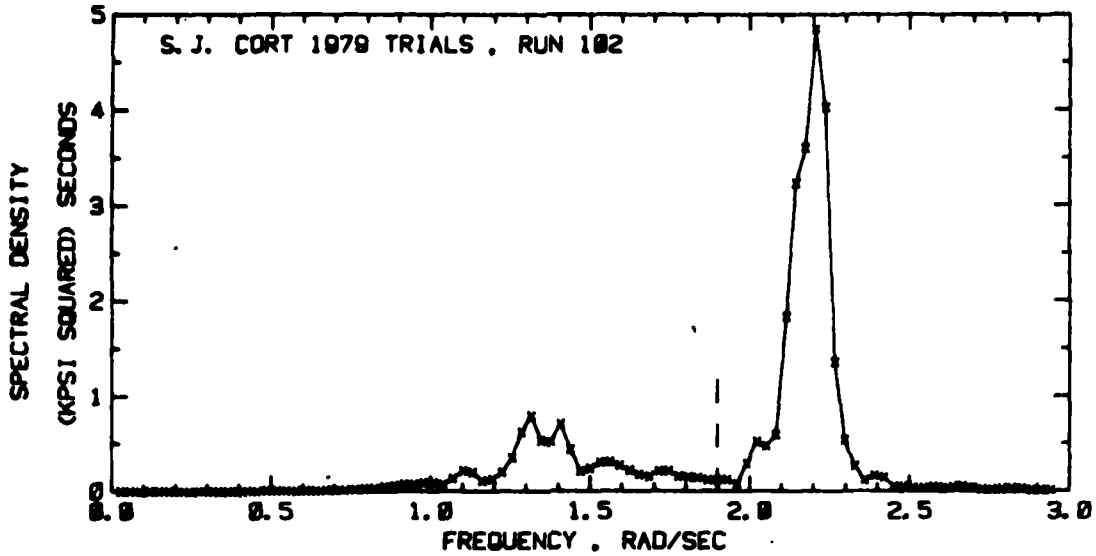

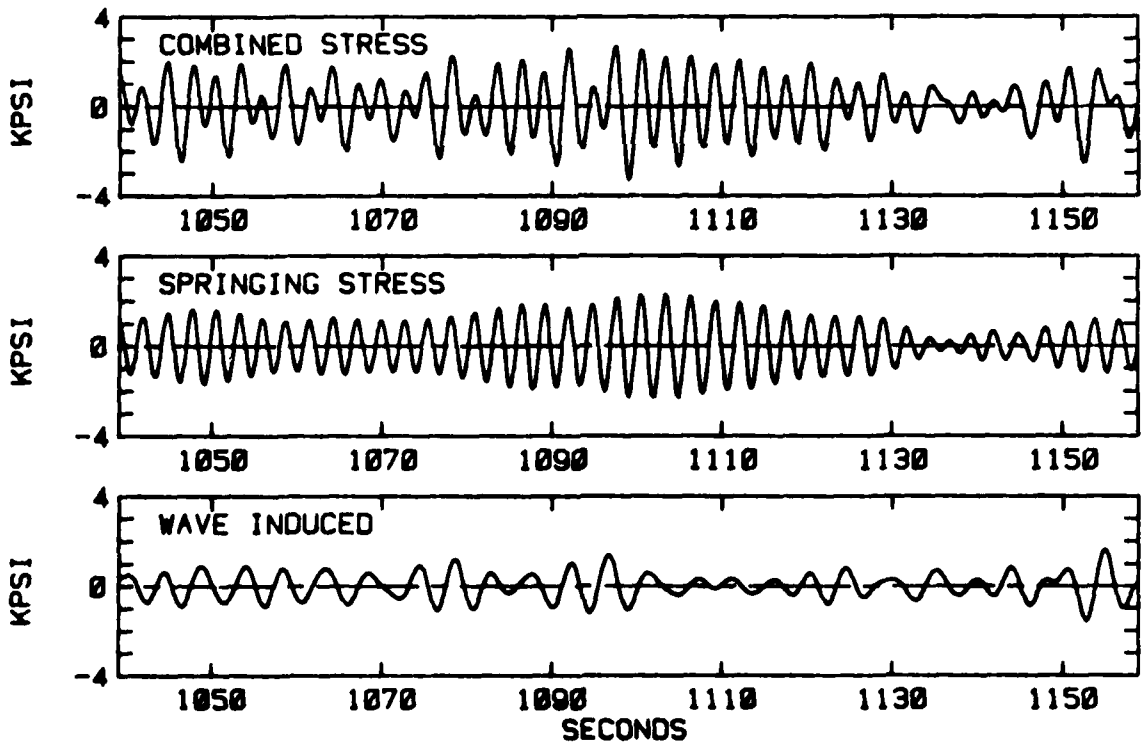

FIGURE D-7 BOTTOM BENDING STRESS SPECTRUM AND REPRESENTATIVE TIME HISTORIES--RUN 102 (1979)

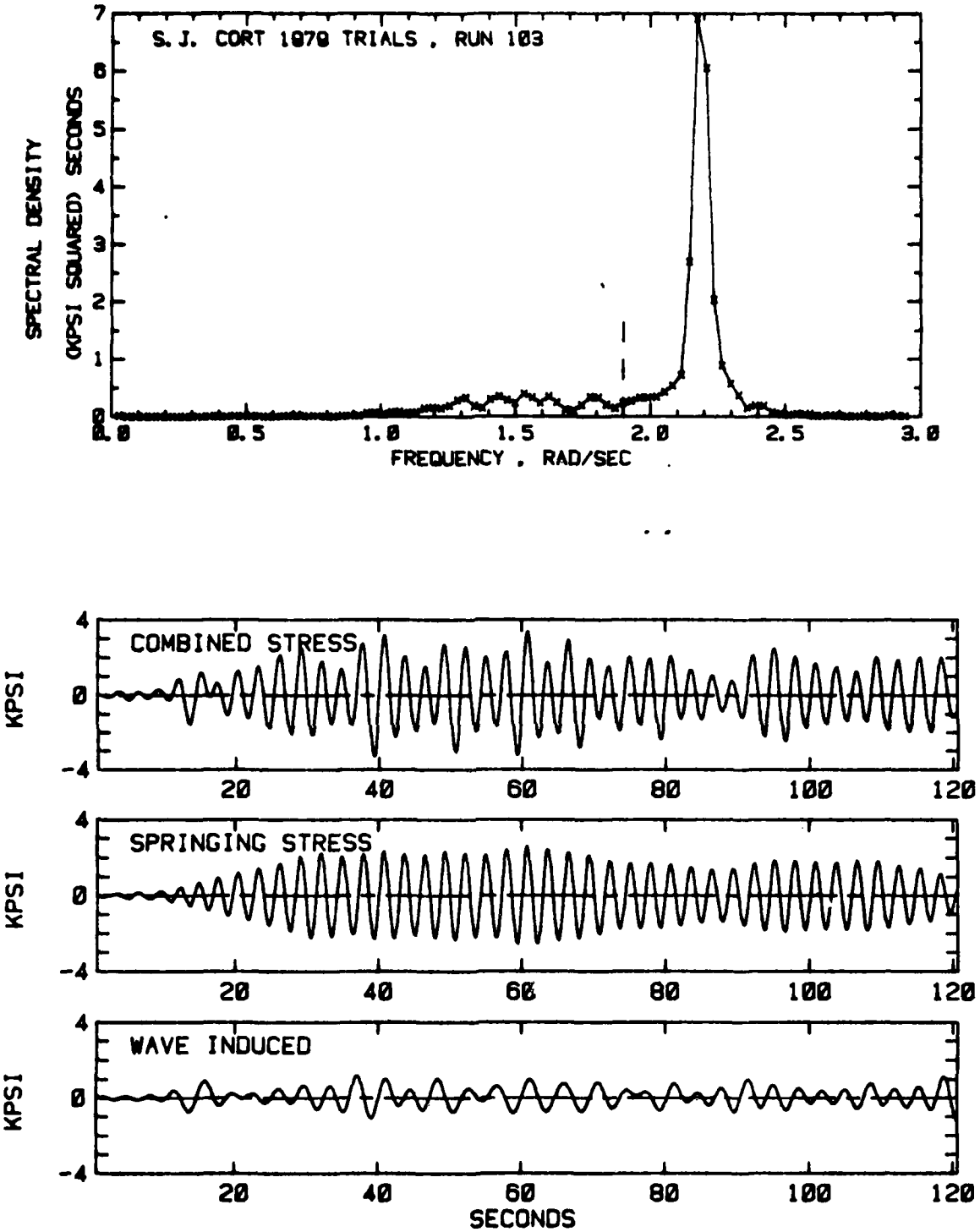

FIGURE D-8 BOTTOM BENDING STRESS SPECTRUM AND REPRESENTATIVE TIME HISTORIES--RUN 103 (1979)

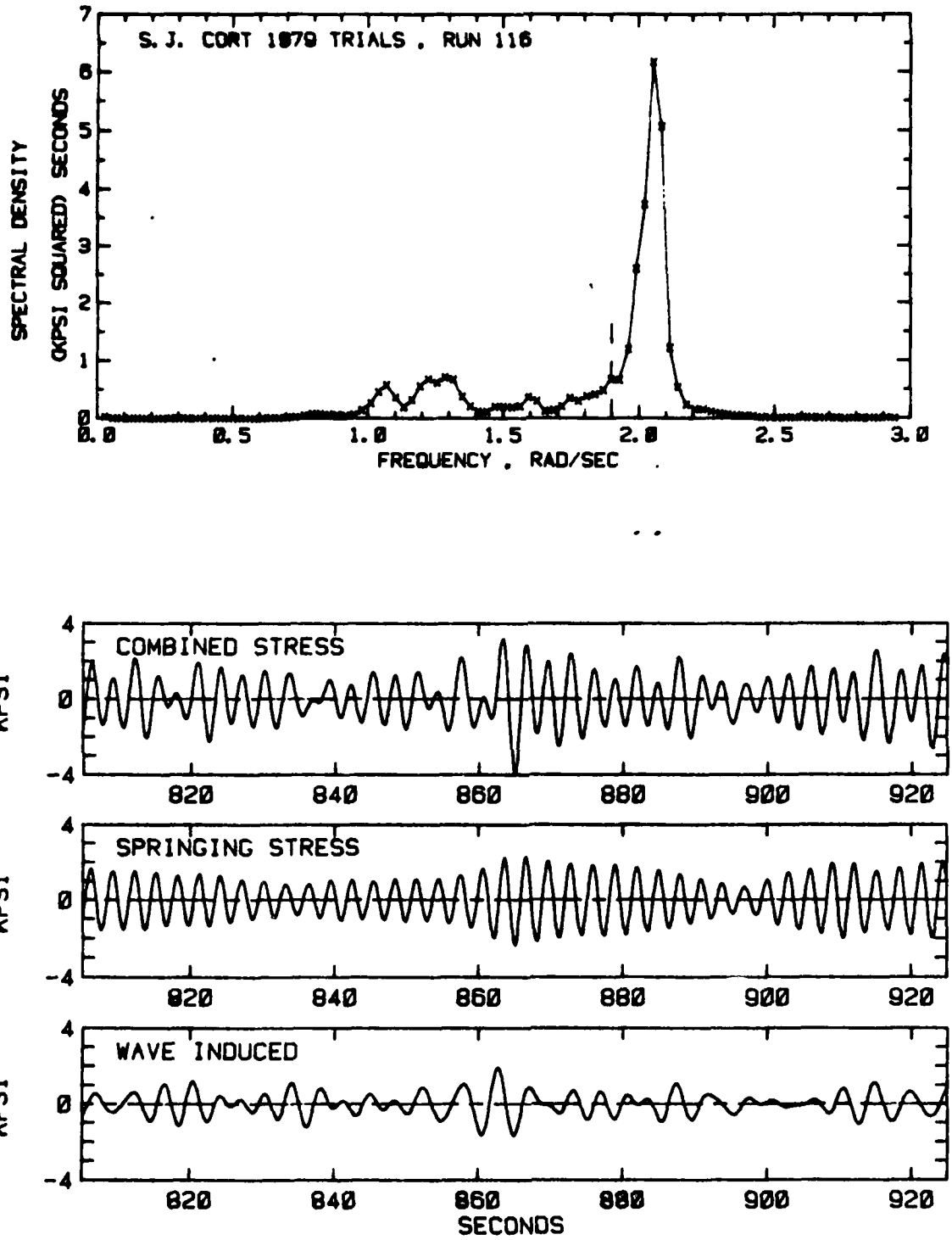

FIGURE D-9 BOTTOM BENDING STRESS SPECTRUM AND REPRESENTATIVE TIME HISTORIES--RUN 116 (1979)

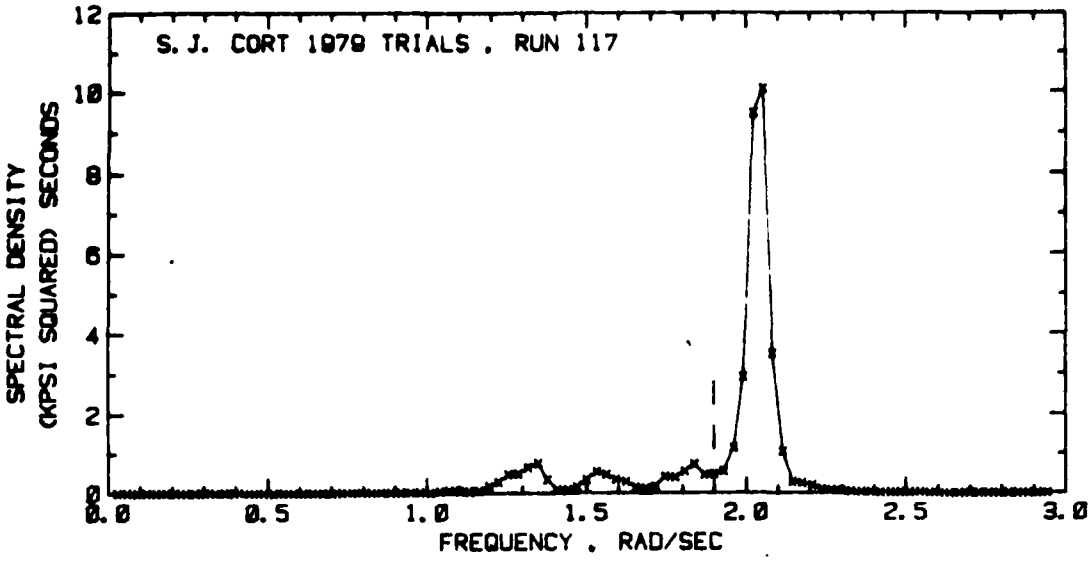

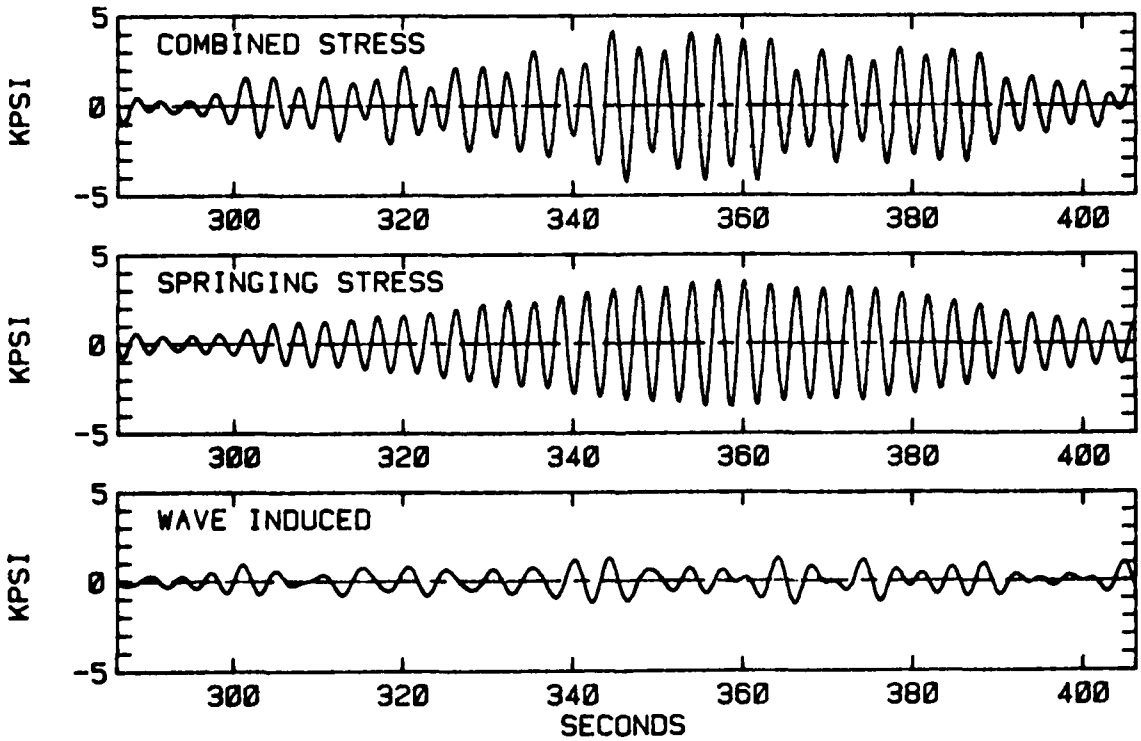

FIGURE D-10 BOTTOM BENDING STRESS SPECTRUM AND REPRESENTATIVE TIME HISTORIES--RUN 117 (1979)

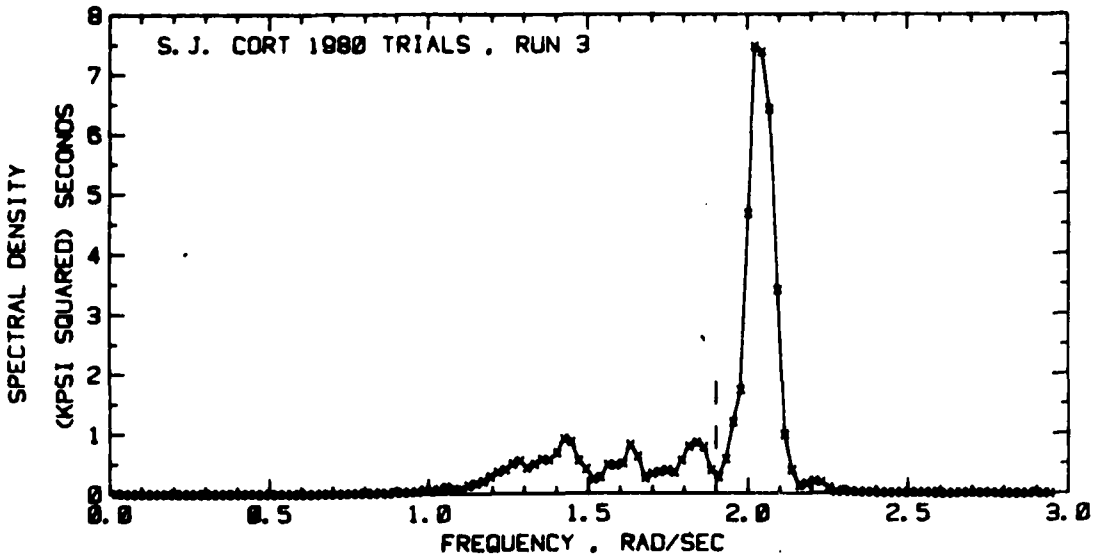

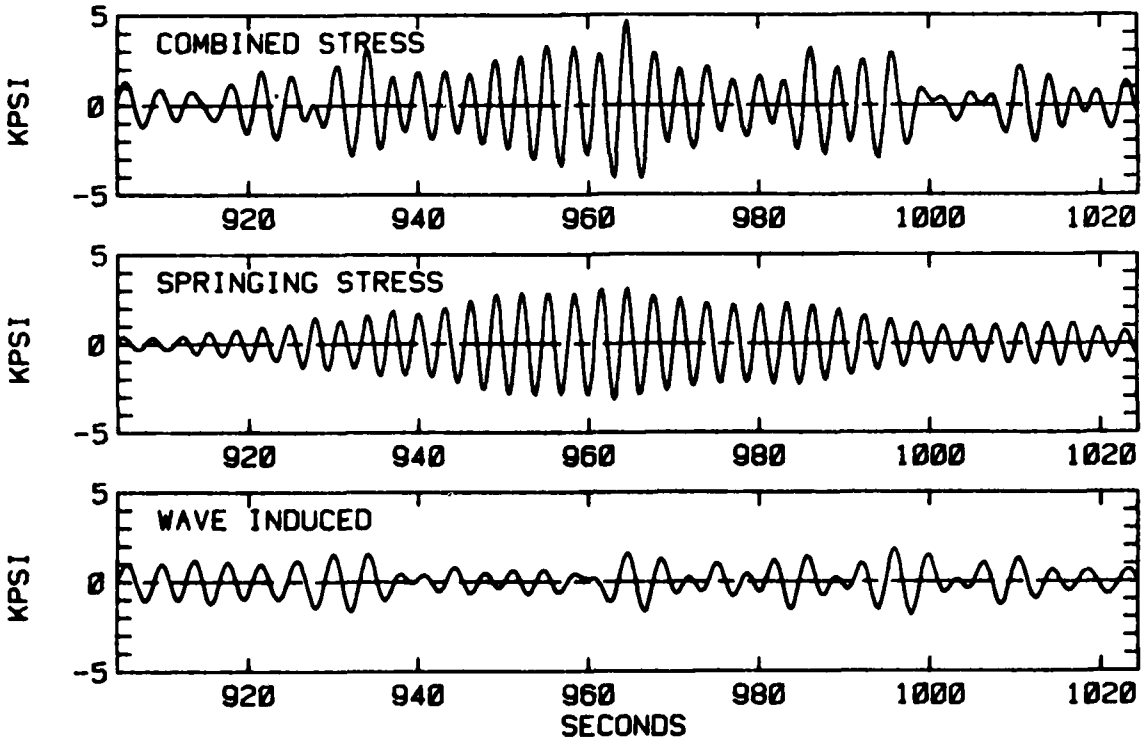

FIGURE D-11 BOTTOM BENDING STRESS SPECTRUM AND REPRESENTATIVE TIME HISTORIES--RUN 3 (1980)

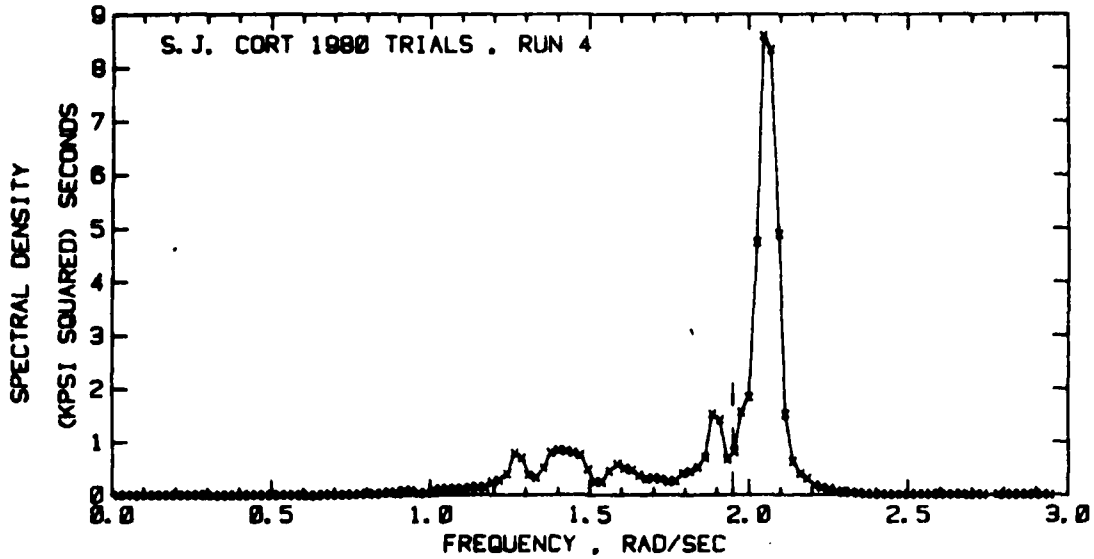

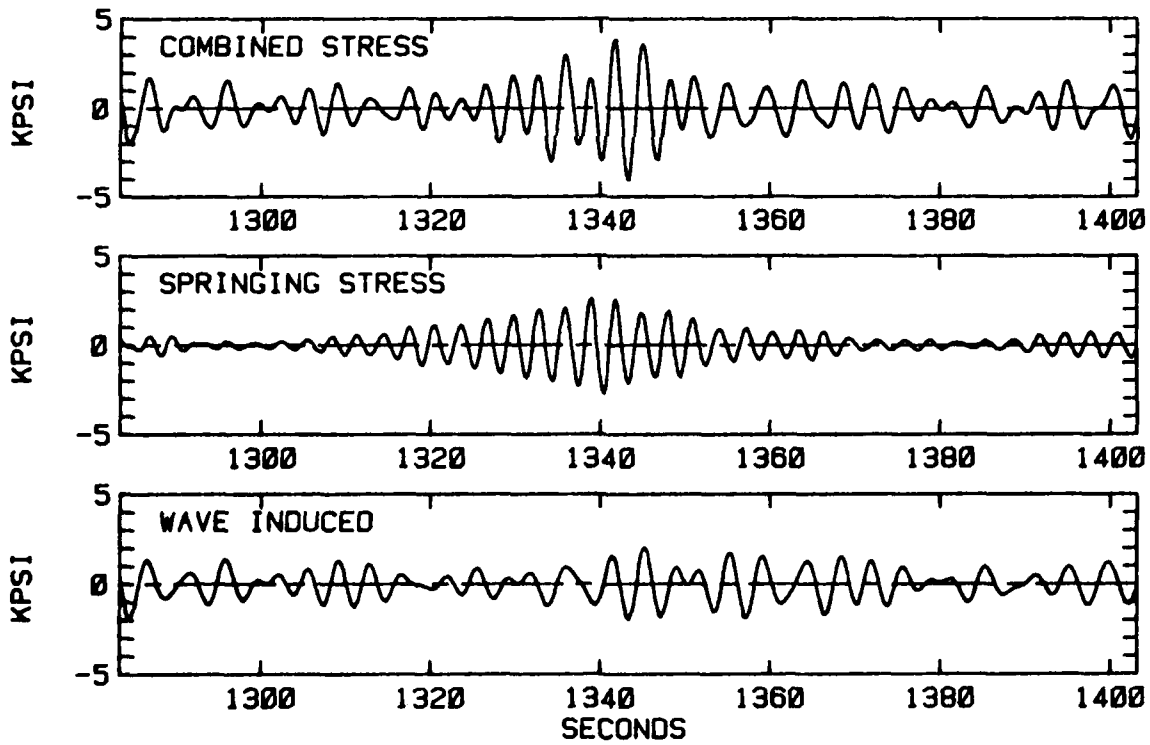

FIGURE D-12 BOTTOM BENDING STRESS SPECTRUM AND REPRESENTATIVE TIME HISTORIES--RUN 4 (1980)

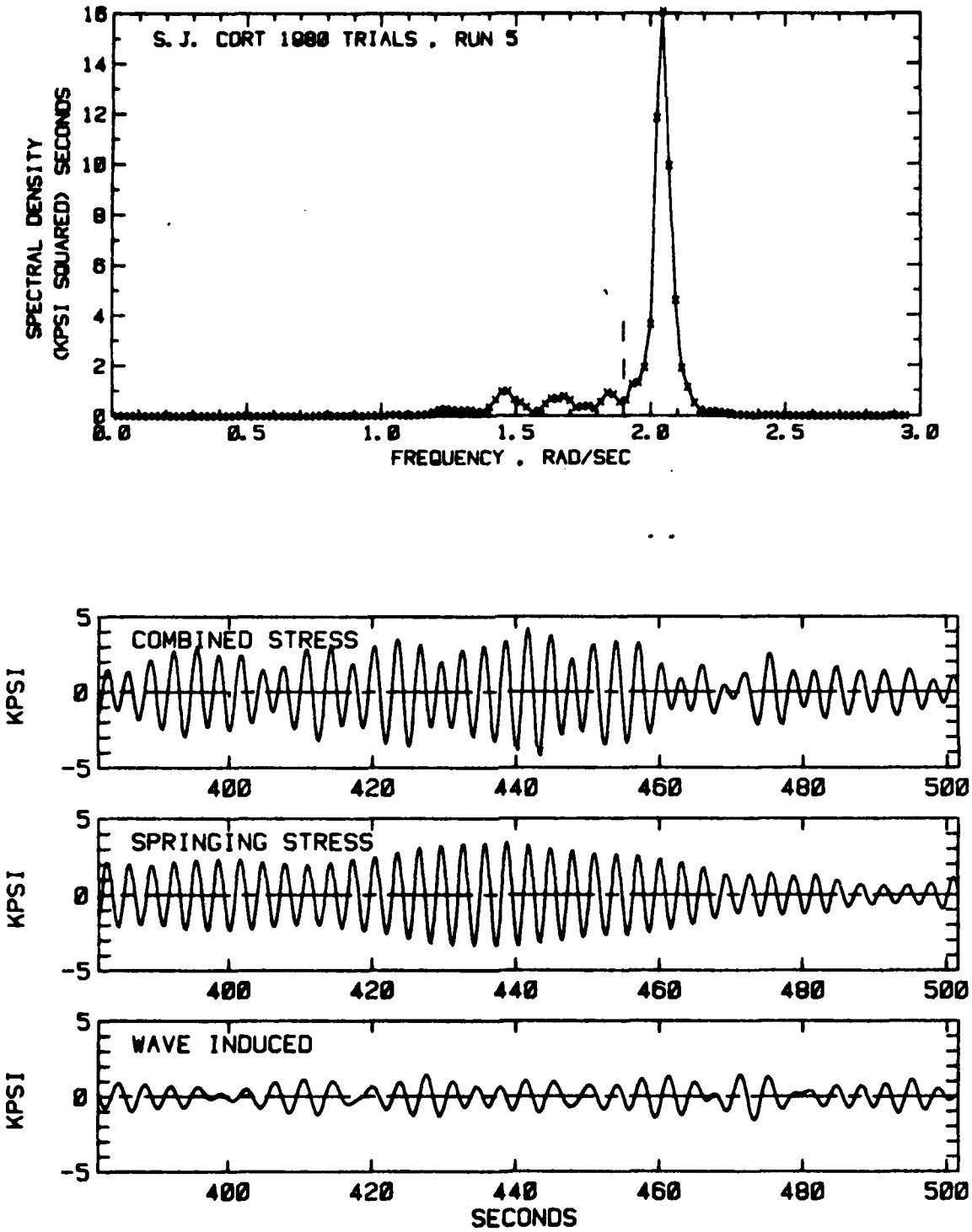

FIGURE D-13 BOTTOM BENDING STRESS SPECTRUM AND REPRESENTATIVE TIME HISTORIES--RUN 5 (1980)

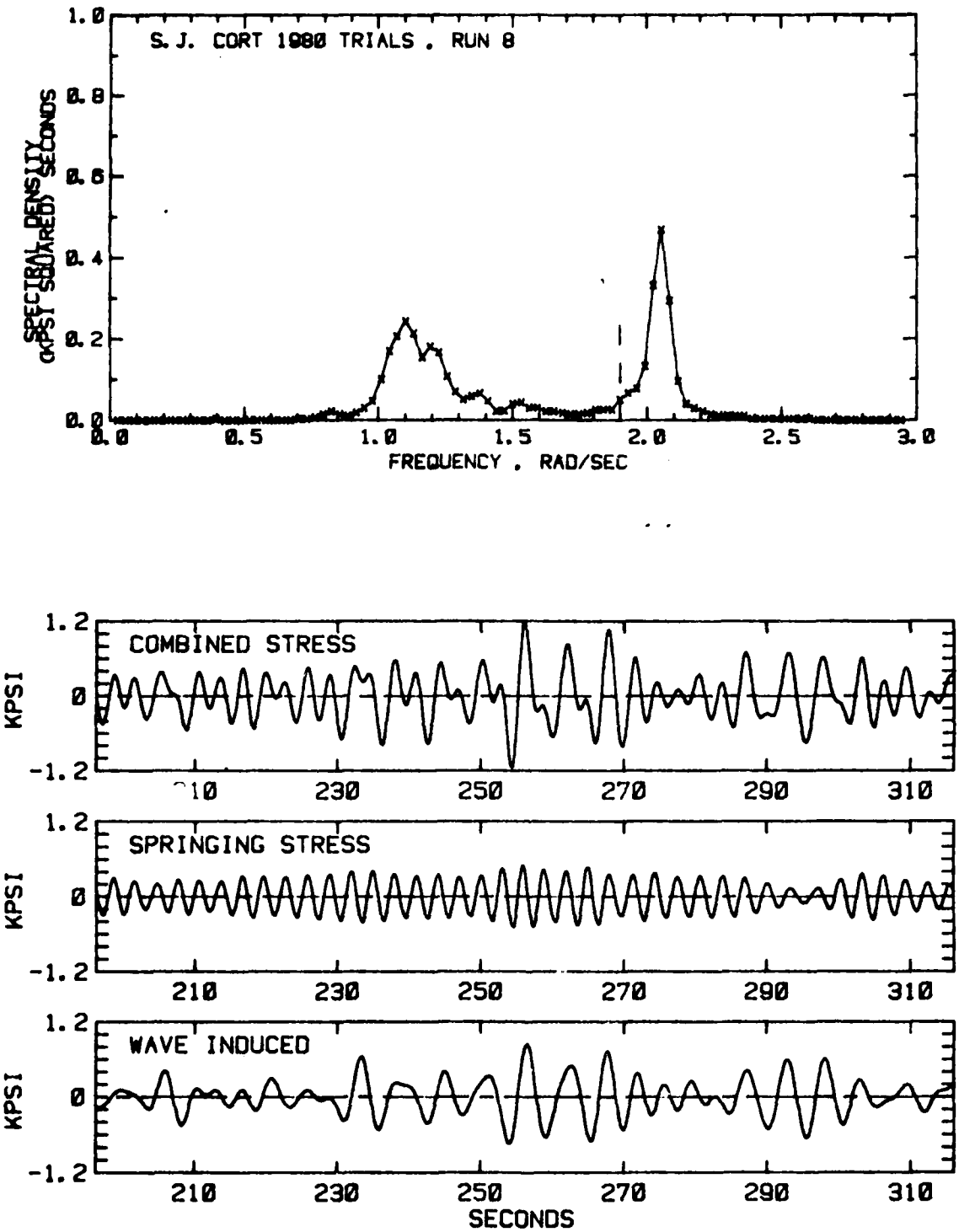

FIGURE D-14 BOTTOM BENDING STRESS SPECTRUM AND REPRESENTATIVE TIME HISTORIES--RUN 8 (1980)

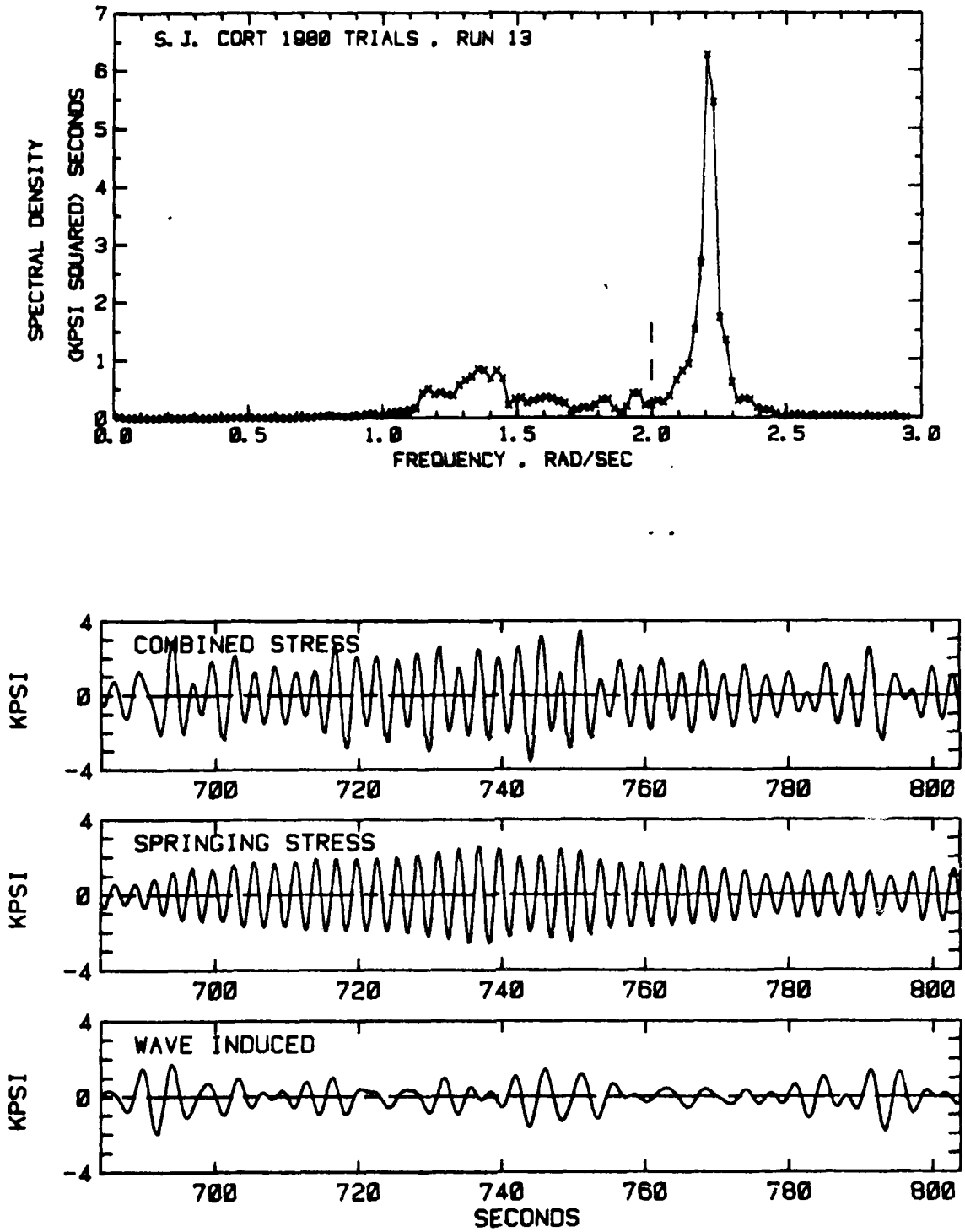

FIGURE D-15 BOTTOM BENDING STRESS SPECTRUM AND REPRESENTATIVE TIME HISTORIES--RUN 13 (1980)

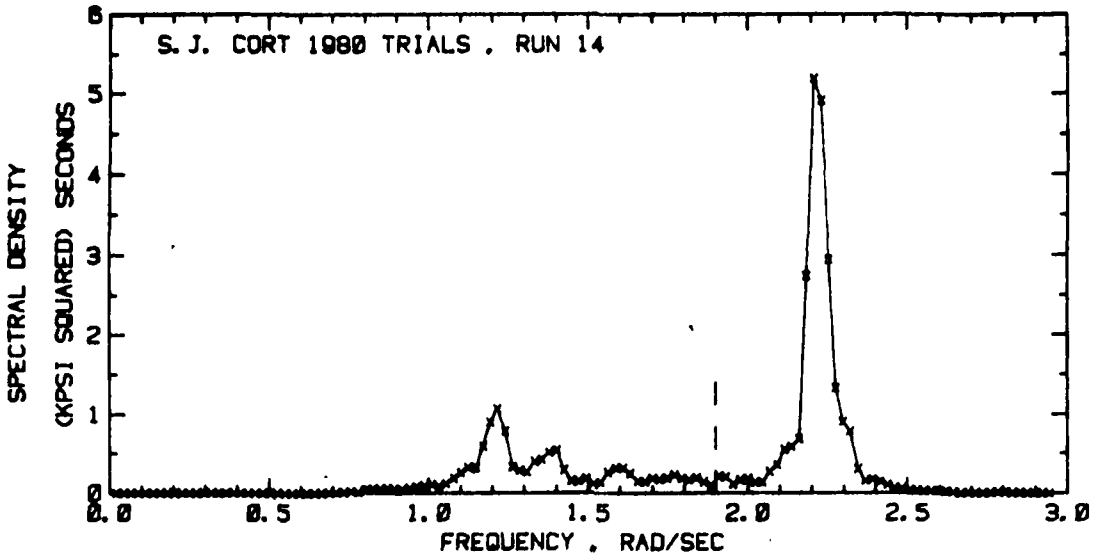

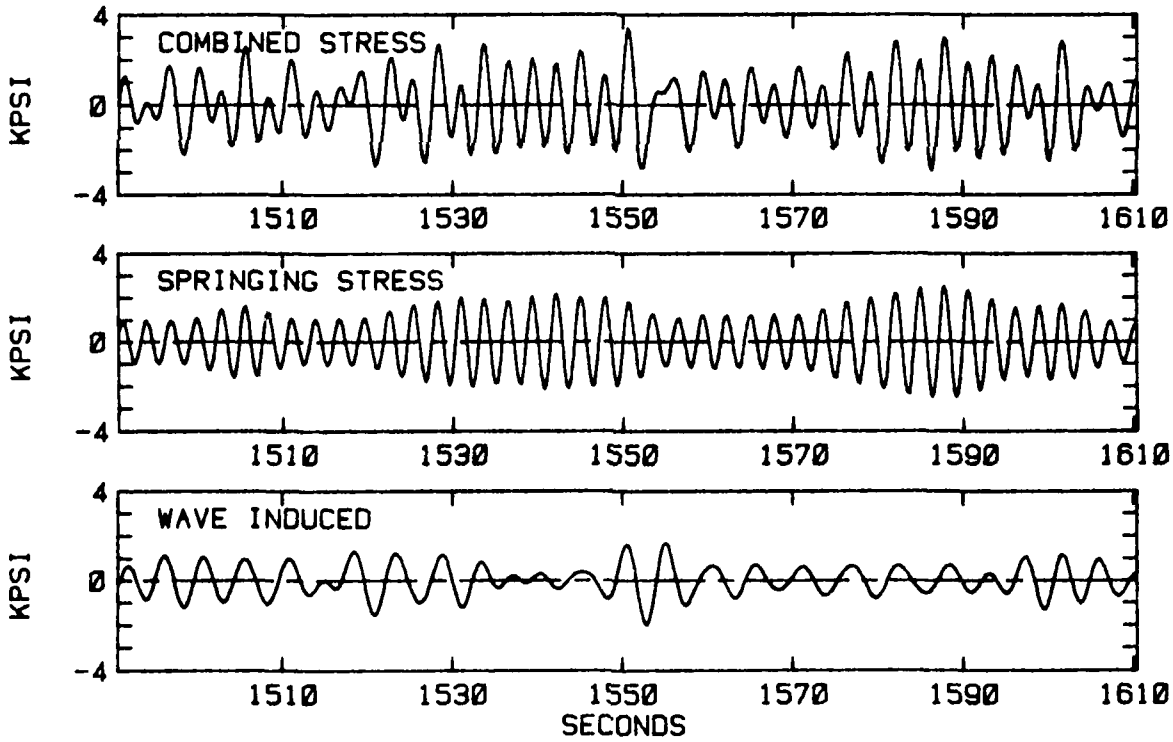

FIGURE D-16 BOTTOM BENDING STRESS SPECTRUM AND REPRESENTATIVE TIME HISTORIES--RUN 14 (1980)

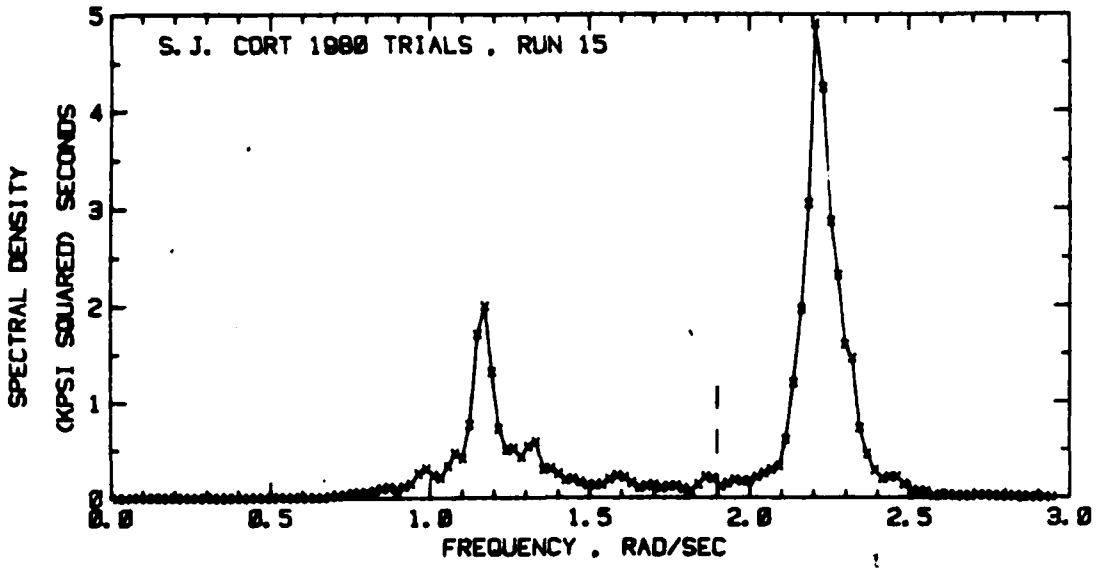

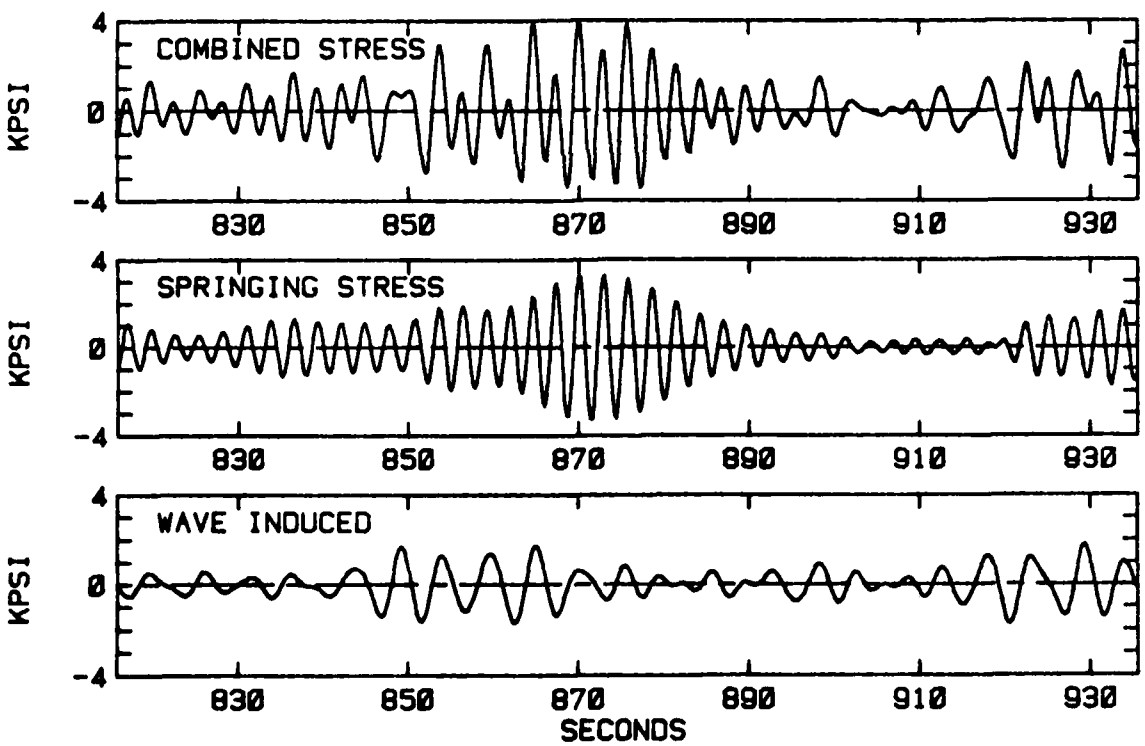

FIGURE D-17 BOTTOM BENDING STRESS SPECTRUM AND REPRESENTATIVE TIME HISTORIES--RUN 15 (1980)

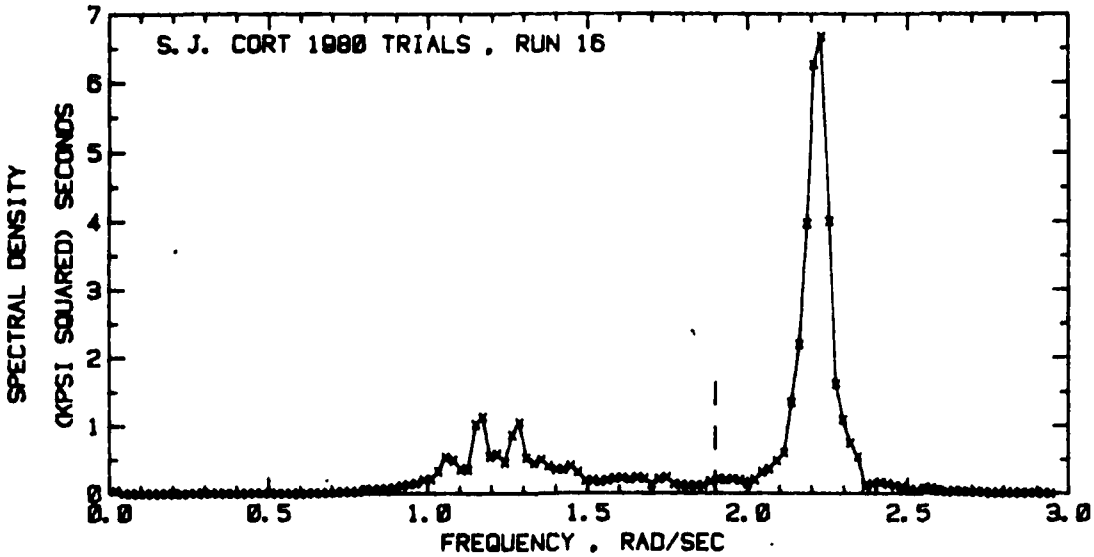

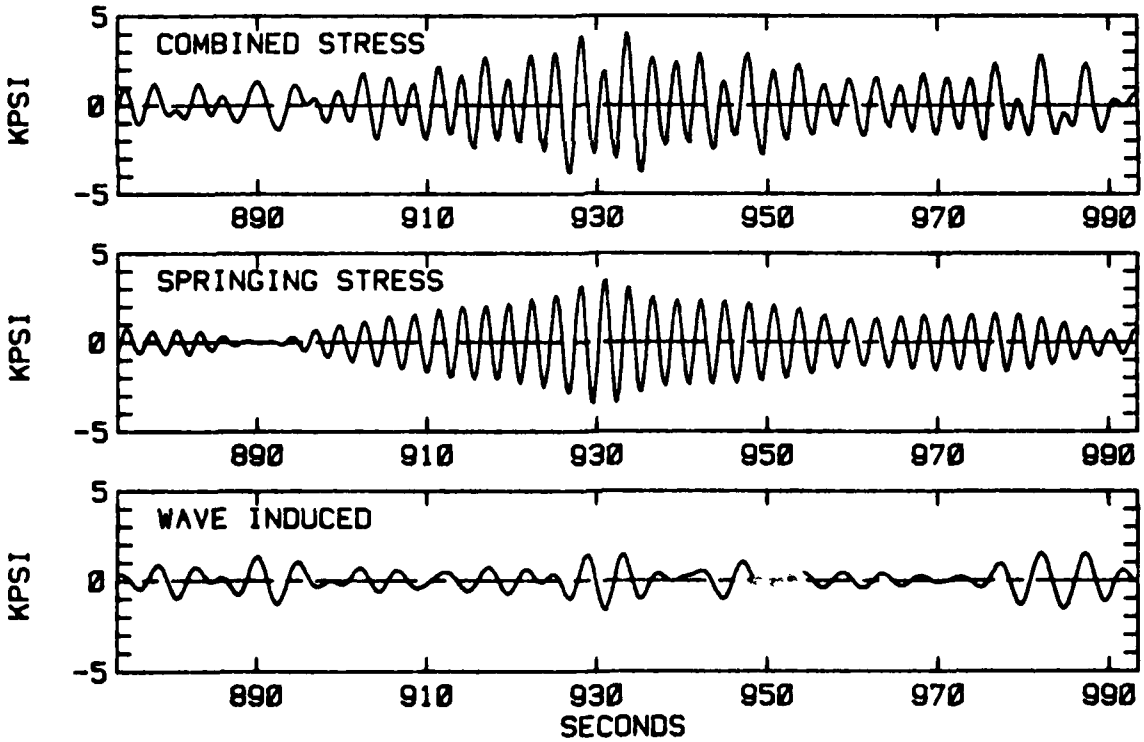

FIGURE D-18 BOTTOM BENDING STRESS SPECTRUM AND REPRESENTATIVE TIME HISTORIES--RUN 16 (1980)

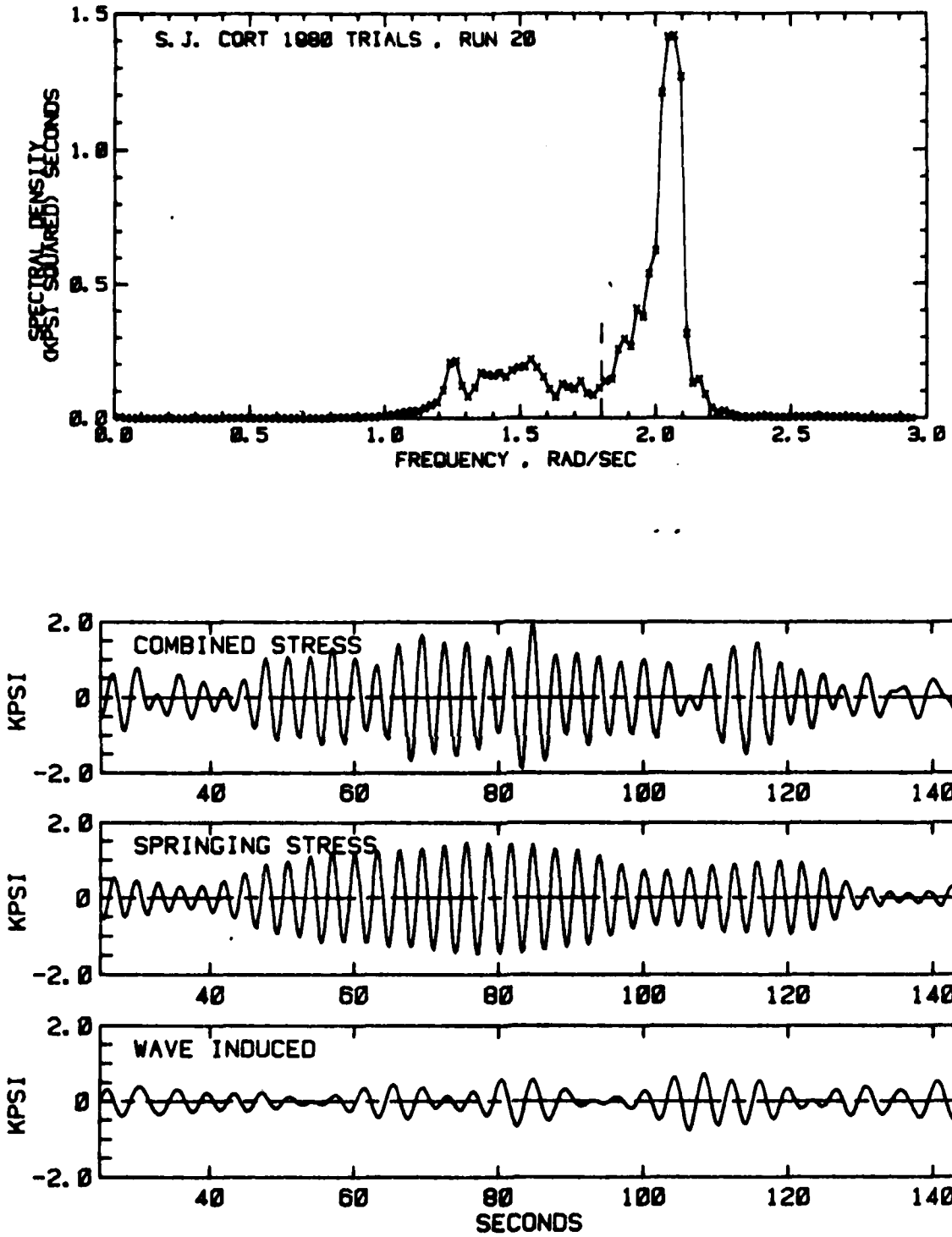

FIGURE D-19 BOTTOM BENDING STRESS SPECTRUM AND REPRESENTATIVE TIME HISTORIES--RUN 20 (1980)

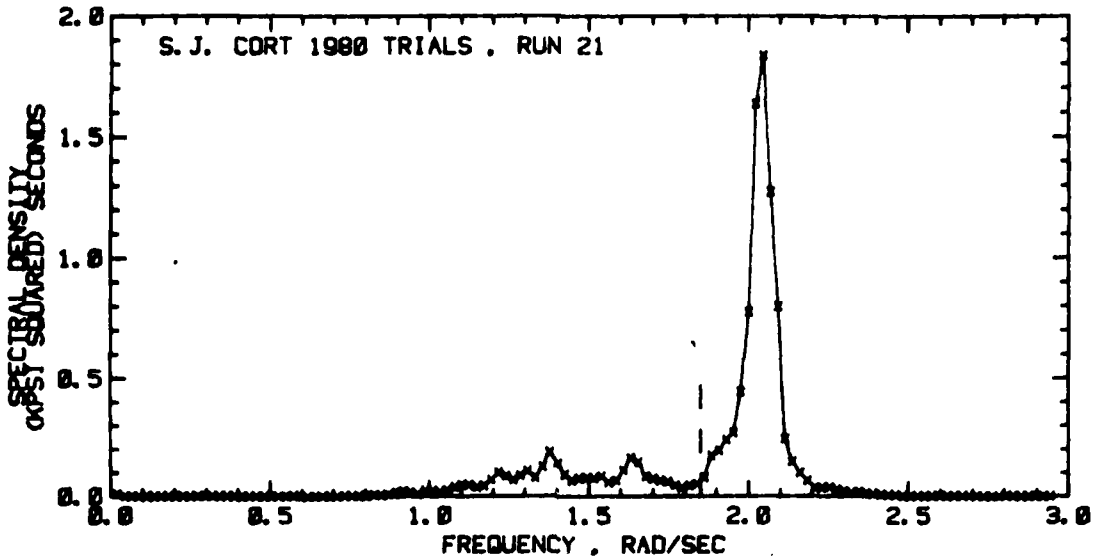

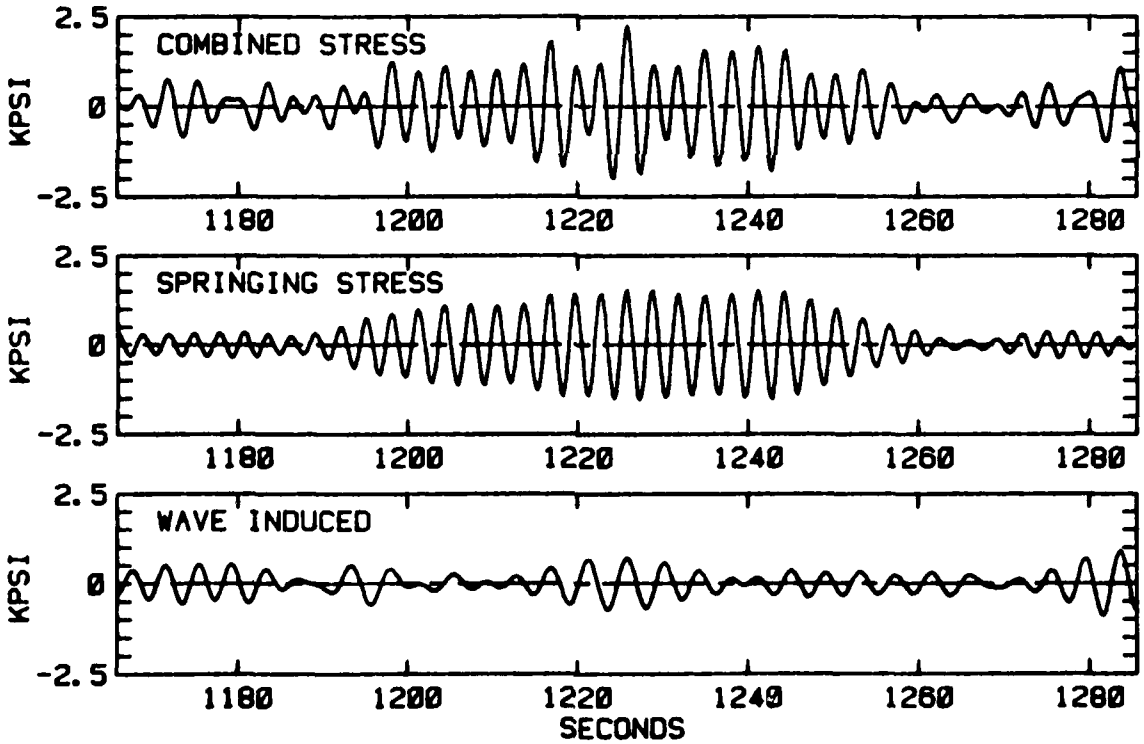

FIGURE D-20 BOTTOM BENDING STRESS SPECTRUM AND REPRESENTATIVE TIME HISTORIES--RUN 21 (1980)

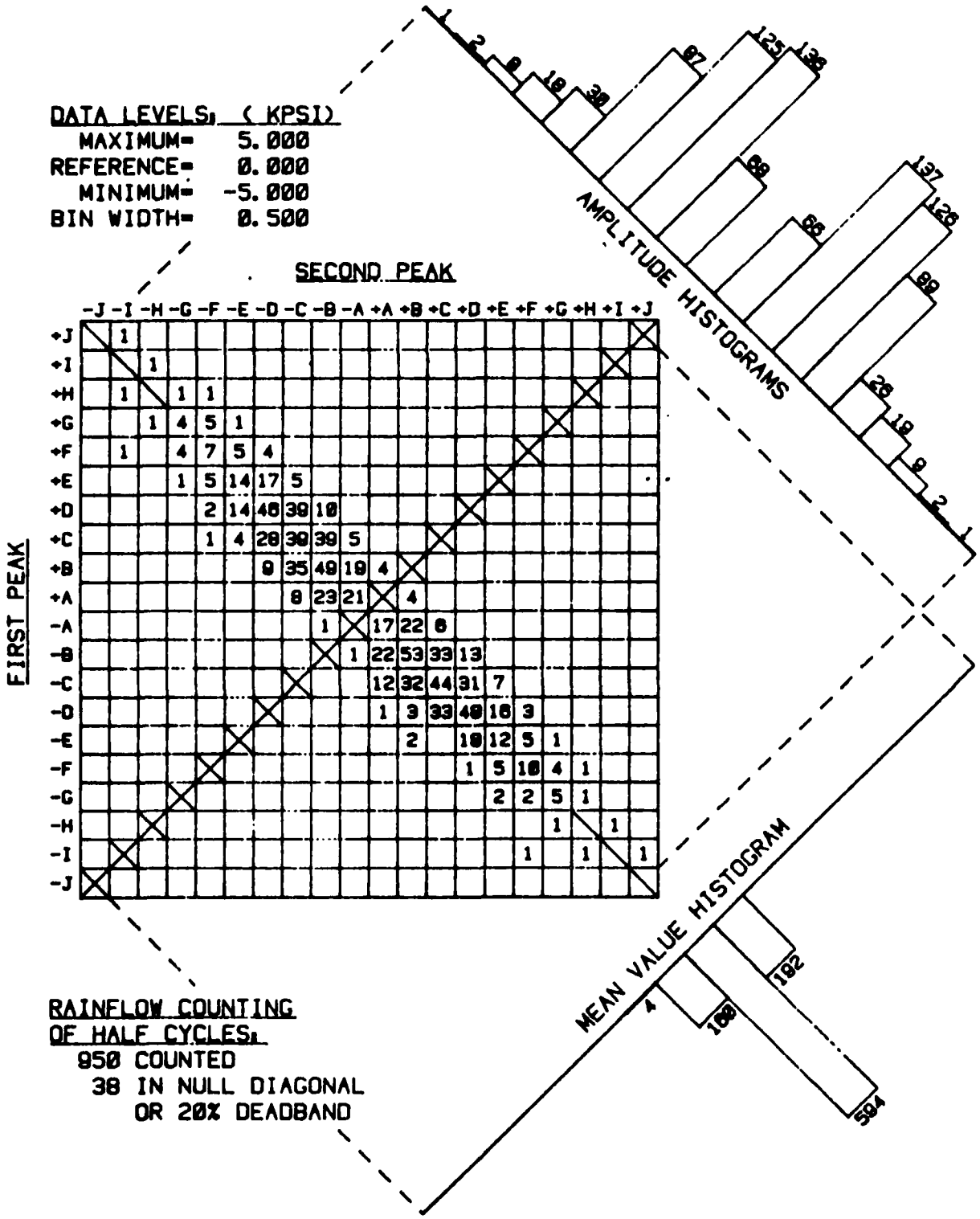

FIGURE D-21 HALF CYCLE COUNT MATRIX: COMBINED BOTTOM BENDING STRESS, RUN 3 (1980)

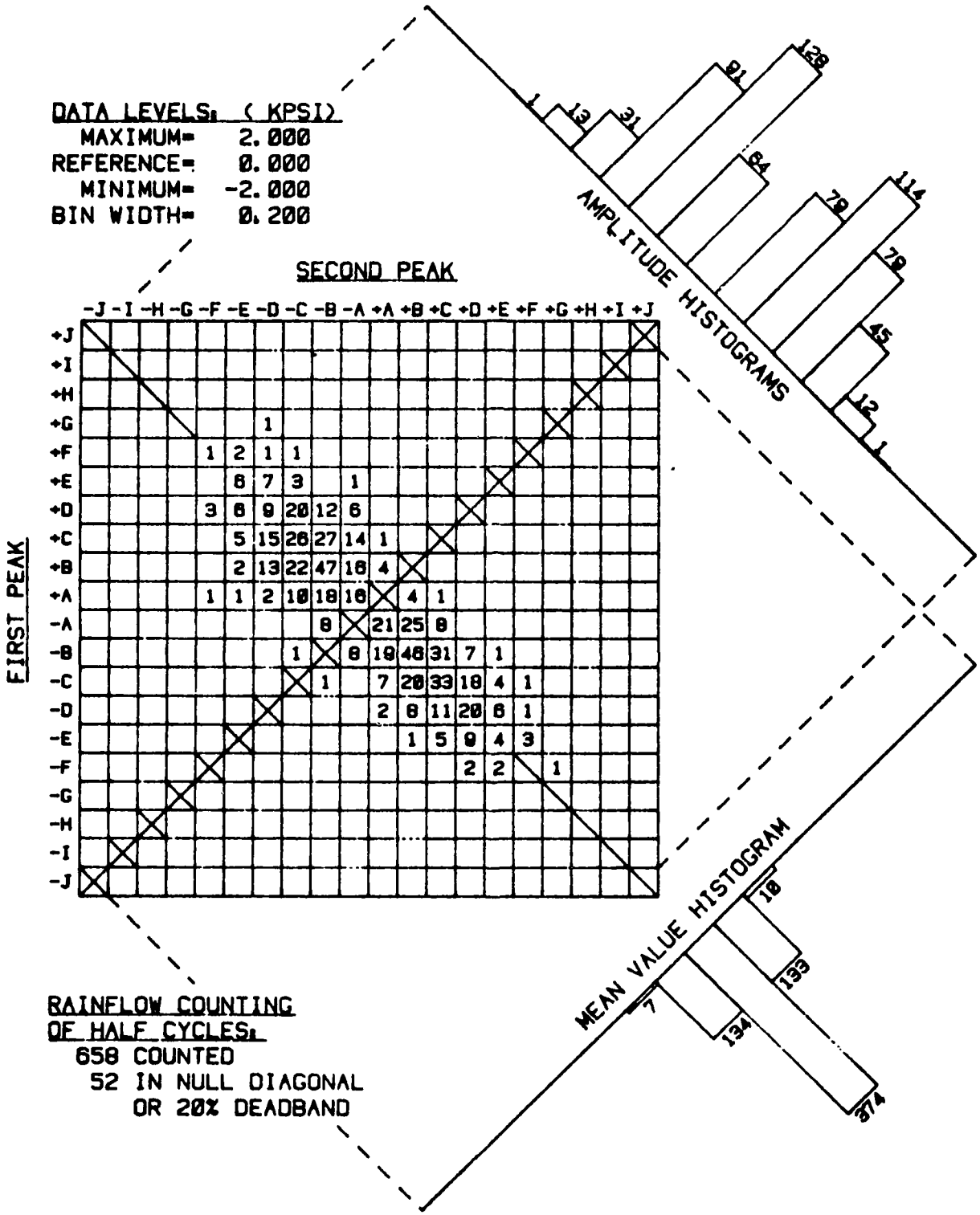

FIGURE D-22 HALF CYCLE COUNT MATRIX: COMBINED BOTTOM BENDING STRESS, RUN 8 (1980)

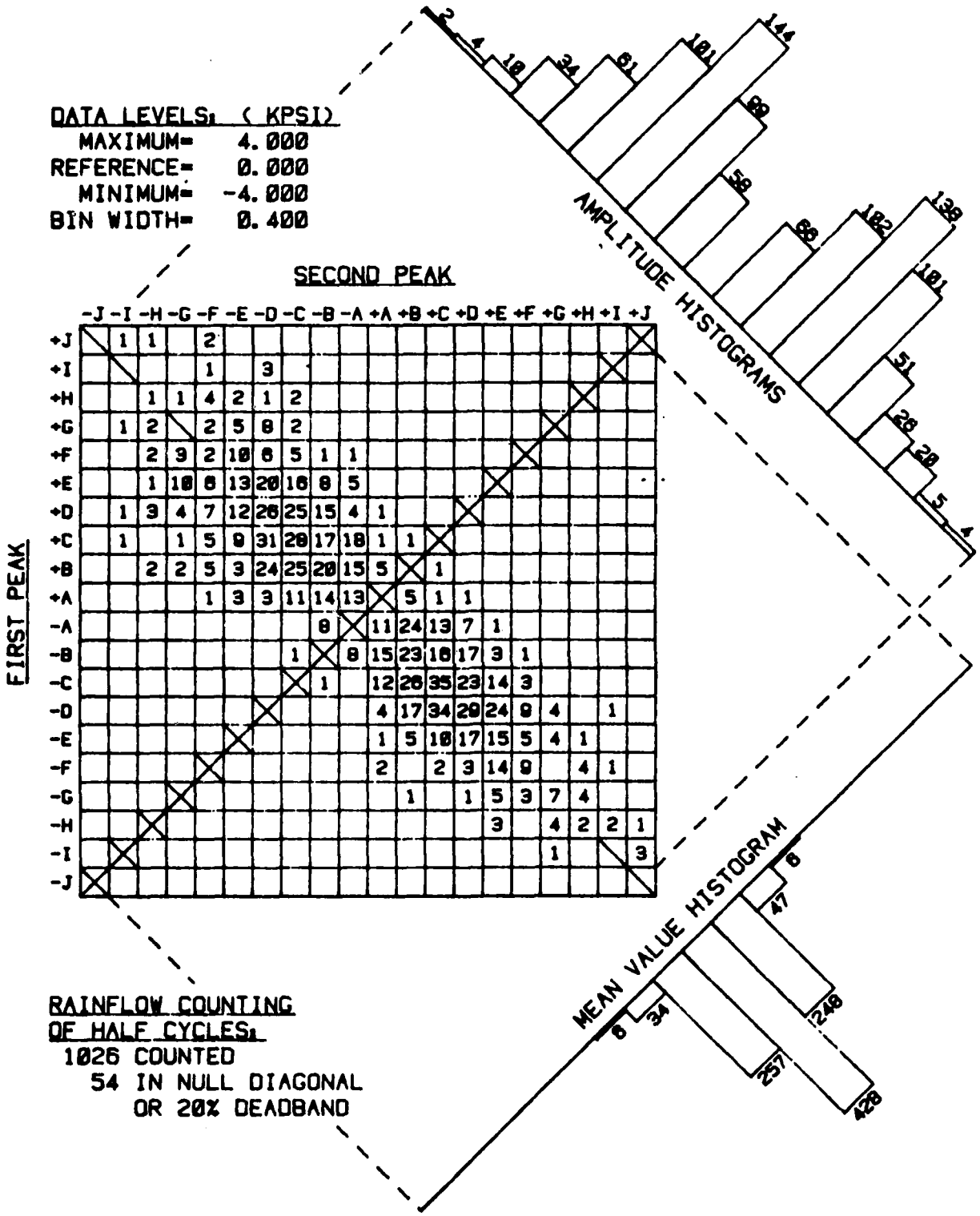

FIGURE D-23 HALF CYCLE COUNT MATRIX: COMBINED BOTTOM BENDING STRESS, RUN 15 (1980)

APPENDIX E

SIMULATION OF DATA

Time Domain Simulations

As noted in Appendix D, the spectral densities shown in Figures D-1 through D-20 are the essential input data to the numerical simulation system of Reference 2. Indeed, the files from which the spectra were plotted were in the required form for the simulation. A "cut-off" frequency to separate wave induced and springing frequency components is noted in the figures. Two specifications not previously mentioned which were incorporated in the input files were the codes for number of points and the delta-time for the simulation. These were selected to be 8192 points at Δt of 0.15 seconds. This is the combination recommended in Reference 2 and results in time domain samples just over 20 minutes in length. Once this much input data is available for each run, up to 30 statistically independent 20 minute time domain samples of combined, springing and wave induced stress can be simulated in accordance with the programs documented in Reference 2.

Generation of Maxima and Minima

The "data base generator" program documented in Reference 2 more or less automatically produces files of maxima and minima of each simulated record once the simulated digital time histories are available, and this program was of course used in the present instance.

Simulation of Data for Subsequent Analysis

The overall objective was to attempt further qualification of the simulation by comparison of statistics from the simulation with those derivable from the full scale data. That which was available from the full scale data for present purposes was twenty 20 or 25 minute runs--essentially twenty short term samples from twenty conceptually infinite populations. It appeared reasonable for present purposes to mimic this

situation and produce one short term simulation corresponding to each of the 20 full scale spectra which were available. In this regard the fact that the simulations of Reference 2 are pseudo-random had to be taken into account. In effect, if all twenty simulations were made by entering the programmed random number sequence at the same point, very similar short term statistics would result for the many runs in the set where the spectra are qualitatively and quantitatively similar. This of course would distort purely statistical comparisons, and the situation was avoided by using a different entry point in the random number sequence for each simulation. What was in fact done was to assign programmed entry points 1 through 20 to 1979 Run 74, etc., through 1980 Run 21, with the final result that the maxima and minima from a twenty minute simulation of each of the spectra shown in Figures D-1 through D-20 was made available. As far as can be determined, each of the simulations is statistically independent of any of the others.

APPENDIX F

STATISTICAL INDEPENDENCE OF MAXIMA

Introduction

Virtually any of the available statistical inference procedures which may be brought to bear upon the problem of comparing the statistics of maxima from the simulations with those from observed data require that the sample being considered be a random sample from the population. The raw material for the analysis was ordered sets of all the maxima and minima in each of the real and simulated records. It is clear from an inspection of any of the springing stress records in Figures D-1 through D-20 that succeeding maxima must be correlated in some way and thus that the sample formed by all the maxima in a record cannot be considered to be random in the required sense.

The "Run" Test

The required sense is that each element of the sample be statistically independent of any other element, that is, the probability structure of the $(j+1)^{th}$ element of the sample in no way depends upon the value of the jth. The "Run" test (Reference 6) is a standard non-parametric statistical procedure used to indicate the presence of trends or sequential correlation in a given sample. In this test it is hypothesized that each observation is independent of its neighbors. Under this hypothesis the probability of a sample point being greater or less than the sample median does not change from observation to observation. This makes possible the construction of sampling distribution for the number of "runs" of data greater than or less than the median. With this in hand the sample size determines a confidence interval on the number of runs which should be contained in the data. In performing the test on a given sample, the number of runs of data above and below the median is computed and compared with the confidence interval. If the number of runs in the sample is within the interval the test is passed, which is to say that the hypothesis of statistical independence is accepted. All the run testing

to be noted was performed at the conventional 5% level of significance. This simply means that the test is designed in such a way that a 5% probability is accepted that the independence hypothesis will be rejected when it is in fact true.

Application to Short Term Stress Maxima and Minima

Counting both the real and simulated data, the three components of stress, and the fact that minima exist when multiple maxima are present, there are 240 ordered samples in the present data sub-set. Some 96% of these samples fail the run test at the 5% level of significance--a result not at all surprising. The way around this is the same as noted in References 12* and 13*. Essentially the run test is repeated for decimated samples which are produced when only every j^{th} sample element is used ($j=1,2....$). From these results it is possible to find an increment, J_c, such that when every $(J_c)^{th}$ sample element is used to form a decimated sample, that sample will pass the run test at the 5% level of significance. The value of J_c found for each sample is then taken as a specification in the sense that it is assumed that the result of a J_c^{th} decimation will be a random sample. There is no guarantee that this procedure will always lead to success, but previous experience with real and contrived data suggests that it elimates the worst effects of serial correlation.

---

*12. Miles, M.D., "On the Short-Term Distribution of the Peaks of Combined Low Frequency and Springing Stresses," Hull Stresses in Bulk Carriers in the Great Lakes and Gulf of St. Lawrence Wave Environment, Society of Naval Architects and Marine Engineers, T & R Symposium S-2 (1971).

*13. Dalzell, J. F. et al, "Examination of Service and Stress Data of Three Ships for Development of Hull Girder Load Criteria," SSC-287, Ship Structure Committee, 1979, AD-A072910.

Summary of Run Test Results

The essential results of all the run tests performed are summarized in Table F-1. The numbers given are the decimation specification, J_c. For each data run there are naturally 12 sets of data; maxima and minima for each of the three components of stress, for both the observed data and the simulation.

Several comments may be made about the contents of the table. First, the decimation specification for the maxima of a run seldom differ by more than one from the specifications for the corresponding minima. This holds for both the real data and the simulation. As far as the run tests are concerned, both the real and simulated data are statistically symmetric. Since the simulation is a statistically symmetric process by the nature of its basic assumptions the result is at least half that expected.

It is clear that the general nature of the simulated time histories parallels that of the real ones. Decimation specifications for wave induced stress are nearly constant over both the simulated and real data sets. There is more variability in the specifications for springing. A brief inspection of the springing spectra suggests that the run to run variability is in the correct direction, the narrower the spectrum the larger the increment. It is believed that the results from the springing simulation are not significantly different from those from the real springing data. Of the 20 comparisons for springing maxima, 6 specifications are the same, and in the remaining 14 the specification for the simulation is larger than that for the real data in exactly half the cases. The numbers for the combined stress data are quite strongly influenced by the relative magnitudes of wave induced and springing stresses. It is thought that the specifications for combined stress observation and simulation are not significantly different in 17 out of the 20 runs. The three runs where something is different are 77, 102 and 15. Why the wide disparity between observation and simulation occurs in these cases could not be determined. The time histories look alike--perhaps these are cases where the indpendent assumption was rejected when it was true (or vice versa).

TABLE F-1

SUMMARY OF RUN TEST RESULTS

(Decimation Specification, J_c)

		COMBINED STRESS				SPRINGING STRESS				WAVE INDUCED STRESS			
		MAXIMA		MINIMA		MAXIMA		MINIMA		MAXIMA		MINIMA	
YEAR	RUN	OBS.	SIM.	OBS.	SIM.	OBS.	SIM.	OBS.	SIM.	OBS.	SIM.	OBS.	SIM.
1979	74	2	2	2	2	6	5	6	5	2	2	2	3
	75	2	2	2	3	9	5	9	5	2	2	2	2
	77	1	4	1	4	4	6	5	5	2	3	2	3
	99	4	6	4	6	6	8	6	8	2	3	2	2
	100	4	3	4	4	6	8	6	8	2	2	2	2
	101	5	7	6	7	7	8	7	8	2	2	2	2
	102	1	4	1	4	6	6	6	6	2	2	2	2
	103	4	5	4	5	5	6	5	6	2	2	2	2
	116	3	2	4	2	7	5	5	5	1	2	1	2
	117	4	6	4	7	6	8	6	9	2	2	2	2
1980	3	4	3	4	2	9	6	9	6	2	2	2	2
	4	4	2	4	3	9	8	9	8	2	2	2	2
	5	5	5	5	5	9	7	9	8	2	2	2	2
	8	3	3	2	3	6	6	7	5	3	3	2	2
	13	3	3	3	3	8	8	7	7	2	2	3	2
	14	1	3	1	3	7	7	7	6	2	3	2	2
	15	1	9	1	7	9	11	8	11	2	3	2	2
	16	3	3	3	3	7	5	6	5	2	2	2	2
	20	2	3	3	3	6	6	6	6	2	2	3	2
	21	5	4	4	5	6	6	6	5	2	2	2	2

APPENDIX G

COMPARISONS OF STATISTICS FROM REAL DATA AND SIMULATIONS

Introduction

With the problem of statistical independence within each of the 240 ordered sets of maxima and minima approximately taken care of by the decimation procedure just described, it remained to compare the statistics of observation and simulation. A reasonable overall approach appeared to be as follows. The state-of-art statistical model which has been adopted for the combined stress response is that the stress is a linear response to zero mean ergodic Gaussian-wave excitation. These assumptions being made, it follows theoretically that the stress is also a zero mean ergodic Gaussian process, and is statistically symmetric. The theoretical probability density function of the maxima of such a process is known (Reference 14* for example). Accordingly, the hypothesis was made that the density of maxima of real data follows the theoretical and the remainder of the work essentially involved testing this hypothesis in a number of ways relative to both real and simulated data.

The Hypothesized Probability Density

The theoretical probability density of maxima (in the notation of Reference 14) is as follows:

$$p(\eta) = \frac{1}{\sqrt{2\pi}} \left[\varepsilon \operatorname{Exp}\left[-\eta^2/2\varepsilon^2\right] + \sqrt{1-\varepsilon^2}\, \eta \operatorname{Exp}\left[-\eta^2/2\right] \cdot \phi\left[\eta \sqrt{(1-\varepsilon^2)/\varepsilon^2}\,\right]\right] \qquad \text{(G-1)}$$

---

*14. Cartwright, D. E., and Longuet-Higgins, M. S., "The Statistical Distribution of the Maxima of a Random Function," Proc. Royal Society, A, 237, 1956.

where:

η = reduced variate

= X/σ

X = the (dimensional) maxima of the process

σ = the RMS of the process (square root of variance)

ε^2 = spectrum broadness parameter

$$\phi(a) = \int_{-\infty}^{a} \text{Exp}\,[-t^2/2]\,dt$$

The maxima and minima of the theoretical process are statistically symmetric so that if the minima are denoted by Y, the reduced variate becomes $\eta = -Y/\sigma$. When ε approaches unity (zero) the density approaches the normal (Rayleigh).

Parameter Fitting

In order to make statistical comparisons the analytical expression must be fitted to the data. Two approaches are available. The parameters σ and ε are functions of the 0th, 2nd, and 4th moments of the spectrum:

$$\sigma^2 = m_o$$

$$\varepsilon^2 = 1 - m_2^2/m_o m_4 \qquad \text{(G-2)}$$

$$\text{and} \quad m_n = \int \omega^n S(\omega)\,d\omega$$

where $S(\omega)$ is the spectrum.

The second apprach involves functions of the sample of maxima (Reference 14). Given a sample of N maxima, $X_1, X_2 \ldots X_n$:

$$\sigma^2 = M_2 - 2M_1^2/\pi$$

$$\varepsilon^2 = (\pi - 4\rho)/(\pi - 2\rho) \qquad \text{(G-3)}$$

where:

$$\rho = M_1^2/M_2$$

$$M_1 = \frac{1}{N}\sum_{i=1} X_i$$

$$M_2 = \frac{1}{N}\sum_{i=1} X_i^2$$

The approach used in fitting the RMS parameter, σ, varied according to the stress component. In the case of the combined stress, σ from the approach given in Equation G-2 is given in Tables A-1 and B-1 and these were the values used for both simulated and real data. The second approach (Equation G-3) was used for springing and wave induced stresses since it was desired to produce some measure by which the simulations could be compared to the real maxima. The results of this latter process are summarized in Table G-1. All estimates shown were made from the decimated samples dictated by the analysis of the preceeding appendix. It is clear that the differences in the estimates of σ from simulation and observation are relatively small--sample to sample variations in the RMS computed from spectra of samples of the present length are typically of the magnitude of the differences shown. It is also clear that the differences between the estimates of maxima and minima are exceedingly small in both simulation and observation, further evidence of statistical symmetry.

The approach used in fitting the broadness parameter was that using the samples of maxima and minima, Equation G-3. This method was utilized for all three components of stress. The results are summarized in Table G-2. Estimates for observation and simulation are generally of the same magnitude, but with some glaring exceptions. The method, Equation G-3 involves subtraction of two numbers of roughly the same magnitude in the present case and it is suspected that considerable scatter results. Something like the same magnitude of variation was experienced when similar estimates were made for the maxima and minima of a large number of stress records in Reference 13.

"Goodness of Fit" Tests

The basic question it was desired to answer next was:

> Could the maxima and minima from the real data have been drawn from a population having the theorectical density function, Equation G-1?

With respect to the objective of comparing simulation and real data,

TABLE G-1

VALUES OF SPRINGING AND WAVE INDUCED RMS STRESS DEDUCED FROM THE SAMPLES OF MAXIMA AND MINIMA

		SPRINGING STRESS				WAVE INDUCED STRESS			
		MAXIMA		MINIMA		MAXIMA		MINIMA	
YEAR	RUN	OBS.	SIM.	OBS.	SIM.	OBS.	SIM.	OBS.	SIM.
1979	74	0.69	0.72	0.68	0.73	0.57	0.52	0.56	0.51
	75	0.85	0.79	0.85	0.78	0.64	0.66	0.63	0.66
	77	0.81	0.76	0.81	0.77	0.68	0.72	0.71	0.74
	99	0.81	0.89	0.81	0.87	0.40	0.38	0.40	0.40
	100	0.85	0.79	0.85	0.79	0.55	0.57	0.51	0.54
	101	0.97	1.13	0.97	1.12	0.65	0.61	0.59	0.64
	102	0.80	0.83	0.80	0.83	0.52	0.51	0.50	0.50
	103	0.88	0.92	0.87	0.93	0.44	0.41	0.44	0.43
	116	0.79	0.73	0.81	0.72	0.58	0.60	0.58	0.60
	117	1.00	1.02	1.00	0.99	0.52	0.52	0.52	0.53
1980	3	0.95	0.85	0.93	0.86	0.62	0.61	0.61	0.62
	4	0.92	0.82	0.91	0.81	0.65	0.67	0.69	0.66
	5	1.12	1.22	1.12	1.22	0.57	0.61	0.56	0.62
	8	0.22	0.22	0.23	0.22	0.27	0.29	0.27	0.28
	13	0.77	0.76	0.73	0.76	0.58	0.58	0.58	0.59
	14	0.78	0.72	0.79	0.75	0.54	0.52	0.53	0.54
	15	0.90	1.01	0.84	1.00	0.61	0.64	0.63	0.62
	16	0.90	0.86	0.91	0.85	0.61	0.59	0.62	0.56
	20	0.48	0.46	0.47	0.46	0.30	0.31	0.30	0.31
	21	0.47	0.40	0.46	0.40	0.26	0.29	0.26	0.28

TABLE G-2

VALUES OF SPECTRAL BROADNESS PARAMETER, ε^2,

ESTIMATED FROM SAMPLES OF MAXIMA AND MINIMA

		COMBINED STRESS				SPRINGING STRESS				WAVE INDUCED STRESS			
		MAXIMA		MINIMA		MAXIMA		MINIMA		MAXIMA		MINIMA	
YEAR	RUN	OBS.	SIM.	OBS.	SIM.	OBS.	SIM.	OBS.	SIM.	OBS.	SIM.	OBS.	SIM.
1979	74	0.00	0.07	0.05	0.03	0.00	0.00	0.00	0.00	0.00	0.12	0.02	0.09
	75	0.08	0.18	0.17	0.14	0.09	0.09	0.09	0.00	0.07	0.17	0.07	0.14
	77	0.05	0.21	0.15	0.25	0.00	0.04	0.00	0.06	0.12	0.11	0.19	0.15
	99	0.05	0.14	0.04	0.11	0.05	0.02	0.06	0.01	0.08	0.05	0.10	0.09
	100	0.03	0.12	0.15	0.20	0.08	0.00	0.06	0.00	0.15	0.18	0.11	0.10
	101	0.00	0.03	0.05	0.07	0.00	0.01	0.01	0.03	0.28	0.10	0.13	0.19
	102	0.00	0.18	0.01	0.21	0.00	0.14	0.00	0.13	0.11	0.11	0.02	0.14
	103	0.02	0.13	0.03	0.12	0.00	0.00	0.00	0.00	0.04	0.16	0.13	0.14
	116	0.08	0.02	0.13	0.03	0.00	0.00	0.00	0.00	0.14	0.16	0.16	0.16
	117	0.10	0.05	0.01	0.15	0.06	0.00	0.05	0.00	0.12	0.10	0.11	0.05
1980	3	0.16	0.02	0.13	0.07	0.14	0.00	0.12	0.00	0.08	0.10	0.02	0.08
	4	0.14	0.09	0.07	0.00	0.11	0.01	0.08	0.00	0.08	0.20	0.17	0.15
	5	0.03	0.08	0.05	0.09	0.00	0.02	0.00	0.08	0.03	0.03	0.00	0.07
	8	0.14	0.25	0.17	0.15	0.00	0.00	0.00	0.00	0.21	0.19	0.20	0.14
	13	0.15	0.12	0.11	0.18	0.00	0.00	0.00	0.01	0.17	0.09	0.06	0.09
	14	0.13	0.09	0.11	0.18	0.03	0.04	0.01	0.04	0.07	0.13	0.07	0.14
	15	0.21	0.05	0.15	0.24	0.09	0.09	0.11	0.09	0.17	0.06	0.14	0.18
	16	0.23	0.18	0.12	0.14	0.07	0.00	0.11	0.00	0.09	0.11	0.13	0.08
	20	0.05	0.09	0.01	0.12	0.05	0.00	0.02	0.00	0.14	0.08	0.13	0.07
	21	0.13	0.11	0.10	0.15	0.00	0.00	0.00	0.00	0.05	0.07	0.07	0.11

the question comes to whether or not standard statistical test procedures can detect any significant difference between the two.

There were two goodness of fit tests applied to all the data, and a third, largely graphical test, to about half the data. The first steps in applying the tests have been described: decimation and the fitting of parameters.

The first test is the conventional Chi-Square Test, Reference 6. In this test, the parameters of the hypothesized distribution are fitted to the sample data, the data are sorted into class intervals and the sample chi-square statistic computed in the usual way. All tests were performed using the equi-probability class interval method. In this approach, the boundaries of the class intervals are chosen so that the expected sample frequency is the same in all intervals (and equal to 1/(number of class intervals). The number of class intervals was chosen according to the sample size according to an extrapolation of recommendations given in Reference 6 for the optimization of Chi-Square tests at the 5% level of significance. The expected number of sample points per class interval resulting from this method is as follows:

Sample Size	Expected Number of Sample Points Falling in Each Class Interval
200	13
100	8
50	5
20	3

To evaluate the adequacy of the fit, an evaluation was made of the percentage point of the Chi-Square distribution with (number of class intervals - 3) degrees of freedom corresponding to the sample Chi-Square statistic.

The second test was the Kolmogorov-Smirnov test as outlined in Reference 15*. In this test the maximum deviation between the sample distribution and the hypothesized distribution is computed. A statistic, approximately Chi-Square distributed with 2 degrees of freedom, is formed by multiplying the squared maximum deviation by four times the sample size. The percentage point of the Chi-Square distribution with 2 degrees of freedom corresponding to this statistic is then evaluated, and this, in turn, is used to interpret the test.

The results of these tests are summarized in Tables G-3 through G-5. Table G-3 pertains to combined stress, Table G-4 to springing stress, and Table G-5 to wave induced stress. The number of points in the decimated samples is included in each case. The results of the tests are given as the "level of significance" which would have had to be chosen in the test design in order that the hypothesis be accepted that the data could have been drawn from the theoretical population. These tests are statistical hypothesis tests and it may be in order to discuss some of the caveats before interpreting the results.

No hypothesis test can indicate with absolute certainty that something is true or false. In all cases, there is a "level of significance" of some sort designed into the test. The level of significance can be interpreted as the probability of rejecting a hypothesis on the basis of an individual sample when it is really true. Unfortunately, a designed zero level of significance corresponds to an automatic acceptance of the hypothesis regardless of its truth. The usual philosophy is to design the test for a 5 or sometimes 10% probability of failure, and to make pass/fail deteriminations rigorously on this basis for each individual case. If an individual case is failed at the nominal level of significance, the meaning of the failure

---

*15. Ochi, M. K. and Bolton, W. E., "Statistics for Prediction of Ship Performance in a Seaway," International Shipbuilding Progress, 1973.

TABLE G-3

RESULTS OF THE CHI-SQUARE AND KOLMOGOROV-SMIRNOV GOODNESS OF FIT TESTS APPLIED TO THE OBSERVED AND SIMULATED COMBINED STRESS MAXIMA AND MINIMA

		# POINTS IN SAMPLE				CHI-SQUARE TEST PASSING SIGNIFICANCE LEVELS				KOLMOGOROV-SMIRNOV TEST PASSING SIGNIFICANCE LEVELS			
		MAXIMA		MINIMA		MAXIMA		MINIMA		MAXIMA		MINIMA	
YEAR	RUN	OBS.	SIM.	OBS.	SIM.	OBS.	SIM.	OBS.	SIM.	OBS.	SIM.	OBS.	SIM.
1979	74	193	198	193	198	9.1	75.8	10.0	73.3	28.0	34.8	10.5	46.7
	75	195	196	195	130	70.4	43.7	3.2	76.3	66.1	36.6	52.7	27.6
	77	388	96	388	96	10.9	68.9	55.6	41.5	16.6	48.9	41.1	20.1
	99	100	68	99	68	58.3	6.7	37.3	49.3	40.3	17.7	6.8	24.4
	100	100	134	100	100	63.3	7.9	37.7	19.5	78.7	46.9	23.4	29.4
	101	80	58	67	58	40.7	17.3	75.7	93.8	34.8	12.3	44.2	40.9
	102	408	99	407	99	5.5	63.1	31.7	11.0	39.6	32.6	41.8	47.5
	103	101	82	101	82	93.2	41.9	38.3	44.5	54.9	21.4	13.9	38.7
	116	124	186	93	187	25.2	22.5	55.7	83.3	47.2	12.9	46.5	31.2
	117	93	63	93	54	43.1	3.2	10.6	15.6	67.9	9.3	28.9	60.4
1980	3	124	122	124	184	42.4	95.0	4.6	71.3	52.7	66.3	19.5	19.5
	4	123	187	123	125	31.6	5.5	43.5	3.5	36.6	11.1	45.4	22.8
	5	101	76	101	76	46.9	72.0	63.7	13.8	15.8	28.5	61.2	13.7
	8	118	117	178	116	56.1	69.4	66.7	76.2	46.2	42.5	37.1	58.7
	13	178	134	178	134	15.6	46.0	62.3	80.8	37.5	65.3	40.8	78.5
	14	537	135	538	134	14.1	12.3	8.0	88.3	14.5	38.4	31.7	66.6
	15	540	45	541	58	82.2	26.9	16.3	8.9	51.0	25.8	38.8	12.0
	16	177	137	177	136	74.4	88.9	75.8	2.8	26.2	74.7	58.8	17.7
	20	246	122	165	122	90.8	35.8	1.6	5.8	52.4	70.4	11.8	55.4
	21	100	94	126	76	80.2	73.1	88.9	62.4	69.6	44.6	65.2	14.0

TABLE G-4

RESULTS OF THE CHI-SQUARE AND KOLMOGOROV-SMIRNOV GOODNESS OF FIT TESTS APPLIED TO THE OBSERVED AND SIMULATED SPRINGING STRESS MAXIMA AND MINIMA

		# POINTS IN SAMPLE				CHI-SQUARE TEST PASSING SIGNIFICANCE LEVELS				KOLMOGOROV-SMIRNOV TEST PASSING SIGNIFICANCE LEVELS			
		MAXIMA		MINIMA		MAXIMA		MINIMA		MAXIMA		MINIMA	
YEAR	RUN	OBS.	SIM.	OBS.	SIM.	OBS.	SIM.	OBS.	SIM.	OBS.	SIM.	OBS.	SIM.
1979	74	67	81	67	82	64.9	29.6	95.4	26.2	77.1	9.2	83.2	29.1
	75	46	83	46	83	14.4	23.5	23.8	40.3	26.8	57.9	28.8	51.8
	77	104	69	83	83	61.3	88.2	33.3	65.5	49.0	74.7	61.0	56.7
	99	70	59	69	69	$\boxed{2.5}$	79.3	13.2	72.3	33.0	47.5	38.2	69.2
	100	70	53	70	53	47.5	35.9	41.4	47.1	43.4	48.1	43.6	52.4
	101	60	53	60	52	88.5	90.2	91.4	6.0	75.7	58.0	82.0	61.0
	102	69	70	69	70	7.4	41.4	10.9	81.2	$\boxed{2.6}$	45.0	5.8	37.0
	103	83	70	83	70	56.7	67.7	37.9	9.1	30.2	54.9	36.9	26.7
	116	55	78	77	79	11.2	82.3	30.7	30.8	26.0	32.9	33.7	16.4
	117	65	48	65	43	62.2	85.4	41.3	31.9	46.7	27.2	50.9	24.0
1980	3	57	65	57	65	9.1	54.9	8.1	5.8	25.5	80.1	26.8	69.0
	4	58	49	58	49	93.8	52.0	44.7	71.5	77.0	67.7	66.8	76.0
	5	57	55	58	49	62.6	8.0	73.1	22.9	59.0	46.4	80.2	9.5
	8	65	65	55	78	7.9	32.6	53.7	37.8	63.1	43.3	78.5	25.8
	13	70	53	81	60	26.3	64.6	22.1	18.8	39.4	50.8	29.9	58.7
	14	81	61	81	71	18.9	12.6	27.6	41.1	45.1	47.6	52.8	58.8
	15	63	39	71	39	$\boxed{1.5}$	62.9	5.7	45.5	26.4	66.9	34.2	48.3
	16	81	85	94	85	91.2	50.8	5.6	79.1	76.0	25.3	47.5	15.5
	20	86	65	86	65	82.9	80.6	60.8	35.3	60.3	56.3	66.8	70.7
	21	86	65	87	78	15.2	27.6	65.5	67.3	58.7	29.0	74.9	10.8

TABLE G-5

RESULTS OF THE CHI-SQUARE AND KOLMOGOROV-SMIRNOV GOODNESS OF FIT TESTS APPLIED TO THE OBSERVED AND SIMULATED WAVE INDUCED STRESS MAXIMA AND MINIMA

		# POINTS IN SAMPLE				CHI-SQUARE TEST PASSING SIGNIFICANCE LEVELS				KOLMOGOROV-SMIRNOV TEST PASSING SIGNIFICANCE LEVELS			
		MAXIMA		MINIMA		MAXIMA		MINIMA		MAXIMA		MINIMA	
YEAR	RUN	OBS.	SIM.	OBS.	SIM.	OBS.	SIM.	OBS.	SIM.	OBS.	SIM.	OBS.	SIM.
1979	74	155	154	155	103	74.2	76.1	94.9	13.6	61.7	64.7	73.7	50.2
	75	151	150	151	149	12.2	46.8	71.3	62.7	45.4	20.6	67.3	58.4
	77	143	96	144	96	54.6	29.3	60.1	46.1	33.9	52.9	57.5	71.4
	99	152	153	152	153	28.9	83.9	0.9	0.0	41.8	69.3	7.9	26.8
	100	135	133	136	133	48.7	66.3	31.6	31.5	25.7	50.7	47.5	59.1
	101	138	136	138	136	9.0	1.2	43.3	17.7	23.9	35.9	55.4	50.3
	102	140	141	140	141	83.0	72.8	84.5	56.4	57.1	51.3	72.3	64.4
	103	149	151	149	151	22.1	59.4	62.7	54.3	55.8	28.5	62.9	26.6
	116	295	145	296	146	65.4	20.1	29.3	69.6	43.4	42.8	20.3	62.6
	117	155	150	155	150	2.2	58.4	43.5	30.8	8.5	39.8	72.3	71.9
1980	3	202	152	203	152	37.9	92.5	6.8	52.1	51.0	43.3	19.2	33.9
	4	213	155	212	155	82.9	22.3	49.1	49.7	52.2	29.0	47.3	72.9
	5	207	159	207	159	20.2	11.8	19.5	29.5	15.1	66.2	14.2	60.0
	8	85	84	128	126	59.2	49.4	75.6	99.5	68.9	41.1	55.1	72.9
	13	199	149	133	150	86.2	4.5	42.4	19.9	66.1	26.5	73.6	32.2
	14	182	94	182	141	69.9	52.1	87.5	16.5	39.3	53.5	61.6	50.2
	15	172	87	172	129	66.9	20.2	68.4	89.6	68.5	25.6	50.7	58.8
	16	180	134	180	133	25.0	2.4	22.3	17.7	59.4	45.6	45.9	30.8
	20	192	146	128	146	85.4	93.4	34.1	66.1	46.6	64.8	40.3	52.1
	21	191	143	191	143	32.9	77.6	2.2	46.0	44.0	65.3	13.8	33.3

is assessed in terms of the level of significance at which the test would be passed. Thus if a particular sample fails at the 5% level of significance but would have passed had the test been designed for 4%, the failure is not considered too significant. If the test could only be passed if the test had been designed for 0.1% level of significance, the failure must be considered highly significant. Conversely, if the tests could be passed if the design had been for an 80% level of significance it would be nearly impossible to reject the hypothesis--in terms of the contents of the tables the higher the number the better the fit. For the conventional 5% level of significance design only cases where the numbers given are below 5% would be considered failures.

It may be noted that if repeated tests of independent samples truly drawn from a hypothesized population are made at the 5% level of significance, it would be expected in the long run that the rate of failure would approach 5%. Extrapolating this a bit, if it is hypothesized that one of the present stress components always follows the theoretical density and tests are made on many samples the failure rate should be roughly 5% if the hypothesis is always true, and a very much larger rate if the hypothesis is not always (or never) true.

Returning to the results in Tables G-3 through G-5 it may be noted that all the passing levels of significance below 5% have been boxed in. These are the tests which were failed at the 5% level of significance. A great number of the tests pass at very high levels of significance. In the 240 Kolmogorov-Smirnov tests which were performed, only one failure (Table G-4) is noted. Out of the 240 Chi-Square tests performed 15 were failed at the 5% level of significance, a rate of 6%. Considering the number of failures of all the Chi-Square tests on the simulated data, the seven failures noted translate to a rate of 5.8% versus a failure rate of 6.7% for the real data.

If any particular column in the tables is considered, the expected number of failures would be one. However it would not be at all unusual in a relatively small number of tests to experience

twice the nominal failure rate even if the hypothesis was always true. In this context it is worth noting that in two columns of the tables three failures are noted. One of these two is that for observed combined stress minima, Table G-3. The other is that for the simulated wave induced stress maxima, Table G-5. The simulated stresses are supposed to follow the theoretical distribution. The fact that the detailed incidence of failures for a part of the simulation is perhaps a bit higher than expected is possibly due to imperfections in the test procedure--specifically the approach to the estimation of broadness parameter.

The results in the tables suggest two things. First, the fit of real data to the theoretical distribution is statistically indistinguishable from the fit of simulated data. Second, the hypothesis that the maxima and minima of the real data fit the theoretical density should be generally accepted.

There is third type of test of goodness of fit which is essentially graphical. This is to plot the sample probabilities on a suitable probability paper and compare the sample points to the straight line which is the best fit to the sample. Since the theoretical density contains two parameters, only one of which can be used to form a non-dimensional variate, there are an infinite number of probability papers possible for this distribution--one for each conceivable choice of broadness parameter, ε^2. However, if the necessary graphical work is automated, it is not difficult to prepare a new probability paper for the fitted value of broadness parameter for each sample. This course was taken in the present instance and applied to a portion of the available samples. The results are included in Figures G-1 through G-28, which are bound at the end of this appendix.

Each figure pertains to either the maxima or minima in the decimated samples produced for combined, springing, and wave induced stress. Since this effort was intended largely to confirm the findings just noted it was decided to apply the procedure to half the real data,

choosing either maxima or minima according to which appeared to be the worst fits to the distribution. In the event the fits of both maxima and minima were done for 1978 Runs 77 and 117, and 1980 Runs 8 and 15. Data from only two simulated runs were plotted, but in each case both the maxima and minima were included. The figures where a comparison of observed and simulated results can be made are Figures G-7 through G-9 for Run 101, and Figures G-22 through G-25 for 1980 Run 15.

In any probability paper what is being plotted is the value of reduced variate which corresponds to the sample probability, as a function of the dimensional value of the variate. The theoretical distribution is thus always a straight line in the present case because of the definitions, Equation G-1. In the present plots the reduced variate scale is shown on the right, and the probability scale to the left. The horizontal scale is the dimensional variate when maxima are involved, and the negative of the sample minima when minima are indicated. The sample distribution, shown as square symbols, is that derived from the class intervals used in the Chi-Square tests previously described. Thus the spacing of points along the horizontal axis varies because of the equi-probability approach to determining class intervals. The sample extremes are plotted as plus signs in each case. Following Reference 16* the probabilities assigned to the largest and smallest values in a sample of N are N/(N+1) and 1/(N+1) respectively.

In the graphical approach to goodness of fit it is necessary to provide some way of indicating the significance of the inevitable deviations between the sample probabilities and the theoretical straight line. The "90% control curves" shown on the plots are the approach to this problem noted in Reference 16, which was derived from the asymptotic distribution of the nth highest value in a sample.

---

*16. Gumbel, D. E., "Statistics of Extremes," Columbia University Press, New York, 1958.

Between probability levels of 0.1 and 0.9 the 90% control curves are formed by adding and subtracting a quantity, δ, from the value of sample variate corresponding to the fitted theoretical distribution at probability level P, and δ is defined as follows:

$$\delta = \frac{1.65}{p(\eta_*)} \sqrt{\frac{P(1-P)}{N}}$$

where: $p(\eta_*)$ = theoretical probability density corresponding to η_*.

η_* = the reduced variate corresponding to probability P.

σ = sample standard deviation (RMS)

N = sample size.

The 90% control curves are extended above and below probability levels of 0.9 and 0.1 by drawing straight lines to the 90% confidence bounds on the sample extremes. Once all the graphical work is done, the results are interpreted quite simply. If the sample probabilities (excluding extremes) all fall within the 90% control curves it is accepted that the deviations between sample and theory are not statistically significant, and thus that the sample may reasonably be supposed to come from the hypothesized distribution.

Conclusions based upon Figures G-1 through G-28 are somewhat in the eye of the beholder. It is believed however the the graphical results bear out the numerical results indicated previously. There are two exceptions in the 84 plots shown. It is difficult to be convinced that the springing minima for observed data, Run 102 (Figure G-10) fit the theoretical distribution well enough to pass the numerical tests at the 5% level of significance. Precisely the same difficultly is presented by the graphical result for simulated minima of combined stress, Run 15 (Figure G-25). Again, there is at least one oddity in both the observed and the simulated data.

Analysis of Sample Extremes

The extremes of each sample of maxima and minima were noted in passing in the discussion of the graphical goodness of fit tests. In the present context there can be little interest in the smallest value of a maximum unless it is negative and of the same magnitude as the largest positive maximum. Nowhere in the current data is this true and accordingly only the largest values of each sample were further analyzed.

As in all previous analyses the questions of interest are:

> Are the extremes statistically symmetrical, are the differences between observation statistically significant and could the observed sample extremes reasonably have been experienced in a sample drawn from the theoretical population of maxima of Gaussian processes?

The statistical questions were approached by working out the 90% confidence bounds on the largest in a sample of the decimated sizes indicated in Tables G-3 through G-5, assuming the theoretical probability density of Equation G-1, the fitted values of broadness parameter, Table G-2, and the general expression for the probability density of the largest member in a sample, Reference 16. Similar to the hypothesis tests previously mentioned, it is expected that the sample extremes should in a long run of independent samples be included within the confidence bounds so constructed in 9 out of 10 samples.

Tables G-6 through G-8 summarize the sample extremes for maxima and minima and indicate as well whether the extreme was within the 90% confidence bounds. Table G-6 summarizes the combined stress results, Table G-7 those for springing stress, and Table G-8 the results for the wave induced stress extremes. The columns which serve to indicate if the extreme fell within the 90% confidence bounds contain a "Y" to indicate yes that it did, and an "N-High" or "N-Low" to indicate that

TABLE G-6

SUMMARY OF COMBINED STRESS SAMPLE EXTREMES

		SAMPLE MAXIMA				SAMPLE MINIMA			
YEAR	RUN	OBSERVED EXTREME (KPSI)	OBS. WITHIN 90% BOUNDS?	SIMULATED EXTREME (KPSI)	SIM. WITHIN 90% BOUNDS?	OBSERVED EXTREME (KPSI)	OBS. WITHIN 90% BOUNDS?	SIMULATED EXTREME (KPSI)	SIM. WITHIN 90% BOUNDS?
1979	74	3.1	Y	3.0	Y	-3.3	Y	-2.9	Y
	75	4.0	Y	3.6	Y	-3.8	Y	-3.7	Y
	77	3.1	N-LOW	3.5	Y	-4.5	Y	-3.3	Y
	99	3.0	Y	3.6	N-HIGH	-2.8	Y	-3.4	N-LOW
	100	3.1	Y	3.9	Y	-3.8	Y	-3.7	Y
	101	3.4	Y	4.7	N-HIGH	-3.6	Y	-4.4	N-LOW
	102	2.9	N-LOW	4.0	N-HIGH	-3.3	Y	-3.5	Y
	103	3.4	Y	3.5	Y	-3.3	Y	-3.7	Y
	116	3.3	Y	3.5	Y	-4.0	Y	-3.5	Y
	117	4.1	Y	3.9	Y	-4.2	Y	-4.2	N-LOW
1980	3	4.7	N-HIGH	3.7	Y	-4.1	Y	-3.8	Y
	4	3.9	Y	3.8	Y	-4.1	Y	-3.4	Y
	5	4.2	Y	4.8	Y	-4.2	Y	-4.7	Y
	8	1.2	Y	1.4	Y	-1.2	Y	-1.2	Y
	13	3.5	Y	3.1	Y	-3.6	Y	-3.0	Y
	14	3.4	Y	3.0	Y	-3.0	Y	-3.2	Y
	15	3.9	Y	3.9	N-HIGH	-3.5	Y	-4.0	N-LOW
	16	4.1	Y	3.9	Y	-3.9	Y	-3.7	Y
	20	2.0	Y	2.2	N-HIGH	-1.9	Y	-2.0	Y
	21	2.2	N-HIGH	1.5	Y	-2.0	Y	-1.6	Y

TABLE G-7

SUMMARY OF SPRINGING STRESS SAMPLE EXTREMES

		SAMPLE MAXIMA				SAMPLE MINIMA			
YEAR	RUN	OBSERVED EXTREME (KPSI)	OBS. WITHIN 90% BOUNDS?	SIMULATED EXTREME (KPSI)	SIM. WITHIN 90% BOUNDS?	OBSERVED EXTREME (KPSI)	OBS. WITHIN 90% BOUNDS?	SIMULATED EXTREME (KPSI)	SIM. WITHIN 90% BOUNDS?
1979	74	2.0	Y	2.1	Y	-2.0	Y	-2.2	Y
	75	2.7	Y	2.5	Y	-2.8	Y	-2.4	Y
	77	2.6	Y	3.0	N-HIGH	-2.7	Y	-3.0	Y
	99	2.6	Y	2.8	Y	-2.7	Y	-2.8	Y
	100	2.5	Y	2.2	Y	-2.5	Y	-2.2	Y
	101	2.8	Y	4.3	Y	-2.8	Y	-4.2	N-LOW
	102	2.3	Y	2.8	Y	-2.3	Y	-2.9	Y
	103	2.6	Y	3.0	Y	-2.6	Y	-3.0	Y
	116	2.9	Y	2.1	Y	-3.0	Y	-2.1	Y
	117	3.5	Y	3.2	Y	-3.5	Y	-3.1	Y
1980	3	3.9	N-HIGH	2.9	Y	-3.8	N-LOW	-2.9	Y
	4	2.8	Y	2.4	Y	-2.8	Y	-2.4	Y
	5	3.4	Y	3.8	Y	-3.4	Y	-3.8	Y
	8	.74	Y	.75	Y	- .75	Y	- .76	Y
	13	2.6	Y	2.2	Y	-2.6	Y	-2.2	Y
	14	2.5	Y	2.5	Y	-2.5	Y	-2.5	Y
	15	3.3	Y	3.3	Y	-3.3	N-LOW	-3.4	Y
	16	3.5	N-HIGH	2.8	Y	-3.4	Y	-2.8	Y
	20	1.5	Y	1.4	Y	-1.5	Y	-1.3	Y
	21	1.5	Y	1.3	Y	-1.5	Y	-1.3	Y

TABLE G-8

SUMMARY OF WAVE INDUCED STRESS SAMPLE EXTREMES

		SAMPLE MAXIMA				SAMPLE MINIMA			
YEAR	RUN	OBSERVED EXTREME (KPSI)	OBS. WITHIN 90% BOUNDS?	SIMULATED EXTREME (KPSI)	SIM. WITHIN 90% BOUNDS?	OBSERVED EXTREME (KPSI)	OBS. WITHIN 90% BOUNDS?	SIMULATED EXTREME (KPSI)	SIM. WITHIN 90% BOUNDS?
1979	74	1.7	Y	1.8	Y	-1.7	Y	-1.9	Y
	75	2.7	N-HIGH	2.8	N-HIGH	-2.3	Y	-2.8	N-LOW
	77	2.2	Y	2.6	Y	-2.5	Y	-2.5	Y
	99	1.3	Y	1.2	Y	-1.3	Y	-1.2	Y
	100	2.0	Y	2.0	Y	-1.8	Y	-1.9	Y
	101	2.0	Y	2.2	Y	-1.8	Y	-2.4	Y
	102	1.7	Y	1.8	Y	-1.6	Y	-1.8	Y
	103	1.5	Y	1.5	Y	-1.7	Y	-1.6	Y
	116	1.9	Y	2.6	N-HIGH	-1.8	Y	-2.4	Y
	117	1.8	Y	1.9	Y	-1.8	Y	-2.0	Y
1980	3	2.1	Y	2.0	Y	-2.1	Y	-2.1	Y
	4	2.4	Y	2.4	Y	-2.2	Y	-2.2	Y
	5	1.8	Y	2.1	Y	-1.9	Y	-1.9	Y
	8	.94	Y	1.0	Y	-1.1	Y	-1.0	Y
	13	1.8	Y	2.2	Y	-2.0	Y	-2.1	Y
	14	1.7	Y	1.7	Y	-2.0	Y	-1.8	Y
	15	1.8	Y	2.0	Y	-2.2	Y	-2.0	Y
	16	2.0	Y	1.9	Y	-2.0	Y	-2.1	Y
	20	1.2	Y	1.0	Y	-1.1	Y	-1.1	Y
	21	.96	Y	.86	Y	- .96	Y	- .90	Y

it did not and that the sample extreme value was higher than the upper bound or lower than the lower bound. "Low" indications for minima are meant in the algebraic sense--the sample extreme was further away from the sample mean than was expected when "Low" is noted.

Considering all 240 of the sample extremes noted in Tables G-6 through G-8, just over 90% were found to lay within the 90% bounds. Similarly, 88% of the simulated extremes are within the bounds, as are 92% of the real extremes. One out of ten extremes is on average expected to lay outside the bounds even when the sampling is truly form the hypothesized population. Twice this number is not uncommon when relatively small numbers of samples are involved. The detailed results in each of the individual columns of the tables are thus fairly well in line with expections, with the exception of the simulated combined stress maxima, Table G-6. The slightly higher than expected number of simulated combined stress extremes which are out of bounds may in part be due to the use of the same estimate of RMS combined stress in both real and simulated data, or in the relatively crude approach to estimation of broadness parameter.

Considering the size of the 90% confidence bounds (which may be noted graphically in Figures G-1 through G-28) the differences are very slight between the magnitude of extreme positive and negative stresses in the same run. The differences between the simulated and real extremes are generally of the same or smaller magnitude than half the width of the 90% bounds. In effect, within the sample size dictated by the existing observations, the difference between simulated and observed extremes appears statistically insignificant.

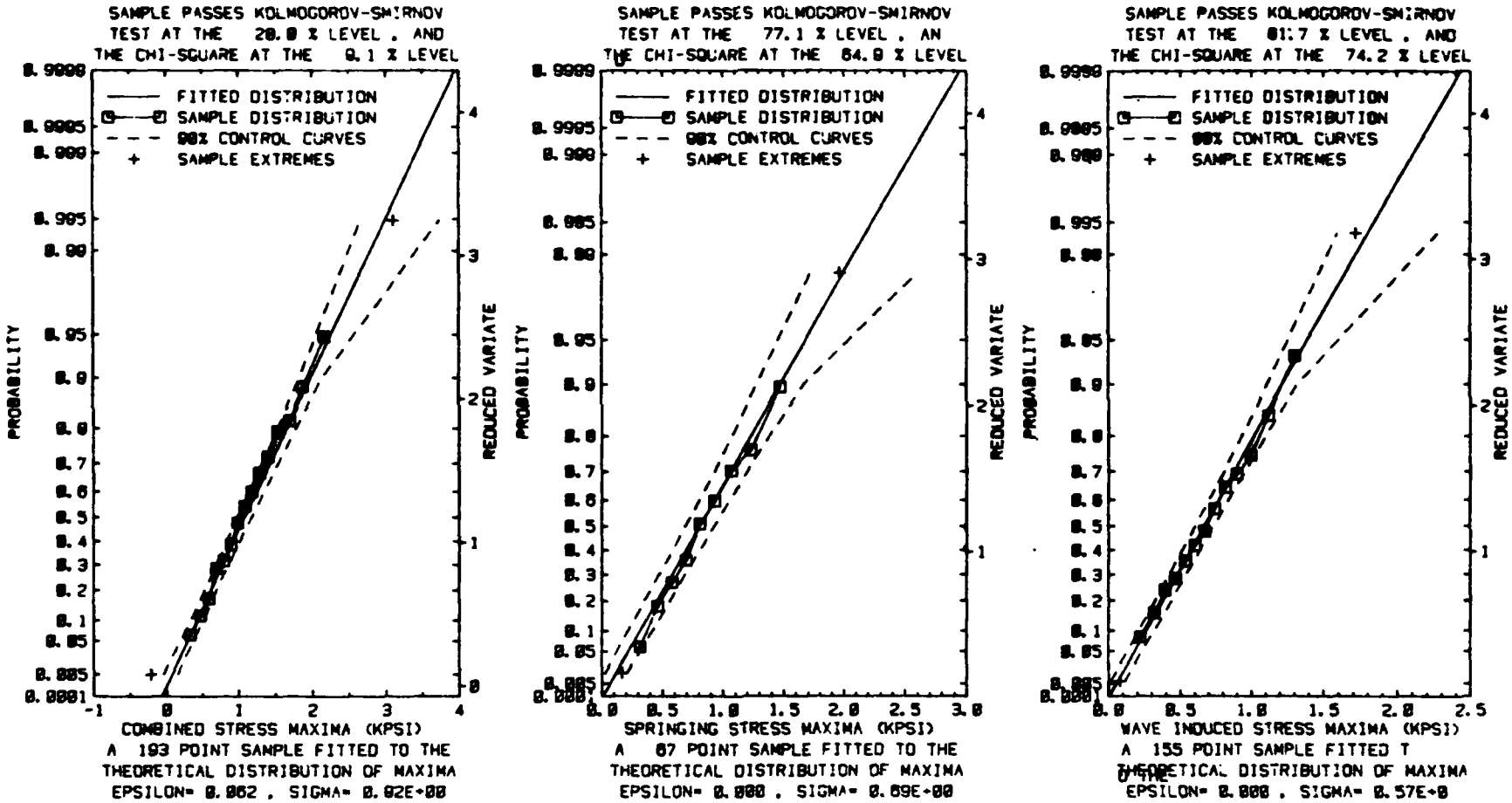

FIGURE G-1 SAMPLE DISTRIBUTIONS, OBSERVED DATA (MAXIMA) RUN 74 (1979)

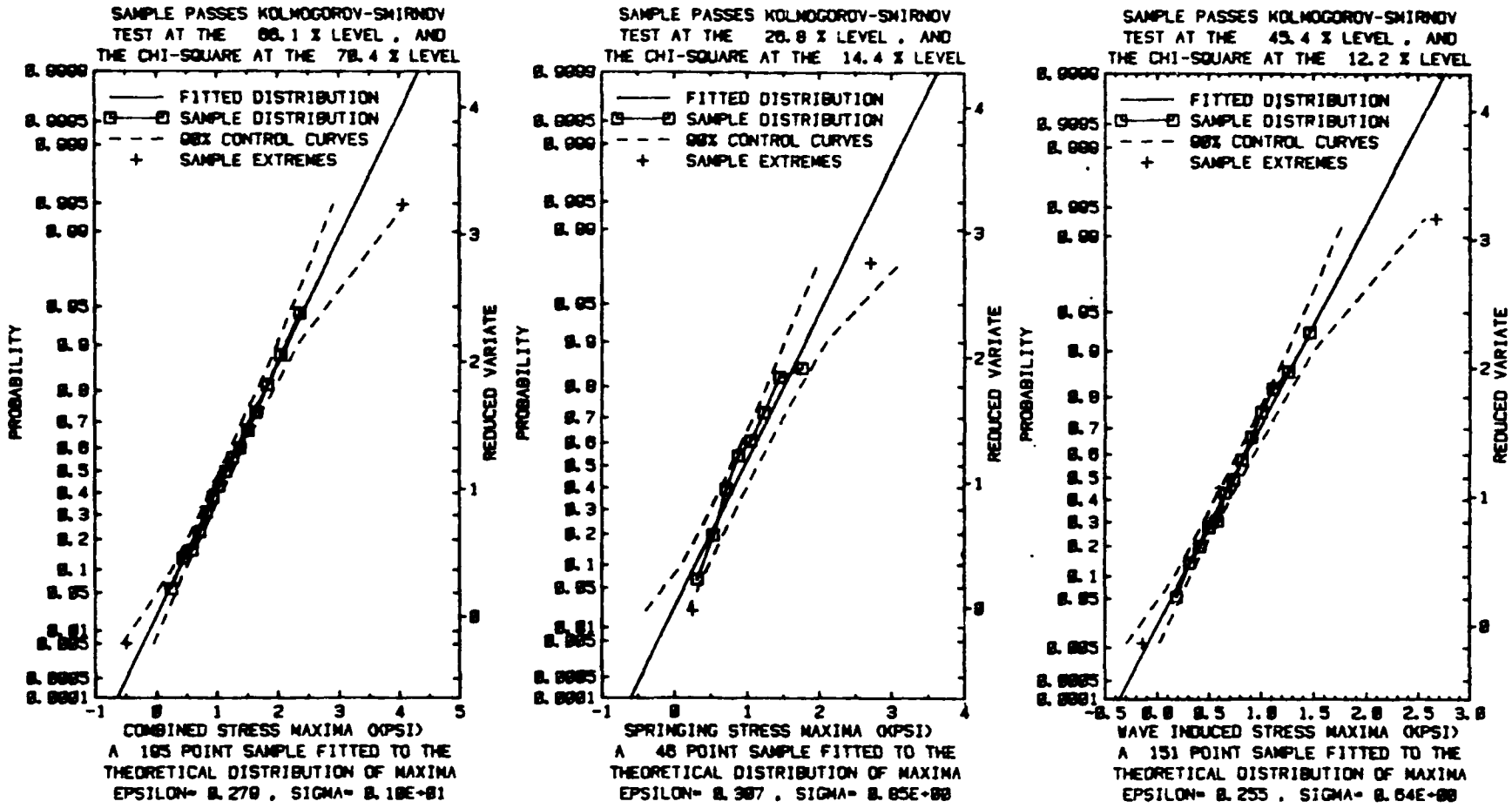

FIGURE G-2 SAMPLE DISTRIBUTIONS, OBSERVED DATA (MAXIMA), RUN 75 (1979)

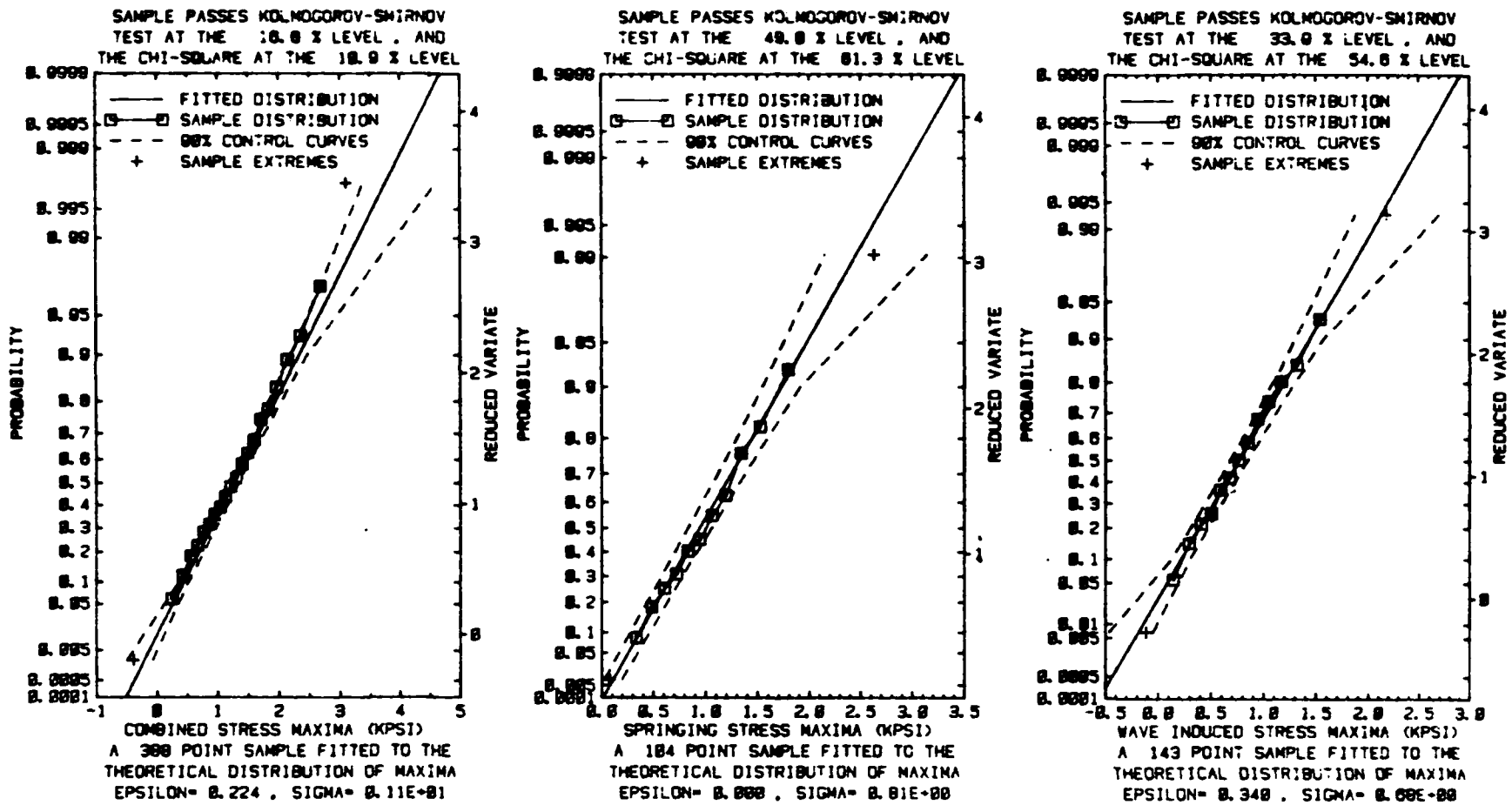

FIGURE G-3 SAMPLE DISTRIBUTION, OBSERVED DATA (MAXIMA), RUN 77 (1979)

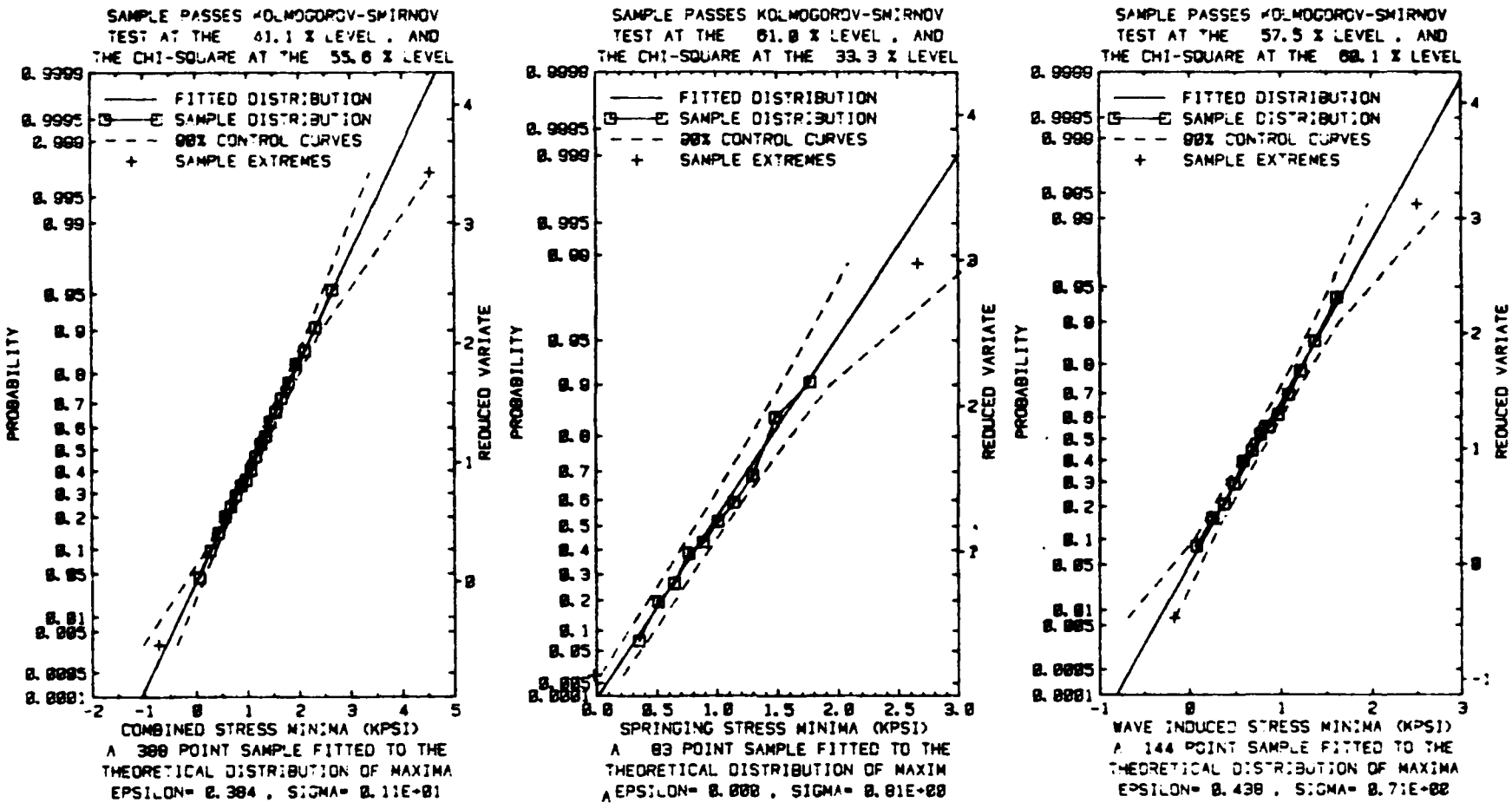

FIGURE G-4 SAMPLE DISTRIBUTIONS, OBSERVED DATA (MINIMA), RUN 77 (1979)

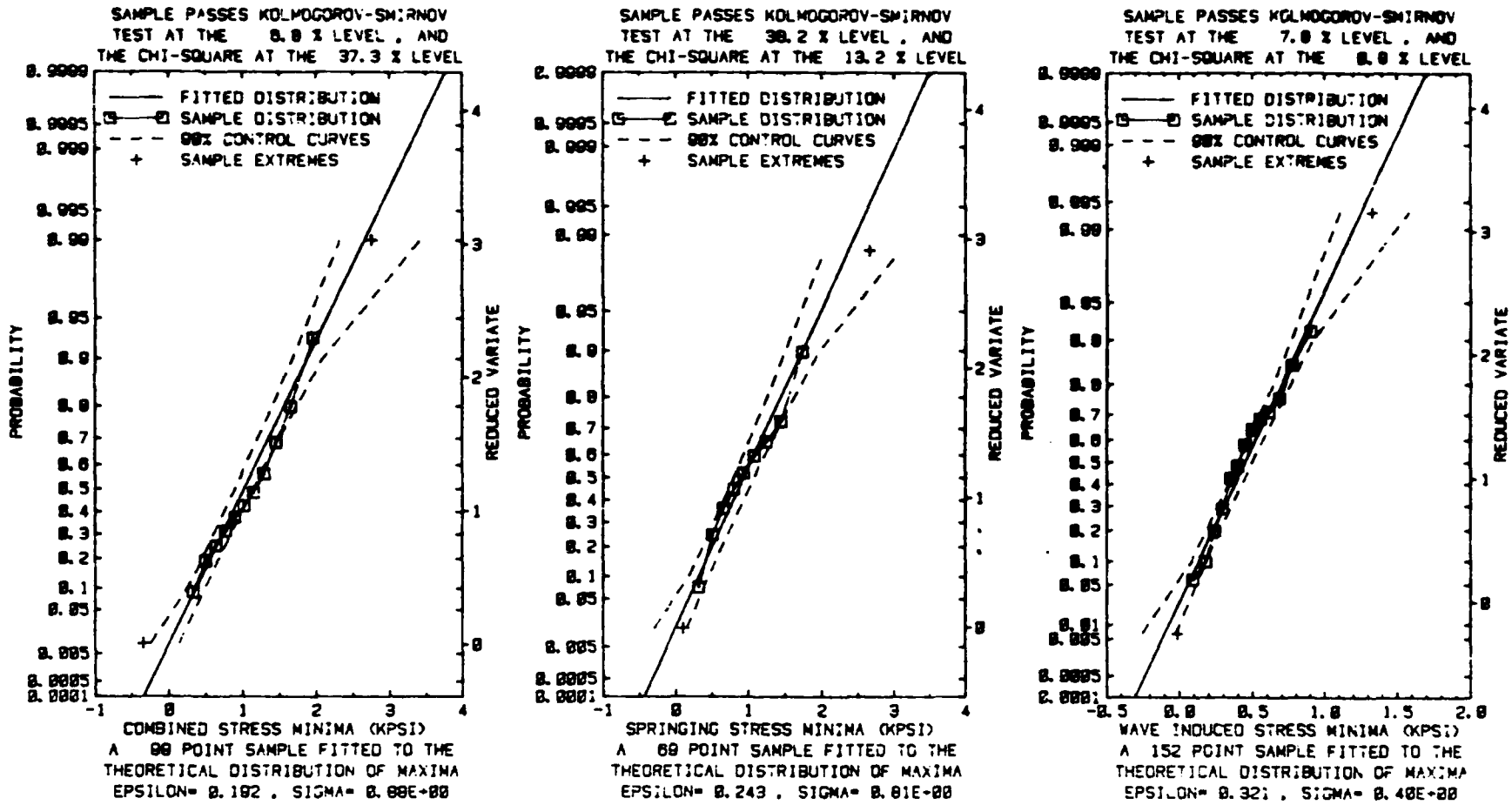

FIGURE G-5 SAMPLE DISTRIBUTIONS, OBSERVED DATA (MINIMA), RUN 99 (1979)

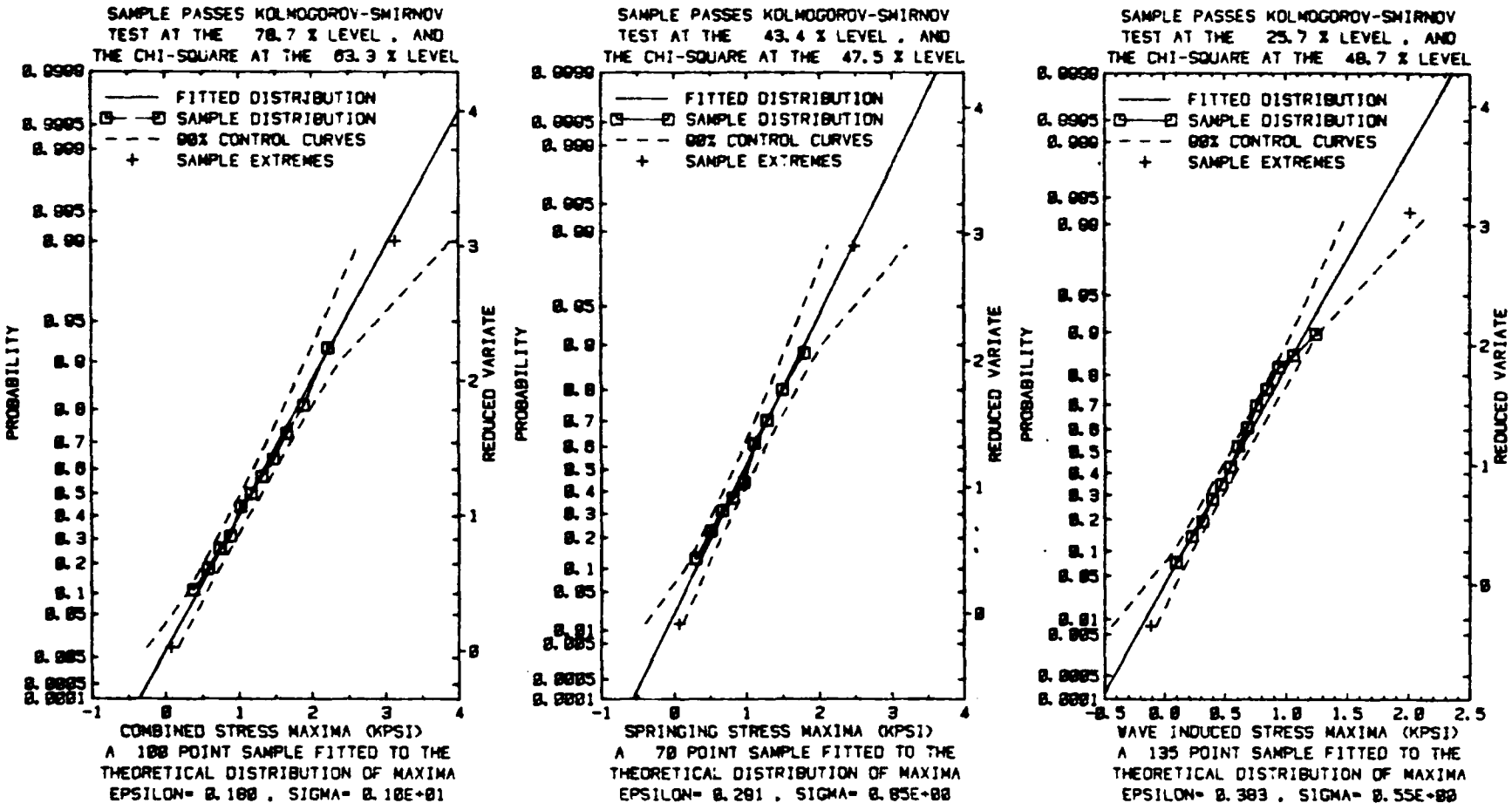

FIGURE G-6 SAMPLE DISTRIBUTIONS, OBSERVED DATA (MAXIMA), RUN 100 (1979)

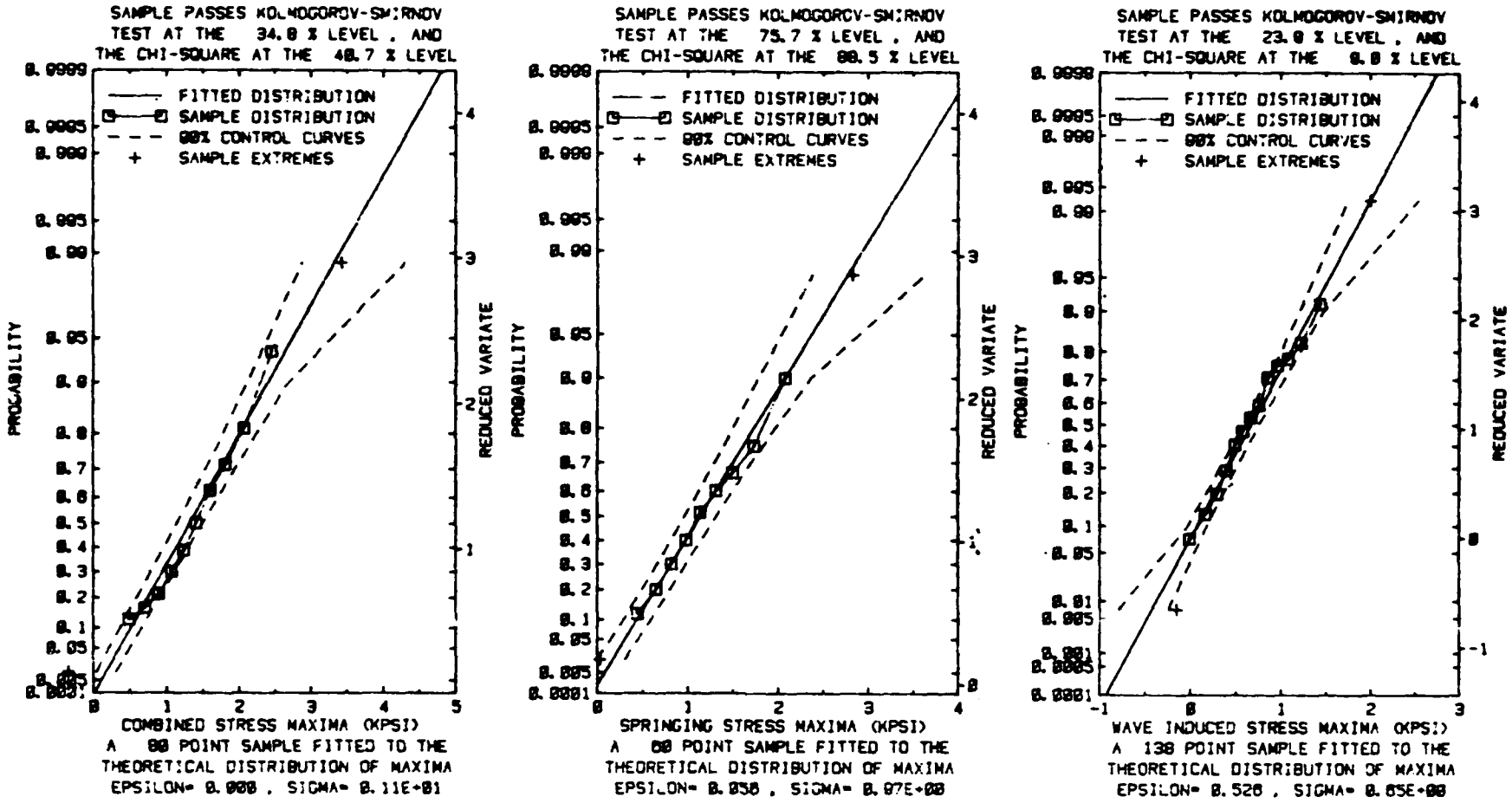

FIGURE G-7 SAMPLE DISTRIBUTIONS, OBSERVED DATA (MAXIMA), RUN 101 (1979)

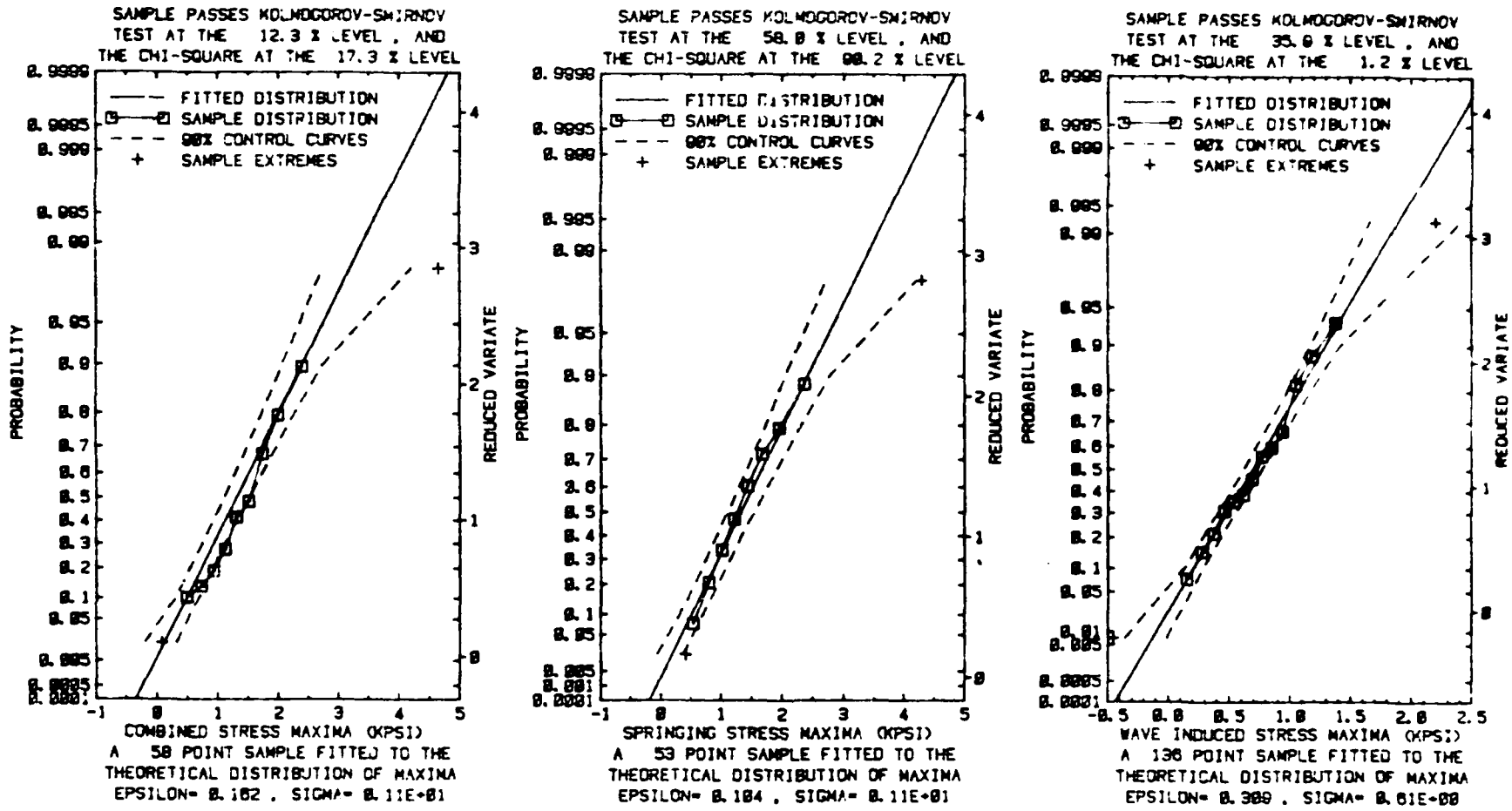

FIGURE G-8 SAMPLE DISTRIBUTIONS, SIMULATED DATA (MAXIMA), RUN 101 (1979)

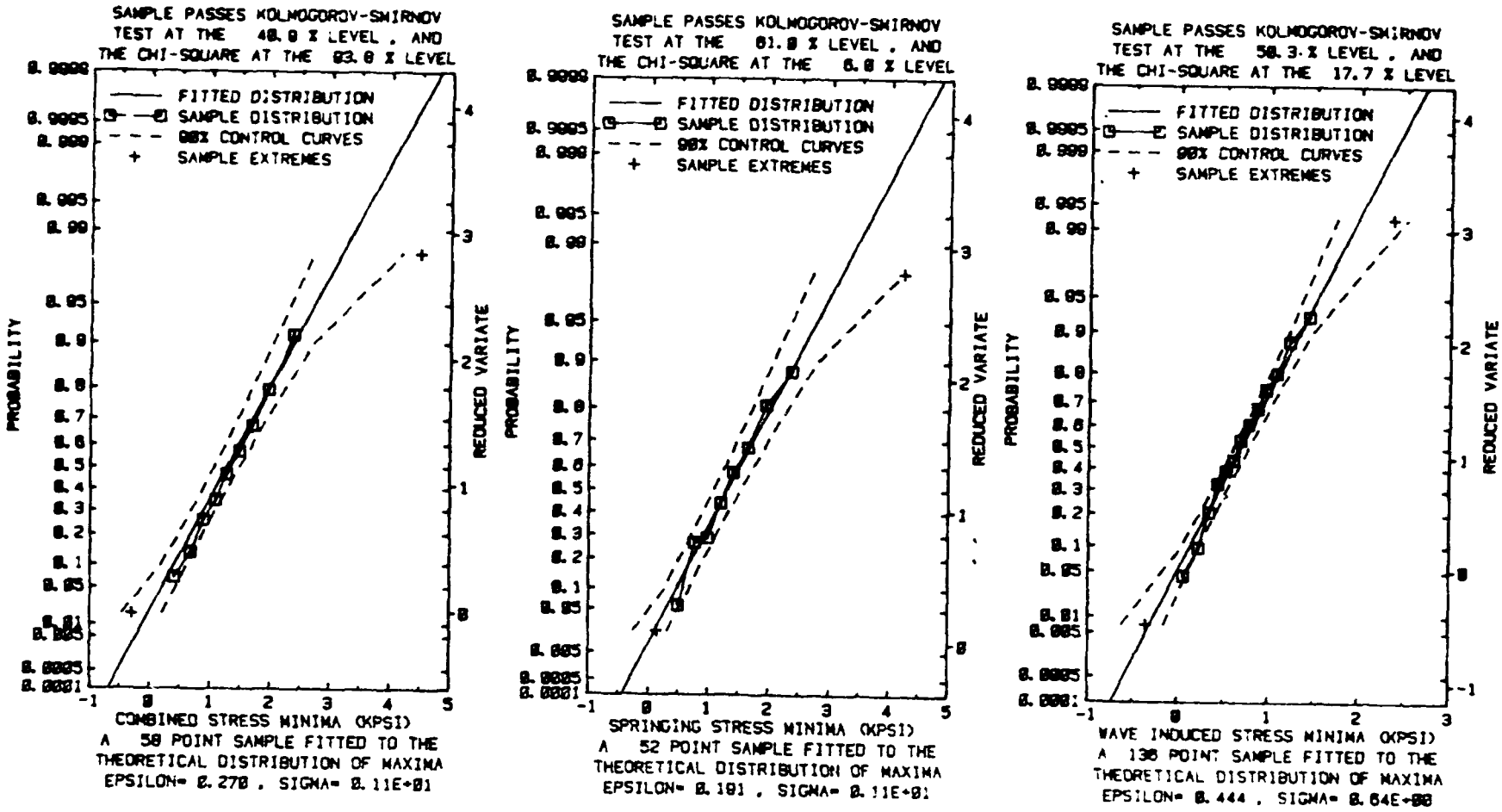

FIGURE G-9 SAMPLE DISTRIBUTIONS, SIMULATED DATA (MINIMA), RUN 101 (1979)

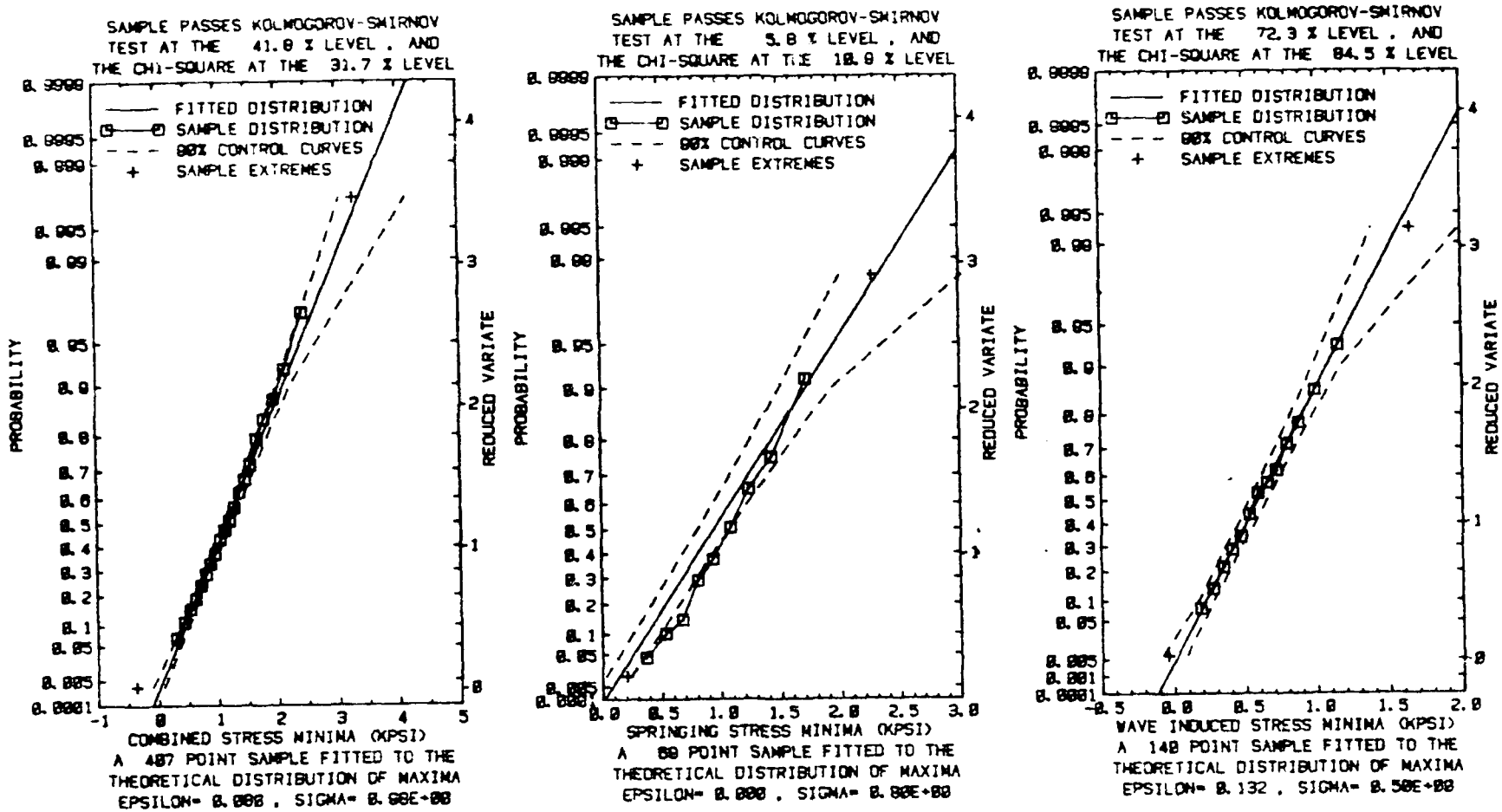

FIGURE G-10 SAMPLE DISTRIBUTIONS, OBSERVED DATA (MINIMA), RUN 102 (1979)

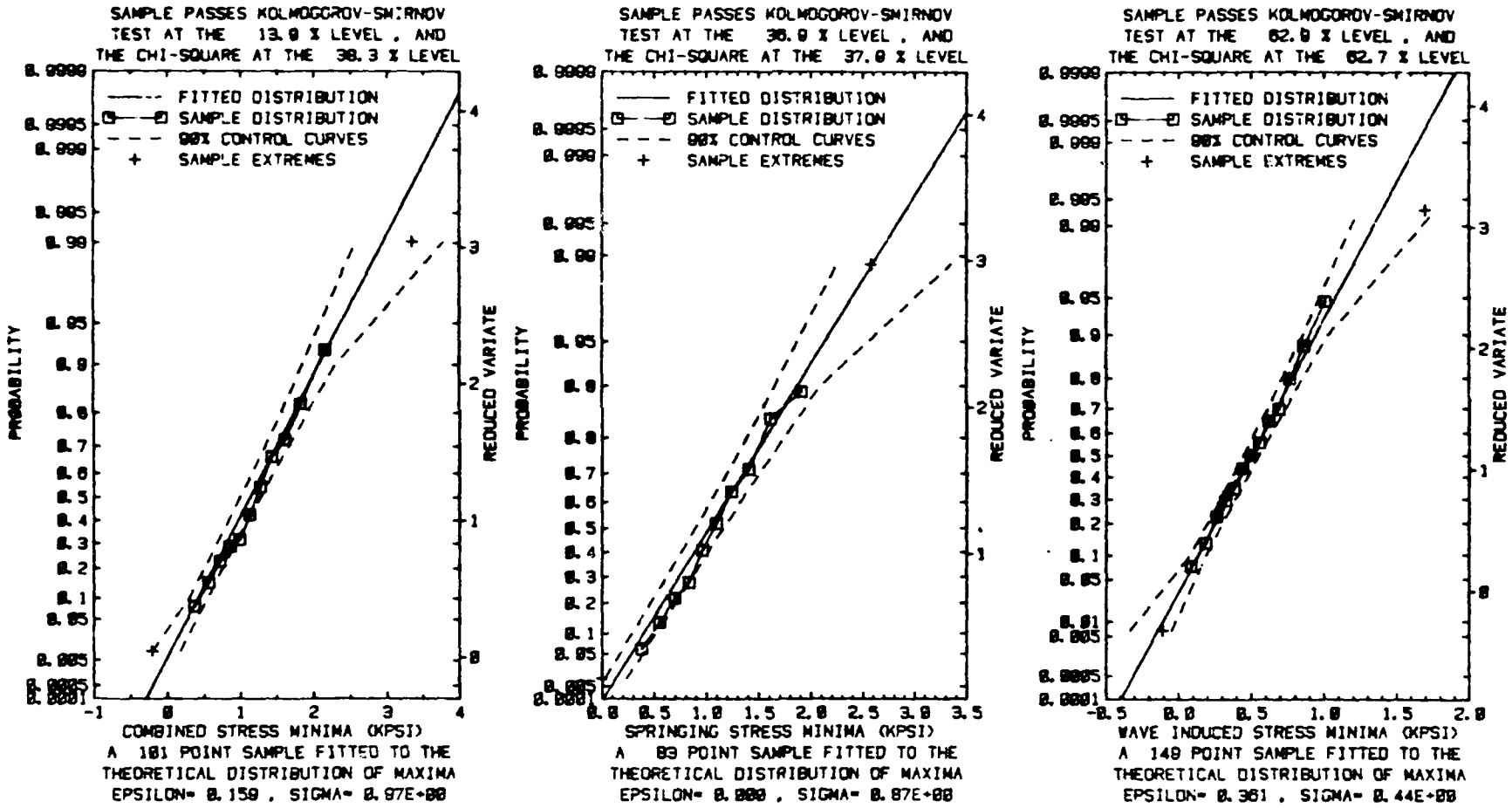

FIGURE G-11 SAMPLE DISTRIBUTIONS, OBSERVED DATA (MINIMA), RUN 103 (1979)

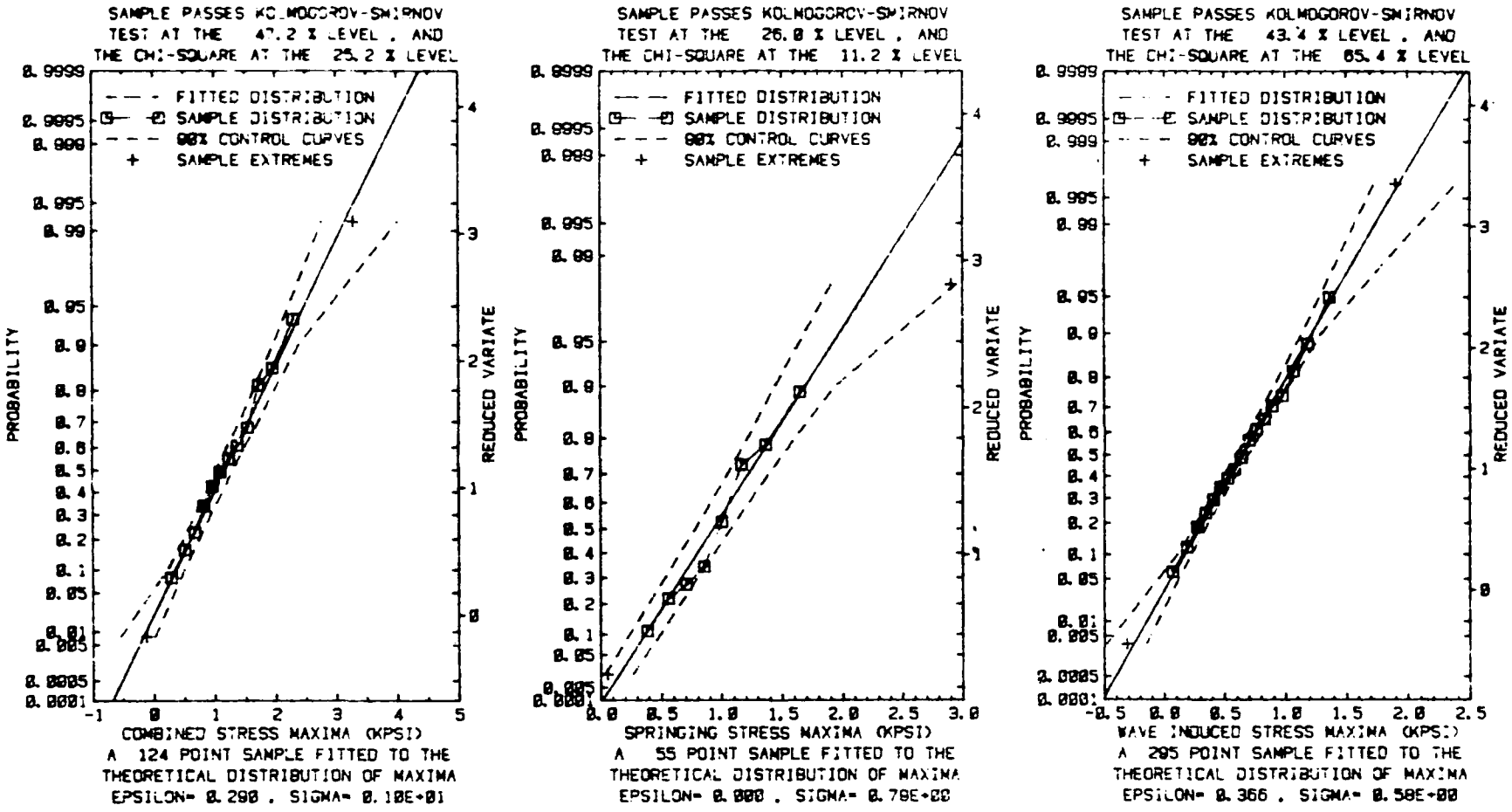

FIGURE G-12 SAMPLE DISTRIBUTIONS, OBSERVED DATA (MAXIMA), RUN 116 (1979)

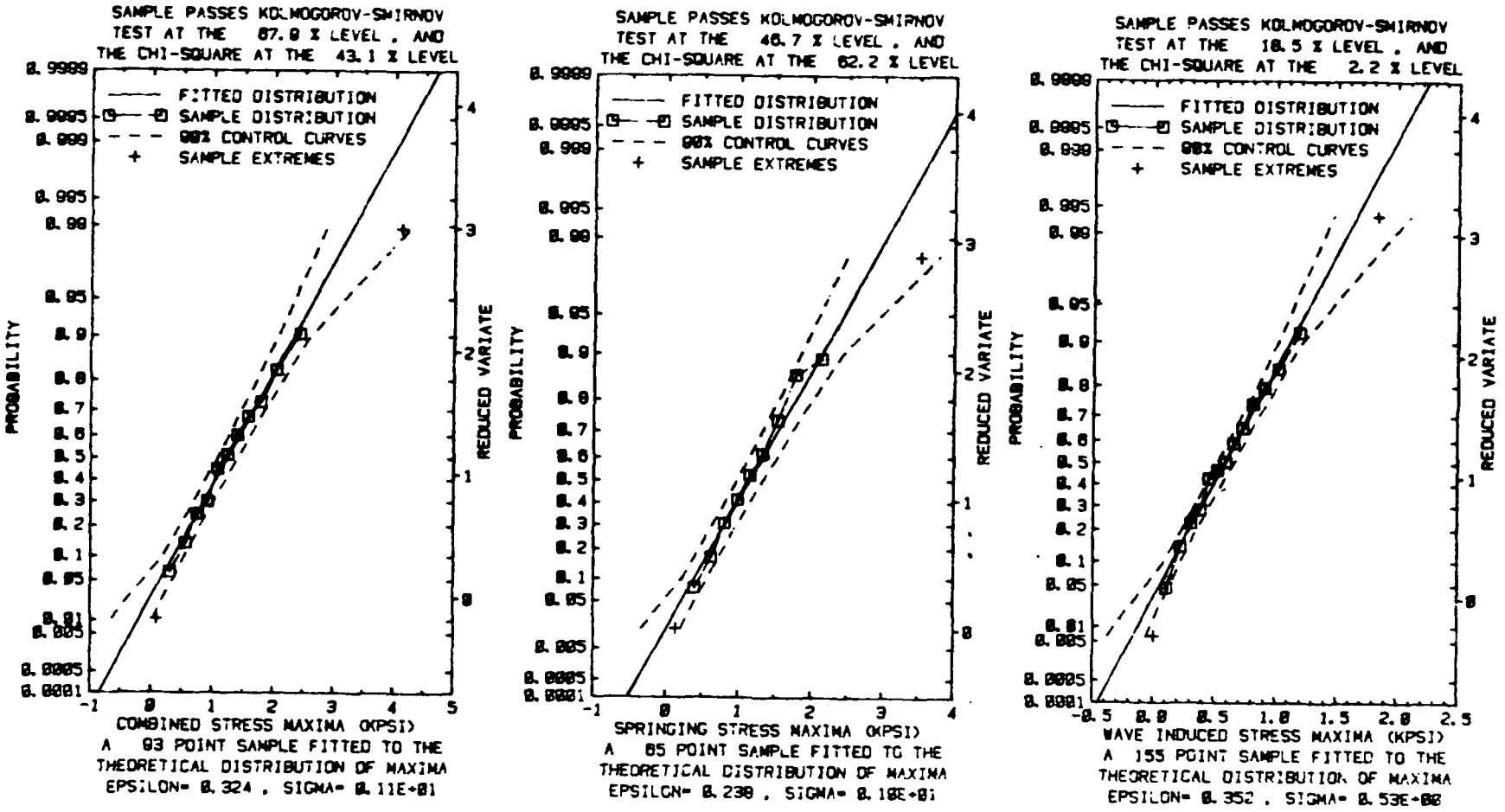

FIGURE G-13 SAMPLE DISTRIBUTIONS, OBSERVED DATA (MAXIMA), RUN 117 (1979)

117

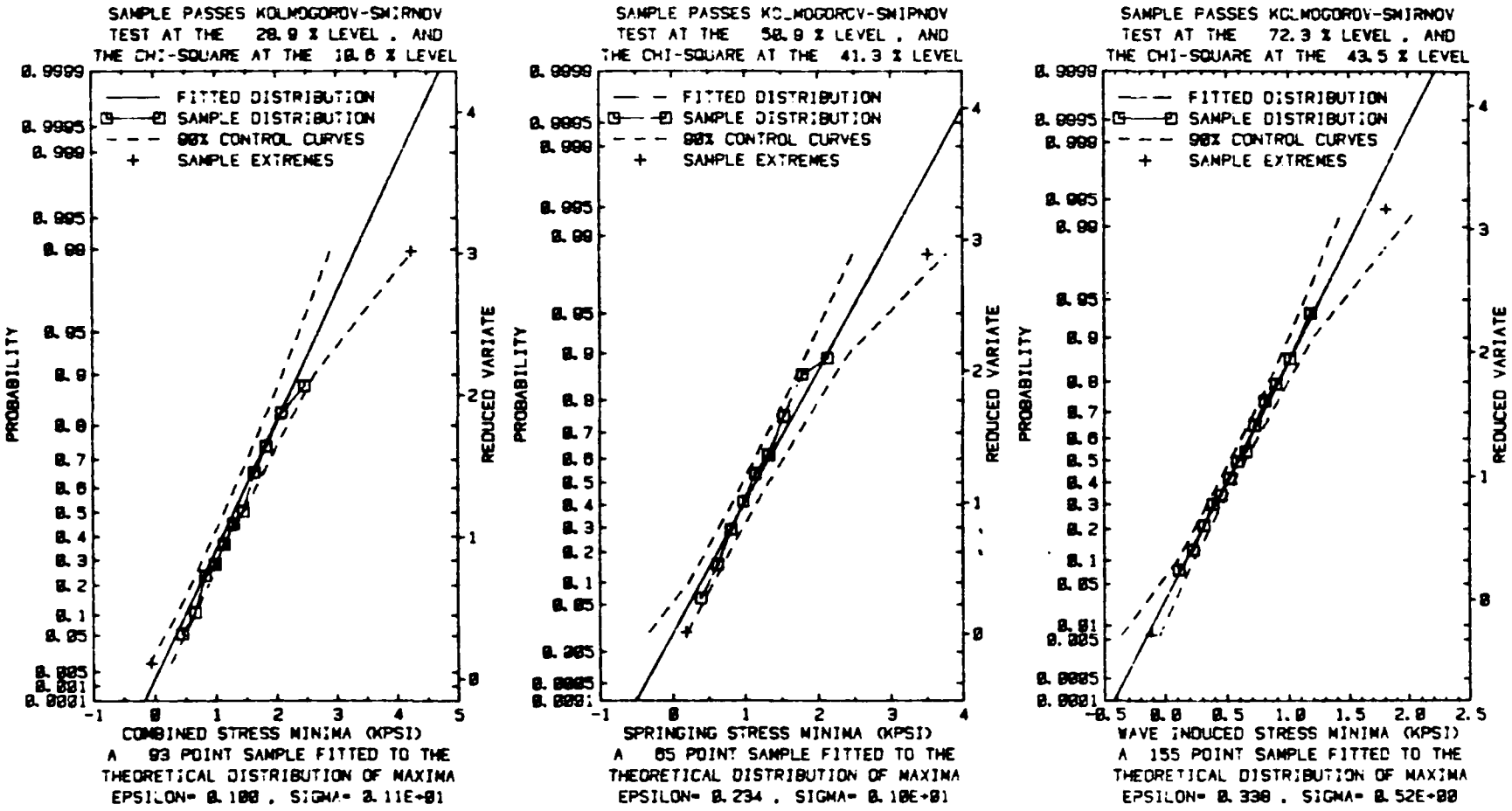

FIGURE G-14 SAMPLE DISTRIBUTIONS, OBSERVED DATA (MINIMA), RUN 117 (1979)

117

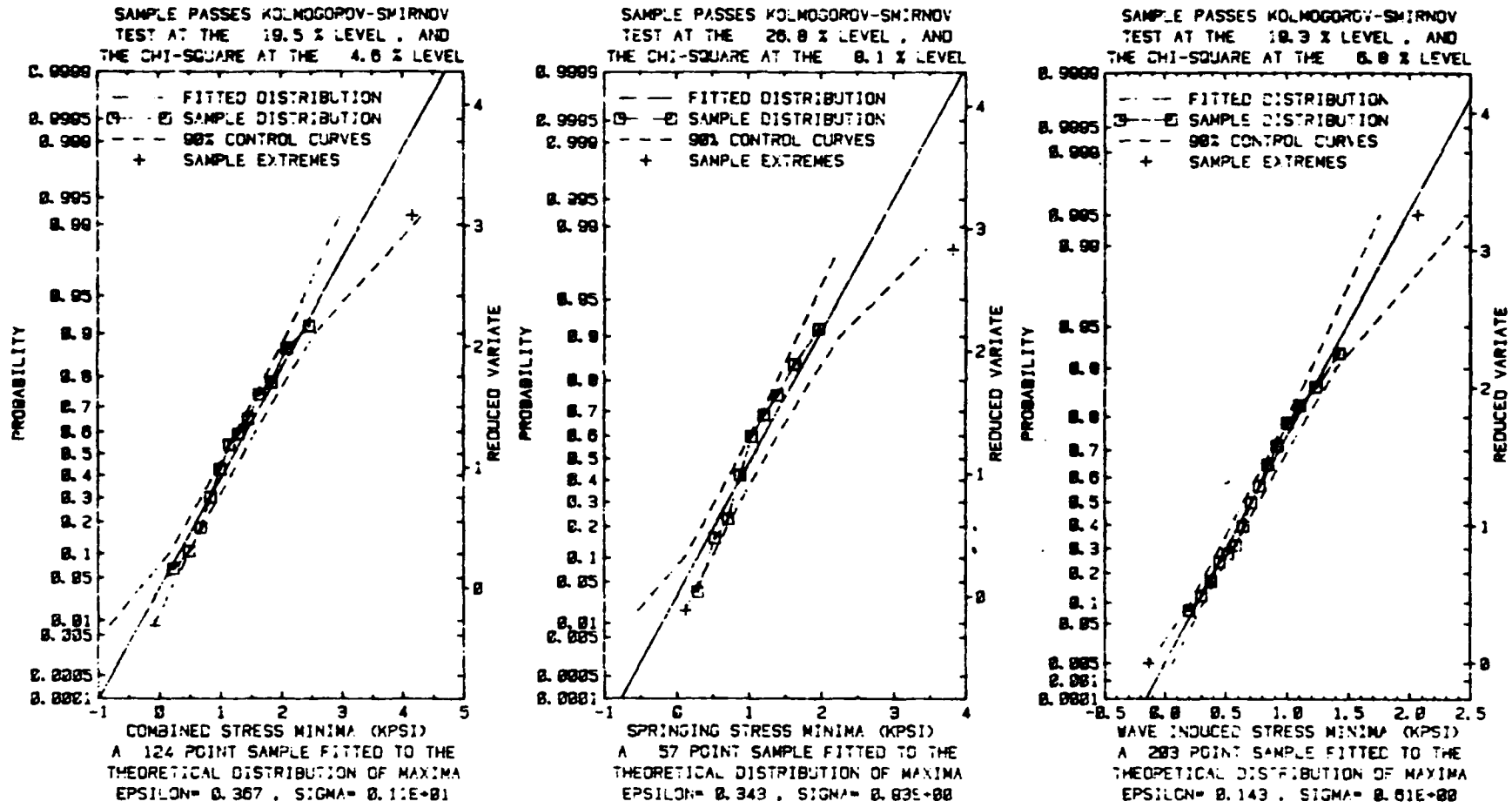

FIGURE G-15 SAMPLE DISTRIBUTIONS, OBSERVED DATA (MINIMA), RUN 3 (1980)

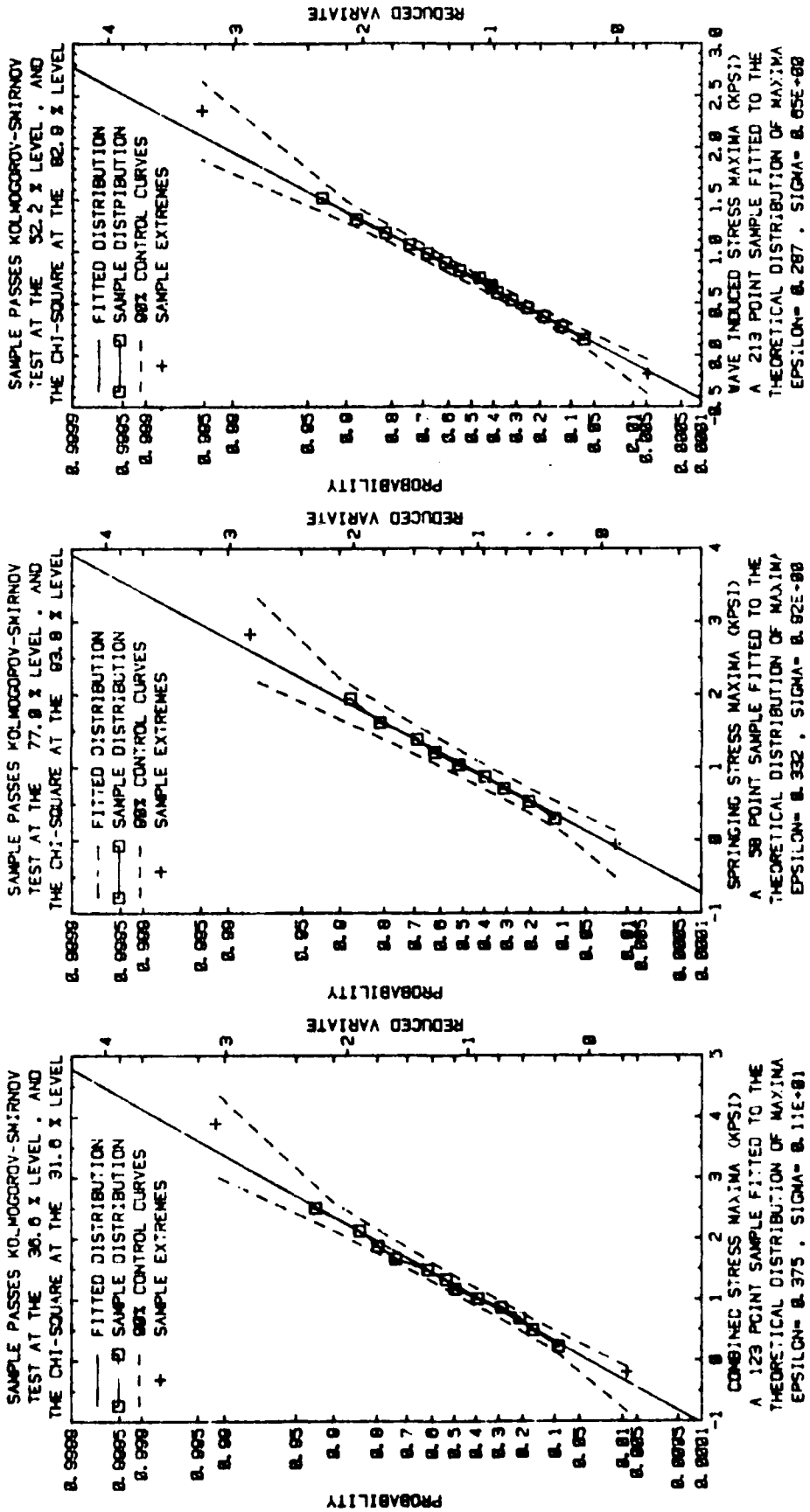

FIGURE G-16 SAMPLE DISTRIBUTIONS, OBSERVED DATA (MAXIMA), RUN 4 (1980)

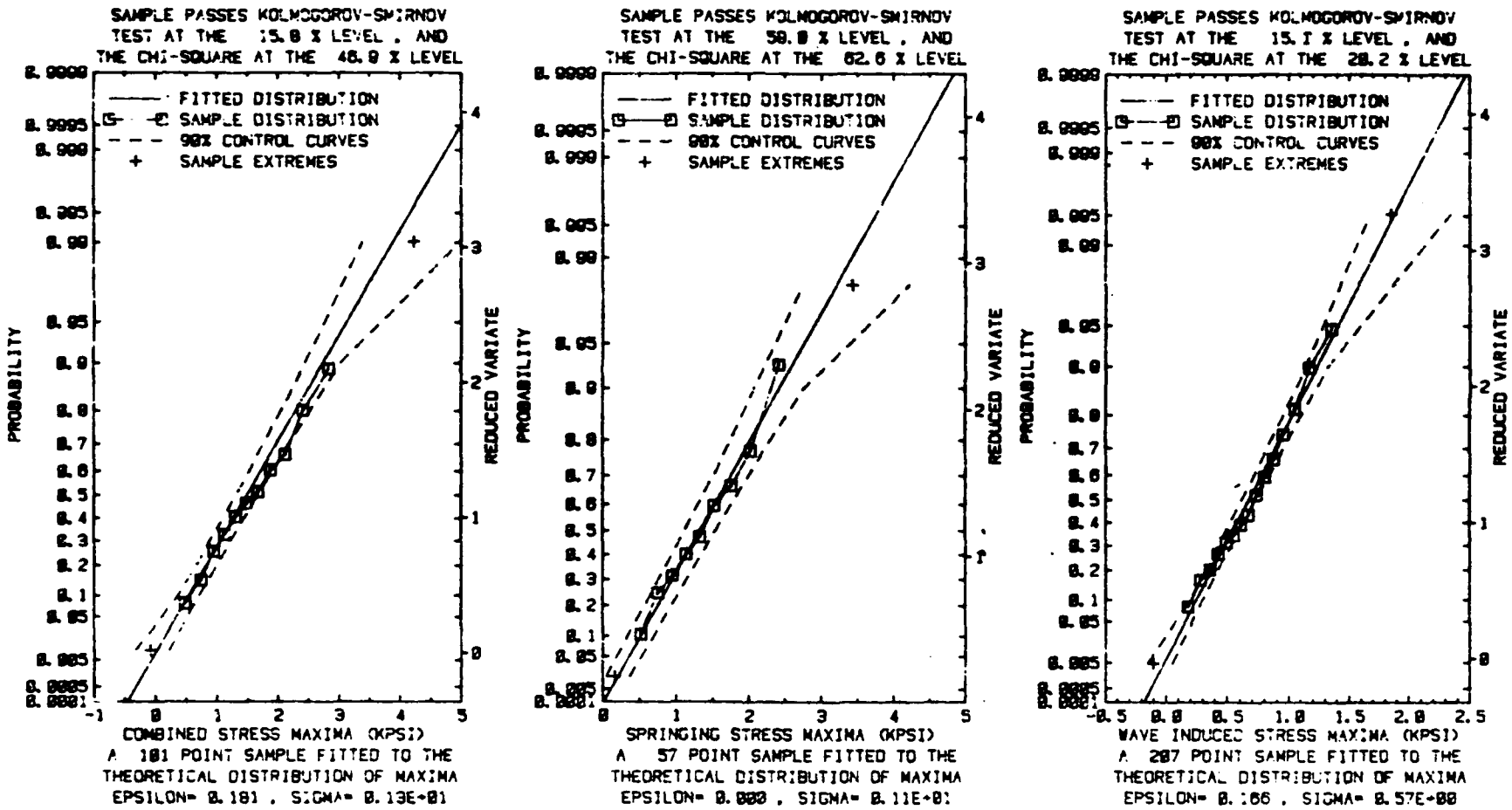

FIGURE G-17 SAMPLE DISTRIBUTIONS, OBSERVED DATA (MAXIMA), RUN 5 (1980)

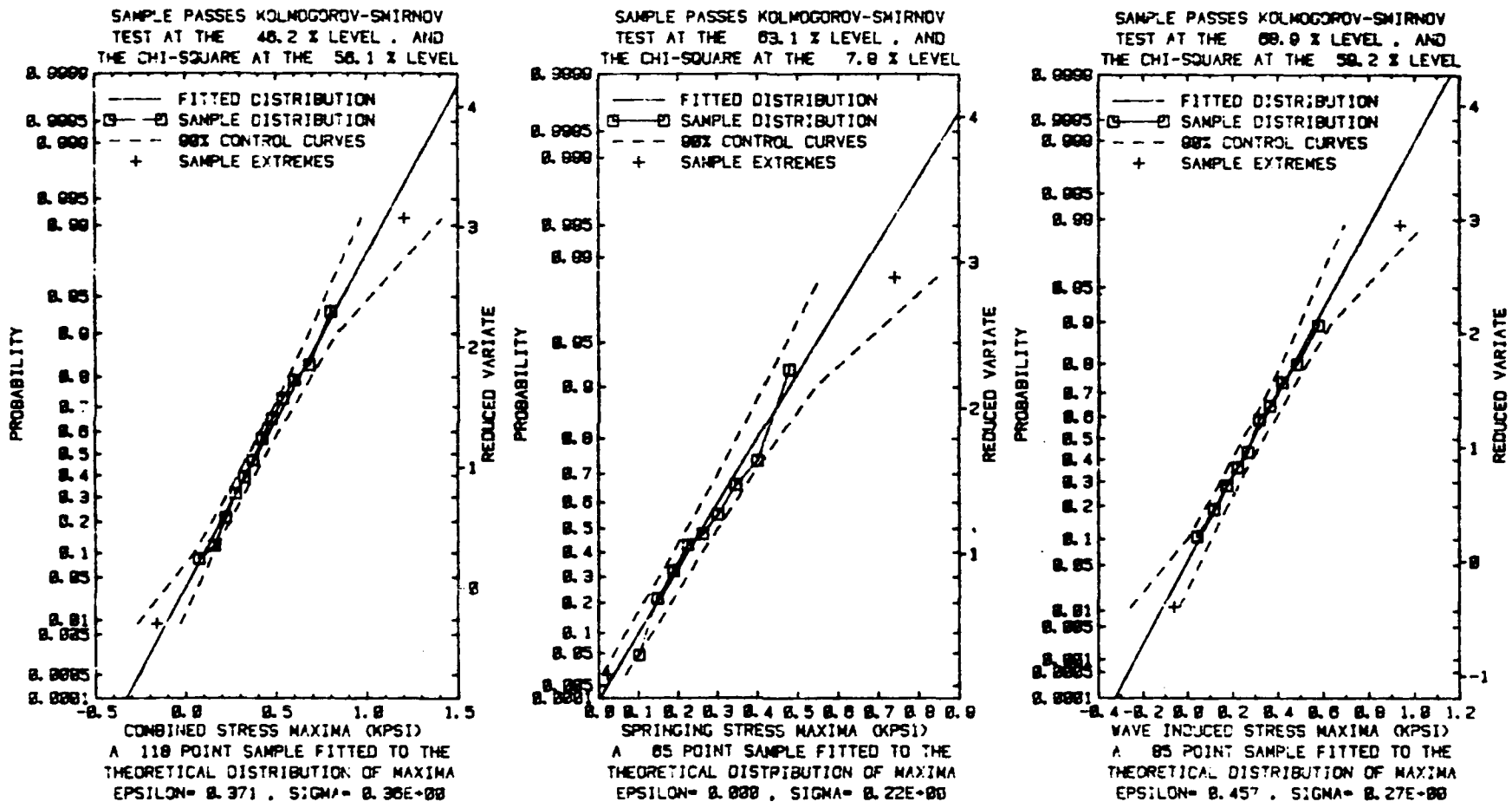

FIGURE G-18 SAMPLE DISTRIBUTIONS, OBSERVED DATA (MAXIMA), RUN 8 (1980)

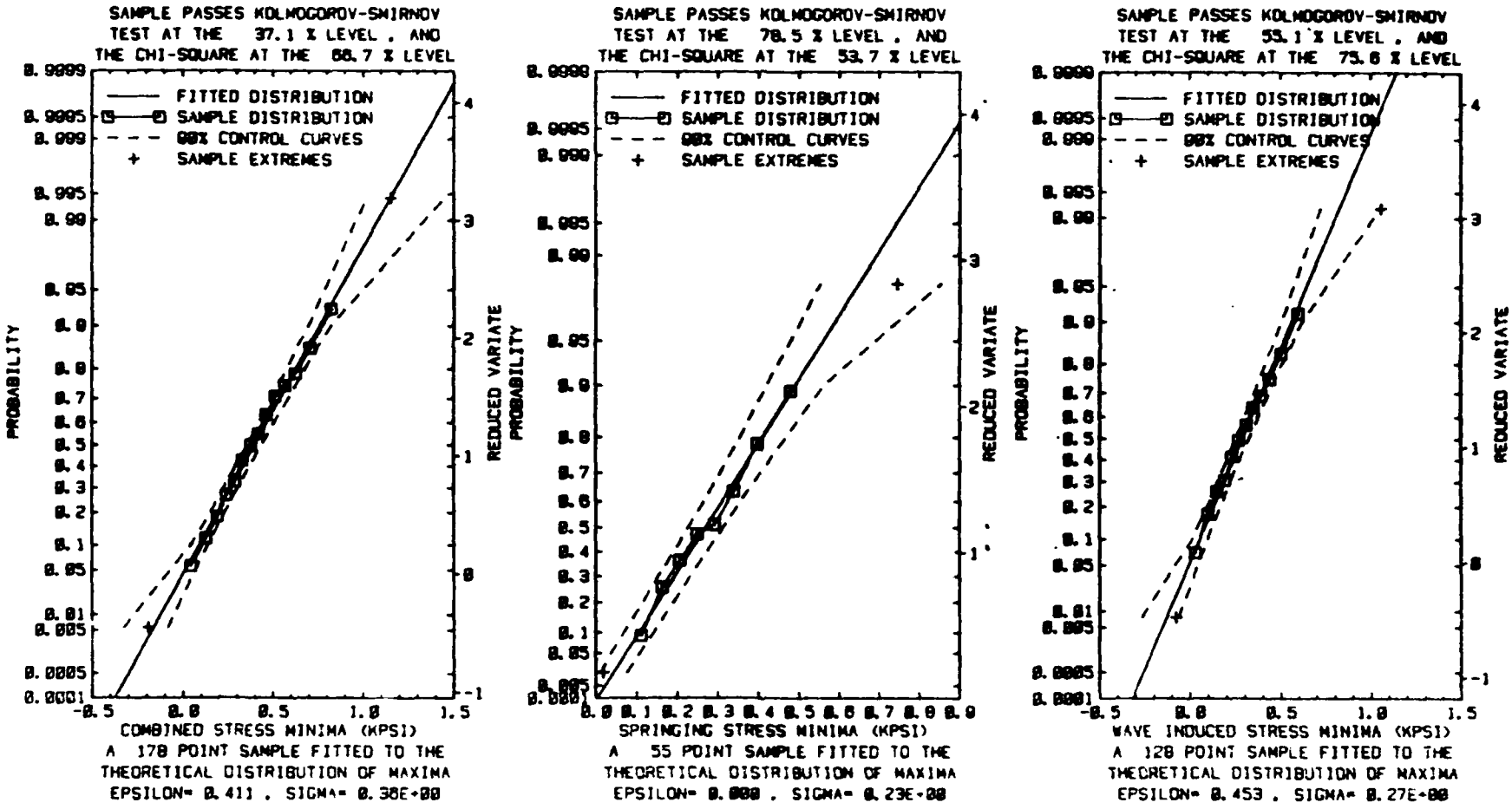

FIGURE G-19 SAMPLE DISTRIBUTIONS, OBSERVED DATA (MINIMA), RUN 8 (1980)

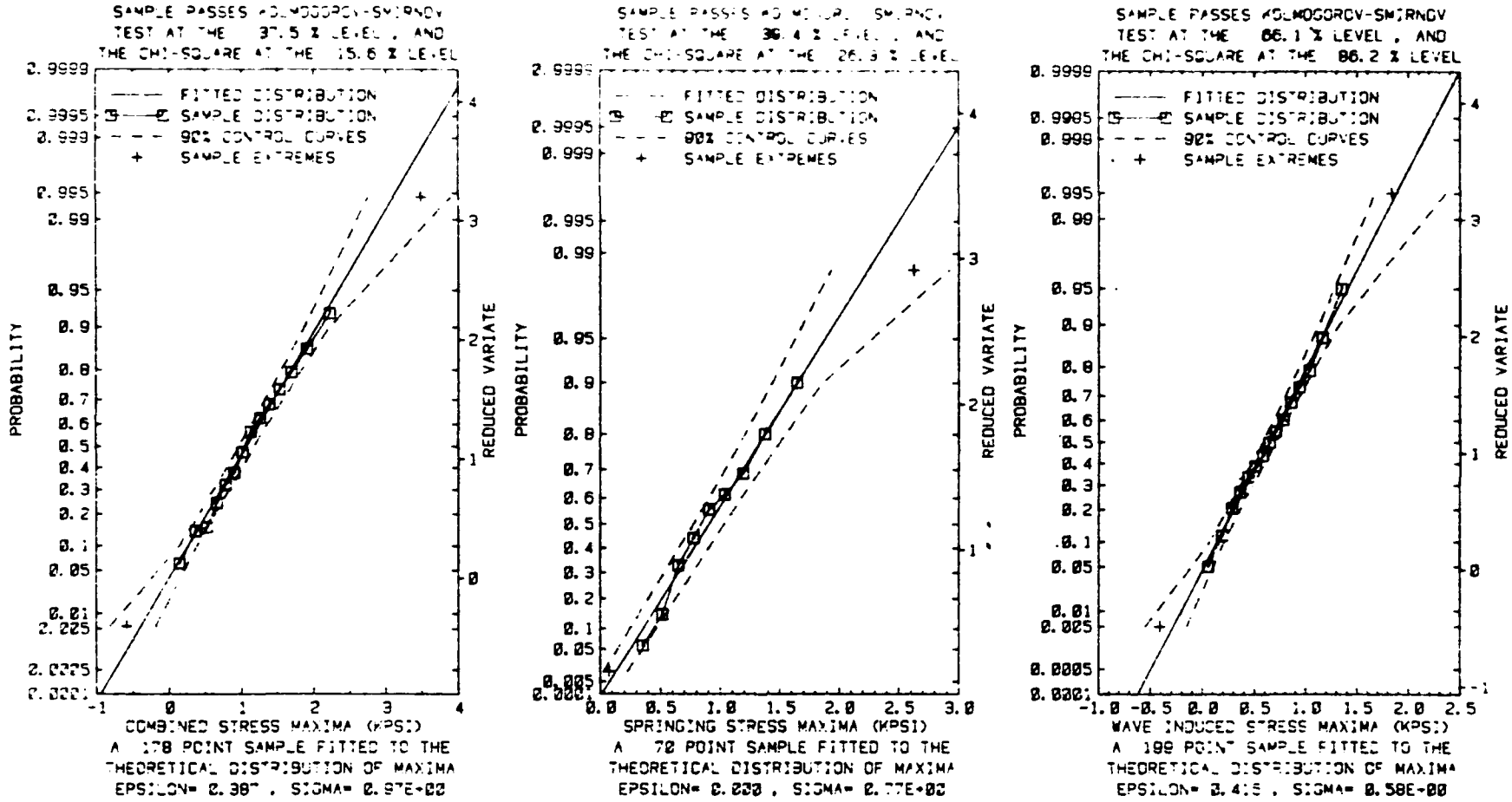

FIGURE G-20 SAMPLE DISTRIBUTIONS, OBSERVED DATA (MAXIMA), RUN 13 (1980)

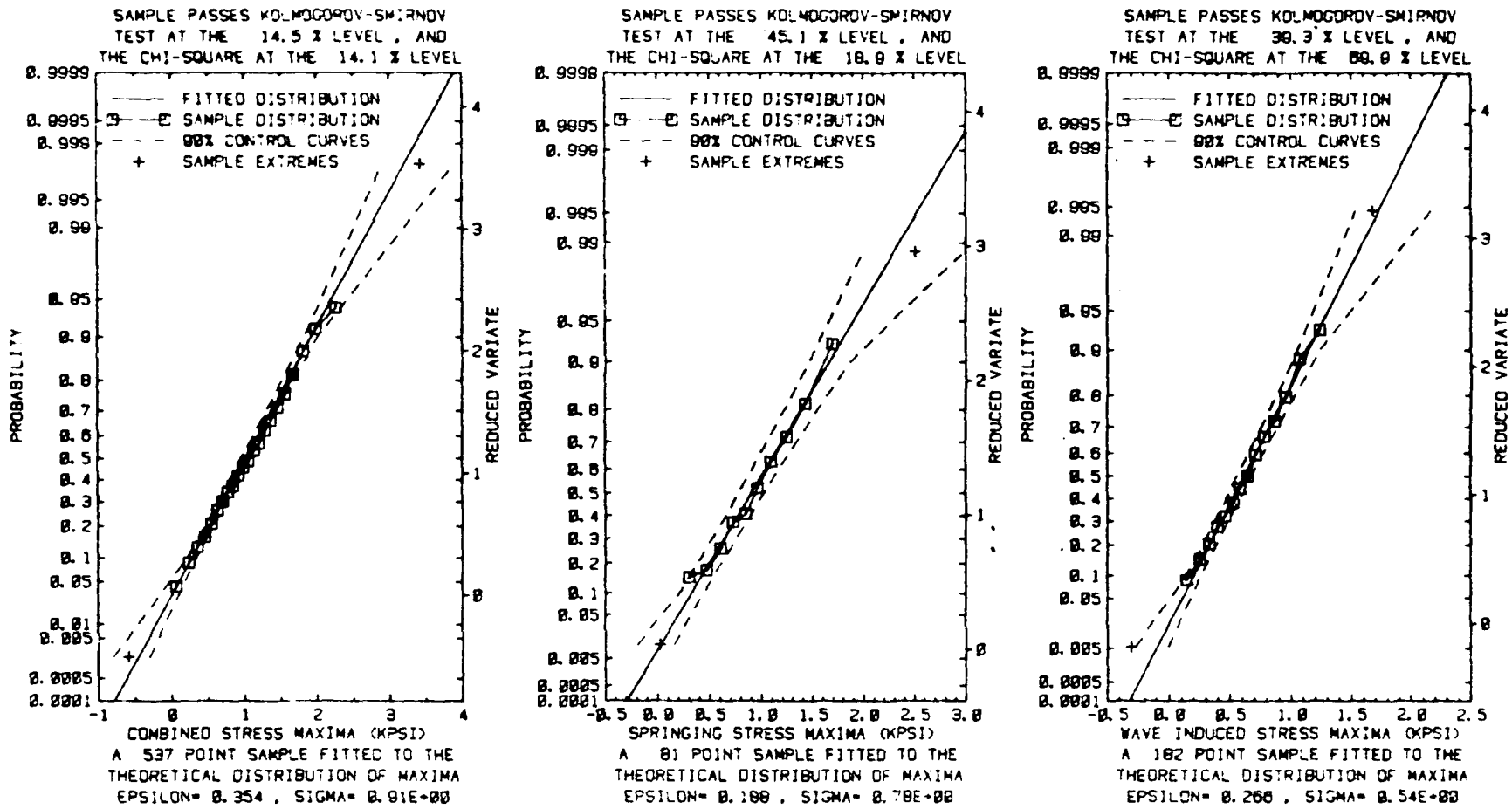

FIGURE G-21 SAMPLE DISTRIBUTIONS, OBSERVED DATA (MAXIMA), RUN 14 (1980)

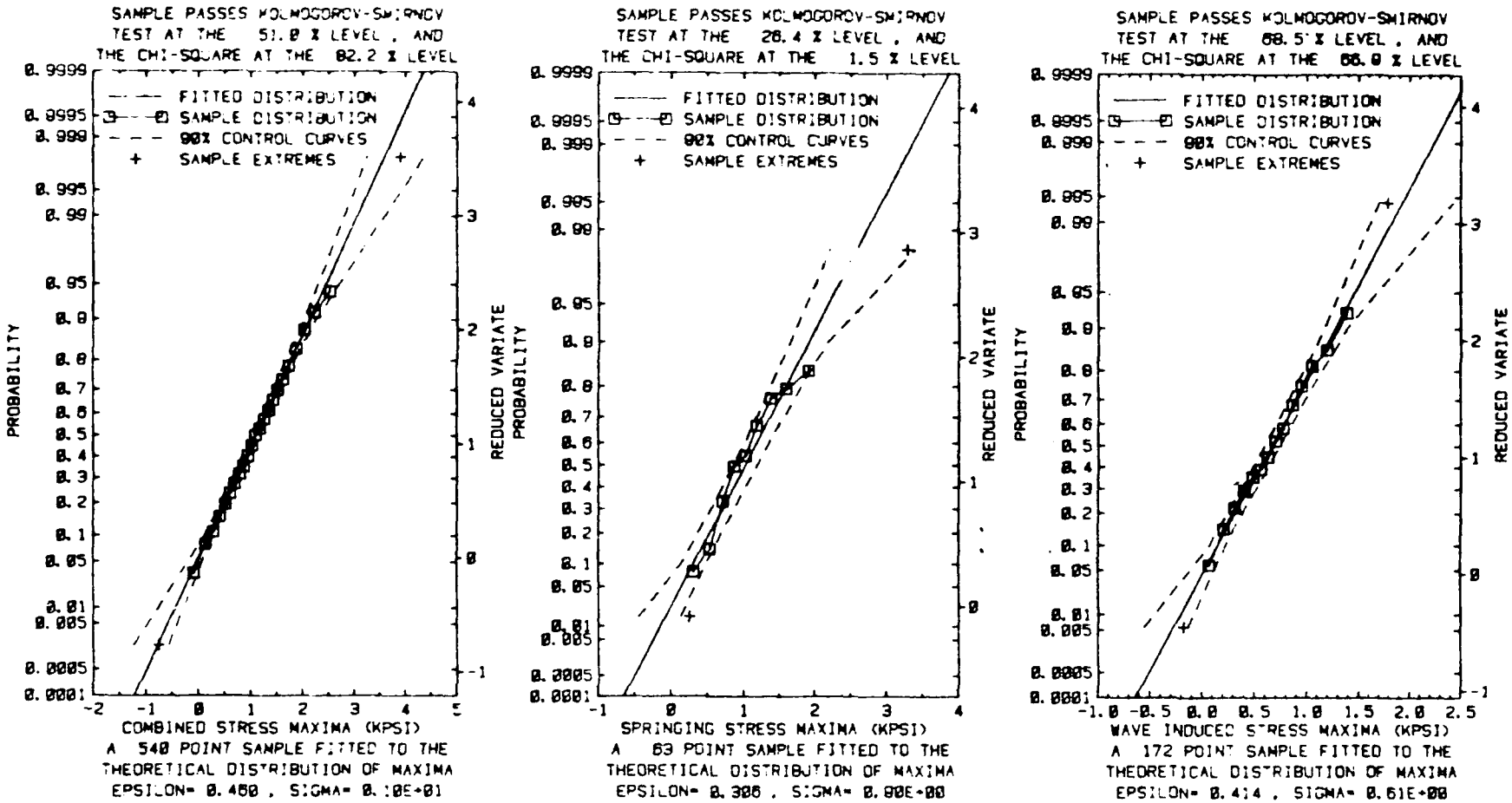

FIGURE G-22 SAMPLE DISTRIBUTIONS, OBSERVED DATA (MAXIMA), RUN 15 (1980)

15

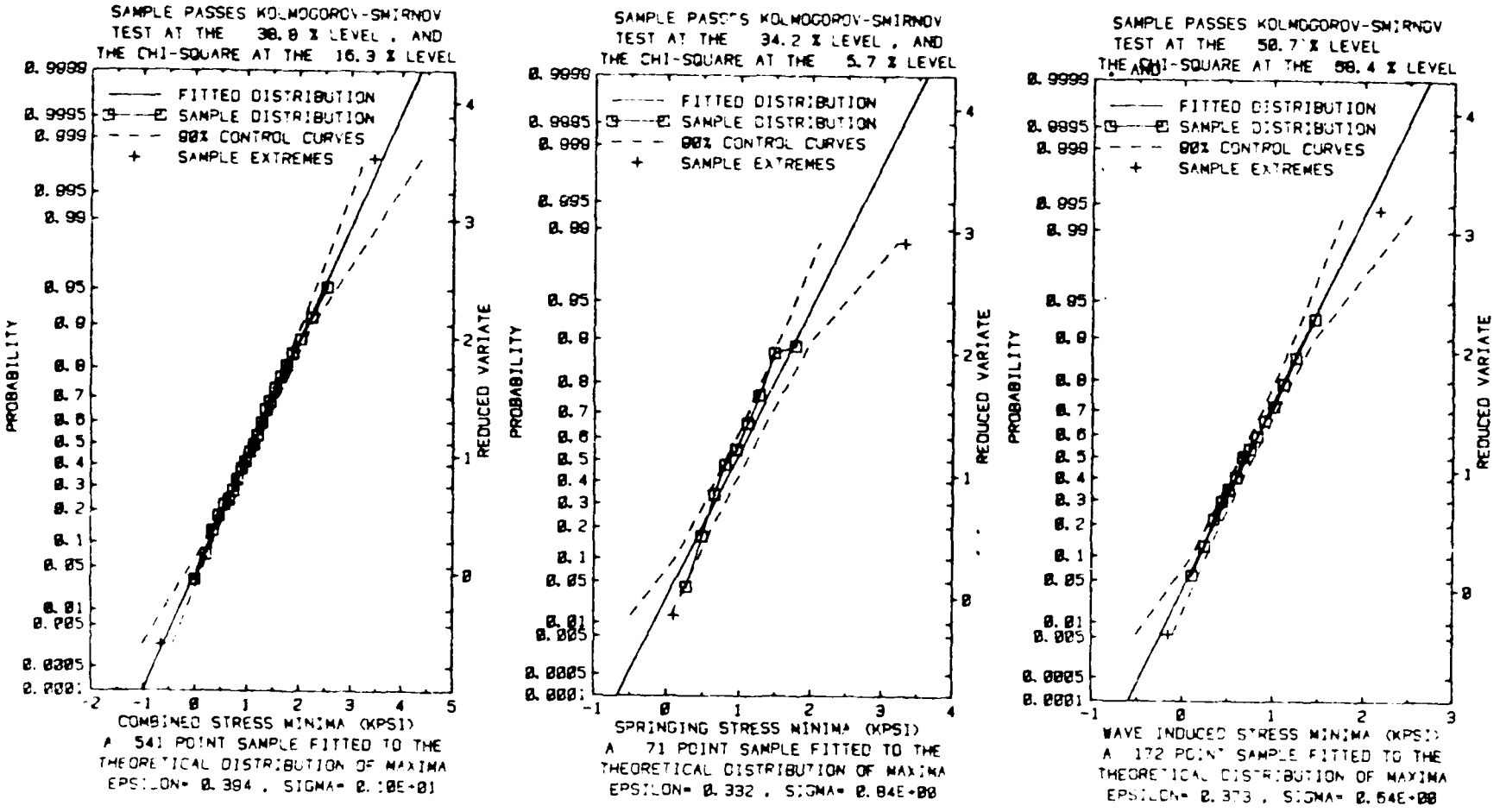

FIGURE G-23 SAMPLE DISTRIBUTIONS, OBSERVED DATA (MINIMA), RUN 15 (1980)

AD-A127 226 AN ANALYSIS OF FULL SCALE MEASUREMENTS ON M/V STEWART J CORT DURING THE 1..(U) STEVENS INST OF TECH HOBOKEN NJ DAVIDSON LAB J F DALZELL FEB 82 SIT-DL-81-9-2221 3/3

UNCLASSIFIED USCG-D-25-82 DTCG23-81-C-2031 F/G 13/10 NL

END
FILMED
DTIC

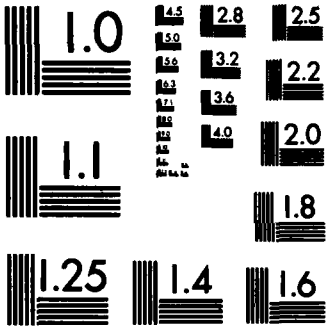

MICROCOPY RESOLUTION TEST CHART
NATIONAL BUREAU OF STANDARDS-1963-A

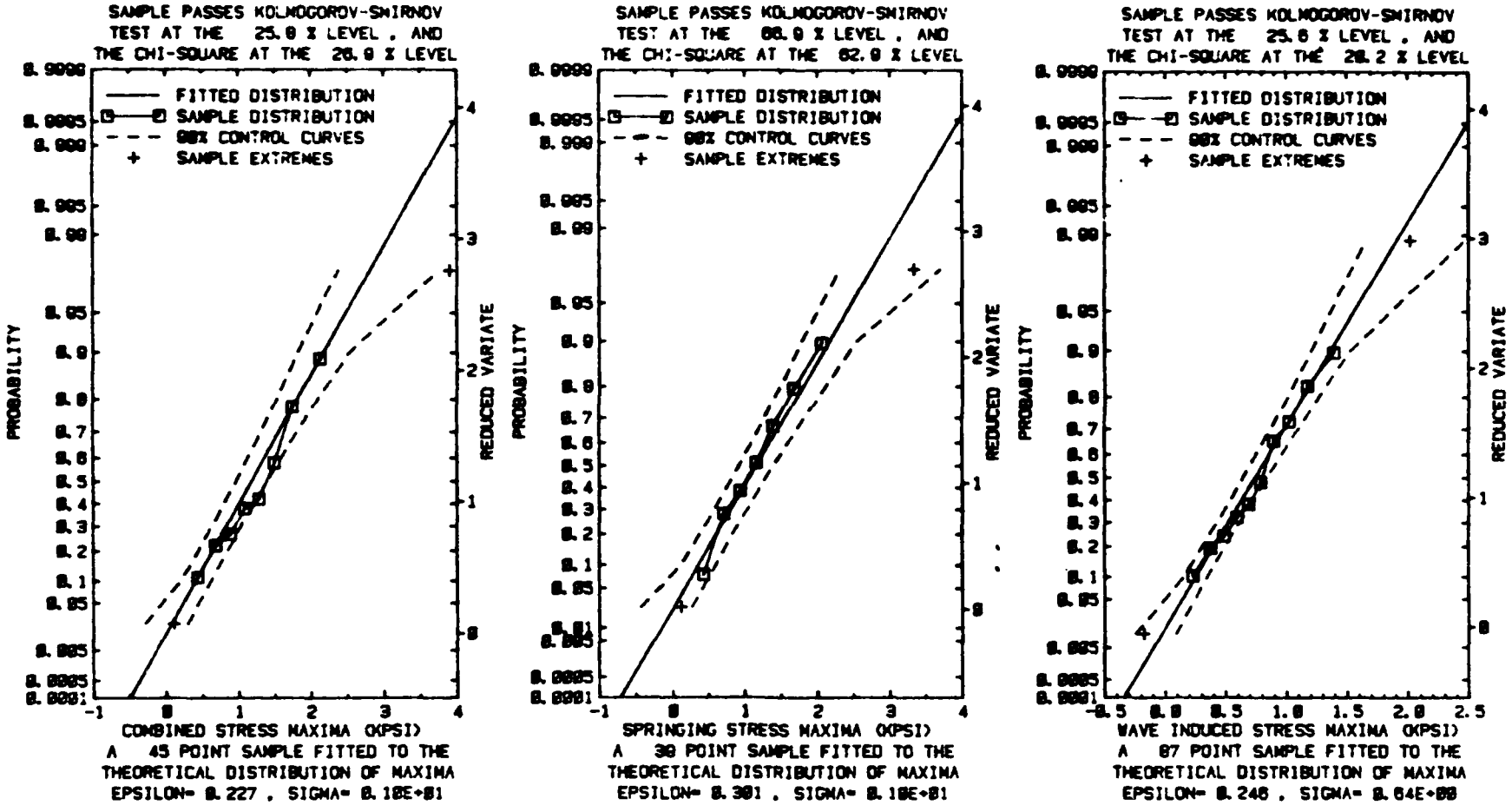

FIGURE G-24 SAMPLE DISTRIBUTIONS, SIMULATED DATA (MAXIMA), RUN 15 (1980)

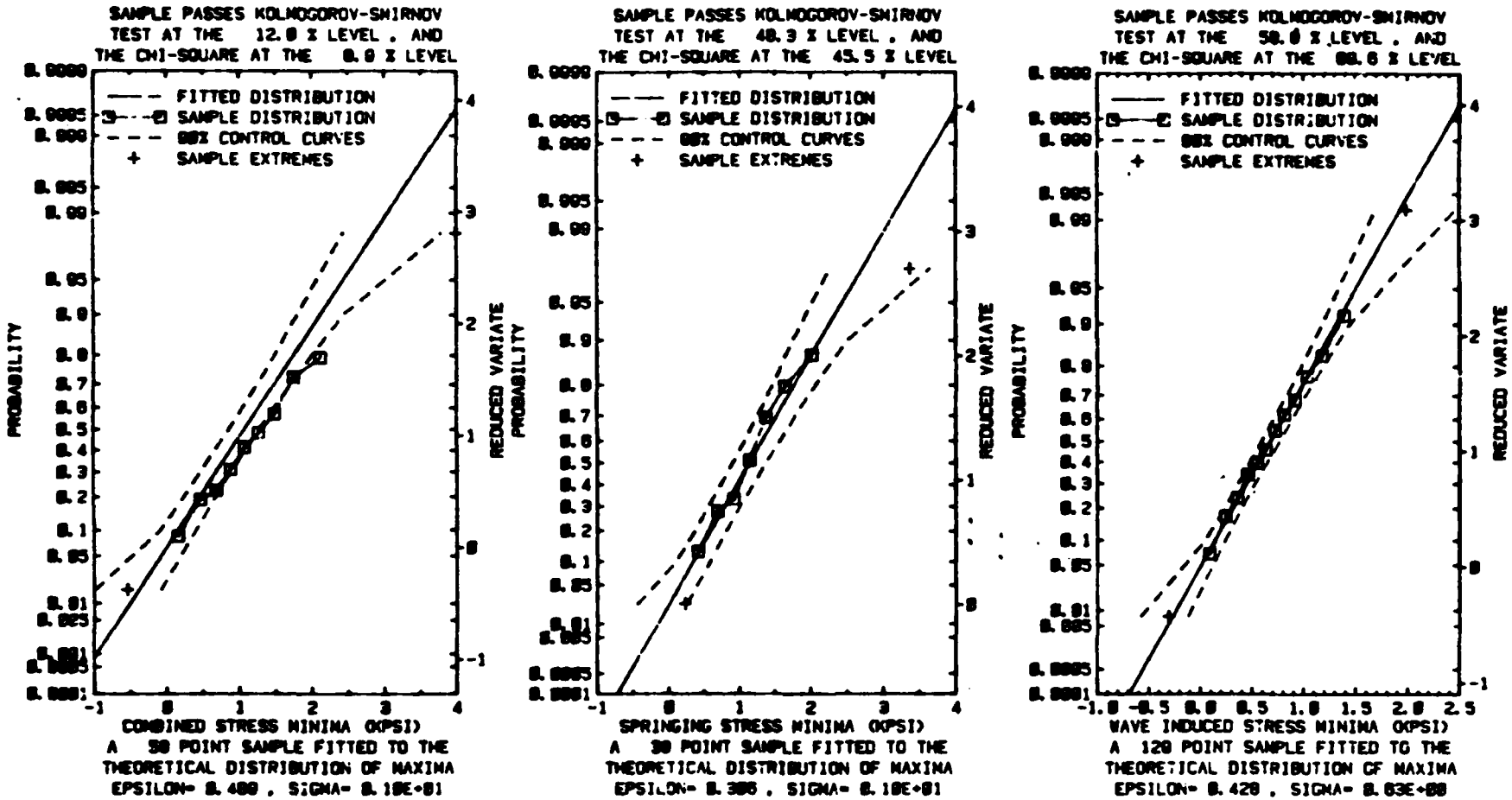

FIGURE G-25 SAMPLE DISTRIBUTIONS, SIMULATED DATA (MINIMA), RUN 15 (1980)

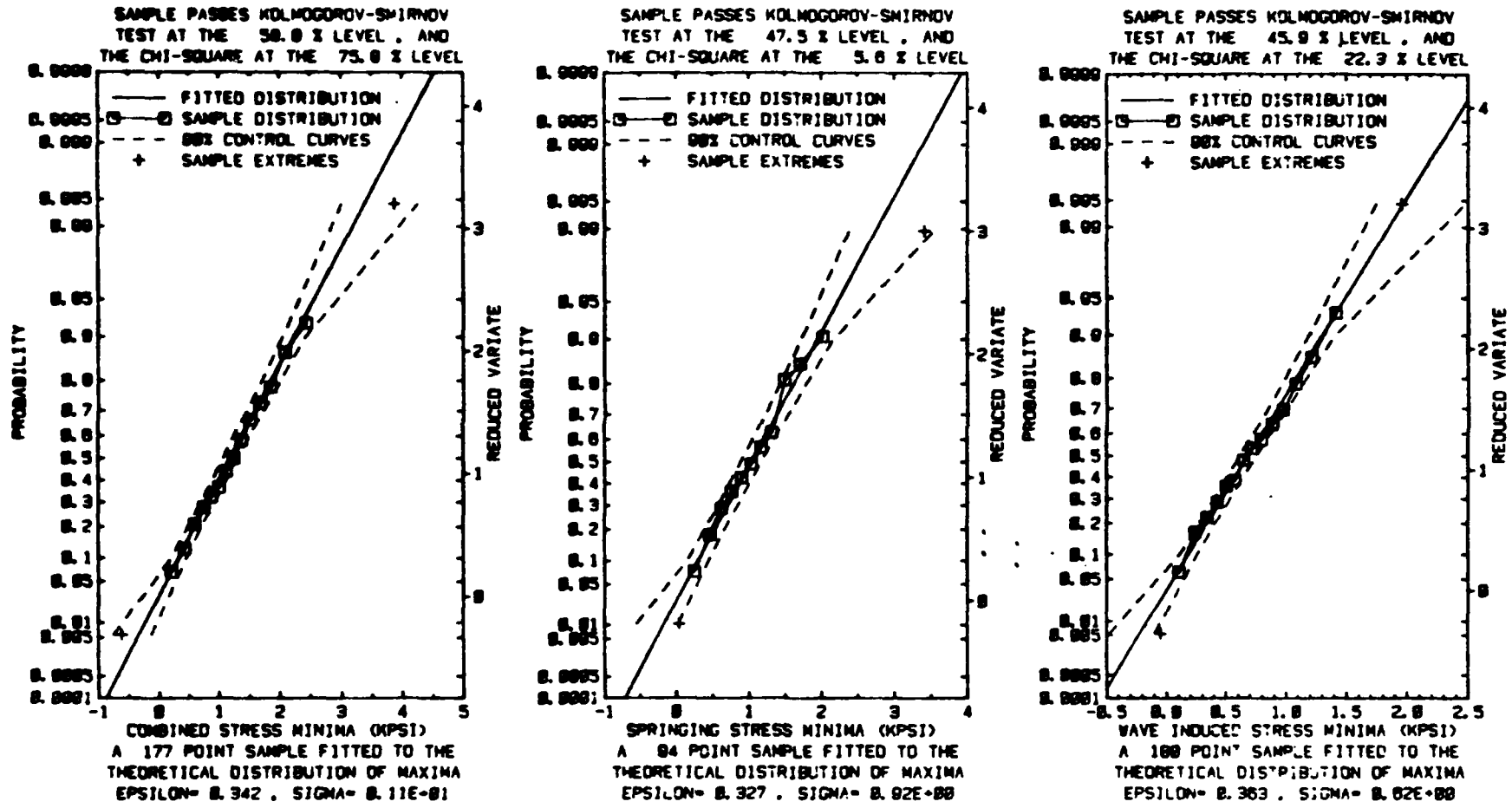

FIGURE G-26 SAMPLE DISTRIBUTIONS, OBSERVED DATA (MINIMA), RUN 16 (1980)

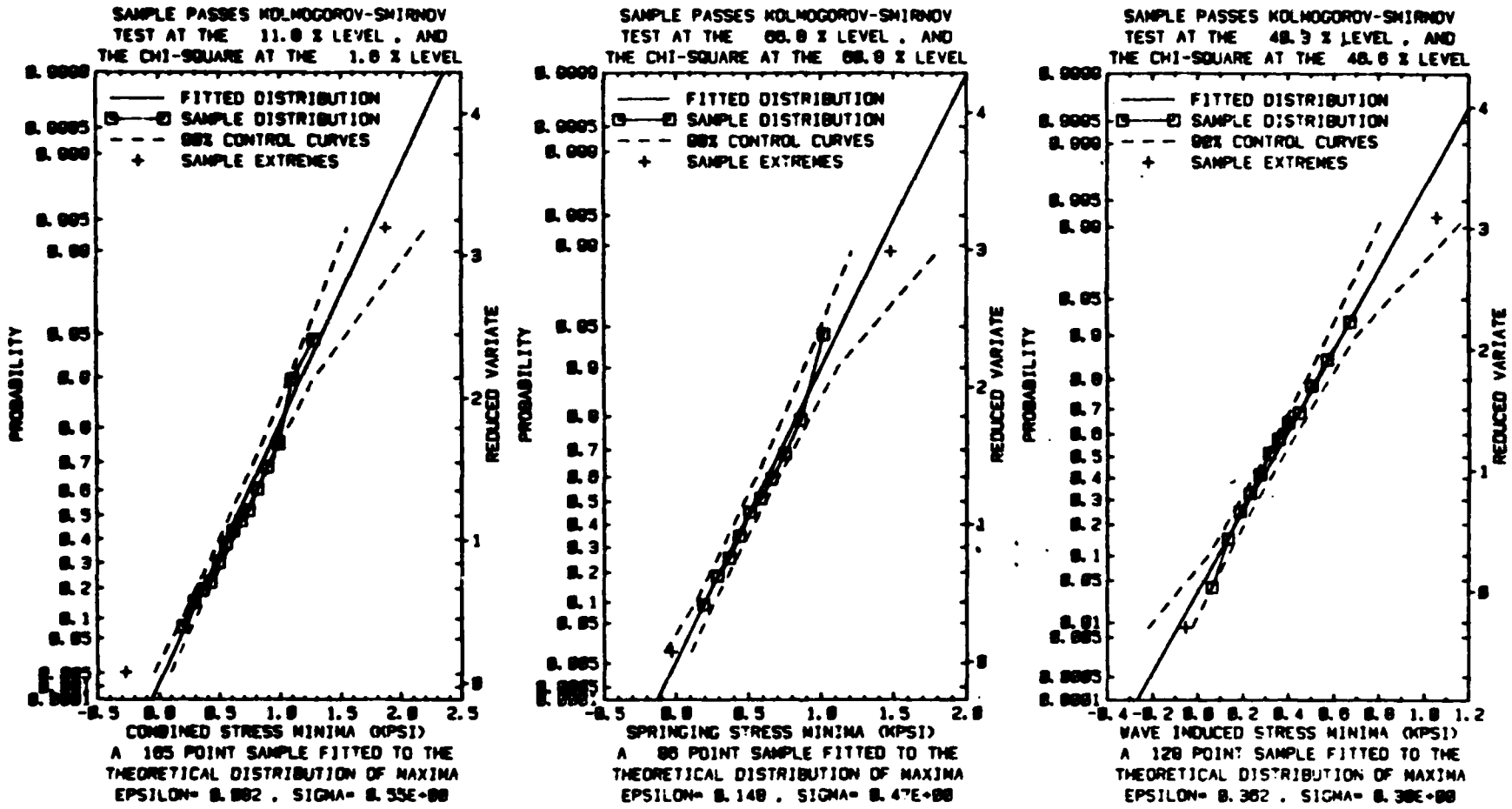

FIGURE G-27 SAMPLE DISTRIBUTIONS, OBSERVED DATA (MINIMA), RUN 20 (1980)

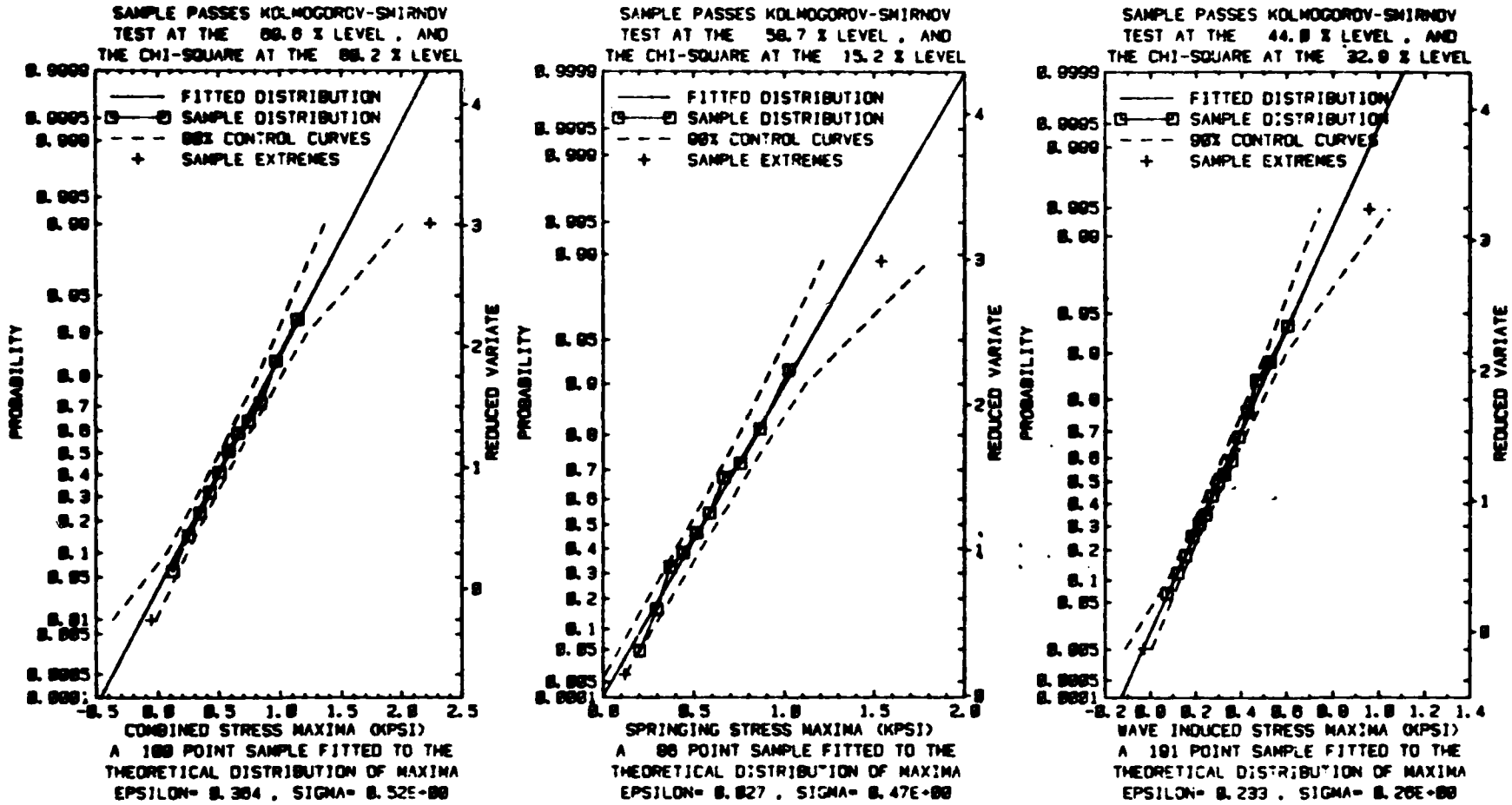

FIGURE G-28 SAMPLE DISTRIBUTIONS, OBSERVED DATA (MAXIMA), RUN 21 (1980)

REFERENCES

1. Swanek, R. A. and Kihl, D. P., "Investigation of Springing Responses on the Great Lakes Ore Carrier M/V STEWART J. CORT," Structures Department, David W. Taylor Naval Ship Research and Development Center, CG-D-17-81, December 1980, NTIS AD A100 293.

2. Dalzell, J. F., "Numerical Simulation of Combined, Springing and Wave Induced Stress Response," Davidson Laboratory Report SIT-DL-81-9-2141, Coast Guard Report CG-M-6-81, August 1981.

3. Hammond, D. L., "Great Lakes Wave Height Radar System," Prepared by the Naval Research Laboratory, issued as Coast Guard Report CG-D-6-80, January 1980,

4. Dalzell, J. F., "Wavemeter Data Reduction Method and Initial Data for the SL-7 Containership," Ship Structure Committee, SSC-278, September 1978, AD A062391.

5. Lacoss, T., "Data Adaptive Spectral Analysis Methods," Geophysics, Vol. 36, No. 4, August 1971, pp. 661.

6. Bendat, J. S. and Piersol, A. G., "Random Data: Analysis and Measurement Procedures," John Wiley & Sons, Inc., 1971.

7. Nuttal, A. H., "Spectral Estimation by Means of Overlapped Fast Fourier Transform Processing of Windowed Data," Report 4196, Naval Underwater Systems Center, October 1971.

8. Pierson, W. J., Jr., "On the Phases of the Motions of Ships in Confused Seas," New York University, Report 9, NONR 285(17), November 1957.

9. Dalzell, J. F., "Application of Cross-Bi-Spectral Analysis to Ship Resistance in Waves," SIT-DL-72-1606, Davidson Laboratory, May 1972, AD-749102.

10. Dalzell, J. F., "Application of the Functional Polynomial to the Ship Added Resistance Problem," Eleventh Symposium on Naval Hydrodynamic, London, 1976.

11. Walden, D. A. and Noll, M. D., "Springing Research of a Great Lakes Ore Carrier," Coast Guard Report No. CG-D-13-82, April 1981.

12. Miles, M. D., "On the Short Term Distribution of the Peaks of Combined Low Frequency and Springing Stresses," Hull Stresses in Bulk Carriers in the Great Lakes and Gulf of St. Lawrence Wave Environment, Society of Naval Architects and Marine Engineers, T & R Symposium S-2, 1971.

REFERENCES

(Cont'd)

13. Dalzell, J. F. et al, "Examination of Service and Stress Data of Three Ships for Development of Hull Girder Load Criteria," SSC-287, Ship Structure Committee, 1979, AD-A072910.

14. Cartwright, D. E. and Longuet-Higgins, M. S., "The Statistical Distribution of the Maxima of a Random Function," Proc. Royal Society, A, 237, 1956.

15. Ochi, M. K. and Bolton, W. E., "Statistics for Prediction of Ship Performance in a Seaway," International Shipbuilding Progress, 1973.

16. Gumbel, D. E., "Statistics of Extremes," Columbia University Press, New York, 1958.

17. Teledyne Materials Research, "Instrumentation of M/V STEWART J. CORT, 1972 Season," TMR Report E-1419(i), June 1973.

18. Antoinides, G., Schauer, R., Kilcullen, A., and Sigman, R., "Analysis of Springing Stresses on S.S. CHARLES M. BEEGHLY and M/V STEWART CORT," CG-D-163-75, U.S. Coast Guard, Department of Transportation, July 1975, AD-A018 569.

19. Stiansen, S. G., Mansour, A., and Chen, Y. N., "Dynamic Response of Large Great Lakes Bulk Carriers to Wave Excited Loads," Trans. SNAME, Vol. 85, 1977, pp 174-208.

20. American Bureau of Shipping, "Rules for Building and Classing Bulk Carriers for Service on the Great Lakes," American Bureau of Shipping, New York, 1978.

21. Gran, S., "Statistical Description of Wave Induced Vibratory Stresses in Ships," Det norske Veritas Report No. 80-1171, Coast Guard Report No. CG-M-2-81, NTIS AD A111186, December 1980.

METRIC CONVERSION FACTORS

Approximate Conversions to Metric Measures

Symbol	When You Know	Multiply by	To Find	Symbol
		LENGTH		
in	inches	*2.5	centimeters	cm
ft	feet	30	centimeters	cm
yd	yards	0.9	meters	m
mi	miles	1.6	kilometers	km
		AREA		
in^2	square inches	6.5	square centimeters	cm^2
ft^2	square feet	0.09	square meters	m^2
yd^2	square yards	0.8	square meters	m^2
mi^2	square miles	2.6	square kilometers	km^2
	acres	0.4	hectares	ha
		MASS (weight)		
oz	ounces	28	grams	g
lb	pounds	0.45	kilograms	kg
	short tons (2000 lb)	0.9	tonnes	t
		VOLUME		
tsp	teaspoons	5	milliliters	ml
Tbsp	tablespoons	15	milliliters	ml
fl oz	fluid ounces	30	milliliters	ml
c	cups	0.24	liters	l
pt	pints	0.47	liters	l
qt	quarts	0.95	liters	l
gal	gallons	3.8	liters	l
ft^3	cubic feet	0.03	cubic meters	m^3
yd^3	cubic yards	0.76	cubic meters	m^3
		TEMPERATURE (exact)		
°F	Fahrenheit temperature	5/9 (after subtracting 32)	Celsius temperature	°C

*1 in = 2.54 (exactly). For other exact conversions and more detailed tables, see NBS Misc. Publ. 286, Units of Weights and Measures, Price $2.25, SD Catalog No. C13.10:286.

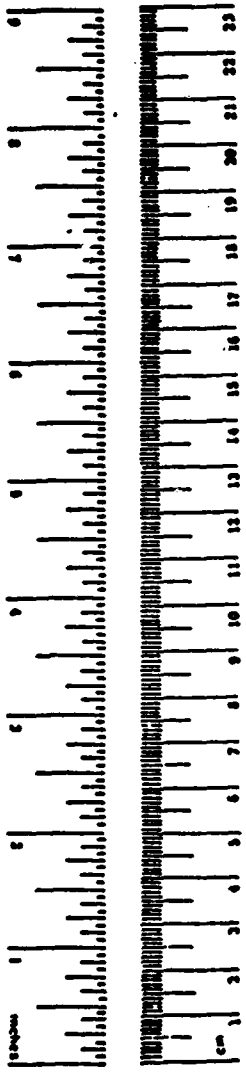

Approximate Conversions from Metric Measures

Symbol	When You Know	Multiply by	To Find	Symbol
		LENGTH		
mm	millimeters	0.04	inches	in
cm	centimeters	0.4	inches	in
m	meters	3.3	feet	ft
m	meters	1.1	yards	yd
km	kilometers	0.6	miles	mi
		AREA		
cm^2	square centimeters	0.16	square inches	in^2
m^2	square meters	1.2	square yards	yd^2
km^2	square kilometers	0.4	square miles	mi^2
ha	hectares (10,000 m^2)	2.5	acres	
		MASS (weight)		
g	grams	0.035	ounces	oz
kg	kilograms	2.2	pounds	lb
t	tonnes (1000 kg)	1.1	short tons	
		VOLUME		
ml	milliliters	0.03	fluid ounces	fl oz
l	liters	2.1	pints	pt
l	liters	1.06	quarts	qt
l	liters	0.26	gallons	gal
m^3	cubic meters	35	cubic feet	ft^3
m^3	cubic meters	1.3	cubic yards	yd^3
		TEMPERATURE (exact)		
°C	Celsius temperature	9/5 (then add 32)	Fahrenheit temperature	

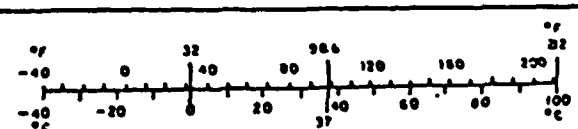

5-8

DTI